

Functional Dissection of Genetic Associations to Osteoarthritis

Madhushika Ratnayake

Thesis submitted for the Doctor of
Philosophy

Institute of Cellular Medicine

December 2013



Abstract

Osteoarthritis is a common, multifactorial disease, characterised by the progressive loss of articular cartilage from synovial joints. It has a major genetic component that is polygenic in nature. The aim of my thesis was to explore functional effects of several osteoarthritis susceptibility loci.

I have carried out functional studies on five genes in total, covering three osteoarthritis susceptibility loci, including *GDF5*, *MICAL3* and *CHST11*. I used protein, gene and allelic expression analyses.

Firstly, I assessed whether human chondrocytes would respond in a predictable manner to GDF5. Reduced expression of *GDF5* (chromosome 20q11.22) correlates with an increased risk for osteoarthritis and I assessed what effect providing exogenous GDF5 to chondrocytes had on expression of target genes. I observed that chondrocytes responded to exogenous GDF5 in a highly discordant manner. Secondly, I carried out gene and allelic expression analyses on *MICAL3* (chromosome 22q11.21), to investigate if the association to osteoarthritis at this locus is mediated by an influence on gene expression. I observed allelic expression imbalance (AEI) at this locus, however, this did not correlate with genotype at the associated polymorphism in the human joint tissues investigated. I then focused on the susceptibility locus at *CHST11* (chromosome 12q23.3). AEI was common at this gene, although a correlation with genotype at the associated polymorphism was not observed in the human joint tissues investigated. I carried out sequence analysis of *CHST11* in osteoarthritic patients to identify rare amino acid coding variants, and found no evidence for any accounting for disease susceptibility. I explored the role of *CHST11* in mesenchymal stem cells during chondrogenesis and observed that *CHST11* knockdown leads to gene expression changes in chondrocyte marker genes and a reduction in cartilage extracellular matrix synthesis.

My studies highlight the complexity in performing functional studies to identify and characterise the causal polymorphisms influencing osteoarthritis susceptibility.

Dedication

To my darling Ammi

Acknowledgements

I would like to thank my supervisor John Loughlin for the constant support, supervision, guidance and useful suggestions throughout my PhD. I also acknowledge my second supervisor Mauro Santibanez-Koref for his advice, suggestions and statistical support during my PhD.

I thank Mark Birch for gifting me with the Smad responsive reporter construct and Matt Barter for providing me with recombinant TGF- β 1 for experiments outlined in Chapter 3. Matt Barter also provided me with mesenchymal stem cells and assisted me in carrying out experiments involving mesenchymal stem cells, described in Chapter 7.

Furthermore, I would like to thank Athanasia Gravani, Mike Cunnington, Martina Elias, Steven Woods and Jonathan Baker for their time, help and advice with various laboratory experiments. I am also thankful to members of the Osteoarthritis Genetics Group, especially Catherine Syddall, Andrew Dodd, Emma Raine and Louise Reynard for their help, guidance and friendship throughout my PhD. I am also grateful for members of the Musculoskeletal Research Group for all their help.

Special thank you to my best friend Arunkumar Krishnakumar for the fantastic support, encouragement and friendship throughout my PhD, particularly whilst writing my thesis.

I would like to thank National Institute for Health Research for funding my research.

Finally, thank you to my dear parents, family and friends for all their support and motivation that they have given me over the duration of my PhD.

Table of Contents

Chapter 1: General introduction.....	1
1.1 Background to osteoarthritis	1
1.1.1 Defining OA	2
1.1.2 Incidence and prevalence of OA	2
1.1.3 Treatment of OA	2
1.2 The normal structure and function of the synovial joint	4
1.2.1 Articular cartilage.....	4
1.2.2 Subchondral bone	8
1.2.3 The joint capsule, synovium and synovial fluid	8
1.2.4 Meniscus	8
1.2.5 Tendons and ligaments	9
1.2.6 Fatpad	9
1.3 Synovial joint and articular cartilage formation	9
1.4 Pathology of OA	11
1.4.1 Articular cartilage.....	11
1.4.2 Subchondral bone	13
1.4.3 Synovium.....	14
1.4.4 Joint capsule, meniscus and ligaments	14
1.5 Effect on joint homeostasis during the pathogenesis of OA	14
1.5.1 Cytokines.....	15
1.5.2 Growth factors	15
1.5.3 Enzymes	16
1.5.4 Transcription factors	17
1.5.5 Other mediators.....	17
1.6 Risk factors of OA.....	18
1.6.1 Age	18
1.6.2 Sex.....	18
1.6.3 Obesity	19
1.6.4 Genetics	20
1.7 Studies to identify alleles implicated in OA	21
1.7.1 Candidate gene studies.....	21
1.7.2 Genome-wide linkage studies.....	22
1.7.3 Genome-wide association scans.....	23
1.8 Measuring functional effects of polymorphisms	25

1.9 Aims.....	28
1.9.1 Aim 1: Investigation of the effect of exogenous growth factor GDF5 on primary chondrocytes.....	28
1.9.2 Aim 2: Allelic expression analysis of the osteoarthritis susceptibility locus that maps to <i>MICAL3</i>	28
1.9.3 Aim 3: Assessing whether the OA associated locus mapping to chromosome 12q23.3 mediates its effect by influencing the expression of <i>CHST11</i>	28
1.9.4 Aim 4: Search for rare variants in the coding region of <i>CHST11</i>	29
1.9.5 Aim 5: The role of CHST11 in chondrocyte differentiation.....	29
Chapter 2: Materials and methods.....	30
2.1 Tissue collection and grinding.....	30
2.2 Nucleic acid extraction from ground joint tissue.....	30
2.3 Complementary DNA (cDNA) synthesis.....	31
2.4 Polymerase Chain Reaction (PCR).....	32
2.5 SW1353 cell culture.....	33
2.6 Bacterial cell transformation with Smad 1/5/8 reporter vector.....	33
2.7 Plasmid DNA purification using MiniPrep.....	34
2.8 Plasmid DNA purification using MaxiPrep.....	34
2.9 Transfection of SW1353 cells with Smad 1/5/8 luciferase reporter vector.....	35
2.10 Cartilage digestion and chondrocyte culture.....	35
2.11 Stimulation of cells with exogenous growth factors (GDF5, TGF- β 1, IL-1 α and OSM).....	36
2.11.1 Monolayer culture with exogenous growth factors post transfection.....	36
2.11.2 Monolayer culture for western blot analysis.....	36
2.11.3 Monolayer culture for gene expression analysis.....	37
2.12 Luciferase activity reading.....	37
2.13 Protein extraction.....	38
2.14 Protein quantification using Bradford assay.....	38
2.15 Western blot.....	39
2.15.1 Gel preparation.....	39
2.15.2 Sample preparation.....	40
2.15.3 Running the gel.....	40
2.15.4 Transfer of proteins to PVDF membrane.....	40
2.15.5 Blocking.....	41
2.15.6 Detection.....	41
2.15.7 Stripping membrane.....	42

2.16 Cell lysis and reverse transcription of cell lysates.....	42
2.17 Gene expression analysis using real time quantitative PCR	42
2.18 Qualitative gene expression analysis	45
2.19 Database searching for polymorphisms	46
2.20 Restriction Fragment Length Polymorphism (RFLP) Analysis	46
2.21 Allelic Expression Imbalance (AEI) analysis using Sequenom iPLEX assays	49
2.22 Allelic Expression Imbalance (AEI) analysis using real time quantitative PCR genotyping assays	53
2.23 OA patients used for coding DNA variant detection in <i>CHST11</i>	54
2.24 Sequence analysis of the three exons of <i>CHST11</i>	54
2.25 Human mesenchymal stem cell culture.....	58
2.26 siRNA transfection	58
2.27 Differentiation of transfected hMSC to chondrocytes	59
2.28 Cartilage disc grinding.....	60
2.29 RNA extraction (Trizol/chloroform method)	61
2.30 Micromass culture of transfected chondrocytes and mesenchymal stem cells.....	61
2.31 Alcian blue staining	62
2.32 Statistical analysis	62
2.32.1 Luciferase activity	62
2.32.2 Gene expression analysis post stimulation with exogenous growth factors.....	62
2.32.3 Gene expression stratified by genotype	63
2.32.4 Allelic expression imbalance analysis	63
2.32.5 Gene expression analysis post transfection with <i>CHST11</i> siRNA.....	63
2.32.6 Alcian blue staining	63
Chapter 3: Investigation of the effect of exogenous growth factor GDF5 on primary chondrocytes.....	64
3.1 Introduction	64
3.2 Results.....	69
3.2.1 GDF5 receptor gene expression in OA and NOF tissue.....	69
3.2.2 The GDF5 proteins used.....	70
3.2.3 Analysis of dose-dependent response to exogenous GDF5 in SW1353 cells using a luciferase reporter assay.....	71
3.2.4 Activation of Smad signalling in chondrocytes after stimulation with GDF5	76
3.2.5 Changes in gene expression in response to exogenous GDF5 in OA chondrocytes ..	77
3.2.6 Changes in gene expression in response to IL-1 α and oncostatin M in OA chondrocytes.....	90

3.3 Discussion.....	93
Chapter 4: Allelic expression analysis of the osteoarthritis susceptibility locus that maps to <i>MICAL3</i>	96
4.1 Introduction	96
4.2 Results.....	100
4.2.1 Qualitative gene expression analysis of <i>BCL2L13</i> , <i>BID</i> and <i>MICAL3</i> in joint tissue cDNAs.....	100
4.2.2 <i>BCL2L13</i> , <i>BID</i> and <i>MICAL3</i> expression in cartilage tissue stratified by genotype at rs2277831	103
4.2.3 Database searching for polymorphisms	106
4.2.4 Allelic expression imbalance at <i>BCL2L13</i> , <i>BID</i> and <i>MICAL3</i> in cartilage tissue	108
4.3 Discussion.....	117
Chapter 5: Assessing whether the OA associated locus mapping to chromosome 12q23.3 mediates its effect by influencing the expression of <i>CHST11</i>	119
5.1 Introduction	119
5.2 Results.....	123
5.2.1 Qualitative gene expression analysis of <i>CHST11</i> in joint tissue cDNAs.....	123
5.2.2 Gene expression of <i>CHST11</i> in hip OA versus NOF cartilage	127
5.2.3 Database searching for common non-synonymous mutations in <i>CHST11</i>	128
5.2.4 <i>CHST11</i> expression in cartilage, fatpad and synovium tissue stratified by genotype at rs835487	128
5.2.5 Allelic expression imbalance of <i>CHST11</i> in cartilage, fatpad and synovium tissue..	131
5.3 Discussion.....	140
Chapter 6: Sequence analysis of <i>CHST11</i> coding exons.....	143
6.1 Introduction	143
6.2 Results.....	143
6.3 Discussion.....	144
Chapter 7: The role of <i>CHST11</i> in chondrocyte differentiation	145
7.1 Introduction	145
7.2 Results.....	146
7.2.1 Validation of the Transwell culture of mesenchymal stem cells as a tool to investigate chondrogenesis	146
7.2.2 <i>CHST11</i> expression in mesenchymal stem cells during differentiation into chondrocytes.....	147
7.2.3 Effect of <i>CHST11</i> knockdown in human mesenchymal stem cells during differentiation into chondrocytes.....	147
7.2.4 Proteoglycan quantification in <i>CHST11</i> knocked-down mesenchymal stem cells ..	158

7.2.5 Gene expression changes after <i>CHST11</i> knockdown in OA and NOF chondrocytes	160
7.2.6 Proteoglycan quantification in <i>CHST11</i> knocked-down OA chondrocytes	164
7.3 Discussion	166
Chapter 8: General discussion	169
Appendix 1	177
Appendix 2	177
Conference attendances	177
Publications	177
References	179

Figures and tables

Figure 1.1: Normal knee joint compared to an osteoarthritic knee joint.....	1
Figure 1.2: Components of the cartilage extracellular matrix.....	6
Figure 1.3: Four different zones of normal adult articular cartilage	7
Figure 1.4: Major steps involved in synovial joint formation	11
Table 1.1: The eight signals from the arcOGEN GWAS.	25
Table 2.1:BSA standard curve for protein quantification	39
Table 2.2: Primer and probe sequences for real time quantitative PCR	44
Table 2.3:Reaction mix for TaqMan assays.....	45
Table 2.4: PCR primer sequences used to detect gene expression in joint tissues.....	46
Table 2.5: PCR primer sequences used to detect expression of different transcript isoforms of <i>CHST11</i> in joint tissues.....	46
Table 2.6: RFLP assays used for genotyping	48
Table 2.7: Sequenom assays designed to the seven SNPs from chr22q11.21	50
Table 2.8: Extension primer mix prepared for multiplex 1(A) and 2(B).....	51
Table 2.9: Real time quantitative genotyping assays used for AEI analyses	53
Table 2.10: Primers designed to amplify and sequence the <i>CHT11</i> coding region.	55
Figure 2.1: Amplimers designed for sequence analysis of <i>CHST11</i> coding region.	57
Table 2.11: Mastermixes for siRNA transfection	59
Figure 3.1: GDF5 signalling.....	65
Table 3.1: Human conditions associated with <i>GDF5</i> mutations.....	67
Figure 3.2: GDF5 receptor gene expression profile in 10 OA and 10 NOF cartilage tissue	69
Figure 3.3: GDF5 receptor gene expression in OA chondrocytes cultured in monolayer	70
Table 3.2: Partial amino acid sequences of the GDF5 proteins used.	71
Figure 3.4: Luciferase activity in response to GDF5 treatment	72
Figure 3.5: Luciferase activity readings generated in SW1353 cells in response to exogenous GDF5	75
Figure 3.6: Western blot images at 15 minutes, 30 minutes, 1 hour and 2 hours post stimulation with GDF5	76

Table 3.3: Details of the OA patients studied and of the growth factors used to stimulate their chondrocytes.....	78
Figure 3.7: Gene expression changes in cells treated with mouse GDF5 compared to untreated cells..	80
Figure 3.8: Gene expression changes in cells treated with wildtype human GDF5 compared to untreated cells.....	81
Figure 3.9: Gene expression changes in cells treated with human GDF5 variant A compared to untreated cells.....	82
Figure 3.10: Gene expression changes in cells treated with human GDF5 variant B compared to untreated cells.....	83
Figure 3.11: Gene expression changes in cells treated with human TGF- β 1 compared to untreated cells	84
Table 3.4: Significant (P<0.05) fold changes in gene expression in response to stimulation with wildtype mouse GDF5.....	85
Table 3.5: Significant (P<0.05) fold change in gene expression in response to stimulation with wildtype human GDF5	86
Table 3.6: Significant (P<0.05) fold change in gene expression in response to stimulation with human GDF5 variant A.....	87
Table 3.7: Significant (P<0.05) fold change in gene expression in response to stimulation with human GDF5 variant B.....	88
Table 3.8: Significant (P<0.05) fold change in gene expression in response to stimulation with TGF- β 1.....	89
Table 3.9: P-values calculated using the Wilcoxon signed rank test for each target gene following growth factor stimulation.	90
Figure 3.12: Fold change in <i>MMP1</i> and <i>MMP13</i> gene expression in response to IL-1 α and OSM simulation for 24 hours.	91
Table 3.10: Significant (P<0.05) fold change in gene expression in response to stimulation with IL-1 α and OSM	92
Table 3.11: P-values calculated using the Wilcoxon signed rank test for each target gene following IL-1 α and OSM stimulation.....	92
Figure 4.1: The eight protein coding transcript isoforms of <i>BCL2L13</i>	97
Figure 4.2: The six protein coding transcript isoforms of <i>BID</i>	98
Figure 4.3: The fifteen protein coding transcript isoforms of <i>MICAL3</i>	98

Table 4.1: The fifteen protein coding <i>MICAL3</i> transcript isoform names and their corresponding ensembl transcript IDs	99
Figure 4.4: <i>BCL2L13</i> expression in joint tissue cDNAs.	101
Figure 4.5: <i>BID</i> expression in joint tissue cDNAs.	102
Figure 4.6: <i>MICAL3</i> expression in joint tissue cDNAs.....	102
Figure 4.7: <i>MICAL3</i> ensembl transcript IDs ENST00000441493, ENST00000577821 and ENST00000579997 expression in joint tissue cDNAs.....	103
Figure 4.8: Expression of (A) <i>BCL2L13</i> , (B) <i>BID</i> and (C) <i>MICAL3</i> stratified by the genotype at the OA associated SNP rs2277831 in cartilage tissue from 55 OA patients	105
Table 4.2: The eight transcript SNPs studied at chr22q11.21.....	107
Figure 4.9: Linkage disequilibrium around <i>BCL2L13</i> , <i>BID</i> and <i>MICAL3</i> showing the eight transcript SNPs and the associated SNP rs2277831	108
Table 4.3: Allelic expression imbalance analysis for 33 patients.....	113
Figure 4.10: Allelic expression imbalance in patients 11, 30 and 9, who showed the largest allelic ratios at <i>BCL2L13</i> (rs2587100), <i>BID</i> (rs11538) and <i>MICAL3</i> (rs5992854) respectively.	114
Figure 4.11: Allelic expression imbalance at the transcript SNPs, stratified by genotype at rs2277831.	116
Figure 5.1: Association plot of the chromosome 12q23.3 hip-OA signal from the arcOGEN GWAS.....	119
Figure 5.2: The five protein coding transcript isoforms of <i>CHST11</i>	120
Figure 5.3: <i>CHST11</i> expression in joint tissue cDNAs.....	124
Figure 5.4: <i>CHST11</i> transcript isoform expression in joint tissue cDNAs.....	126
Figure 5.5: <i>CHST11</i> expression relative to housekeeping genes in cartilage from hip OA and NOF patients.	127
Figure 5.6: Expression of <i>CHST11</i> stratified by the genotype at the OA associated SNP rs835487 in cartilage.....	129
Figure 5.7: Expression of <i>CHST11</i> stratified by the genotype at the OA associated SNP rs835487 in fatpad and synovium.....	130
Table 5.1: The SNPs studied for AEI analysis of <i>CHST11</i>	131
Figure 5.8: Allelic expression imbalance in patients 12 and 44, who showed the largest allelic ratios in OA cartilage and NOF cartilage, respectively	132

Figure 5.9: Allelic expression imbalance stratified by genotype at rs835487 in (A) the 39 hip or knee OA patients, (B) the 11 hip OA patients and (C) the 5 NOF patients.....	134
Figure 5.10: Allelic expression imbalance in patients 51 and 16, who showed the largest allelic ratios in fatpad and synovium, respectively.	135
Figure 5.11: Allelic expression imbalance stratified by genotype at rs835487	136
Table 5.2: Allelic expression analysis of <i>CHST11</i> in cartilage from 39 OA patients, heterozygous at rs2463018.....	138
Table 5.3: Allelic expression analysis of <i>CHST11</i> in cartilage from 5 NOF patients, heterozygous at rs2463018.....	139
Table 5.4: Allelic expression analysis of <i>CHST11</i> in fatpad from 17 OA patients, heterozygous at rs2463018.....	139
Table 5.5: Allelic expression analysis of <i>CHST11</i> in synovium from 12 OA patients, heterozygous at rs2463018.....	140
Figure 6.1: Electropherogram showing the partial sequence of <i>CHST11</i> exon 3, that harbours the novel mutation (G/C).	143
Figure 6.2: RFLP carried out on hip OA patients.	144
Figure 7.1: <i>CHST11</i> expression relative to housekeeping genes in MSCs from donors A and B during differentiation into chondrocytes.	147
Figure 7.2: <i>CHST11</i> expression in MSCs transfected with a non-targeting (NT) siRNA and with an anti- <i>CHST11</i> siRNA.	148
Figure 7.3: Western blot analysis on protein extracted from day 7 cartilage discs formed during MSC chondrogenesis.	148
Figure 7.4: The change in wet mass in cartilage discs formed by MSCs from donors A and B during chondrogenesis.....	149
Table 7.1: List of the genes that were studied in this chapter, their protein products and their role in cartilage.....	151
Figure 7.5: Fold change in gene expression in <i>CHST11</i> knocked-down cells compared to control cells in MSCs from donors A and B during chondrogenesis.....	153
Table 7.2: Significant ($P < 0.05$) fold change in gene expression following <i>CHST11</i> knockdown in days 0, 3, 7 and 14 MSC discs, relative to control discs..	154
Table 7.3: P-values calculated using the Wilcoxon signed rank test for each target gene following <i>CHST11</i> knockdown.....	155

Figure 7.6: <i>CHST11</i> expression in MSCs transfected with a non-targeting (NT) siRNA and with an anti- <i>CHST11</i> siRNA	158
Figure 7.7: Western blot analysis on protein extracted from micromass cultures of MSCs from donors A and B.	159
Figure 7.8: Alcian blue staining in micromasses cultured from cells transfected with (A) a non-targeting siRNA and (B) with an anti- <i>CHST11</i> siRNA.	159
Figure 7.9: Absorbance at 600 nm per microgram of protein in micromasses cultured from MSCs transfected with a non-tarting (NT) siRNA and with an anti- <i>CHST11</i> siRNA.. ..	160
Table 7.4: Details of the nine patients studied.	162
Figure 7.10: Effect of <i>CHST11</i> knockdown in knee OA, hip OA and NOF chondrocytes... ..	163
Table 7.5: Significant (P<0.05) fold change in gene expression following <i>CHST11</i> knockdown in days 0, 3, 7 and 14 MSC discs, relative to control discs.	163
Figure 7.11: <i>CHST11</i> expression in cells transfected with a non-targeting (NT) siRNA and with an anti- <i>CHST11</i> siRNA.	164
Figure 7.12: Alcian blue staining in micromasses cultured from cells transfected with a non-targeting (NT) siRNA and with an anti- <i>CHST11</i> siRNA.....	165
Figure 7.13: Absorbance at 600 nm per microgram of protein in micromasses cultured from cells transfected with a non-tarting (NT) siRNA and with an anti- <i>CHST11</i> siRNA	165

Abbreviations

3'UTR	Three prime untranslated region
5'UTR	Five prime untranslated region
ADAMTS	A disintegrin and metalloproteinase with a thrombospondin motif
AEI	Allelic expression imbalance
APS	Ammonium persulphate
arcOGEN	Arthritis Research Campaign Osteoarthritis Genetics
BD	Brachydactyly
BMI	Body mass index
BMP	Bone morphogenetic protein
BP	Brachypodism
BSA	Bovine serum albumin
cDNA	Complementary DNA
CHST11	Carbohydrate sulfotransferase 11
CS	Chondroitin sulphate
DMEM	Dulbecco's Modified Eagle Medium
DNA	Deoxyribonucleic acid
DS	Dermatan sulphate
DZ	Dizygotic
ECM	Extracellular matrix
eQTL	Expression quantitative trait locus
FBS	Fetal bovine serum
GAG	Glycosaminoglycan
GAPDH	Glyceraldehyde 3-phosphate dehydrogenase
GDF5	Growth and differentiation factor-5
gDNA	Genomic DNA
GWAS	Genome-wide association scan
HRP	Horseradish peroxidase
IL-1	Interleukin-1
KL	Kellgren and Lawrence
KS	Keratan sulphate
LD	Linkage disequilibrium

MAF	Minor allele frequency
MMP	Matrix metalloproteinase
MRI	Magnetic resonance imaging
mRNA	Messenger RNA
MSC	Mesenchymal stem cell
MZ	Monozygotic
NOF	Neck-of-femur fracture
NTsiRNA	Non-targeting siRNA
OA	Osteoarthritis
OSM	Oncostatin M
PBS	Phosphate buffered saline
PCR	Polymerase chain reaction
RFLP	Restriction fragment length polymorphism
RNA	Ribonucleic acid
RT	Reverse transcription
siRNA	Small interfering RNA
SNP	Single nucleotide polymorphism
TBS	Tris buffered saline
TGF-β	Transforming growth factor beta
THR	Total hip replacement
TIMP	Tissue inhibitor of metalloproteinases
TJR	Total joint replacement
TKR	Total knee replacement

Chapter 1: General introduction

1.1 Background to osteoarthritis

Osteoarthritis (OA) is the most common form of arthritis and is the leading cause of disability in adults (Guccione *et al.*, 1994). OA is characterised by the progressive loss of articular cartilage, which is a smooth protective layer covering the ends of articulating joints. In addition to cartilage breakdown, OA is characterised by the abnormal formation of new bone (osteophytes), subchondral bone thickening (sclerosis) and synovial proliferation and inflammation (Figure 1.1). Other components of the joint also undergo changes in structure and function, including the ligaments, tendons, capsule and synovial joint lining (Wieland *et al.*, 2005). OA can affect any joint in the body, however the joints that are most affected are the hands, knees, hips and spine.

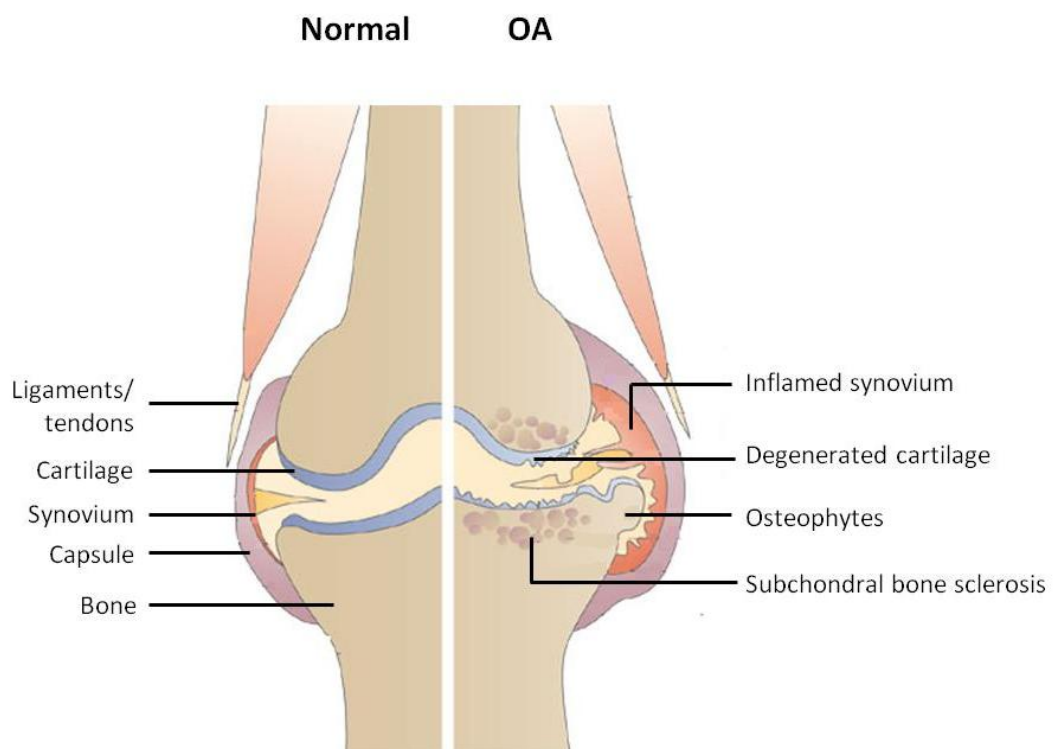


Figure 1.1: Normal knee joint compared to an osteoarthritic knee joint.

Degeneration of cartilage, osteophyte formation, subchondral bone sclerosis and synovial inflammation are observed in OA. Adapted from Wieland *et al.*, 2005.

1.1.1 Defining OA

The commonly used standard for defining the presence of hand, hip or knee OA is the Kellgren and Lawrence (KL) grade. This is a radiographic grading system which scores the severity of OA on a scale of 0 to 4, with definite radiographic OA being defined as a KL grade of or greater than 2 (Kellgren and Lawrence, 1963). The scoring system is based on the degree of the osteophyte formation, joint space narrowing and bone sclerosis. OA can be described in a joint specific manner (hand, hip or knee OA) or if several joints are affected, it can be described as generalised OA.

1.1.2 Incidence and prevalence of OA

The risk of developing symptomatic knee OA is reported to be 40% for men and 47% for women, with an elevated risk in obese individuals (Murphy *et al.*, 2008). The incidence of hand, hip and knee OA is estimated at 100, 88 and 240 cases per 100,000 person-years respectively (Oliveria *et al.*, 1995).

The prevalence of moderate to severe radiographic hand, hip and knee OA is reported to be 4.4 million, 210,000 and 0.5 million individuals in the UK, respectively (Arthritis Research Campaign, 2002; Arthritis and Musculoskeletal Alliance, 2004).

1.1.3 Treatment of OA

Pharmacological intervention

There is currently no cure for OA, therefore pharmacological management of OA involves the control of symptoms such as pain and function of the joints. Analgesics such as paracetamol and non-steroidal anti-inflammatory drugs (NSAIDs) are commonly used to relieve pain in hand, knee and hip OA (Jordan *et al.*, 2003; Zhang *et al.*, 2010). Furthermore, corticosteroid and hyaluronic acid administration to intra-articular joints is widely used in the management of knee OA, which acts to reduce pain and inflammation at the joints (Arroll and Goodyear-Smith, 2004; Bannuru *et al.*, 2009). In addition, nutritional supplements including glucosamine, chondroitin sulphate and vitamins are less commonly used for the management of OA (Vlad *et al.*, 2007; Vallières and du Souich, 2010; Wandel *et al.*, 2010).

Non-pharmacological intervention

Non-pharmacological approaches are used in combination with pharmacological intervention in the treatment of OA. These include educating patients in disease management, exercise, weight reduction and diet, as well as providing patients with physical aids such as orthoses (braces), insoles and walking aids (Heuts *et al.*, 2004).

Surgical intervention

Surgery in OA is considered at the end stage of the disease, after failure of other non-surgical therapies. Total joint replacement or arthroplasty is currently regarded as the most cost-effective, successful and effective treatment of OA (Ethgen *et al.*, 2004; Hawker *et al.*, 2009). This procedure eliminates pain and disability in end stage OA and can restore the function of the impaired joints to near-normal. However, joint replacement surgery can fail due to aseptic loosening and particle-induced osteolysis (Colizza *et al.*, 1995; Delaunay *et al.*, 2010; Huber *et al.*, 2010). This is a consequence of the degradation of the orthopaedic implant, resulting in bone loss. Therefore, newer designs utilising alternative materials and bearings such as ceramic and metal-on-metal bearings are being introduced to reduce wear (Delaunay *et al.*, 2010).

Other non-arthroplasty procedures include osteomy, arthroscopic debridement and arthrodesis. Osteomy is used to correct alignment in anatomic abnormalities of the hip or knee, mostly in younger patients (Coventry, 1979). Arthroscopic debridement is used to remove osteophytes in hip and knee OA, and arthrodesis or fusion is most frequently used to rescue failed joint replacements (Insall, 1967; Callaghan *et al.*, 1985; Conway *et al.*, 2004).

Cell-based approaches

The development of cellular therapies to repair articular cartilage in OA is an emerging area of research. These approaches are aimed at younger patients, and aim to culture new articular chondrocytes to replace the damaged cartilage (Khan *et al.*, 2010; Roberts *et al.*, 2011). If successful, these procedures may reduce pain, disability and enhance function in patients and may delay the need for joint replacement.

Autologous chondrocyte implantation (ACI) is currently used in clinical practice, where chondrocytes harvested from knee articular cartilage are cultured *ex vivo* and then re-implanted into damaged areas of the articular surface (Brittberg *et al.*, 1994; Giannoni *et al.*, 2005; Minas and Bryant, 2005). However, this approach is limited by the size of the cartilage biopsy required to obtain a sufficient number of cells (Oldershaw, 2012). Therefore, mesenchymal stem cells (MSCs) isolated from bone marrow or synovium have been considered as an alternative cell source. MSCs can be isolated from different tissue types including bone marrow, synovium, synovial fluid, adipose tissue, skeletal muscle, placenta, and umbilical cord (Oldershaw, 2012). These cells can be expanded *ex vivo* to obtain high cell numbers, which can overcome the limitations faced by ACI (Hardingham *et al.*, 2006; Khan *et al.*, 2009). Under appropriate conditions, MSCs can be differentiated into chondrocytes, osteoblasts and adipocytes *in vitro* (Dominici *et al.*, 2006), and such a technique is described by (Murdoch *et al.*, 2007) for chondrogenic differentiation using Transwell culture (Murdoch *et al.*, 2007).

1.2 The normal structure and function of the synovial joint

Synovial joints are composed of articular cartilage, subchondral bone, joint capsule, synovial fluid, synovium, ligaments and tendons, with knee joints containing a pair of menisci and a fatpad. All tissues of the joint have a highly specialised structure and function, and coordinate smooth pain-free movements, contributing to the ultimate function of the joint system.

1.2.1 Articular cartilage

Articular cartilage is a smooth frictionless surface with a thickness of approximately 3 mm in humans that covers the edges of skeletal bones, and acts as a gliding surface to dissipate the shearing and compressive stresses applied across the articulating joints (Wieland *et al.*, 2005).

Articular cartilage has no blood or nerve supply and the only type of cell present within this tissue is called the chondrocyte. These cells are responsible for the synthesis, secretion and maintenance of the extracellular matrix (ECM), composed of fibrillar and non-fibrillar components. The fibrillar matrix consists of a network rich in type II collagen, and other minor collagens including collagen type IX, XI and XVI. The non-fibrillar matrix components include proteoglycans such as aggrecan, decorin, biglycan

and fibromodulin (Goldring, 2006). The major proteoglycan, aggrecan, is made up of a core protein with three globular domains (G1, G2 and G3; Poole, 2005). G1 domain is bound non-covalently to hyaluronic acid (HA), and is stabilised by link protein. These then bind non-covalently to the collagenous network (Figure 1.2; Poole, 2005). Many glycosaminoglycan (GAG) chains consisting of keratan sulphate (KS) and chondroitin sulphate (CS) are present between the G2 and G3 domains of aggrecan. These GAGs are rich in carboxyl and sulphate groups that attract water molecules, thereby creating a swelling pressure, which is restricted heavily by the collagenous network (Poole, 2005). Water is the major constituent of articular cartilage and occupies approximately 70% of the tissue, hence water retention is very important for the function of articular cartilage (Allan, 1998; Knudson and Knudson, 2001). Water is expelled under compression to uphold mechanical loads and during unloading, the tissue is rehydrated and tissue elasticity is restored. Therefore, proteoglycans together with the collagenous network acts to withstand tensile and shear forces within the tissue and maintains the structural integrity of cartilage (Poole, 2005). In addition to collagens and proteoglycans, other structural proteins which help maintain the structure and function of the ECM include matrilin-3, cartilage oligomeric matrix protein (COMP) and fibronectin (Reginato and Olsen, 2002).

The articular cartilage is divided into four zones characterised by the shape of the chondrocytes and the arrangement of the matrix fibrils (Figure 1.3; Aigner *et al.*, 2006a). The superficial zone chondrocytes are small and round in appearance and the collagen fibrils are very thin and are arranged in parallel to the surface. Furthermore, the collagen content is greatest in this zone, due to the greater shear forces of articulation exerted on the surface. The middle zone chondrocytes are larger in size and the collagen fibrils are thicker and are arranged in random (Aigner and McKenna, 2002). The deep zone chondrocytes are arranged in perpendicular columns and the collagen content is the lowest in this zone (Salter, 1998). However, the aggrecan content is at the highest in this zone and is the lowest in the superficial zone (Poole, 2005). The collagen fibrils in the deep zone are arranged vertically, and extend through the tidemark, which is the boundary between articular cartilage and the calcified cartilage, into the calcified zone. The collagen fibrils in the calcified zone are arranged perpendicularly to the subchondral bone, and penetrate into it, anchoring the calcified

zone to the underlying bone, thereby forming a strong bond which can help resist shear forces of articulation (Aigner and McKenna, 2002; Salter, 1998). The ECM in the calcified zone is partly calcified and contains type X collagen, a marker of hypertrophy.

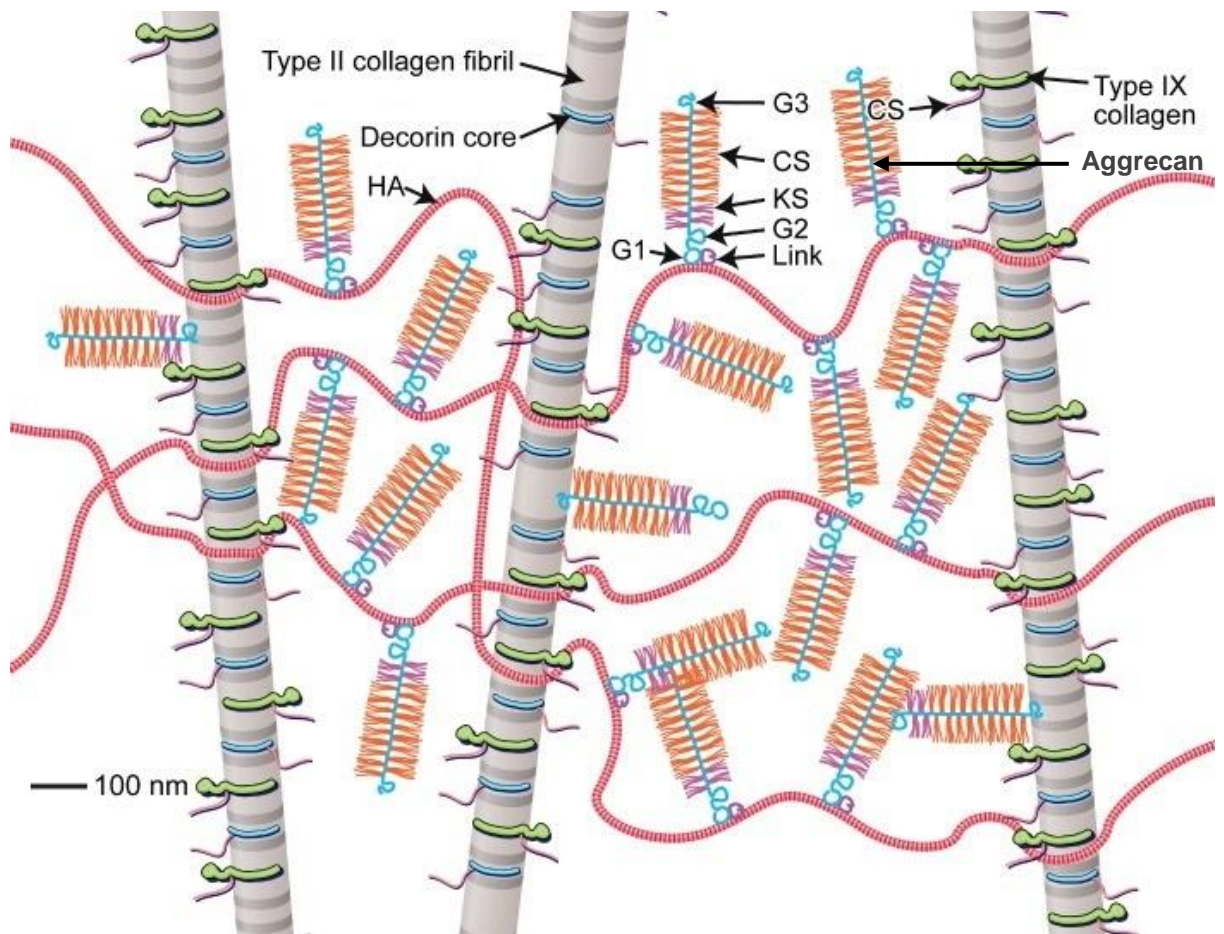


Figure 1.2: Components of the cartilage extracellular matrix

Aggrecan molecules (shown in blue) are bound to hyaluronan (HA), which then interact with type II collagen fibrils to form the cartilage extracellular matrix, to maintain its structural integrity. Keratan sulphate (KS) and chondroitin sulphate (CS) are present on aggrecan molecules in between the G2 and G3 globular domains. Adapted from Poole (2005).

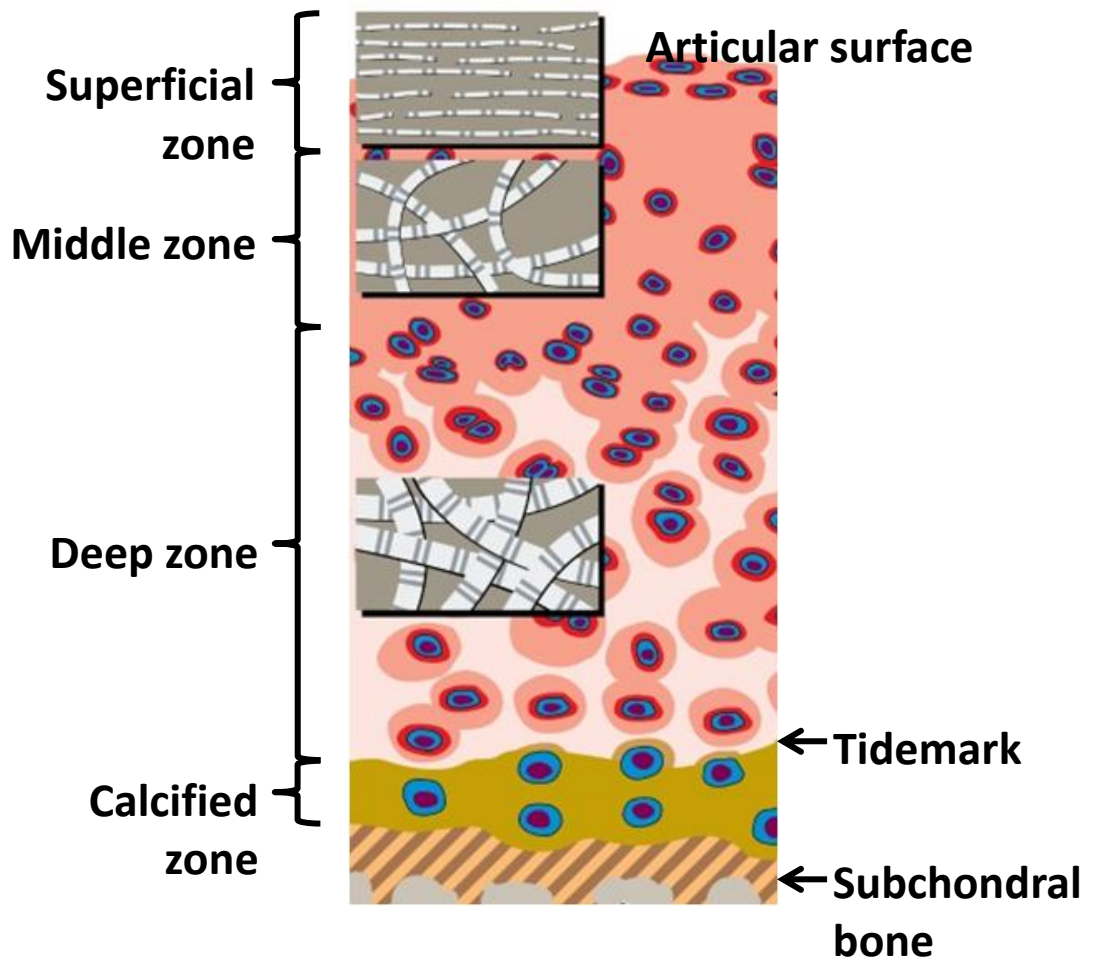


Figure 1.3: Four different zones of normal adult articular cartilage

The chondrocytes within each zone are illustrated in blue. The boxes shaded in grey show the arrangement of the type II collagen fibrils in the superficial, middle and deep zones.

Adapted from Poole (2005).

1.2.2 Subchondral bone

The subchondral bone lies beneath the calcified cartilage, thereby providing support to the cartilage, and consists of the subchondral plate and the cancellous bone, which lies beneath the plate. The cancellous bone contains trabeculae, which are arranged in different directions to distribute the stresses and help with shock absorption (Burr, 2004). The bone is comprised of a collagenous matrix rich in type I collagen fibrils and mineral crystals made of calcium hydroxyapatite (Wehrli, 2007). The bone contains two types of cells, which are important in bone turnover and remodelling. Osteoclasts are involved in the resorption of old bone and osteoblasts are responsible for the deposition of new bone (Wehrli, 2007). The subchondral bone is also highly vascular and neural, and blood vessels and nerve fibres are contained in structures called Haversian canals that run parallel to the cartilage surface.

1.2.3 The joint capsule, synovium and synovial fluid

The joint capsule is a fibrous tissue that is attached to the distal end of the bone, and contains blood vessels, lymphatic vessels and nerve fibres. It also contributes to the movement of the joint and provides mechanical stability. The inside of the capsule is lined by the synovium, which is approximately three cells deep (Aigner and McKenna, 2002). The synovium consists of two cell types. Type A synovial cells line the joint cavity and are involved in endocytosis of bacteria and viruses, thereby maintaining an aseptic environment within the joint-space. Type B synovial cells are fibroblast-like cells that synthesise and secrete two key components of synovial fluid: lubricin, a lubricant important for the articulation of the joints, and hyaluronic acid, which is important in maintaining the viscosity of the synovial fluid (Allan, 1998). The synovial fluid provides low friction between articulating surfaces by coating the joint surfaces. It also provides nutrition to the joint by acting as a medium through which nutrients and oxygen can diffuse from the synovium to the cartilage (Aigner *et al.*, 2006a).

1.2.4 Meniscus

The meniscus is a fibrocartilaginous tissue composed mainly of type I collagen fibrils. The pair of menisci in the knee joint is attached to the joint capsule and act as shock absorbers and distribute the intra-articular load within the joint to help with stability (Makris *et al.*, 2011).

1.2.5 Tendons and ligaments

Tendons and ligaments play an important role in the movement and stability of the joint. Tendons attach muscle to bone and ligaments attach bone to bone and are predominantly composed of type I collagen fibrils, which help resist tensile stress (Woo SL-Y *et al.*, 1992).

1.2.6 Fatpad

The infrapatellar fatpad of the knee is a fibrous tissue composed of adipocytes. It protects exposed articular surfaces by adapting to the changing contours of articulating surfaces during joint movement and also assists in the distribution of synovial fluid within the joint (Resnick, 1995; Vahlensieck *et al.*, 2002).

1.3 Synovial joint and articular cartilage formation

Joint development starts with the formation of mesenchymal condensations, mediated by cell adhesion molecules including Cadherins and N-CAM, and the appearance of an interzone, which determines the future site of joint formation (Pacifici *et al.*, 2005).

The interzone contains closely packed fibroblast-like cells that show a more flattened shape. In humans, these cells form a layer that is two to three cells in thickness (Figure 1.4; Archer *et al.*, 2003). GDF5, which encodes growth and differentiation factor-5 is expressed in these cells and is believed to promote joint function and mediate the differentiation of interzone cells into chondrocytes (Francis-West *et al.*, 1999a; Merino *et al.*, 1999a; Storm and Kingsley, 1999). Also, noggin and chordin, which are GDF5 antagonists, are also expressed in the interzone cells in order to regulate the pace and degree of chondrocyte differentiation during joint development (Brunet *et al.*, 1998; Francis-West *et al.*, 1999b). Wnt-14 is another molecule important for the formation of joints, and is believed to act upstream of GDF5, playing a role in maintaining the mesenchymal character of interzone cells by preventing chondrogenesis (Hartman and Tabin, 2000; Archer *et al.*, 2003).

Once the joint site is specified by the formation of the interzone, the opposing sides of the synovial joint physically separate to form a synovial cavity (Figure 1.4). Several mechanisms have been proposed to explain this phenomenon including apoptosis, mechanical factors, interzone degradation by enzymatic activities, and the differential growth and matrix synthesis of the opposing sides of the cavity (Archer *et al.*, 2003). It

is now believed that hyaluronan (HA) synthesis and accumulation mediated by embryonic limb movement lead to the loss of tissue integrity in the interzone, thus initiating the formation of a fluid-filled cavity (Dowthwaite *et al.*, 1998).

Subsequently, as the synovial space cavitation progresses, the opposite sides of the joints begin the process of morphogenesis leading to the maturation of the joint, forming articular cartilage and the synovial cavity enveloped by the joint capsule.

The cells of the outer layers of the interzone differentiate into chondrocytes, forming the articular cartilage. The transcription factor ERG plays a vital role in this process by imposing a stable and immature chondrocyte phenotype, preventing endochondral ossification and in the induction of differentiation of immature chondrocytes to permanent articular chondrocytes (Iwamoto *et al.*, 2000). Immature chondrocytes express collagen types I, III and V, which are replaced by collagen types II, IX and XI and aggrecan as the cells differentiate into articular chondrocytes (Archer *et al.*, 2003). Endochondral ossification starts during joint formation in the embryo and continues after birth in cartilaginous growth plates in long bones, which is required for bone growth (Kronenberg, 2003). Hypertrophic chondrocytes which undergo endochondral ossification do not express type II collagen and express high levels of type X collagen, MMP13, VEGF and RUNX2. The hypertrophic zone undergoes matrix remodelling, chondrocyte apoptosis and vascular invasion, thus replacing nonvascular cartilage tissue with highly vascularised bone (Kronenberg, 2003).

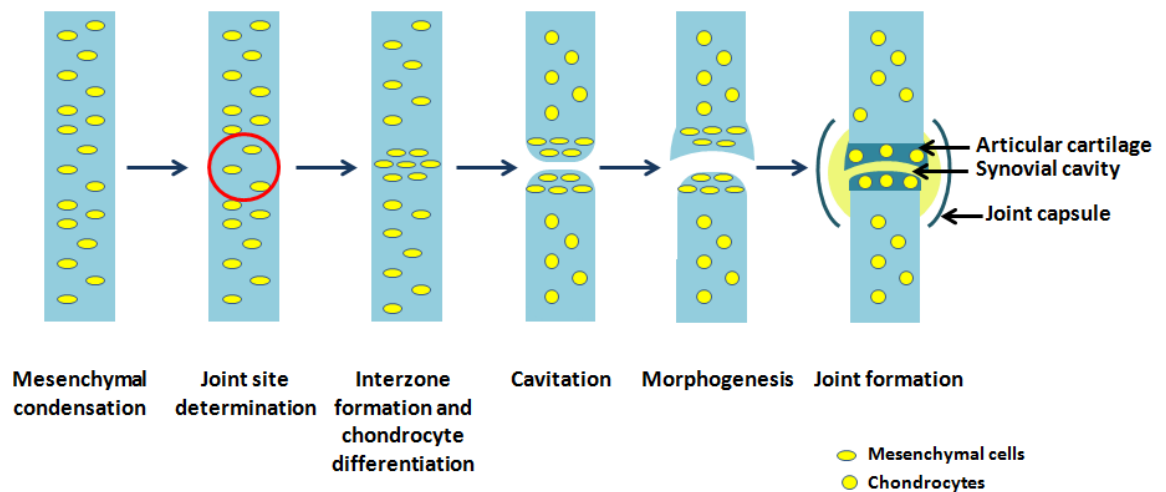


Figure 1.4: Major steps involved in synovial joint formation

The joint site is determined in the mesenchyme condensations, forming an interzone. Subsequently, joint cavitation occurs to physically dissociate the opposite sides of the synovial joint. The cells adjacent to the interzone start to differentiate into chondrocytes. Joint morphogenesis occurs and leads to joint maturation with the formation of articular cartilage, synovial cavity and the joint capsule. Adapted from Pacifici *et al.*, 2005.

1.4 Pathology of OA

The imbalance between the mechanical stresses applied within a joint, mainly at load bearing sites, and the functional ability of the cartilage to manage these stresses can account for the development of OA. The cellular response to damage can bring about degenerative and reparative structural changes in the joint tissues, which can lead to joint failure. It is still unclear which tissue of the joint harbours the most damage in OA as all tissues of the joint, including cartilage, subchondral bone, menisci, synovium and ligaments show pathological changes in the early stages of OA (Lohmander, 2000). Also, the sequence of degradative events that undergo during OA is unknown, for example, both the cartilage and the subchondral bone can show damage concomitantly, or follow or precede damage in one tissue (Dieppe and Lohmander, 2005).

1.4.1 Articular cartilage

The loss of the protective function of articular cartilage results in terminal joint failure, therefore a range of abnormal changes in cartilage is observed in OA.

The loss of articular cartilage is a result of the depletion and destruction of the ECM. In early stages of OA, the type II collagen network is disrupted either by direct physical stresses or by the action of collagenases, mainly matrix metalloproteinase-13 (MMP13; (Wu *et al.*, 2002). This is accompanied by proteoglycan loss, initially in the superficial zone, and then in deeper zones as the disease progresses, due to the increased expression and activity of ADAMTS (a disintegrin and metalloproteinase with a thrombospondin motif) aggrecanases (Song *et al.*, 2007). As a result, the cartilage swells due to increased water content and a reduction in the tensile strength and stiffness of the ECM ensues.

OA cartilage shows fibrillations, fissures and erosions, and therefore appears discoloured and rough, with a fragmented surface (Aigner *et al.*, 2006a). Fibrillations are surface discontinuities that result from the loss of type II collagen fibrils and proteoglycans from the cartilage surface. As the fibrillations extend from the superficial zone to deeper zones, they appear as vertical cracks or fissures. With time, as more and more cartilage tissue is lost, erosions appear and eventually the subchondral bone is exposed (Lorenz and Richter, 2006). Furthermore, vascular invasion from the subchondral bone contributes to further cartilage thinning. This occurs as capillaries penetrate the calcified zone, resulting in the duplication or multiplication of the tidemark, thereby blurring the boundary between calcified and uncalcified cartilage (Lane and Bullough, 1980; Revell *et al.*, 1990).

As the ECM is depleted, the chondrocytes are exposed to abnormal extracellular stimuli such as increased amounts of growth factors and cytokines (Aigner *et al.*, 2007). In response, chondrocytes undergo cell proliferation or cell death, mainly through apoptosis. Increase in cell proliferation can be an attempt to repair damaged cartilage, and can be observed microscopically by the increased amounts of small chondrocyte aggregates. These are seen initially in the superficial zone at early stages of OA, and then in deeper zones as OA progresses (Goldring and Goldring, 2010). Thin superficial pannus-like tissue can be observed in some OA cartilage, as an attempt to replace the damaged cartilage with a fibrocartilage, containing an abnormal arrangement of collagen fibrils. Loss of chondrocytes due to apoptosis, which can be seen under the microscope as areas of empty chondrocyte lacunae, further

contributes to the loss of ECM, cartilage structure and regulation of tissue homeostasis (Blanco *et al.*, 1998; Kühn *et al.*, 2004).

1.4.2 Subchondral bone

Changes seen in subchondral bone in OA include sclerosis, osteophyte formation, cyst formation and osteonecrosis.

Subchondral bone sclerosis is the thickening of the subchondral plate and the cancellous bone, resulting from an imbalance between bone synthesis and resorption (Lajeunesse and Reboul, 2003; Buckland-Wright, 2004). In late stage OA, increased bone thickening is seen in areas where there is a significant reduction in the protective layer of cartilage, suggesting that a change in mechanical forces may result in bone remodelling (Goldring and Goldring, 2010). However, it is also reported that bone remodelling occurs in early stages of OA, perhaps contributing to cartilage loss as a result of the alteration of biomechanical properties of the remodelled bone (Hutton *et al.*, 1986; Buckland-Wright *et al.*, 1991). An increase in the number of trabeculae in the cancellous bone and a decrease in the separation between trabeculae are also seen in OA (Buckland-Wright, 2004). Although this increases the mineral content and volume of cancellous bone, this also renders the bone mechanically weak due to the irregular arrangement of trabeculae.

Osteophytes are newly synthesised bony projections seen at joint margins. These are believed to be formed from periosteal or perichondrial stem cells, which are differentiated into chondrocytes, thus, mature osteophytes are capped with hyaline and fibrocartilage tissue (van der Kraan and van den Berg, 2007; Goldring and Goldring, 2010). Some evidence suggests that osteophyte formation is a consequence of a reparative response to protect cartilage, however, others have reported that osteophyte formation leads to cartilage loss (Wieland *et al.*, 2005; Goldring and Goldring, 2010).

Subchondral bone cysts are seen mainly in regions with severe cartilage loss, which appear as fluid filled sacs protruding from the joint. These are perhaps formed as a consequence of synovial fluid flowing into the subchondral bone under high pressure (Landells, 1953; Freund, 1940).

Osteonecrosis is seen at articular surfaces in severe OA, where the subchondral bone is exposed. Loss of articular cartilage results in an increased load and pressure being applied on the subchondral bone, leading to subchondral plate fracture. This can cause vascular occlusion, thereby obstructing blood flow to the subchondral bone which is then weakened and can collapse under normal mechanical stresses (Kiaer *et al.*, 1990).

1.4.3 Synovium

Although OA is not regarded as an inflammatory condition, synovial inflammation (synovitis) is commonly seen in OA patients (Wieland *et al.*, 2005; Aigner *et al.*, 2006a). When the ECM is degraded in OA, the breakdown products including chondroitin sulphate peptides, proteoglycan fragments and type II collagen peptides are infiltrated into the synovial fluid (Aigner *et al.*, 2006a). This can result in synovial hyperplasia, where the normal flat synovium changes into a more villous structure. The abnormal synovium is seen close to areas with severe cartilage loss, and is thought to secrete catabolic molecules such as MMPs, resulting in more ECM breakdown (Wieland *et al.*, 2005; Aigner *et al.*, 2006a).

1.4.4 Joint capsule, meniscus and ligaments

Abnormalities in other tissues of the joint in OA are less well characterised compared to articular cartilage, subchondral bone and synovium, but nonetheless exhibit extensive changes.

The joint capsule undergoes thickening and fibrosis in OA, leading to a shortened capsule. This can result in more mechanical forces being applied on the articular cartilage, which can disrupt the ECM (Aigner *et al.*, 2006a).

In OA, meniscal tears, fibrillations and fissures are frequently observed (Noble and Hamblen, 1975; Englund *et al.*, 2009). In addition, calcification within the meniscus is also seen in late stage OA (Noble and Hamblen, 1975; Sun *et al.*, 2010).

It has been reported that ligaments show thickening and fissuring in OA at the site where they attach to bone.

1.5 Effect on joint homeostasis during the pathogenesis of OA

Joint homeostasis is crucial in maintaining the structure and function of the joint and involves maintaining a careful balance between anabolic and catabolic activities. The

damage caused by continuous mechanical stress and catabolic enzymatic action in cartilage is counteracted by the anabolic activities of articular chondrocytes. In healthy cartilage, the anabolic and catabolic processes are maintained in equilibrium by chondrocytes. In OA, joint homeostasis is disturbed and this balance is tipped towards catabolism, leading to cartilage degradation (Aigner *et al.*, 2006b). The balance between anabolism and catabolism is tightly regulated by a network of anabolic and catabolic factors including cytokines, growth factors, enzymes, transcription factors and other mediators whose expression levels are affected during the progression of OA.

1.5.1 Cytokines

Inflammatory cytokines play a catabolic role during the progression of OA and these include interleukins (IL) and tumour necrosis factor- α (TNF- α). IL-1 β levels are increased during OA and is found in synovial fluid in OA joints (Schlaak *et al.*, 1996). TNF- α acts in synergy with IL-1 β and this leads to an increase in MMP13 levels, which promote the breakdown of the ECM (Saklatvala, 1986; Lefebvre *et al.*, 1990). Chondrocytes synthesise more prostaglandin E and bone morphogenetic protein-2 (BMP2) in response to an increase in catabolic cytokines, which increase type II collagen expression, as an attempt to compensate for the loss of ECM (Goldring *et al.*, 1996; Fukui *et al.*, 2003).

1.5.2 Growth factors

Transforming Growth Factor- β (TGF- β) is a potent regulator of chondrocyte proliferation and differentiation. The effects of TGF- β are mediated through TGF- β type I receptor and TGF- β type II receptor, which upon ligand binding, phosphorylate and activate Smad 2 and Smad 3 (Wrana *et al.*, 1994; Heldin *et al.*, 1997). These form a complex with Smad 4, which then translocates into the nucleus to regulate gene expression of *COL2A1* and *ACAN* (Edwards *et al.*, 1987; Izumi *et al.*, 1992). Therefore, TGF- β can counteract the effects induced by IL-1 β in OA. The expression of both TGF- β receptors and Smad 2 are down regulated in OA, resulting in a reduction in response to this growth factor, leading to a reduction in anabolism in OA chondrocytes (Blaney Davidson *et al.*, 2005).

Bone morphogenetic proteins (BMPs) are members of the TGF- β superfamily and have roles in cell proliferation, differentiation, apoptosis and tissue homeostasis (Hogan, 1996). The most well characterised BMPs in articular cartilage are BMP2, BMP4, BMP7 and GDF5 (also known as BMP14). In OA, both *BMP2* and *GDF5* are upregulated, perhaps as an attempt to repair damaged cartilage (Karlsson *et al.*, 2010; Xu *et al.*, 2012). Exogenous BMP2, BMP7 and GDF5 have been shown to have anabolic effects in chondrocytes including increased proteoglycan synthesis, measured by sulphate incorporation assays (Chubinskaya *et al.*, 2008).

Insulin-like growth factor-1 (IGF1) is another growth factor essential for normal cartilage homeostasis, and has roles in promoting ECM synthesis and inhibiting matrix degradation (Luyten *et al.*, 1988; Trippel *et al.*, 1989). Both IGF1 and its receptor are elevated in OA chondrocytes (Middleton *et al.*, 1996). However, the levels of IGF binding protein-3 is also elevated in OA, which interferes with IGF1 ligand receptor interaction, thereby reducing the ability of chondrocytes to respond to IGF1, despite its high expression in OA (Chevalier and Tyler, 1996; Eviatar *et al.*, 2003).

Fibroblast growth factor-2 (FGF2) is elevated in OA and was initially thought to have anabolic roles in cartilage, due to its effects on increased cell proliferation (Orito *et al.*, 2003; Hiraide *et al.*, 2005; Chen *et al.*, 2006). However, more recent evidence suggests that FGF2 is responsible for the increase of the ratio of type I collagen to type II collagen, producing more fibrous cartilage tissue (Muddasani *et al.*, 2007; Im *et al.*, 2008). It is also reported that FGF2 can counteract the effects mediated by IGF1 and BMP7 and can also induce MMP13 expression (Loeser *et al.*, 2005; Muddasani *et al.*, 2007; Im *et al.*, 2008). FGF18 in contrast has anabolic roles in chondrocytes and promotes ECM biosynthesis (Ellsworth *et al.*, 2002; Moore *et al.*, 2005). FGF18 also inhibits noggin, a BMP antagonist, hence facilitating anabolism in chondrocytes, whereas FGF2 induces its expression (Reinhold *et al.*, 2004; Li *et al.*, 2008).

1.5.3 Enzymes

MMP1 and *MMP13*, whose products are responsible for the breakdown of type II collagen in the cartilage ECM, are upregulated in OA (Karlsson *et al.*, 2010). This is a consequence of the activation of NF- κ B and AP1 pathways by the catabolic cytokines including IL-1 β and TNF- α , which are produced at high levels in OA chondrocytes

(Brenner *et al.*, 1989; Conca *et al.*, 1989). MMP1 and MMP13 cleave the triple helical structure of type II collagen fibrils, making them susceptible for further degradation by MMP9 (Hashimoto *et al.*, 2008).

ADAMTS4 and ADAMTS5 are the major aggrecanases responsible for aggrecan breakdown in OA. ADAMTS4 has been shown to be regulated by IL-1 and TNF- α , whose upregulation in OA can in turn upregulate *ADAMTS4* (Bondeson *et al.*, 2006; Ahmad *et al.*, 2009). Also, *ADAMTS5* gene expression is upregulated in OA, thus leading to increased ECM breakdown in OA (Karlsson *et al.*, 2010).

1.5.4 Transcription factors

Sex determining region-Y box-9 (SOX9) is a transcription factor crucial for mesenchymal chondrogenesis in embryonic development and regulates gene expression of *COL2A1*, which encodes the α -1 chain of type II collagen and *ACAN*, which encodes aggrecan (Sekiya *et al.*, 2000; Stokes *et al.*, 2001). It has been reported that IL-1 β and TNF- α , which are upregulated in OA activate NF- κ B signalling. This leads to the inhibition of SOX9 binding to the *COL2A1* enhancer, to exert their catabolic effects in OA (Murakami *et al.*, 2000; Sitcheran *et al.*, 2003). NF- κ B signalling is also involved in the induction of MMP1, MMP9 and MMP13 expression, which contribute to the breakdown of type II collagen (Yan *et al.*, 2001; Vincenti and Brinckerhoff, 2002). AP1 is another transcription factor involved in cartilage homeostasis and most MMPs contain AP-1 binding sites in their promoters. AP1 is activated by TGF- β , FGF2 and TNF- α , which are upregulated in OA, thereby further increasing levels of collagenases in OA cartilage (Yan and Boyd, 2007).

1.5.5 Other mediators

Nitric oxide (NO) is produced by OA chondrocytes and is an inflammatory catabolic mediator (Abramson, 2008). Mechanical factors and increased levels of IL-1 β and TNF- α in OA chondrocytes lead to the overproduction of inducible nitric oxide synthase (iNOS) (Goldring and Berenbaum, 2004). This results in high levels of NO, which has shown to mediate a range of catabolic effects in chondrocytes including MMP activation, reduction in matrix biosynthesis, chondrocyte apoptosis and activation of the NF- κ B pathway, further leading to cartilage degradation (Taskiran *et al.*, 1994; Häuselmann *et al.*, 1998; Sasaki *et al.*, 1998).

IL-1 β and TNF- α also induce prostaglandin E synthase and cyclo-oxygenase-2 (COX2), which are responsible for the production of prostaglandin E2, an important mediator of inflammation and pain in OA (Thorén and Jakobsson, 2000).

1.6 Risk factors of OA

Several risk factors affect the development and progression of OA including advancing age, sex, obesity and genetic predisposition. Over time, these factors can initiate and promote abnormal biochemical alterations in joints, which may contribute to the characteristic features associated with OA, resulting in pain, disability and poor quality of life.

1.6.1 Age

Age is the major risk factor for OA and estimates show that 60-90% of adults over the age of 65 and over 30% of adults aged between 45 and 64 years are affected with OA, whilst it is rare before the age of 40 (WHO Scientific Group, 2003). Several factors associated with age can induce mechanical stress on the joint cartilage, such as altered gait, changes in proprioception, muscle weakness and changes in body mass. Also, chondrocytes in the articular cartilage, which are responsible for the production and maintenance of the cartilaginous matrix, show an age-related reduction in response to anabolic growth factors and synthesise less extracellular matrix components such as proteoglycans (Martin and Buckwalter, 2002). This suggests that the ability of chondrocytes to maintain and repair the tissue is decreased with age, leading to age-related changes in morphology of the articular cartilage. Furthermore, aged cartilage shows increased expression of pro-apoptotic genes, including *Fas*, *FasL*, *BCL2* and *CASP8*, which may promote apoptosis of chondrocytes (Kim *et al.*, 2000; Allen *et al.*, 2004). This will lower cartilage matrix protein synthesis, such that the chondrocytes lose the ability to repair damaged tissue and this further increases tissue degradation, resulting in the loss of articular cartilage and hence leading to OA.

1.6.2 Sex

Sex is another risk factor correlated with OA, which is supported by the significant increase in the risk for OA prevalence in the knee and hand in females compared to males in a meta-analysis performed by Srikanth *et al.* (2005). The authors also reported a significantly higher incidence of knee and hip OA in females compared to

males, whilst post-menopausal females present with more severe knee OA. Although the cause for this is poorly understood, evidence suggests that this may be an effect of menopause, hence oestrogen deficiency in earlier life may play a role (Wluka *et al.*, 2000). It is reported that articular chondrocytes express oestrogen receptors, which once activated can promote proteoglycan synthesis, supporting the theory that oestrogen deficiency post-menopause can lead to OA in women (Richmond *et al.*, 2000). However, there is as yet no strong evidence for this correlation, as data from clinical trials regarding effects of oestrogen replacement therapy in OA have been conflicting (Nevitt *et al.*, 2001; Hanna *et al.*, 2004). A review of various studies that compared magnetic resonance imaging (MRI) features of OA with sex shows that women have thinner and more reduced volume of knee cartilage compared to men, possibly from early childhood (Maleki-Fischbach and Jordan, 2010), which can account for the higher prevalence of OA in women. However, it is unclear if the rate of cartilage degradation is higher in women than that in men.

1.6.3 Obesity

Obesity is identified as a risk factor for knee OA, as an increase in mechanical forces experienced by this joint type can accelerate the degenerative process (Anderson and Felson, 1988). A positive correlation has been made between high body mass index (BMI) and elevated risk for knee OA (Marks and Allegrante, 2002). Furthermore, a meta-analysis showed that individuals who were obese (BMI above 30) had a 2.96 fold higher risk of developing knee OA and those who were overweight (BMI of 25-30) showed a 2.18 fold higher risk of developing knee OA compared to those with a normal BMI (BMI less than 25; Blagojevic *et al.*, 2010). In addition, most obese patients show varus knee deformities, where the distal part of the leg below the knee is deviated inwards, resulting in an increased strain on the knee, contributing to the rapid degeneration of the joint (Leach *et al.*, 1973). Although this can contribute to OA, it has been shown that an increase in BMI increases risk for knee OA regardless of knee alignment, hence other mechanisms may be involved (Niu *et al.*, 2009). Obesity is also associated with hand OA, further supporting the notion that obesity mediates risk for OA, but not only through mechanical effects (Sayer *et al.*, 2003; Haara *et al.*, 2004). It is hypothesised that obesity may confer an increased risk for OA through metabolic or inflammatory mediators that act on joint tissues (Manek *et al.*, 2003; Garstang and

Stitik, 2006). As opposed to knee OA, hip OA is not strongly correlated with obesity, although it has been reported that high BMI increases risk for hip replacement due to OA in women (Karlson *et al.*, 2003; Sharma *et al.*, 2006).

1.6.4 Genetics

A genetic predisposition is another important risk factor for OA, evidence for which comes from numerous epidemiological studies. Early family studies by Stecher (1941) showed that the risk of developing hand OA was two to three times elevated in mothers and sisters of patients. A link between genetics and OA was also shown in a study by Kellgren *et al.* (1963) where the occurrence of generalised nodal OA was found to be twice as frequent in first degree relatives (parents, siblings and offspring) compared to controls. However, family studies provided limited information as gathering family history from patients was unreliable, and there were difficulties in matching individuals with respect to age, especially since OA is strongly age-related. Also, shared family environment may also contribute to risk for OA, which was difficult to control, thus making it hard to make comparisons between studies (Spector and MacGregor, 2004).

Twin studies are a more robust method to separate the effects of genetic factors and the shared environmental factors as they naturally control for age. Twin studies compare the concordance rates of the trait of interest between monozygotic (MZ) twins, who share 100% of their genes at birth, with dizygotic (DZ) twins, who share on average 50% of their genes. A lower concordance in DZ twins implies the existence of genetic effects on the trait, whilst an incomplete concordance in MZ twins implies the existence of non-genetic, environmental effects on the trait. Heritability, which is the proportion of the causation of the trait that has a genetic basis, can then be determined. The heritability of radiographic OA of the hand and knee in women was estimated to be in the order of 39% to 65%, independent of known environment or demographic confounding factors, in a twin study performed using 130 MZ and 120 DZ female twins aged between 48 to 69 years (Spector *et al.*, 1996). Another twin study performed by the same group estimated the heritability for hip OA in women to be 60% (MacGregor *et al.*, 2000).

Genetic susceptibility in OA is thought to be transmitted in a complex, non-Mendelian manner, as OA is a multifactorial and heterogeneous disease and genetic differences can be seen between sexes, joint sites and disease characteristics (Spector and MacGregor, 2004; Loughlin, 2001; Peach *et al.*, 2005). Therefore, genetics can account for approximately 50% of the variation seen in disease susceptibility at a population level (Spector and MacGregor, 2004).

1.7 Studies to identify alleles implicated in OA

As OA has been shown to be heritable, it is of interest to identify the genes that are responsible for disease susceptibility. Multiple studies have been carried out to determine susceptibility loci associated with OA through candidate gene studies, genome-wide linkage studies and genome-wide association scans.

1.7.1 Candidate gene studies

Candidate gene studies were initially an attractive method to identify OA susceptibility genes, by taking a hypothesis-driven approach. These studies examined a panel of genes that have shown association in a related disease or which encode a protein that plays a vital role in the pathogenesis of a particular disease (Newman and Wallis, 2002). In early OA candidate gene studies, genes that harbour mutations in rare inherited monogenic diseases in which individuals often present symptoms of early onset, severe secondary OA were selected (Loughlin, 2001; Reginato and Olsen, 2002). Examples include chondrodysplasias, often caused by mutations in genes encoding ECM components of cartilage including *COL2A1*, which encodes the $\alpha 1$ chain of type II collagen, *COL9A1*, encoding the $\alpha 1$ chain of type IX collagen, *COL11A2*, encoding the $\alpha 2$ chain of type XI collagen), *COMP*, encoding cartilage oligomeric matrix protein, and *ACAN*, which encodes aggrecan (Olsen, 1995; Reginato and Olsen, 2002; Peach *et al.*, 2005). However, these studies were limited by small sample size and yielded negative or inconclusive data. This may indicate that these genes have not undergone mutational events to predispose individuals to primary OA or even if mutated, the effect of these polymorphisms can only influence a small proportion of OA heritability (Jakkula *et al.*, 2005). A weakness in this approach is that these studies depend on prior knowledge of the target, so only a few genes have been analysed, thus many important genes may have been over-looked.

Other candidate gene studies have looked at genes whose products are involved in pathologic changes in OA bone, such as sclerosis and higher mineral density (Loughlin, 2003; Peach *et al.*, 2005). *VDR*, which encodes the vitamin D receptor, and *ESR1*, which encodes the oestrogen receptor- α , have been assessed as they are shown to be involved in the regulation of bone mass and bone density (Loughlin, 2001; Bandrés *et al.*, 2005). Studies have shown an association between mutations in *VDR* and knee (Keen *et al.*, 1997; Uitterlinden *et al.*, 1997; Uitterlinden *et al.*, 2000), spine (Jones *et al.*, 1998; Videman *et al.*, 1998) and hand OA (Solovieva *et al.*, 2006), although this was not replicated in other studies where hip, knee and hand OA were assessed (Aerssens *et al.*, 1998; Huang *et al.*, 2000; Loughlin *et al.*, 2000). Similar discordant results were observed with *ESR1*, where association to knee OA was reported (Bergink *et al.*, 2003; Jin *et al.*, 2004), however this was not replicated in other knee or hip OA studies (Loughlin *et al.*, 2000; Fytili *et al.*, 2005). These discrepancies can arise from utilising a small sample size, which can produce false positive or false negative signals, as well as variations in study cohorts such as sex, ethnicity, age and joint site analysed (Loughlin, 2001; Solovieva *et al.*, 2006).

Two compelling OA associations have been identified by a Japanese group through candidate gene studies in *ASPN*, which encodes asporin (Kizawa *et al.*, 2005), and in *GDF5* (Miyamoto *et al.*, 2007). The protein products of these two genes are involved in signal transduction during cartilage development (Loughlin, 2005b). *ASPN* was selected as a candidate based on the role of its protein product, which is a member of the family of small leucine-rich proteoglycans (SLRPs), in binding to TGF- β (Kizawa *et al.*, 2005). A variable tandem repeat sequence in *ASPN* showed association to hip and knee OA. A subsequent study by this group identified an association of the single nucleotide polymorphism (SNP) rs143383 in *GDF5* with hip and knee OA in Japanese and Chinese populations (Miyamoto *et al.*, 2007). The same SNP was then shown to be associated with knee OA in European populations (Chapman *et al.*, 2008). This was the first clear example of an OA susceptibility gene affecting different ethnic groups.

1.7.2 Genome-wide linkage studies

As candidate gene studies rely on prior knowledge of the disease process, they are prone to ignoring novel disease pathways (Peach *et al.*, 2005). Genome-wide linkage scans examine affected families for the co-segregation of various markers and defined

OA phenotypes. However, these studies have limitations. For example, due to the late onset of OA, it can be difficult to study the parents of the affected individuals. To overcome this, studies utilise affected sibling pairs instead (ASPs; Loughlin, 2002).

Several OA linkage scans on patients affected by hip, knee or hand OA have been performed in small families of affected relatives collected in the UK, Finland, Iceland and the USA (Loughlin, 2003). These studies have mapped susceptibility loci to chromosomes 2, 4, 6, 7, 11, 16, 19 and the X chromosome (Moskowitz *et al.*, 2007). Although no susceptibility genes have been identified by linkage alone, candidate gene studies within regions that showed linkage have yielded moderately supportive evidence for several OA associated genes. Examples of these include *IL1RN* (interleukin-1 receptor antagonist; Meulenbelt *et al.*, 2004), *MATN3* (matrilin 3; Stefánsson *et al.*, 2003), *FRZB* (frizzled-related protein 3; Loughlin *et al.*, 2004) and *BMP5* (bone morphogenetic protein 5; Southam *et al.*, 2004).

1.7.3 Genome-wide association scans

Linkage scans have yielded susceptibility regions which can contain a large number of genes, making it cumbersome to find causal loci (Loughlin, 2005a). Genome-wide association scans (GWASs) have emerged as an attractive method to identify disease susceptibility loci. This has become possible owing to the completion of the human genome project and the cost-effective high throughput genotyping arrays (Barrett and Cardon, 2006; Pe'er *et al.*, 2006). Also, genomic databases such as HapMap can be utilised to select a number of tag SNPs which is estimated to be 300,000 to 600,000 to cover the entire genome, instead of studying 10 million common SNPs (International HapMap Project, 2013). GWASs are typically performed on large (over 2000 individuals) cohorts of cases and controls who are unrelated to each other and drawn from the same population (Barrett and Cardon, 2006; Chanock *et al.*, 2007). They provide quite narrow, refined genomic intervals to be examined further, compared to linkage scans, hence are higher in resolution. A particular allele, if associated with disease, will be observed more frequently than expected in affected individuals (cases) than in controls.

Although GWASs are able to identify susceptibility loci, they can generate false positives due to multiple testing and population stratification. Therefore, high

resolution studies with broad coverage of the genome, a large sample size and several replication studies are needed to be performed to eliminate false positives and to increase reliability (Reynard and Loughlin, 2013). There have been three GWASs reported in OA that combined these requirements. They are the Rotterdam study, Tokyo study and arcOGEN (arthritis research campaign osteoarthritis genetics) study.

The Rotterdam study identified a locus on chromosome 7q22 that harbours six genes (*PRKAR2B*, *HBP1*, *COG5*, *GPR22*, *DUS4L*, *BCAP29*), which showed association to knee OA in Dutch Caucasians (Kerkhof *et al.*, 2010). None of these genes had been previously implicated in OA, therefore were not obvious OA candidates. The Tokyo study identified a locus that maps to the HLA locus on chromosome 6p, in knee OA in Japanese populations (Nakajima *et al.*, 2010).

The arcOGEN study was conducted in two stages using cases and controls from the UK and tested 550,000 polymorphisms (Reynard and Loughlin, 2013). All cases of OA showed radiographic evidence and over 80% had undergone joint replacement surgery, and had therefore reached a severe clinical end point of OA. The first stage of arcOGEN studied 3177 cases and 4894 controls and identified three association signals, although none reached genome-wide significance of $P \leq 5.0 \times 10^{-8}$ (Panoutsopoulou *et al.*, 2011). These signals mapped to *MICAL3* in hip and/or knee OA, to *C6orf130* in knee OA and to *COL11A1* in hip OA. The second stage of the arcOGEN study employed 7410 cases and 11,009 controls, and identified eight compelling signals, of which five surpassed genome-wide significance (Table 1.1, Zeggini *et al.*, 2012). Of interest, *RUNX2* (chromosome 6p), *PTHLH* (chromosome 12p) and *CHST11* (chromosome 12q) can be regarded as plausible candidates for OA susceptibility due to their roles in cartilage biology. *RUNX2* and *PTHLH* encode runt-related transcription factor-2 and parathyroid hormone-related protein, respectively, and are involved in endochondral ossification (Kronenberg, 2006; Komori, 2010; Wysolmerski, 2012). *CHST11* encodes carbohydrate sulfotransferase-11, which catalyses the transfer of sulphate groups to chondroitin, a constituent of the GAG chains of cartilage proteoglycans (Okuda *et al.*, 2000). The majority of the arcOGEN signals however do not contain obvious OA candidates. Most of the arcOGEN signals emerged after stratification by sex and joint type (Reynard and Loughlin, 2013). For example, the signal on chromosome 6p was associated only in male OA cases whilst several others were associated only in female

OA. Furthermore, some signals were associated only in knee OA (chromosome 3q) and some only in hip OA (chromosomes 6q, 9q, 12p and 12q; Table 1.1). These observations further highlight that OA is a multifactorial disorder and that its genetic predisposition operates in a sex-specific and joint-specific manner.

SNP	Chromosome	Nearest genes	Strata	P-value
rs11177/rs6976	3p	<i>GNL3/GLT8D1</i>	TJR	7.24×10^{-11}
rs12107036	3q	<i>TP63</i>	TKR-female	6.71×10^{-8}
rs10948172	6p	<i>SUPT3H, RUNX2</i>	Male	7.92×10^{-8}
rs9350591	6q	<i>FILIP1</i>	Hip	2.42×10^{-9}
rs4836732	9q	<i>ASTN2</i>	THR-female	6.11×10^{-10}
rs10492367	12p	<i>KLHDC5, PTHLH</i>	Hip	1.48×10^{-8}
rs835487	12q	<i>CHST11</i>	THR	1.64×10^{-8}
rs8044769	16q	<i>FTO</i>	Female	6.85×10^{-8}

Table 1.1: The eight signals from the arcOGEN GWAS.

TJR, Total joint replacement; TKR, total knee replacement; THR, total hip replacement

Adapted from Zeggini *et al.* (2012).

1.8 Measuring functional effects of polymorphisms

Polymorphisms in susceptibility loci can influence the variation in disease susceptibility and the response to therapies. Therefore, it is important to identify and characterise susceptibility loci further, in order to increase the understanding of the underlying mechanisms involved in the development and progression of the disease under investigation.

DNA polymorphisms can give rise to phenotypic differences by altering the coding sequence of a protein coding gene, by interrupting the regulation of gene expression, by causing differential mRNA splicing or by affecting translation. Polymorphisms in regulatory elements that cause gene expression changes account for a majority of phenotypic diversity observed within and among species (Wang and Sadée, 2006).

Gene expression levels are under control by *cis* and *trans* acting regulators. It is believed that an average individual is heterozygous at functional *cis* regulatory sites in more than 40% of all genes (Rockman and Wray, 2002). The effect of *cis* regulatory elements can be context specific, such that they may cause an increase in expression of one allele relative to the other in one tissue type, but can cause repression or may not show any effect in another tissue type (Koch *et al.*, 2006). *Cis* variants regulate target gene expression either by affecting the transcription level of a gene or by influencing the stability of the mRNA.

It is possible to measure the overall expression of a particular gene using quantitative methods such as real time polymerase chain reaction (PCR) and stratify gene expression by the genotype at a polymorphism which has shown association in the disease under investigation. This will detect if a change in the expression of this gene is mediated or marked by the associated variant and can quantify *cis* and *trans* effects acting at this locus. However, this method is subject to generating false negative results due to the natural fluctuation in gene expression observed among individuals.

It has been challenging to quantify effects caused by *cis*-acting factors alone, due to the inability to distinguish these from gene expression variance caused by *trans*-acting factors. As a solution, the relative expression of each allele of a gene of interest can be measured to determine the proportion of *cis* acting regulation that influences gene expression (Yan *et al.*, 2002). This can be carried out by allelic expression imbalance (AEI) studies that measure expression of one allele relative to the other at a heterozygous locus in a transcribed region of a gene. This method assumes that in the absence of *cis*-acting polymorphisms, the level of expression from one allele should equal that of the other in the same tissue type, as both alleles are exposed to the same environmental as well as *trans* acting factors (Wang and Sadée, 2006). On the other hand, if an individual shows AEI, this individual may be heterozygous for a *cis* regulatory polymorphism which affects transcription, mRNA stability, splicing or translational efficiency of the target gene. Such allelic expression imbalances are measured by determining the amount of mRNA molecules relative to the amount of genomic DNA molecules for each allele in the same tissue. Each allele acts as an internal control for the other as it measures allelic variation within an individual, thus

eliminating effects caused by environmental and trans-acting factors, tissue quality and preparation (Wilkins *et al.*, 2007).

Several techniques can be used to detect AEI, including real-time allele-specific PCR or primer extension assays such as Sequenom iPLEX assays. In these methods, the region surrounding the polymorphism is first amplified using genomic and complementary DNA (cDNA) as templates.

The real-time PCR method uses TaqMan probes designed for the two different alleles which are differentially labelled with a fluorescent dye. During the PCR, a different fluorophore will be emitted for each allele, which will allow the differentiation between the two alleles. The increase in emission can be measured for each allele, which will enable the quantification of one allele relative to the other in cDNA and genomic DNA.

Primer extension assays use an extension primer designed to anneal immediately adjacent to the polymorphic locus in the amplified template. The extension reaction mix contains dideoxynucleotide (ddNTP) terminators so that during the extension, the primers are extended by a single base complementary to the allele present. Sequenom iPLEX assays use mass modified ddNTP terminators. The products are run on the Sequenom MassARRAY analyzer which uses MALDI-TOF mass spectrometry, enabling the detection of the mass of the extended primer which determines the sequence amplified. Therefore, the amount of each allele present at the polymorphic site can be quantified. The Sequenom assays can be multiplexed to allow the analysis of up to 40 SNPs (Gabriel *et al.*, 2009). In order to measure AEI using these methods, a ratio is calculated between the amounts of each allele at a locus in cDNA, which is then normalised against that calculated for genomic DNA from the same sample.

1.9 Aims

The overall aim of my thesis is to explore the functional effects of OA susceptibility loci.

1.9.1 Aim 1: Investigation of the effect of exogenous growth factor GDF5 on primary chondrocytes

As noted earlier, a SNP in the 5'UTR of *GDF5* (rs143383, C/T) was reported as being associated with OA in Japanese and Chinese (Miyamoto *et al.*, 2007) and European (Chapman *et al.*, 2008) populations. Functional studies carried out on this SNP showed that there was up to 27% reduced transcription from the T allele relative to the C allele in OA patients heterozygous at this locus (Southam *et al.*, 2007). These findings suggest that a slight reduction in *GDF5* expression increases the risk for OA. My aim was to determine if this deficit could be attenuated by the application of exogenous GDF5 protein. I have assessed what effect exogenous GDF5 will have on primary OA chondrocyte gene expression.

1.9.2 Aim 2: Allelic expression analysis of the osteoarthritis susceptibility locus that maps to MICAL3

The first stage of the arcOGEN study produced evidence of an association of the SNP rs2277831 to primary hip and/or knee OA, with a P-value of 2.3×10^{-5} and an odds ratio of 1.07 for allele G (Panoutsopoulou *et al.*, 2011). rs2277831 is an A/G transition located within an intron of the gene *MICAL3*, which maps to chromosome 22q11.21. The association interval marked by rs2277831 encompasses two additional genes, *BCL2L13* and *BID*. My aim was to explore whether the OA association to rs2277831 is mediated by an influence on *MICAL3*, *BCL2L13* or *BID* expression.

1.9.3 Aim 3: Assessing whether the OA associated locus mapping to chromosome 12q23.3 mediates its effect by influencing the expression of CHST11

The arcOGEN study reported a SNP rs835487 (G/A) on chromosome 12q23.3 as being associated with hip OA, with an odds ratio of 1.13 for allele G and a P-value of 1.64×10^{-8} (Zeggini *et al.*, 2012). The SNP is located within intron 2 of *CHST11*, which encodes carbohydrate sulfotransferase-11. As discussed earlier, this enzyme catalyses the transfer of sulphate groups to chondroitin, to form chondroitin-4 sulphate. This is a major constituent of the GAG chains in the cartilage ECM. Its role in cartilage biology

combined with previous reports that showed an upregulation of *CHST11* in knee and hip OA (Karlsson *et al.*, 2010; Xu *et al.*, 2012), make it an attractive candidate for OA susceptibility. My aim was to study *CHST11* as an OA susceptibility locus by the use of total and allelic expression analyses to determine if the association to rs835487 is mediated by a change in *CHST11* expression.

1.9.4 Aim 4: Search for rare variants in the coding region of CHST11

There are no common coding variants in *CHST11* recorded in online public databases, which are based on population samples. The aim of this chapter was to search for rare penetrant variants that can account for OA susceptibility. I therefore sequenced 192 male and female hip OA patients to look for rare variants in the coding exons of *CHST11*.

1.9.5 Aim 5: The role of CHST11 in chondrocyte differentiation

The critical role of *CHST11* during skeletal development has been demonstrated previously in mice and zebrafish, where knockout mice showed severe chondrodysplasias whilst the knockout zebrafish showed multiple embryonic morphological defects including a ventrally bent trunk and a curled tail (Klüppel *et al.*, 2005; Mizumoto *et al.*, 2009; CL Hammond, personal communication, 18th July 2012). My aim was to study the role of *CHST11* during chondrogenesis by using iliac crest derived mesenchymal stem cells from young donors. *CHST11* mRNA and *CHST11* protein were knocked-down in these cells and the cells were then differentiated into chondrocytes using Transwell culture (Murdoch *et al.*, 2007). Gene expression of a panel of marker genes for various metabolic processes in chondrocytes were analysed in the knocked-down cells compared to control cells. The GAG content and the wet mass were also compared to assess the role of *CHST11* in chondrocyte matrix synthesis.

Chapter 2: Materials and methods

2.1 Tissue collection and grinding

See Appendix 1 for ethics statement. Cartilage, fatpad, meniscus, synovium, osteophyte and cancellous bone were collected from OA patients that had undergone joint replacement surgery. Cartilage tissue from neck-of-femur fracture (NOF) patients was collected as healthy controls. The tissues were removed from the joint on the same day as the surgery using a scalpel blade, washed in Phosphate Buffered Saline (PBS; Lonza, Slough, UK) and stored at -80 °C. Prior to tissue grinding, all surfaces, forceps, grinding vials and balls were cleaned with RNase-Zap (Ambion, Life Technologies, Paisley, UK) and 70% ethanol made up with diethylpyrocarbonate (DEPC)-treated water (Invitrogen, Life Technologies, Paisley, UK). The tissue to be ground was placed on dry ice and transferred to a grinding vial with a grinding ball. The vials were cooled in liquid nitrogen, clamped to a Mixer Mill MM200 (Retsch, Castleford, UK) and oscillated at a frequency of 20 Hz for 90 seconds. The cycles were repeated until the tissue was powderised, cooling the vials in liquid nitrogen between every cycle. The ground tissue was stored at -80 °C for nucleic acid extraction.

2.2 Nucleic acid extraction from ground joint tissue

DNA and RNA were extracted from ground cartilage using E.Z.N.A DNA/RNA isolation kit (VWR International, Lutterworth, UK). The tissue samples were kept on dry ice and 0.25 g of tissue were transferred to eppendorf tubes, four tubes per sample (1 g in total). One tube was to be used for DNA extraction and the remaining three for RNA. GTC lysis buffer was prepared by adding 20 µl of β-mercaptoethanol per 1 ml of buffer and 700 µl of this was added to each sample. The mixture was vortexed thoroughly to homogenise and centrifuged at 11700 rpm for 5 minutes. The supernatant from one of the tubes was transferred to a HiBind DNA column placed in a 2 ml collection tube. The supernatants from the remaining three tubes were transferred to 700 µl of chilled 70% DEPC-treated ethanol and 750 µl of the mix was transferred to RNA columns placed in 2 ml collection tubes. The tubes were centrifuged at 10300 rpm for 1 minute. The flow through from the RNA columns was discarded. The flow through from the DNA column was added to the remaining supernatant/ethanol mix equally. The mix was transferred to the RNA columns, which were centrifuged at 10300 rpm for 1 minute, and the flow through was discarded. To the RNA columns, 500 µl of RNA Wash Buffer I was added

and centrifuged at 11700 rpm for 1 minute, and the flow through was discarded. Next, 500 µl of RNA Wash Buffer II was added to RNA columns and 500 µl of Buffer HB was added to DNA columns. The columns were centrifuged at 11700 rpm for 1 minute and the flow through was discarded. A further 500 µl of RNA Wash Buffer II was added to RNA columns and 700 µl of DNA Wash Buffer was added to the DNA column. The tubes were centrifuged at 11700 rpm for 1 minute. The collection tubes were discarded and were replaced with fresh collection tubes. The tubes were centrifuged at 13000 rpm for 2 minutes to dry the columns. The columns were transferred to fresh 1.5 ml tubes and 50 µl of DEPC water was added to RNA columns and 50 µl of Elution Buffer was added to the DNA column. The tubes were centrifuged at 11700 rpm for 1 minute, and the elution was repeated. The eluted RNAs were combined and labelled. The RNA columns were transferred to fresh 1.5 ml tubes and were washed twice with 50 µl of DEPC water by centrifuging at 11700 rpm for 1 minute to obtain any remaining DNA. This was combined with the eluate from the DNA column.

One microlitre of the sample was used to quantify the nucleic acid using a NanoDrop 1000 spectrophotometer. Three microlitres of RNaseOUT RNase inhibitor (Invitrogen) were added to RNA samples which were then centrifuged in a DNA 120 SpeedVac system (Thermo Scientific, Epsom, UK) along with the DNA samples. The DNA and RNA pellets were resuspended in DEPC water and made to 50 ng/ml and 250 ng/ml respectively. DNA samples were stored at -20 °C and RNA samples at -80 °C until further use.

2.3 Complementary DNA (cDNA) synthesis

RNA extracted from cells and patient tissue was reverse transcribed to synthesise cDNA. RNase-free pipettes and tubes were used throughout to ensure that the RNA did not degrade. To remove genomic DNA (gDNA) contamination, 4 µl of 250 ng/µl RNA was incubated at 37 °C for 30 minutes with 1 µl of Turbo DNase (2 units; Ambion), 1 µl of DNase buffer (10X; Ambion) and 4 µl of DEPC-treated water (Invitrogen). This was then heated to 75 °C for 10 minutes with 1.8 µl of 100 mM Ethylenediaminetetraacetic acid (EDTA; Sigma-Aldrich, Poole, UK) to inactivate the DNase.

The reverse transcription (RT) of RNA was carried out using the SuperScript First-Strand Synthesis System for RT-PCR (Invitrogen). The DNase treated RNA was

incubated at 65 °C for 5 minutes with 1 µl of random primers (50 ng/µl), 1 µl of 10 mM dNTP mix (10 mM each of dATP, dCTP, dGTP and dTTP) and 2 µl of DEPC water. A DEPC water blank with no RNA was also used as a negative control. The reaction mix was then left on ice for at least 1 minute followed by incubation at 25 °C for 1 minute with 4 µl of 5X Reaction buffer (250 mM Tris-HCL pH 8.3, 375 mM KCl, 15 mM MgCl₂), 4 µl of MgCl₂ (25 mM), 2 µl of DTT (0.1 mM) and 1 µl of RNaseOUT RNase inhibitor (40 U/µl; Invitrogen). SuperScript II RT enzyme (200 U/µl; Invitrogen) was diluted four times using DEPC water and 1 µl (50 U) of this was added to the reaction and mixed by pipetting. The RT reaction was carried out by incubating at 25 °C for 10 minutes, 42 °C for 50 minutes and 70 °C for 15 minutes. Finally, 1 µl of RNaseH (5 U/µl; New England Biolabs, Hitchin, UK) was added and the reaction mixture was incubated at 37 °C for 20 minutes.

The synthesised cDNA and the DEPC water blank were PCR amplified using primers that amplify cDNA and gDNA producing different sized PCR products, to distinguish cDNA products from any products resulting from residual gDNA contamination (forward primer 5'TCGAAGAGTGAACCAGCCTT3' and reverse primer 5'GAAGGCCAGGAATTGCACCATCC3' which target *HBP1*). The PCR products were electrophoresed through a 2% (weight/volume) agarose gel containing 1 µl of ethidium bromide (10 mg/ml) per 100 ml of agarose and were visualised under UV light using a G:BOX gel doc system (Syngene, Cambridge, UK). Only cDNA samples that produced the appropriate bands specific for cDNA (152 bp in size), and not for gDNA or the DEPC water blank, were taken forward for subsequent analysis. These cDNA samples were stored at -20°C until further use.

2.4 Polymerase Chain Reaction (PCR)

Genomic DNA and cDNA from cell lines and patient tissues were amplified in a 15 µl reaction using 1 µl of template DNA (50ng/µl) or 0.5 µl of cDNA synthesised from 1 µg of RNA. The PCR was first optimised using different MgCl₂ concentrations (ranged between 1 and 3 mM) and annealing temperatures (ranged between 55 °C and 70 °C). The reaction contained 0.075 µl of 100 µM forward and reverse primers (Sigma), 0.375 µl of 10 mM dNTPs (Bioline, London, UK), 1.5 µl of 10X PCR buffer (500 mM KCl, 100 mM Tris-HCl pH 8.3; Applied Biosystems, Life Technologies, Paisley, UK), 0.6 -1.8 µl of 25 mM MgCl₂ (final concentration of 1-3 mM; Applied Biosystems), 0.08 µl of AmpliTaq

Gold DNA polymerase (5 U/ μ l, Applied Biosystems) and was made up to 15 μ l with water (Sigma). The PCR cycle conditions were 94 °C for 14 minutes, followed by 35 cycles of 94 °C for 30 seconds, 55 °C to 70 °C for 30 seconds and 72 °C for 30 seconds and 72 °C for 5 minutes. Five microlitres of PCR product mixed with loading dye was electrophoresed through a 2% agarose gel containing ethidium bromide and was visualised under UV light to ensure the PCR amplification was successful.

2.5 SW1353 cell culture

Cell culture was carried out under sterile conditions at all times. A cryovial containing one million SW1353 human chondrosarcoma cells was removed from liquid nitrogen storage and thawed rapidly for 30 seconds in a 37 °C water bath. The cells in the vial were diluted in 1 ml of pre-warmed Dulbecco's Modified Eagle Medium: Nutrient Mixture F-12 (DMEM / F-12; Gibco, Life Technologies, Paisley, UK) supplemented with 10% FBS (Gibco), 2 mM glutamine (Sigma), 100 U/ml penicillin and 100 μ g/ml streptomycin mix (Sigma). The cells were then resuspended in 10 ml of complete media and transferred to a 75 cm² cell culture flask (VWR) and placed in a cell culture incubator maintained at 37 °C with 0.5% CO₂. The media was changed 24 hours after resurrection and the cells were passaged 1 in 3 when they reached 80% confluence. This was achieved by removing the media, washing cells with PBS and incubating the flask containing the cells with 1 ml of 0.05% trypsin (Gibco) at 37 °C for 5 minutes. The cells were resuspended in 4 ml of complete media to inactivate the trypsin and pelleted at 1100 rpm for 5 minutes. The media was removed and the cell pellet was resuspended in 30 ml of complete media and 10 ml was transferred to a fresh 75 cm² cell culture flask.

2.6 Bacterial cell transformation with Smad 1/5/8 reporter vector

The experiments were carried out under sterile conditions. Smad 1/5/8 binding elements were cloned to a pGL3 basic vector (Promega) which was a kind gift from Dr. Mark Birch. One vial of chemically competent MACH bacterial cells (Invitrogen, cat no. C8620-03) was removed from -80 °C and was allowed to defrost on ice. Two microlitres of vector DNA was added to the cells and the vial was left on ice for 20 minutes. The cells were heat shocked at 42 °C for 30 seconds and placed immediately on ice for 2 minutes. The vial was incubated at 37 °C at 200 rpm for one hour with 200 μ l of Super Optimal broth with Catobolite repression (S.O.C) medium (Invitrogen Cat no. 15544-

034). Eighty microlitres of cells were spread on Lysogeny Broth (LB) agar (Sigma) plates containing Ampicillin (Sigma) using a sterile glass spreader. The plates were incubated at 37 °C overnight to allow colonies to grow. One positive colony of cells was picked with a sterile autoclaved filter tip and the tip was ejected into 3 ml of LB broth containing 3 µl of Ampicillin in a 15 ml tube. The tube was incubated at 37 °C at 200 rpm overnight. Two hundred microlitres of bacterial culture was mixed with 200 µl of glycerol and stored at -80 °C.

2.7 Plasmid DNA purification using MiniPrep

QIAGEN Plasmid Mini Kit (QIAGEN, Crawley, UK) was used to purify plasmid DNA. Briefly, 1.5 ml of overnight bacterial culture was centrifuged at 7500 rpm for 3 minutes to pellet the bacteria. LB supernatant was removed and the pellet was resuspended in 100 µl of Buffer P1+RNase A. Two hundred microlitres of Buffer P2 was added to the tube and inverted several times and the cells were allowed to lyse for 2 minutes. The lysate was mixed with 150 µl of Buffer P3 and centrifuged at 13000 rpm for 5 minutes. The supernatant was then transferred to a fresh tube and centrifuged at 13000 rpm for 2 minutes. This supernatant was transferred to a fresh tube containing 1 ml of 100% ethanol, and stored at -80 °C for 15 minutes. The tube was centrifuged at 13000 rpm for 5 minutes to pellet the DNA. The supernatant was removed and the DNA pellet was allowed to air dry for 15 minutes and resuspended in 40 µl of DEPC-treated water (Invitrogen) and stored at -20 °C.

2.8 Plasmid DNA purification using MaxiPrep

QIAGEN plasmid maxi kit was used to purify DNA. Ten microlitres of the glycerol stock of a bacterial culture was incubated in 250 ml of LB containing 250 µl of Ampicillin at 37 °C at 200 rpm for 4 hours. The cultures were centrifuged at 6000 x *g* for 15 minutes at 4 °C. The supernatant was removed and the bacterial pellet was resuspended first in 10 ml of Buffer P1, then in 10 ml of Buffer P2 and incubated at room temperature for 5 minutes to allow the cells to lyse. The lysate was mixed with 10 ml of chilled Buffer P3 and incubated on ice for 20 minutes. The lysate was centrifuged at 4 °C at 20,000 x *g* for 30 minutes. The supernatant containing plasmid DNA was centrifuged at 4 °C at 20,000 x *g* for 15 minutes. A QIAGEN-tip 500 was equilibrated by applying 10 ml of Buffer QBT and the column was allowed to empty by gravity flow. The supernatant was applied to the QIAGEN-tip and was allowed to enter the resin by gravity flow. The

QIAGEN-tip was washed with 30 ml of Buffer QC. The DNA was eluted with 15 ml of Buffer QF. The DNA was precipitated by centrifugation with 10.5 ml of isopropanol at 4 °C at 15,000 x g for 30 minutes. The supernatant was removed and the pellet was air dried for 10 minutes and resuspended in 500 µl of water (Sigma) and transferred to a 2 ml screw cap tube. The DNA was washed with 1.25 ml of 100% ethanol and centrifuged for 10 minutes at full speed. The supernatant was removed and the pellet was air dried for 10 minutes. The DNA was resuspended in 300 µl of water and stored at -20 °C.

2.9 Transfection of SW1353 cells with Smad 1/5/8 luciferase reporter vector

SW1353 cells were seeded at 17, 500 cells/well in 48-well cell culture plates (VWR) in 300 µl of media containing 10% FBS. The cells were cultured to 80% confluence, which took 48 hours. Cells were co-transfected with 15 ng of *Renilla* vector DNA (Promega, Southampton, UK) as an internal control and 500 ng of basic pGL3-Smad 1/5/8 vector DNA or basic pGL3 empty vector DNA (Promega) using ExGen 500 *in vitro* transfection reagent (Fermentas, Thermo Scientific, Epsom, UK). A master mix was prepared with 25.35 µl of 0.9% NaCl, 2.5 µl of 200 ng/µl DNA and 0.5 µl of 30 ng/µl *Renilla* DNA. The mix was vortexed briefly and 1.65 µl of ExGen 500 was added and vortexed for 10 seconds. The mix was incubated at room temperature for 10 minutes. The media was aspirated from the wells and 30 µl of the DNA and ExGen 500 mix was added to each well. The wells were filled with 270 µl of complete media and the cells were incubated at 37 °C for 24 hours.

2.10 Cartilage digestion and chondrocyte culture

Articular cartilage was obtained from knee or hip OA patients and neck-of-femur fracture patients after their surgery. The cartilage was removed from the joint using a scalpel and then cut finely. The cartilage was digested by incubating with 1mg/ml hyaluronidase (type I-S from bovine testes; Sigma) in PBS at 37 °C for 15 minutes, then with 2.5 mg/ml trypsin (type III, from porcine pancreas; Sigma) in PBS at 37 °C for 30 minutes. The supernatant was removed and the cartilage was washed with complete DMEM (Gibco) supplemented with 10% FBS (Gibco), 2 mM glutamine (Sigma), 100 U/ml penicillin, 100 µg/ml streptomycin (Sigma) and 50 U/ml nystatin (Sigma) to inactivate the trypsin. The cartilage was then incubated with 2.5 mg/ml bacterial collagenase (type I from *Clostridium histolyticum*; Sigma) in complete DMEM at 35 °C overnight. The supernatant was removed and centrifuged at 1100 rpm for 10 minutes

to collect the cells. The cell pellet was washed with PBS and resuspended in complete DMEM culture media. A cell count was obtained using a haemocytometer.

2.11 Stimulation of cells with exogenous growth factors (GDF5, TGF- β 1, IL-1 α and OSM)

2.11.1 Monolayer culture with exogenous growth factors post transfection

Twenty four hours after transfection, the media was aspirated off and the cells were washed with PBS. The cells were incubated in 150 μ l of serum-free media at 37 °C overnight. The cells were stimulated with four different recombinant GDF5 proteins (mouse GDF5, human wild type GDF5 and two variants, A and B) at 10 ng/ml, 30 ng/ml, 100 ng/ml and 300 ng/ml. Recombinant mouse GDF5 protein (R&D Systems, Abingdon, UK) was diluted serially from a stock concentration of 150 μ g/ml and recombinant human GDF5 and variants A and B (Biopharm GmbH, Heidelberg, Germany) from a stock concentration of 1000 μ g/ml. Recombinant human TGF- β 1 (5 ng/ml; R&D Systems) and BMP2 (100ng/ml; R&D Systems) were also used as positive controls. The proteins were diluted in 150 μ l of serum-free media at double the concentration required and added to 150 μ l of media already in the wells to give the correct final concentration. The experiment was performed in four replicates. The plates were incubated at 37 °C and lysed at 6 hours, 12 hours, 24 hours and 48 hours post stimulation.

2.11.2 Monolayer culture for western blot analysis

Chondrocytes from two OA patients were seeded at 350,000 cells/well in four 6-well cell culture plates (VWR) in 2 ml of serum positive DMEM culture media. Cells from each plate were isolated at four different time points after stimulation (15 minutes, 30 minutes, 1 hour and 2 hours). The cells were cultured at 37 °C until 80% confluent, which took 10-12 days. Chondrocytes were replenished with fresh complete media after three days when the cells had adhered to the bottom of the wells and again every two days.

The cells were then serum-starved by removing the media from the wells, washing the cells with PBS and adding 1 ml of serum-free DMEM culture media (supplemented with 2 mM glutamine, 100 U/ml penicillin, 100 μ g/ml streptomycin and 50 U/ml nyastatin). The plates were incubated at 37 °C overnight.

The cells were stimulated with GDF5 protein at 100 ng/ml in 2 ml of serum free media. At appropriate time points, the cells were lysed for protein extraction.

2.11.3 Monolayer culture for gene expression analysis

Chondrocytes extracted from a total of 20 OA patients were seeded at 10,000 cells/well in four 96-well cell culture plates (VWR). The volume in each well was made to 200 μ l with serum positive complete DMEM culture media. Four plates were prepared to enable the cells to be isolated at four different time points; 6 hours, 12 hours, 24 hours and 48 hours. The cells were cultured at 37 °C with 0.5% CO₂ until 80% confluent, which took 10 to 12 days. The chondrocyte medium was changed after three days when the cells had adhered to the bottom of the wells and again every two days.

The culture media was removed from the wells, the cells were washed with PBS and cultured in 100 μ l of serum-free DMEM culture media at 37 °C overnight.

Six wells in 6, 12, 24 and 48 hour plates were cultured with 100 ng/ml GDF5 protein by preparing a solution of 200 ng/ml of GDF5 with serum-free DMEM media and adding 100 μ l of this to the 100 μ l of serum-free media already in the wells. The untreated control wells (6 wells in each plate) received 100 μ l of serum-free media instead of GDF5.

Three wells in the 24 hour plate were treated with IL-1 α (0.05 ng/ml) and recombinant oncostatin M (OSM) (10 ng/ml) as positive controls for the assay. IL-1 α was a gift from Dr Keith Ray (GlaxoSmithKline, Stevenage, UK) and recombinant OSM was a gift from Dr Amit Patel (Newcastle University, UK). Six wells in the 48 hour plate were treated with recombinant human TGF- β 1 (5 ng/ml; R&D Systems) as positive controls.

The plates were incubated at 37 °C. At appropriate time points, the cells were lysed for RNA extraction.

2.12 Luciferase activity reading

The dual-Luciferase Reporter assay system (Promega) was used to measure luciferase activity in the transfected cells. The media was aspirated off and the cells were washed in PBS. At each time point, 65 μ l of 1X Passive Lysis Buffer (PLB; Promega) was added

to each well. The plates were incubated at room temperature for 20 minutes on a rocker, and stored at -20 °C overnight.

The plates were defrosted and 20 µl of lysate was transferred to a luminometer plate. The plate was placed in a Microumat Plus luminometer (Berthold Technologies, Bad Wildbad, Germany) and 50 µl of Luciferase Assay Reagent II (LAR II; Promega) was added to each well and firefly luciferase activity was measured on the instrument. Next, 50 µl of Stop and Glo Reagent (Promega) was added to each well and *Renilla* luciferase activity was measured as an internal control, which served as the baseline response. The firefly luciferase reading was normalised to the *Renilla* luciferase reading, by dividing the former by the latter, to account for differences in cell viability and transfection efficiency.

2.13 Protein extraction

At specific time points, media was removed from 6-well plates and the cells were washed with PBS. One millilitre of fresh PBS was added to the cells on ice and a cell scraper was used to lift the cells off the wells. The cells in PBS were transferred to a 1.5 ml eppendorf tube and centrifuged at 4 °C, at 13000 rpm for 5 minutes to obtain a cell pellet. The supernatant was removed and the cells were resuspended in 30 µl of protein lysis buffer (50 mM Tris, 10% v/v glycerol, 50 mM NaF, 1 mM EGTA, 1 mM EDTA, 10 mM glycerol phosphate, 1% v/v Triton X-100, 1x complete inhibitor cocktail, 1 µM microcystin-LR and 1mM Na₃VO₄) and left on ice for 20 minutes. The tubes were centrifuged at 13000 rpm for 10 minutes at 4 °C. The supernatant containing whole cell protein was transferred to a fresh 1.5 ml eppendorf and was stored at -80 °C until further use.

2.14 Protein quantification using Bradford assay

To enable equal loading in western blot gels, the amount of whole cell protein was quantified. A protein standard curve was made using Bovine Serum Albumin (BSA; Thermo Scientific). A stock concentration of 2 mg/ml was diluted with protein lysis buffer to achieve concentrations ranging from 0 to 1.5 mg/ml BSA as shown in Table 2.1.

Required concentration for standard curve (mg/ml)	BSA (2 mg/ml) in μ l	Lysis buffer (μ l)
0	0	50.0
0.1	2.5	47.5
0.25	6.25	43.75
0.5	12.5	37.5
0.75	18.75	31.25
1.0	25	25.0
1.25	31.25	18.75
1.5	37.5	12.5

Table 2.1: BSA standard curve for protein quantification

The proteins to be measured were diluted 1 in 10 using protein lysis buffer. Twenty microlitres of samples were loaded onto a 96-well microtiter plate in duplicate. Three hundred microlitres of Bradford Ultra (Expedeon, Harsdon, UK) was added to samples and the absorbance at 595 nm was measured using a microplate reader (Tecan, Reading, UK). The absorbance values were used to plot a BSA standard curve, which was used to then calculate the concentration of the test samples.

2.15 Western blot

2.15.1 Gel preparation

A separating gel and a stacking gel were made up fresh for each experiment. First, the glass plates (Bio-Rad Laboratories, Hemel Hempstead, UK) were cleaned with 100% ethanol and were assembled on a glass holder. A 12% separating gel was made as follows:

- 3.6 ml of 40% bis-acrylamide (NBS biologicals, Huntigdon, UK)
- 3 ml of lower buffer (1.5 M Tris, 0.4% w/v SDS; Sigma), pH 8.8
- 5.4 ml of distilled water
- 60 μ l of 10% ammonium persulphate (Sigma)
- 20 μ l of N, N, N', N'-tetramethylethylenediamine (TEMED; Sigma)

Six millilitres of separating gel were pipetted through the glass plates and 1 ml of isopropanol was added to the top to avoid evaporation. The gel was allowed to set for

half an hour. Once the gel was set, the isopropanol was poured off and a 4.5% stacking gel was made up as follows:

- 1.35 ml of 40% bis-acrylamide
- 3 ml of upper buffer (0.5 M Tris, 0.4% w/v SDS), pH 6.8
- 7.65 ml of distilled water
- 60 µl of 10% ammonium persulphate
- 20 µl TEMED

Three millilitres of stacking gel was pipetted through the glass plates on to the top of the separating gel, and a comb was applied. The gel was allowed to set for 15 minutes, the comb was removed and the wells were washed with distilled water. The glass plates containing the gel in between were removed from the holder and were assembled in a gel tank (Bio-Rad). Ten times running buffer (5.86 g glycine, 20 g of SDS, 60.6 g of Tris base in 2 l of water, pH 8) was diluted in distilled water to make up 1X running buffer, which was poured into the gel tank ensuring the glass plates were fully covered.

2.15.2 Sample preparation

For western blot analysis of anti-phospho Smad 1/5/8 antibody, 10 µg of sample was mixed with 4 µl of 5X Laemmli sample buffer (0.1M Tris-HCL, 0.35M SDS, 20% (v/v) glycerol, 0.01% (v/v) bromophenol blue, 5% (v/v) β-mercaptoethanol) and made up to 20 µl with water. Thirty micrograms of protein in 6 µl of 5X Laemmli sample buffer was made up to 30 µl with water for western blot analysis of anti-CHST11 antibody. The samples were boiled at 95 °C for 5 minutes to denature the proteins.

2.15.3 Running the gel

The samples were loaded onto the gel and 4 µl of pre-stained page ruler ladder (Fermentas) was loaded at the end of the gel, which was run at 100 V.

2.15.4 Transfer of proteins to PVDF membrane

Four pieces of blotting paper (10x7 cm) were soaked in transfer buffer (5.86 g of glycine, 0.65 g SDS, 11.62 g Tris in 400 ml of 100% methanol) for 5 minutes. Whatman Westran Polyvinylidene Fluoride (PVDF; GE Healthcare, Amersham, UK) membrane (9x6 cm) was soaked in 100% methanol for 3 minutes. Once the gel had finished

running, the stacking gel was removed and the separating gel was soaked in transfer buffer for 3 minutes. A complex was assembled on a semi-dry transfer machine with two pieces of blotting paper, the PVDF membrane, the gel, followed by two more pieces of blotting paper. Air bubbles were removed with a roller. The proteins were transferred at 100 mA for 1 hour.

2.15.5 Blocking

Once the transfer was complete, the membrane was blocked in 5% milk, made up with 1 g of dried milk powder (Marvel) in 20 ml of Tris Buffered Saline/Tween-20 (TBS/T; 12.1 g of Tris, 90 g of NaCl and 10 ml of 10X Tween-20 in 1 l of distilled water, pH 7.4) for 30 minutes (for anti-pSmad 1/5/8 and anti- β -actin antibodies) or in 5% BSA for 1 hour (for anti-CHST11 antibody).

2.15.6 Detection

Anti-phospho-Smad1 (Ser463/465)/ Smad5 (Ser463/465)/ Smad8 (Ser426/428; rabbit polyclonal; Cell Signalling, cat no. 9511) and anti-CHST11 (mouse monoclonal; Abcam, cat no. ab57225) antibodies were used at 1 in 2000 dilution in 5% BSA and 0.02% sodium azide. Anti- β -actin (Sigma, cat no. A5316) antibody was used at 1 in 10000 dilution in 5% milk and was used as a loading control. The membrane was incubated with the primary antibody at 4 °C overnight on a rocker.

The membrane was then washed with TBS/T for 20 minutes on a rocker, changing the buffer every 5 minutes. The membrane was incubated for 1 hour at room temperature on a rocker with the corresponding secondary antibody. Either polyclonal goat anti-rabbit IgG (0.25 g/l; Dako, Ely, UK) or polyclonal goat anti-mouse antibody (1 g/l; Dako) were used at 1 in 2000 or 1 in 10000 dilution respectively in 5% milk. Both antibodies were linked to horseradish peroxidase (HRP). The membranes were washed with TBS/T for 30 minutes.

Enhanced chemiluminescent (ECL; GE Healthcare, Amersham, UK) reagent, which acts as a substrate for HRP, was used for visualisation of the proteins using a G: BOX gel doc system (Syngene). ECL was used for membranes incubated with anti- β -actin and ECL advanced was used for membranes incubated with anti-pSmad 1/5/8 and anti-CHST11 due to the low abundance of these proteins. The membranes were exposed 5 times at 20 second intervals to obtain 5 digital images.

2.15.7 Stripping membrane

After the use of anti-CHST11 antibody, the membrane had to be stripped before incubation with anti- β -actin, since both antibodies were raised in mouse. The membrane was incubated in mild stripping buffer (15 g of glycine, 1 g of SDS, 10 ml of Tween-20 in 1 l of distilled water, pH 2.2) at room temperature for 40 minutes. The buffer was replaced after 20 minutes. The membrane was incubated with PBS for 20 minutes and then with TBS/T for 10 minutes at room temperature. The membrane was blocked with 5% milk for 30 minutes.

2.16 Cell lysis and reverse transcription of cell lysates

At appropriate time points, the media was removed from the cells in 96-well plates and the cells were washed with PBS. Thirty microlitres of Cells-to-cDNA II Cell Lysis Buffer (Ambion) was added to each well on ice and the suspension was transferred to a fresh 96-well PCR plate. The plates were heated to 75 °C for 15 minutes. The plates were then stored at -80 °C until all time points were reached.

One microlitre of RNase free DNase I (0.1 U; Qiagen) was added to each well and incubated at 37 °C for 15 minutes and 75 °C for 5 minutes. Eight microlitres of this mix was transferred to a fresh microtitre plate and incubated at 70 °C for 5 minutes with 1 μ l of random primers (0.2 μ g/ μ l; Invitrogen) and 3 μ l of 10 mM dNTP mix (2.5 mM each of dATP, dCTP, dGTP and dTTP; Invitrogen). This mix was then subjected to reverse transcription by adding 4 μ l of 5X RT buffer (Invitrogen), 0.5 μ l of MMLV reverse transcriptase (200 U/ μ l; Invitrogen), 2 μ l of DTT (0.1 M; Invitrogen) and 1.5 μ l of water. The cycle conditions were 37 °C for 50 minutes and 75 °C for 15 minutes. Finally, 30 μ l of water was added to the wells to give a final volume of 50 μ l in each well. The plates were stored at -20 °C until further use.

2.17 Gene expression analysis using real time quantitative PCR

The TaqMan primers and probes listed in Table 2.2 were used to analyse gene expression changes in a panel of selected genes. Some TaqMan assays used commercially available primer-probe mixes (IDT, Glasgow, UK) or a combination of PCR primers (Sigma) and custom designed probes (IDT). The gene expression was measured relative to the housekeeping genes *GAPDH*, *HPRT1* and *18S*.

Gene	Forward primer (5'-3')	Reverse primer (5'-3')	Probe (5'-3')
GAPDH	ACATCGCTCAGACACCATG	TGTAGTTGAGGTCAATGAAGGG	AAGGTCGGAGTCAACGGATTTGGTC
HPRT1	TGCTGAGGATTTGGAAAGGG	ACAGAGGGCTACAATGTGATG	AGGACTGAACGTCTTGCTCGAGATG
18s	CGAATGGCTCATTAATCAGTTATGG	TATTAGCTCTAGAATTACCACAGTTATCC	TCCTTTGGTCGCTCGCTCCTCTCCC
BCL2L13	AGGTATGTCACGCCAAACTG	GGAATGTACTGAGGAGACCAC	TCGTAGCAAACCAGAGGCACCA
BID	ATTAACCAGAACCTACGCACC	TGACCACATCGAGCTTTAGC	CAGAAATGGGATGGACTGAACGGACA
MICAL3	GAACAAAGTGAAGTACATGGCG	TGGCAGAAGTAGCATGTGTC	ATCGGCATACGGAGACAGGGC
BMPR-II	GGCTGACTGGAAATAGACTGG	CACAGTCCCTCAAGTTCACAG	CCTCGCTTATGGCTGCATTATCTTCCTC
BMPR-IA	ACAAAGTTCTGGTAGTGGGTC	CATCCATACTTCTCCATATCGGC	ATTCAGATGGTCCGGCAAGTTGGT
BMPR-IB	CTGCACAGAAAGGAACGAATG	AGGACCAAGAGCAAACACTACAG	TGGAGGCAGTGTAGGGTGTAGGT
MMP13	AAATTATGGAGGAGATGCCATT	TCCTTGGAGTGGTCAAGACCTAA	CTACAACCTGTTTCTTGTGCTGCGCATGA
MMP1	AAGATGAAAGGTGGACCAACAATT	CCAAGAGAATGGCCGAGTTC	CAGAGAGTACAACCTTACATCGTGTGCGGCTC
TIMP1	TTCTGCAATTCCGACCTCG	TCATAACGCTGGTATAAGGTGG	TTGACTTCTGGTGTCCCCACGAAC
COL2A1	ACCTTCATGGCGTCCAAG	AACCAGATTGAGAGCATCCG	AGACCTGAAACTCTGCCACCCTG
SOX9	CTGGTACTTGTAATCCGGGTG	ACTTGCACAACGCCGAG	TCTGGAGACTTCTGAACGAGAGCGA
ACAN	TGTGGGACTGAAGTTCTTGG	AGCGAGTTGTCATGGTCTG	CTGGGTTTTCTGACTCTGAGGGT
CHST11	TGCTTGGGATCCTTTATCCTG	GCTGGATTGGGTTGTAGAGTTC	AATCCCTTTGGTGTGGACATCTGCT
COL10A1	CAAGGCACCATCTCCAGG	TGGGCATTTGGTATCGTTCAG	ACTCCCAGCACGCAGAATCCAT
BGLAP	CAGCGAGGTAGTGAAGAGAC	TGAAAGCCGATGTGGTCAG	TCCCAGCCATTGATACAGGTAGCG
COL1A1	CCCCTGGAAAGAATGGAGATG	TCCAAACCACTGAAACCTCTG	TTCCGGGCA ATCCTCGAGCA
ADAMTS4	CTGGGTATGGCTGATGTGG	TGGCTTGGAGTTGTCATGG	TTCACTGCTGCTCATGAACTGGGT
ADAMTS5	CAAGTGCGGAGTATGTGGAG	GTCTTTGGCTTTGAACTGTCTG	TTTATGTGGGTTGCCCTTCAGGA

<i>IHH</i>	ATGAAGGCAAGATCGCTCG	GATAGCCAGCGAGTTCAGG	TCAAGGACGAGGAGAACACAGGC
<i>RUNX2</i>	AATGGTTAATCTCCGCAGGTC	TGTTTGATGCCATAGTCCCTC	CTGTTGGTCTCGGTGGCTGGTAG

Table 2.2: Primer and probe sequences for TaqMan assays used for real time quantitative PCR.

Two and a half microlitres of the reverse transcribed lysate or cDNA corresponding to 6.25 ng of RNA were mixed with 7.5 µl of assay master mix in wells of a 96 well optical realtime-PCR plate. The reaction components for each assay are shown in Table 2.3. The reactions were then run on either an ABI PRISM 7900HT Standard or Fast Real Time PCR System, under the following cycle conditions: 50 °C for 2 minutes, 95 °C for 10 minutes and 40 cycles of 95 °C for 15 seconds and 60 °C for 1 minute for a standard run or 95 °C for 20 seconds and 40 cycles of 95 °C for 1 second and 60 °C for 20 seconds for a fast run.

18S, MMP1 and MMP13		Assays with primer-probe mix	
TGE	5 µl	TGE/TFU	5 µl
Forward primer	0.2 µl	Primer probe mix	1 µl
Reverse primer	0.2 µl	Water	1.5 µl
Probe	0.4 µl		
Water	2 µl		

Table 2.3: Reaction mix for TaqMan assays. TGE: TaqMan Gene Expression Master Mix (Applied Biosystems), TFU: TaqMan Fast Universal PCR Master Mix (Applied Biosystems)

The relative expression for each gene was analysed using the comparative cycle threshold (Ct) method using SDS 2.3 software (Applied Biosystems).

Ct values for each target gene were normalised to the mean Ct value of the reference genes. Normalised Ct values were calculated using the following formula:

$$\text{Normalised Ct} = 2^{-(\text{target assay Ct} - \text{reference assay Ct})}$$

2.18 Qualitative gene expression analysis

Complimentary DNA synthesised from joint tissue RNA were assessed for gene expression using primers shown in Table 2.4 and Table 2.5. The PCR products were electrophoresed through a 2% agarose gel and visualised following ethidium bromide staining on a gel doc system.

Gene	Forward primer (5'-3')	Reverse primer (5'-3')
<i>BCL2L13</i>	GGAATTGACAAGACGTGGTC	GCTTTCTGTGTGCCAACTCTGG
<i>BID</i>	AGACATCATCCGGAATATTGC	AGACATCATCCGGAATATTGC
<i>MICAL3</i>	CTTCCAGGAGCTCTGTGAC	CCAGTAAGGATAAGTCGATG
<i>MICAL3 (2)</i>	GTGGACTCTGGAAAGCACAG	CAGCTTGGCATTTCAGTTCCTC
<i>CHST11</i>	GGAATCCCTTTGGTGTGGAC	CAGTAGATGAGCTCGTGGTCC

Table 2.4: PCR primer sequences used to detect gene expression in joint tissues

Ensembl transcript ID*	Forward primer (5'-3')	Reverse primer (5'-3')
ENST00000303694	CTATTTCAAAGTATGTTGCACC	CAGTAGATGAGCTCGTGGTCC
ENST00000549260	CTATTTCAAATCATGCGGAGG	CAGTAGATGAGCTCGTGGTCC
ENST00000549016	GTGTTCATAGCAGCATGAGTCACG	CAGTAGATGAGCTCGTGGTCC
ENST00000546689	CTATTTCAAATCATGCGGAGG	GGTAAAATGCCAGGCTGTG
ENST00000547956	CTATTTCAAAGTATGTTGCACC	GGTAAAATGCCAGGCTGTG

Table 2.5: PCR primer sequences used to detect expression of different transcript isoforms of *CHST11* in joint tissues

* <http://www.ensembl.org>

2.19 Database searching for polymorphisms

HapMap genome browser (<http://hapmap.ncbi.nlm.nih.gov/>) was used to query the genotype frequency and linkage disequilibrium (LD) database to search for polymorphisms on chromosome 22q11.21 and 12q23.3 that have been genotyped in the CEU population (individuals of European ancestry). Transcribed polymorphisms in *BCL2L13*, *MICAL3*, *BID* and *CHST11* with high minor allele frequency (greater than 15%) in the population were selected using the National Centre for Biotechnology Information (NCBI) variation database (dbSNP; <http://www.ncbi.nlm.nih.gov/projects/SNP/>).

2.20 Restriction Fragment Length Polymorphism (RFLP) Analysis

Genomic DNA was PCR amplified using primers designed to target the region surrounding the SNP of interest. The primer sequences used for each SNP are shown in Table 2.6.

The PCR products were then incubated with 5µl of a digestion mixture containing the corresponding restriction enzyme (5 U; New England Biolabs), 2 µl of the recommended buffer (10X; New England Biolabs), 0.2 µl of BSA (100X; New England Biolabs) where required and water (Table 2.6). Digestion reactions were incubated for 3 hours at the optimum temperature for the corresponding restriction enzyme. The digested products were electrophoresed through a 2% agarose gel containing ethidium bromide. The genotype of each sample was determined by analysing the sizes of the digestion products.

SNP	Forward primer (5'-3')	Reverse primer (5'-3')	Restriction Enzyme	Digestion conditions
rs4488761	GCTTGTCCCTTCGTTTCTAGG	CAGGATCCATTGCAATCTGC	AluI	NEB 4, 37 °C
rs2587100	GGTTTCTCAGCCTTGGCACTAGT	CTCTCGCTAAAGCAGTGGGTCTCAATAGGGGATGTTCAACA	BstNI	NEB 2, BSA, 60 °C
rs9967	CCACTTGTGAGTGCAACTG	CCTAGCAAGAGACCCATAGAAC	BstNI	NEB 2, BSA, 60 °C
rs11538	CCTTGTGCTGGCAGCAGAG	CCTACCCTAGAGACATGG	Tsp5091	NEB 1, 65 °C
rs2277831	GGATCACCTATGAAGAAAGAC	CAGGGATGGACAGCTAGTGG	MspI	NEB 4, 37 °C
rs5992854	GTCGGCCTTCTTCTTCTTGTGTC	GCTCTTTCACCTTCATCCGAG	BstNI	NEB 2, BSA, 60 °C
rs11917	CCTCAAGCTCACTCCCAAGACCTG	CAGGAGAGGATTAGCTGTGC	HincII	NEB 3, BSA, 37 °C
rs1057721	TCAGCTATGGCTCTTGGGGTAAGGTGGGAG GTAAGCTGGATTG	CATAGTTCGGATCCTGAATGG	PstI	NEB 3, BSA, 37 °C
rs4819639	GGTCATGAAAGTGGGACAGGT	CCGTGGTCTTGTTTTGGGTTCC	AluI	NEB 4, 37 °C
rs835487	GGAGTGAGCCAGAACAGATAAG	CTCTGCTGGACCAAATTCACG	KpnI	NEB 1, BSA, 37 °C
rs835488	TGAATTTGGTCCAGCAGAGTCTGG	GAGCCGGATCAGTATCTAGCAAAACC	HaeIII	NEB 4, 37 °C
rs864454	GCTTCTTAGCACCACTAAGG	GGTTGGCTCTACTGGCTAGACTCCCTCCTAAAGACAAAACCCCATTA	AseI	NEB 3, 37 °C
rs835489	GCACCCCTCATAGGGTCATATAGG	GCTGACGTCCCAACGCAGTGTGTTCTGTGTTGCCA	NcoI	NEB 3, 37 °C
rs835490	CTGGAGATTAGCTGTGTTGTGC	GGTTCCAAAGAGAACAGTTCCG	SmaI	NEB 4, 25 °C
rs1164760	GCTATTTGGAGAGCTTTGCTTG	CTCTCTGACCTCGTTTACTGC	MspI	NEB 4, 37 °C
rs2463018	GGTGAGACTCGTACACTTGG	CTAGCTGTAAGAGGGATGTGG	BCC1	NEB 1, BSA, 37 °C
rs2453155	GCATATCTGAGGTCTTCAAGG	TTTGAGCCTGAGGAGTAGG	NcoI	NEB 3, 37 °C
CHST11 novel variant	CTCTCAAACACTGCTGTCCTGCACC	GCTTTTCAAGCGGTGGTTGATTTCTGGGATGCTGTACTGGTTCAGGGT	HinfI	NEB 4, 37 °C

Table 2.6: RFLP assays used for genotyping

2.21 Allelic Expression Imbalance (AEI) analysis using Sequenom iPLEX assays

Sequenom assays were designed using the online 'MySequenom Genotyping Tools' (<https://www.mysequenom.com/Tools>). A 300 bp sequence surrounding each SNP was imported into the software, which then designs appropriate multiplexed assays. The software validates all primers in the multiplex by aligning them against each other to check for cross-hybridisation. All PCR primers contain a 10 bp tag (ACGTTGGATG) which helps to standardise the primers so that they work more efficiently in a multiplex. The extension primers are designed to anneal immediately adjacent to the polymorphic site and to differ in mass from each other. Table 2.7 lists the assays designed for six transcript SNPs and the OA-associated SNP rs2277831 from chromosome 22q11.21, which were in two multiplex groups.

Multi plex	SNP	Forward primer (5'-3')	Reverse primer (5'-3')	Mass of extension primer	Extension primer sequence (5'-3')
1	rs4488761	ACGTTGGATGTCTCCA ACTGTGACCACTTC	ACGTTGGATGCTTTCTG TGTGCCAACTCTG	5127.3	TTACCTGTGTCCTGTC
1	rs2587100	ACGTTGGATGCCCAGA GATGACAAACGAAA	ACGTTGGATGAAGCAG TGGGTCTCAATAGG	5443.6	GACATTGCCAAATGTCCC
1	rs2277831	ACGTTGGATGTGAAGA AAGACAATGCCAGG	ACGTTGGATGGAAGAA GAAAAGACTGGAGC	6126	AAAGACTGGAGCCATTCTG
1	rs11917	ACGTTGGATGTGGTGT GTTTCTTTGTGAG	ACGTTGGATGAAGCAC GACAACTTGGTTT	7032.6	TGTGTAACCTTTGTTTTTGCCGTT
2	rs9967	ACGTTGGATGAACTCT GGCTAGAGAGACAC	ACGTTGGATGGGCTGA AGAGACCTCAGAAG	5277.5	AAGGCAGGAGGATAACC
2	rs1057721	ACGTTGGATGGCTTTT TAGTGGAGCAAGAG	ACGTTGGATGACACATC ACCGTCAGCTATG	5659.7	GGGAGGTAAGCTGGATTG
2	rs4819639	ACGTTGGATGATGTCC CATCACGGTGCAG	ACGTTGGATGATTCTGC GTCCTGTTCCCTG	6194.1	AGACAGGAGAGCAGCCACAG

Table 2.7: Sequenom assays designed to the seven SNPs from chr22q11.21. The assays were grouped in two multiplexes.

Prior to the experiment, an extension primer mix was prepared by sorting the primers into four groups based on their mass. This is necessary because the primers with the highest mass generate a lower peak intensity compared to primers with a lower mass. Hence, the extension primers are adjusted by concentration to ensure that they generate peaks with equal intensity. Therefore the concentrations were doubled in high and low mass primers in four groups, such that the first group of lower mass primers are mixed at 7 μM , the second at 9.33 μM , the third at 11.66 μM and the highest mass group at 14 μM . The extension primer mixes prepared for the two plexes are shown in Table 2.8.

A

SNP	Mass of extension primer (Da)	Concentration in cocktail (μM)	Volume in cocktail (μl)
rs4488761	5127.3	7.00	8.75
rs2587100	5443.6	9.33	11.66
rs2277831	6126	11.66	14.58
rs11917	7032.6	14	17.50
		Water	322.51
		Total	375

B

SNP	Mass of extension primer (Da)	Concentration in cocktail (μM)	Volume in cocktail (μl)
rs9967	5277.5	7.00	8.75
rs1057721	5659.7	9.33	11.66
rs4819639	6194.1	11.66	14.58
		Water	340.01
		Total	375

Table 2.8: Extension primer mix prepared for multiplex 1(A) and 2(B). Primers with lowest mass were used at 7 μM and those with the highest mass were used at 14 μM .

Patients who were heterozygous for one or more of the six transcript SNPs were selected for AEI analysis. The gDNA and cDNA were amplified in four replicates using the Sequenom primers listed in Table 2.7 in multiplex. A multiplex PCR primer mix was prepared by adding 0.075 μl of each forward and reverse primer at a 100 mM stock concentration to give a final concentration of 0.5 mM for each primer in a 15 μl PCR reaction. This was added to 0.75 μl of 10 mM dNTP mix, 1.875 μl of 10X PCR buffer (500 mM KCl, 100 mM Tris-HCl pH 8.3), 1.2 μl of 25 mM MgCl_2 and 0.2 μl of AmpliTaq Gold DNA polymerase (5 U/ μl , Applied Biosystems). The reaction volume was made to 14.5 μl by the addition of H_2O . Twenty nanograms of genomic DNA and 0.5 μl of cDNA synthesised from 1 μg of RNA were added to the reaction mix. The PCR conditions were; 94 $^\circ\text{C}$ for 14 minutes, 35 cycles of 94 $^\circ\text{C}$ for 30 seconds, 57 $^\circ\text{C}$ for 30 seconds and 72 $^\circ\text{C}$ for 30 seconds and then 72 $^\circ\text{C}$ for 5 minutes. The reactions were performed in four replicates to assess experimental error. A 'no template control' (NTC) was also included in every PCR. The PCR products were analysed on a 2% agarose gel containing ethidium bromide to confirm successful amplification.

A 5 μl aliquot of each PCR product was transferred to a 384-PCR well microtitre plate and was transferred to Newgene (Newcastle upon Tyne, UK), where it was then processed using the protocol summarised below.

Five microlitres of PCR product was incubated with 0.5 U of Shrimp alkaline phosphatase (SAP; Sequenom, Hamburg, Germany) at 37 $^\circ\text{C}$ for 40 minutes and 85 $^\circ\text{C}$ for 5 minutes to dephosphorylate unincorporated dNTPs. The multiplex extension reaction was then carried out in a 9 μl volume with 10X iPLEX buffer, iPLEX termination mix, extension primer mix (primers at 7 to 14 μM each in multiplex pool) and iPLEX enzyme (Sequenom). The extension reaction products were then purified with SpectroCLEAN (Sequenom), a cationic resin that removes residual salts including Na^+ , K^+ and Mg^{2+} from the reaction. The purified products were arrayed on to spots on a SpectroCHIP which contains 3-hydroxypicolinic acid, the appropriate matrix for matrix assisted laser desorption ionisation-time of-flight (MALDI-TOF) mass spectrometry. The chip was placed in a MassARRAY analyzer (Sequenom) mass spectrometer and the spots were excited with a laser under a vacuum. The matrix absorbs the laser light energy causing the sample molecules to vaporise and ionise, which are then transferred electrostatically into the mass spectrometer tube (Gabriel *et al.*, 2009). The

molecules are detected individually at the end of the tube based on their flight time and are analysed by the SpectroTYPER software (Sequenom). A peak is generated for each extension fragment at the expected mass, which corresponds to the amount of each allele in the sample analysed.

The peak height ratios were calculated for genomic DNA and cDNA. The average peak height ratio for gDNA, which represents the 1:1 ratio, was used to normalise the cDNA peak height ratio to generate a normalised allelic ratio using the following formula:

$$\text{Normalised allelic ratio} = \text{Average allelic ratio of cDNA} / \text{average allelic ratio of gDNA}$$

2.22 Allelic Expression Imbalance (AEI) analysis using real time quantitative PCR genotyping assays

Ready-made quantitative real time PCR genotyping assays were used (Table 2.9). These are standard real time assays except that they employ a probe (FAM or VIC labelled) specific to each of the two alleles of a SNP. Real time PCR was carried out according to the manufacturer's instructions. In brief, 4 µl of gDNA diluted to 5 ng/µl or 4 µl of cDNA corresponding to 10ng of RNA were added to 5 µl of TaqMan Universal Master Mix II no UNG (Applied Biosystems) and 0.25 µl of 40X or 0.5 µl of 20X TaqMan assay (Applied Biosystems) in a 10 µl reaction. The samples were then amplified on an ABI PRISM 7900HT Sequence Detection System. Table 2.9 shows the cycle conditions for each assay. The reactions were performed in four replicates for assays rs11538 and rs5992854. For assay rs2463018, 5 replicates were performed for gDNA samples and 5 to 10 replicates were performed for cDNA samples. The allelic ratios were calculated using the formula $(2^{-\text{FAM Ct}}) / (2^{-\text{VIC Ct}})$ and normalised to the allelic ratios of gDNA.

Gene	SNP	PCR cycle conditions
BID	rs11538	50 °C for 2 minutes, 95 °C for 10 minutes and 40 cycles of 92 °C for 15 seconds and 60°C for 1 minute
MICAL3	rs5992854	
CHST11	rs2463018	50 °C for 2 minutes, 95 °C for 10 minutes and 40 cycles of 92 °C for 15 seconds and 60 °C for 90 seconds

Table 2.9: Real time quantitative genotyping assays used for AEI analyses

2.23 OA patients used for coding DNA variant detection in *CHST11*

DNA previously extracted from the peripheral blood of a total of 751 OA hip cases were analysed for DNA variant detection in the *CHST11* coding region. In 192 of the cases the *CHST11* coding sequence was sequenced to detect novel variants, which were then genotyped in the remaining 559 patients to accurately assess allele frequency. The 751 patients were composed of 281 males and 470 females and they derive from a large UK cohort that has been described in detail previously (Southam *et al.*, 2007).

2.24 Sequence analysis of the three exons of *CHST11*

Primers were designed to amplify the coding region of *CHST11* (Table 2.10, Figure 2.1). Exon 1 was amplified with a single primer pair (amplimer 1) as was exon 2 (amplimer 2), whilst two primer pairs (amplimers 3 and 4) were used to amplify the larger exon 3. The primers contained 18 bp tag sequences (M13 forward primer 5'TGTAAAACGACGGCCAGT3'; M13 reverse primer 5'CAGGAAACAGCTATGACC3') to ensure that consistent sequencing conditions could be used. The annealing temperature and final MgCl₂ concentration for the 15 µl PCR reactions for all four amplimers were 55 °C and 1 mM respectively. Each PCR reaction contained 50 ng of genomic DNA. For amplimer 1, 3.75 µl of Betaine (5 M, Sigma) was added to each PCR reaction.

PCR products were incubated with 2.4 µl of SAP (2.4 U; Fisher Scientific, Loughborough, UK), 0.6 µl of Exonuclease I (12 U, New England Biolabs) and 1.4 µl of 10X Exonuclease I reaction buffer (New England Biolabs) at 37 °C for 15 minutes and 80 °C for 15 minutes. One microlitre of PCR product was diluted with 9 µl of water and transferred to Genome Enterprises (Norwich, UK) for Sanger sequencing using the M13 forward primer 5'TGTAAAACGACGGCCAGT3' for amplimers 1, 2 and 3, and the M13 reverse primer 5'CAGGAAACAGCTATGACC3' for amplimer 4.

Amplimer	Target exon	Forward primer (5'-3')	Reverse primer (5'-3')	Size of amplimer (bp)
1	Exon 1	TG TAAAACGACGGCCAGTGCATCTCAGCACTTCCAGACC	CAG GAAACAGCTATGACCGGAGCCGGTAGGAAGAAGAGG	558
2	Exon 2	TG TAAAACGACGGCCAGTATCTAGATCCTTCTGGGTGTG	CAG GAAACAGCTATGACCGGAGAAAGCAACCACTGAAGG	443
3	Exon 3	TG TAAAACGACGGCCAGTAAAGGCATGAGCCACTGCAC	CAG GAAACAGCTATGACCCTTCTGGGTGAACTTGTTG	534
4	Exon 3	TG TAAAACGACGGCCAGTACATGAAGTTCTGTTTGTCC	CAG GAAACAGCTATGACCTAATTCTCACTATGCTGCTCG	661

Table 2.10: Primers designed to amplify and sequence the *CHT11* coding region. The M13 sequences are shown in bold.

Exon 1

ATATATAGATCGTTGGAGCGCAATGAAGTAGCCTTTGGAGAGAAGGGAGAGGGCCCCTCGGACAGCCACA
GCGGCCAGCGCAGCGGCAGCGGCAGCGGCAGCCACCATCACCGCTCGCACCCCAGCCGCCCGGCCGCGC
CAGGCAGCGGCAGCGCCGCCGGCGGGATCGGAGGAGGCGGCAGCGGCAGGAGGAGGAGCAGGAGCGCGC
AGCCAGCGGGTCCACGCATCTCAGCACTTCCAGACCAACTCCGGCACCTTCCACACCCCTGCCCCGGGCTG
GGGGCTCCGAGAGCGGCCGGAAGCGACTCCGATCCTCCCTCTGAGCCTTGCTCAGCTCTGCCCCGCGCC
TCCCGGGCTCCGGTCCGCGCGGGGGTCCCTGCTCCTGCGCCCCGGGCGCGCTTCCCGGACACCCCGGT
CCCCGCAGCCAGGACAAAGCC**ATGAAGCCAGCGCTGCTGGAAGT**GATGAGGATGAACAGAATCTGCCGA
TGGTGTGGCCACTT**GCTTGGGATCCTTTATCCTGGTCATCTTCTATTTCCAAAGTATGTTGCACC**CAG
TAGGGGGCGCGTTAGCGTGGTTTTGTTGGATATTTCTTCTCTCGCGCTCTAGCTCGCTCCGCCTGAT
TTCTGCCTCTTCCAACCTACCTCTCCGCTTCCGCTCTCGGGCTCTGGCTGCCAGAGCTCCTGG
CTGCCAGATCTACCCGGGTCACCGCGTCGGGATGGGGAGGAGAAGGGAAGGTGCTTCGCCCTTCT
TCCTACCGGCTCCGGGCTGGAGGATGGGACCAGGAGGGGCGGTAGTTTTTTTTTTTTTTTTTTTTTTCTTCT
CTTTTTTTCTTTGTGTCCCTTGTCTGTCTGTCTGCGAGGTAGCAGGGAAACGGAGAGGTG

Exon 2

CTTGCTGTCTTGAAGCAGCCATTACGCCATCTTTTTGTAAGTGGTTTCATTTCAATGAGCTTTAGATGCCT
GTCCTGTTTTCTTAAACACTTGCTGGGGAGACTTTTTAGCATGATCTAGATCCTTCTGGGTGTGGAGAT
GCCTGAATGTTGGGAAGACAGACAGCAGCTGTGCTGTTGGAGAAGGGACAGTGTGAAATCTTCCCTTGC
TAGAAGCTGGTTTTCTCTTTCTTTCCCTACTCTGTGCCTTTTTCTTTGACAGA
CAACAAATCTTTGTTGCTCATTTCTGATGAGCCTTCACTTTCTTTCCCTCAG**TCATGCGGAGGAATCCCTT**
TGGTGTGGACATCTGCTGCCGGAAGGGTCCCGAAGCCCCTGCAAGAACTCTACAACCCAATCCAGGTA
AGCTTCAAGCACTCTGTGAGCATGTGAATTTTTTTTTTTTGTAGGTATGGATACTAAAACTCTAAAATT
GTGGTCTTTGGGGATTTAAAACCTTCTTTACAGCCTGGCATTTTACCTTCAGTGGTTGCTTTCTCCGT
CACCTTTTTCTATGTAGCATCTCTGAAAAATCTAGCAGGGATGTTTGAATTAGAGAAATGCCTAGT
TTAGTGCTAAGCATTACAGACCTGCCAGGGTTTTGAACTCCTGAGA

Exon 3

TGAGGTCTCACTATGTTGCCAAGGCTGGTCTTGAACCTTGTTGGCCTCAAGCGATCCTCCTGCCTCAGCTTC
CCAGAGTGCTGGGATTAAGGCATGAGCCACTGCACCAGCTTAGATATGTGTTGAACGGGTGGATTTA
TGATCTACTTGTAGCCAAGTGAAATGTTTCAGGCAAGTACTGAGTCTTATTCGCTTGTGTCTCCTCT
GCAG**CTGGAGCTCTCAAACACTGCTGTCTGCACCAGATGCGGCGGGACCAGGTGACAGACACGTGCCGA**
GCCAAACAGCGCCACAAGCCGTAAGCGGAGGGTCTGACCCCCAACGACCTGAAGCACTTGGTGGTGGATG
AGGACCACGAGCTCATCTACTGTACGTGCCAAGGTGGCTGCACCAACTGGAAGCGGCTCATGATGGT
CCTGACCGGGCGGGGGAAGTACAGCGACCCCATGGAGATCCCGGCAACGAGGCACACGTCCTCGCCAAC
CTGAAGACCCTGAACCAGTACAGCATCCAGAAATCAACCACCGCTTGAAAAGCTACATGAAGTTCCTGT
TTGTCCGGGAGCCCTTCGAGAGGCTAGTGTCCGCTACCGCAACAAGTTCACCCAGAAGTACAACATCTC
CTTCCACAAGCGGTACGGCACCAAGATCATCAAACGCCAGCGGAAGAACGCCACCCAGGAGGCCCTGCGC
AAAGGGGACGATGTCAAATTCGAGGAGTTTGTGGCCTATCTCATCGACCCACACACCCAGCGGGAGGAGC
CTTTCAACGAACACTGGCAAACCGTCTACTCACTCTGCCATCCCTGCCACATCCACTATGACCTCGTGGG
CAAGTACGAGACACTGGAAGAGGATTTAATTACGTCTCGAGCTGGCAGGAGTGGGAGCTACCTGAAG
TTCCCCACCTATGCAAAGTCTACGAGAACTACTGATGAAATGACCACAGAATTTCCAGAACATCAGCT
CAGAGCACAAACGCAGCTGTACGAAGTCTACAAAACCTCGATTTTTTAATGTTCAATTACTCAGTGCCAAG
CTACCTGAAATTTGAAATAAGGGGGTGGGGAGAGGGAGAGAATCATGCTTTTTTAATTTAAGATTTTTTATT
TGTCAAAGAATTATATGGATATTGGGTATTGTTGTAATAATATTTCTTTGGGGATGATGCTGCGAGC
AGCATAGTGAGAATTATTTTAAAATCCTTCGTAGGGAAGGACAGCTGTCTTTCAGGGGAAATAGGATGGG
TCGTCTTGTCTGTAGAAGTGAATACTGCAACACTGTCTCAAAGGTTTCTTGTGTTCTGGTGAATTCAT
GAATTGTGCATTCCATAAATTTCTAATTAATATTTATATAGTTATTTAAACATGGTCTCATTTATTTCTTT
TTGTGGCAGCAAATTTCTAACATCTTTCCAGAAGAAATCTATGATTCCTGCTTTGCTTGTACAGCTCAT
TTGGGGGCATGAATGTTCTCTTACTAACCTCTCATGGAGTCATGTGATAACAGCCATTGTCATGTGTAT
GGATGCCACCATTTCTGAATTTCTGCTAGAAATAAGTAGGTTGCTATTGCACTTAGAGTCATTTTGCAA
GGGACTCATTCCAAACCAATTTCAATCGACCTGAAAGTCCCTTGCCTAAAGAAATGTGATTTTTTTTTTA

ACCCAAGGAGAAAGTTGGTTGTAACAATTTTTACCAGAAATTAGCAATCTGATAGAATAGGCTTTTTTAA
 CAGGAATTTTAAACTGGCGGTGCCAGTTGCAGTGAAGGTGAAGTGGCTATTGCTTTATATTCGACAAATA
 TTTATTGAGCATCTACTATATACTAGGCCCTGAAGATAGAGCGTTGAACAAACCAATAGTCTTGGCCCT
 CAAAAAGCTTTATGTGACATAGAGCATCCAGCTCGACAATTAGCAAACCCCTGATATTTATTCATGGACTT
 GACATGAGGTTTGGACTATTCATGAGCAACAGCAGAAGGTCCATGACCCCTACAAATTTACATTTTTCTA
 TGGCCCATATTTGAAAACCTCACATTCGGAGCAGGCCACTTTATATTCGTGAGTATCCCAAGCTCACTG
 ACCAACAGAAAAGATGCTAAAAAAATGTGTCCCTATCATGTGCCTGCTCCAAGTATGGGTAATGTCTGCC
 TTTAAGCCCCAGAATGGATTCTCCAGGCACAGTGTGGAAGAGTGTGTGGTTGATTAGCAATGTCTGCC
 TGGGTGAGGAAAGGGGAACACTCCTCAAGTGCCTCCTACTGTGCATCTCCATTCAGCCTAGCACCACATCC
 CCATGTAGAAGTGTGTCTTCTACTGCTTGCACAGTACAAGTGTGAAATGCCAAGGTGAGACTCGTACAC
 TTGGGGATTTGCAATGGTTTTTACCCTCATGAAGGTGAGAGTGGACTATTTGTACACATACACACATG
 CACACCCTCTCACGTCTCCAGAGGCTGAAAGACTATCAGCATCTTGGTAACTGCCATGCATGAGCAGCA
 AGGACAGCCTTCCATAATCCATGCCCATTTCTCTGGAAGCCTGGAACTTTTCATTTCTGTTCCTTG
 CTAATTAACATCTAAACATGCTTCTCATTTCCAGCCATTGCTGATGCTTCTCAGTTGAAGTTTGAGCCAC
 ATCCCTCTTACAGCTAGTGAATGAGTTGGTAGCAGCTACTGTATATAATAATAATAATAGTTTTAATAAT
 AGGGGAGGGTGGGATGGGGTGTGGGTAAGTTTTGCCTTTTGTTTTGTTTTGTATGCCGTATATAGTGAAG
 GGGTGAGGATATTCTAAACAAACAAAAATGAATAATTTATTACAGAACTATTAAGATTGTATTGTAA
 AGCTCACAGCAAGCTCAGTGGGCAGCAGCTGCAACATCTCACCGGGGAAATTTATTTTATTTAACGTGAGT
 GAGATGTGGGCCGGAGAAGGTAGCTGAAGCTATTTATAAAACGTTGTGTACCTTCTTCCGAGCTCTCTCC
 CCTTTGTGAAGGGCGCAGCAACTATAACCTTGATGGATGGAGATTTACGCAATGTGTTTTACTGGGTAGA
 GTGACAGACCTTGGCTGTCCCTGGAATTGAGAATCTGGACCTTATTTCCAGGCAGAGAACACTGTCCCA
 GAAATGGGACTTCTGATAATGAAACAGGTTGTCCAACATTTCTAATACGCATTTCTACAGAACACAGGTT
 CCAGGAGCATTCAAGTTGGTGTGATGCAGACTAAGGGTTTGTGGTCAAATATCCTTAAGAAAACAAAGTT
 AAGTCAGTTTCTTTCTGCAAGGACTTTTCCAGCCTCAATGTGTGCTGTGCATGTTGAATCCCCAAAAAT
 AATCCTTGAGTCTGTAGCATTTCCTGAACTTACATGACCAGGATACTCTATTTTGCAGATCACCCACAG
 AGCTAGGGTTCCACCGAGTATACTTTGCTTAGGTTGACTTAGCATATCTGAGGCTTCAAGGATAAAAAAC
 TGCCACCCCAACACCCTTCCATTAATAAAAAAAAAATACAAAAATAGCACCACAGTCTCCATCTGGTTTTATAGC
 AACAGAGGTACTTTATTTAATGAAGCAATGGTTCTAATCCTGGATACTGCCACGGACTACAATTCATCC
 CTCCCAGAGGGAGTGGAGGAAGTCTTGGGTGGTGTGGACAGAAGGAAGAGAGGAGGGGTGAGTGGGGTA
 TAGGGCCCAGGGTGGCTCCCTACTCCTCAGGCTCAAAGGATGCTCAGTGGGAACAGATGATCTCTTGAT
 GAGTGTCTTCTCAGTTTCATAGTTTGAATCGTTCCTGTGTGCTTTTTGGGGGGTTTTCAATGGAAAT
 CACGTTGCTTTGCATTTCTGTGTCCGTCTTTGGTCAGTTGTGCAAGCCTGCTCACTGTCATGTGAAGATG
 GCCTTTCATCTGGCTTCTCTCTTAAGTGAAGAAAGATTGTCTTCCAGGGGACATGACATCAATAGGTTT
 CTGGAATGAGGGACTCTTTCTCCCCGTGTTTTGCTTTGTGTTTACATTTTCTTTTCTAATGGCATTGAAA
 CTTTAAAAAAATGGATTCAACTGTTTTTGCAGAATGTAGAAAGTATTCTGTGTCCCTTGGTTAAAGAAAT
 CCACTTGTGAAGTGTGCCTGGAAAATGAAAGTTTGTGTTTTTAAAGAGGAATATTTGAAACTGCTTTCT
 ATGCATGCTTAGCTGGAGAAAAGTACAGGCAGGCGTCCCATCTCCAGCCACTTCTCAAAGGTGCTGCTG
 TGTTTTAAAGACCAGGTACAGCCAGGGCAGTATTTGCAAGGACATTCCTGCTTACTTTATCCCTTTGGTT
 GGAAAGCTCTAGATGATTCCCGCAGCTCCTCCAGACCCCGCCTCCCTGCCCTCCCAGCTGGTCTGGGAA
 GAGGTGGTCTGTGACCTGTGGTATCTCAGAGGGGACGTTCCCTCCTCCTCCTGTGCACCAGGTGGGCTG
 CACCCTCCTGCCTATTCAGGATGGATGCCACAGGAGCAGCAGGCAGTTCAGTTGCACTG
 GTTCTCCTGGTGGCAAAGGCATGAAGCACAGGGGTCGATTAATCCAGGCTACTAGAAAGCTCCAGAGCAA
 AGTGTGCGGGTCCCACAAATGCTTGGCTGGTGGGGTCTGGATCAGTGTGAGATAGAGTTGGCAGAAGAA
 GCAGAGGCACTCTGCTTGTCTTCCCTAGCCAGTCCCTCCCTACACACACACACACACACACACACACAC
 ACACACAATCTCAGCTGCGCCATTCTGTGCAATCCAGTGACCAAATCCCTTCCCTTGCCCACTCTATGT
 CAGCAGGACTGACCACATCACTCCCCGAGTTCCACCACCAGCATTTCCCTCCAACCTTTTTCCATCACA
 ACCAGTTAGAACCCTACAGGCAACAAGGCCTTCTAGAATCCGCTTAACCCTTGGCTGATAACAGGCAAAT
 TTCAGTCTGCTACACTTTGTTAGGTCCAGAAGGAGCTGCCATACTACTTTCTTATGAGCATGCTCAGTA
 TGGCATATGGACATGTAATGTCACATCTTTGTGGAGTGTGATTTCTTTTTTTCACATATTTGTATGCAGT
 AGAGAGCCTGTTGTAGAAAACGCTCCCTGTATCTTGTGTACTGTAAAGAAAGCTGAATTCACATTGC
 CAACAAAAGCGTGAAAATGTTTCATGAACCTTCCCTCCAGGAAAAGCCATTCAAGCCTGATTATTTTTCTAA
 GTAACCTCAATTAATTTGAAGAAAAAGAA

Figure 2.1: Amplimers designed for sequence analysis of *CHST11* coding region.
Untranslated regions are highlighted in yellow. Exons are highlighted in red with
alternating colours for codons. Primer sequences for amplimers 1, 2 and 3 are underlined.
Primer sequences for amplimer 4 are shown in blue bold text.

2.25 Human mesenchymal stem cell culture

One million cryo-preserved human bone marrow mesenchymal stem cells (hMSC) from two donors (a black male aged 22 and a black female aged 24; Lonza Biosciences) were resurrected from liquid nitrogen storage and cultured in monolayer in Mesenchymal Stem Cell Growth Medium (Lonza, cat no. PT-3001) supplemented with 5 ng/ml fibroblast growth factor-2 (FGF2; R&D Systems) in 75 cm² flasks.

2.26 siRNA transfection

On-TARGETplus SMART pool human *CHST11* siRNA (Dharmacon, Thermo Scientific, cat no. L-008882-01-0005) was resuspended in 250 µl of 1X siRNA Buffer (Dharmacon) to make 20 µM siRNA. On-TARGETplus control pool Non-targeting siRNA (Dharmacon, cat no. D-001810-10-20) at 20 µM was used as a control.

Chondrocytes from eight OA and one NOF patient were cultured in DMEM culture media at 37 °C until they reached 80% confluence. The cells were lifted off the surface using trypsin, counted and seeded at 10,000 cells/well in 200 µl of media in a 96- well plate for gene expression analysis. Eighteen wells of the 96-well microtitre plate were used for six replicates for three different treatments. Untransfected cells and cells transfected with non-targeting (NT) siRNA were used as controls. Six wells were transfected with siRNA against *CHST11*.

For western blot analysis, chondrocytes were seeded at 350,000 cells/well in 2 ml of media in 3 wells of a 6-well plate, for the 3 treatment groups.

Mesenchymal stem cells, once 80% confluent, were trypsinised, counted and seeded in three 10 cm tissue culture dishes (for untransfected, NT siRNA and *CHST11* siRNA) with 1.2 million cells in each dish.

The cells were cultured at 37 °C for 24 hours and transfected with Dharmafect transfection reagent 1 (Dharmacon). Table 2.11 shows the master mixes that were made for each of the culture conditions.

	96-well plate	6-well plate	10 cm culture dish
siRNA (NT or <i>CHST11</i>)	0.5 µl siRNA + 14.5 µl SFM	5 µl siRNA + 245 µl SFM	35 µl siRNA + 665 µl SFM
Transfection reagent	0.26 µl TR + 14.74 µl SFM	3.25 µl TR + 246.75 µl SFM	14 µl TR + 686 µl SFM
Total volume	30 µl	500 µl	1.4 ml

Table 2.11: Mastermixes for siRNA transfection. NT: Non-targeting siRNA, SFM: Serum Free Media

First, siRNA/media mix and transfection reagent/media mix were incubated at room temperature for 5 minutes before combining. Then the reaction mixture was incubated at room temperature for 20 minutes. Cells were transfected in 100 µl, 1 ml and 7 ml in 96-well, 6-well plates and 10 cm dishes respectively, by removing the required amount of media already in the wells. The cells were incubated at 37 °C for 48 hours. The cells in 96-well plates were lysed and the lysate was reverse transcribed for gene expression analyses. The 6-well plates were used for protein extraction and western blot analysis. Following transfection the mesenchymal stem cells were carried forward for chondrocyte differentiation experiments.

2.27 Differentiation of transfected hMSC to chondrocytes

Three 10 cm dishes were cultured with 1.2 million cells each for three different treatment groups; untransfected, cells transfected with NT siRNA and cells transfected with siRNA against *CHST11*. Forty eight hours post transfection, the cells were isolated with trypsin and 1.5 million cells from each dish were centrifuged at 240 x g for 5 minutes at room temperature. The cells from each disc were to be differentiated into three cartilage discs to be processed for gene expression analyses at days 3, 7 and 14 during chondrogenesis. The remaining cells in the dishes were centrifuged, the cell pellet was washed with PBS, resuspended in 250 µl of Trizol reagent (Ambion) and stored at -80 °C to be used as a day 0 time point. RNA was extracted from these cells using the Trizol/Chloroform method and used for gene expression analyses.

The centrifuged cells were washed with pre-warmed PBS and were centrifuged at 240 x g for 5 minutes at room temperature. The PBS was removed and the cells were resuspended in 450 µl of chondrogenic differentiation media consisting of 47.5 ml of

DMEM containing 4.5 g/l glucose (Lonza, cat no. 12-614), 10 ng/ml TGF- β 3 (PeproTech, London, UK) 100 mM dexamethasone (Sigma), 50 μ g/ml ascorbic acid-2-phosphate (Sigma), 40 μ g/ml proline (USB, High Wycombe, UK), 1X Insulin, Transferin, Selenium, Linoleic acid premix (ITS+L; BD Biosciences, Oxford, UK), 500 μ l of 2mM glutamine (Sigma) and 500 μ l of 100 U/ml penicillin and 100 μ g/ml streptomycin mix (Sigma). Millicell 0.4 μ m hanging PET cell culture inserts (Merck Millipore, Watford, UK, cat no. PIHT12L04) were placed in a 24-well plate (VWR) and 150 μ l of cells were transferred to each insert. The plates were spun at 200 x g for 5 minutes at room temperature and 750 μ l of differentiation media were added to the bottom of the wells, such that the cells received media from above and below. The surrounding empty wells were filled with 1 ml of PBS to avoid evaporation and the plates were incubated at 37 °C. The media above and below the inserts were replaced with fresh differentiation media every two days and up to the 14 days.

At each time point, the media from the Transwell inserts was removed and replaced with PBS to wash the membrane and the disc. The membrane containing the disc was cut using a scalpel blade and the disc was weighed on a piece of parafilm to obtain the wet mass. The discs were placed in 1.5 ml eppendorf tubes and stored at -80 °C until all time points were reached.

2.28 Cartilage disc grinding

The eppendorfs containing the cartilage discs were placed on dry ice and 20 μ l of molecular grinding resin (G-Biosciences, St. Louis, USA) was added to each tube. The tubes were spun at 13000 rpm for 30 seconds at room temperature and the water was removed from the tubes. For RNA extraction, the discs were ground using a pestle in 250 μ l of Trizol reagent (Ambion), until the disc disappeared. The tubes were centrifuged at 13000 rpm for 30 seconds at room temperature and the supernatant was transferred to a fresh tube. RNA was extracted using the Trizol/chloroform method. For protein extraction, the discs were ground in 250 μ l of protein lysis buffer using a pestle. Protein extraction was carried out following the method outlined in section 2.13.

2.29 RNA extraction (Trizol/chloroform method)

The cell pellets or ground cartilage discs resuspended in 250 µl Trizol were incubated at room temperature for 5 minutes. To each tube, 50 µl of chloroform (Fisher Scientific) was added and the tubes were shaken vigorously and incubated at room temperature for 2 minutes. The tubes were centrifuged at 4 °C at 13000 rpm for 15 minutes. The aqueous phase was transferred to a fresh tube and mixed with 125 µl of isopropanol. The tubes were vortexed, incubated at room temperature for 10 minutes, and centrifuged at 4 °C at 13000 rpm for 10 minutes. The supernatant was discarded and the pellets were washed with 250 µl of 75% ethanol made up in DEPC-treated water (Invitrogen). The tubes were vortexed and spun at 4 °C at 10000 rpm for 5 minutes. The ethanol was removed, the pellets were left to air dry for 10 minutes and resuspended in 20 µl of DEPC-treated water. The RNA was quantified using a NanoDrop 1000 spectrophotometer and the RNA was stored at -80 °C. One microgram of RNA was used for cDNA synthesis.

2.30 Micromass culture of transfected chondrocytes and mesenchymal stem cells

Chondrocytes and mesenchymal stem cells grown in monolayer were transfected with NT siRNA and siRNA against *CHST11* in 6-well cell culture plates and 10 cm dishes respectively. After 48 hours, the cells were trypsinised, counted and centrifuged to obtain a cell pellet. The cell pellet was resuspended in the required amount of media. Chondrocytes were cultured at high density at 400,000 cells per well in 20 µl of complete chondrocyte growth media in 24-well culture plates. Mesenchymal stem cells were seeded at 250,000 cells per well in 15 µl of differentiation media in 24-well culture plates. The cells were left for two hours in a 37 °C incubator to allow the cells to adhere to the bottom of the wells, and were then submerged in 400 µl of media. Seven replicates were made in total for NT siRNA and *CHST11* siRNA transfected cells. Three replicates were utilised for Alcian blue staining, two replicates for gene expression analysis and two for western blot analysis. The cells were incubated at 37 °C for 5 days. For gene expression and western blot analysis, the media was removed, the cells were washed in PBS and scraped off the surface of the well using a pipette tip. The cells in PBS were transferred to an eppendorf tube and pelleted by centrifugation at 13000 rpm for 5 minutes. RNA was extracted using the Trizol/chloroform method

(Chapter 2.29). Protein was extracted by following the method described in section 2.13.

2.31 Alcian blue staining

The media was removed from the cells and washed in 1 ml of PBS. The cells were fixed with 500 μ l of 100% methanol overnight at -20 °C. The methanol was removed and the cells were washed with 1 ml of distilled water and incubated with 500 μ l of 1% Alcian blue solution (0.5 g Alcian blue 8GX (Sigma) in 50 ml of 0.1 M HCl, pH 1) overnight at room temperature on a rocker. The Alcian blue was removed and the cells were washed with distilled water for two hours. The cells were then incubated with 200 μ l of 6 M guanidine hydrochloride (0.57 g of guanidine hydrochloride (Sigma) per 1 ml of water) for two hours at room temperature on a rocker. One hundred microlitres of guanidine hydrochloride was transferred to a 96-well glass microtiter plate and the absorbance was measured at 600 nm using a microplate reader (Tecan). The absorbance was normalised to the average protein content of the cells (absorbance/ μ g of protein).

2.32 Statistical analysis

GraphPad Prism software was used for generating graphs and statistical analyses. A P-value of less than 0.05 was considered significant.

2.32.1 Luciferase activity

The absorbance measurements for firefly luciferase were divided by that for *Renilla* luciferase. A two tailed student's *t*-test was used to compare the normalised values for untreated cells versus cells stimulated with exogenous growth factors.

2.32.2 Gene expression analysis post stimulation with exogenous growth factors

The gene expression relative to housekeeping genes ($2^{-\Delta\text{Ct}}$) was calculated for each treatment. A two tailed student's *t*-test was performed to compare the untreated cells against the treated cells. A Wilcoxon signed rank test was then performed on the fold change in gene expression for each gene analysed, to determine if the data deviate significantly from a hypothetical value of 1, which signifies no change in gene expression.

2.32.3 Gene expression stratified by genotype

Linear regression analysis was used to determine if the gene expression relative to genotype differed significantly from the null.

2.32.4 Allelic expression imbalance analysis

Tissue samples were considered to show an allelic imbalance if the fold difference in expression from the two alleles was 20% or greater. The normalised allelic expression ratios were plotted against the genotype at the associated SNP. A Kruskal-Wallis test was performed to assess the association between allelic expression imbalance and the genotype.

2.32.5 Gene expression analysis post transfection with CHST11 siRNA

The gene expression relative to housekeeping genes was compared between cells transfected with NT siRNA and cells transfected with siRNA against *CHST11* using a two tailed student's *t*-test. A Wilcoxon signed rank test was then performed on the fold change in gene expression for each gene analysed, to determine if the data deviate significantly from a hypothetical value of 1, which signifies no change in gene expression.

2.32.6 Alcian blue staining

The absorbance measurements were divided by the average protein content of the cells to obtain the absorbance values per microgram of protein. A two tailed student's *t* test was performed to compare the cells transfected with NT siRNA against cells transfected with *CHST11* siRNA.

Chapter 3: Investigation of the effect of exogenous growth factor GDF5 on primary chondrocytes

3.1 Introduction

Growth and differentiation factor-5 (GDF5), also known as cartilage-derived morphogenetic protein-1 (CDMP-1), is closely related to the Bone Morphogenetic Proteins (BMPs) and is a member of the Transforming Growth Factor- β (TGF- β) superfamily. GDF5 is involved in bone and cartilage development, maintenance and repair and is a marker for early joint formation (Luyten, 1997). GDF5 expression is mainly detected during embryonic development, in precartilaginous mesenchymal condensations and cartilaginous cores of the developing long bones (Storm *et al.*, 1994; Storm and Kingsley, 1996). Low expression levels of GDF5 are seen postnatally in cartilage, brain and placenta (Storm *et al.*, 1994; Chang *et al.*, 1994; Krieglstein *et al.*, 1995).

GDF5 protein is synthesised intracellularly, and is then cleaved at a consensus sequence Arg-X-X-Arg to form the mature form, which is then secreted as a dimer. GDF5 signals through BMP receptor type II (BMPR-II), which upon ligand binding, transphosphorylates BMP receptor type IB (BMPR-IB). This leads to the phosphorylation and activation of the downstream Smad1/5/8 signalling pathway (R-Smads). Although GDF5 shows binding affinity towards BMP receptor type IA (BMPR-IA), GDF5 has been shown to exhibit a 17-fold higher affinity towards BMPR-IB, compared to BMPR-IA (Nishitoh *et al.*, 1996). The phosphorylated Smad 1/5/8 then complexes with Smad 1/4 (Co-Smads), which translocates into the nucleus and regulates transcription of target genes (Massagué, 1998; Figure 3.1). These include *COL2A1*, which encodes the α 1 polypeptide chain of type II collagen, and *ACAN*, which encodes aggrecan (Mikic, 2004). GDF5 signalling can be negatively regulated by soluble proteins including noggin, chordin and gremlin (Piccolo *et al.*, 1996; Cho and Blitz, 1998; Merino *et al.*, 1999b). These bind to GDF5 extracellularly and block its interaction with the cell surface receptors (Piccolo *et al.*, 1996; Zimmerman *et al.*, 1996). In addition, GDF5 signalling can be inhibited by the action of inhibitory Smads. Smad 6 binds stably to BMPR-IB, thus competing with Smad 1/5/8 at the receptor level

(Imamura *et al.*, 1997). It has also been shown that Smad 6 can bind to activated Smad 1, therefore competing with Smad 4 to form a complex with Smad 1 (Hata *et al.*, 1998).

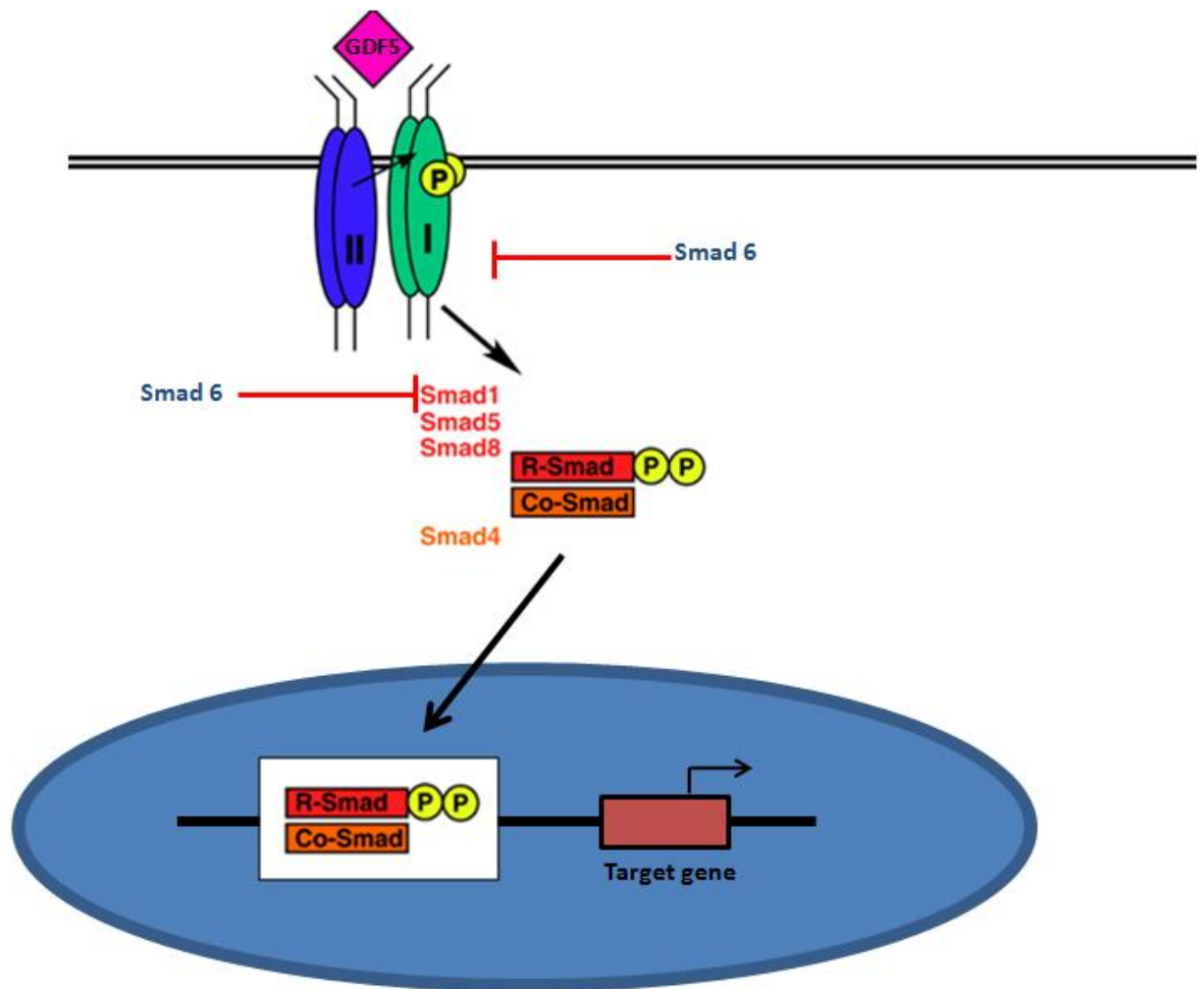


Figure 3.1: GDF5 signalling

GDF5 binding activates BMP receptor type II which in turn activates BMP receptor type IB, leading to the phosphorylation (denoted by P) of Smad 1/5/8 (R-Smads). These form a heterotrimer with Smad 4 (Co-Smads) consisting of two R-Smad molecules and one Co-Smad. This translocates to the nucleus to activate target gene transcription. Adapted from (Varga and Wrana, 2005).

The importance of GDF5 in the development of synovial joints has been shown in mouse models and human diseases. The presence of a frame shift mutation in *GDF5* in the brachypodism (bp) mouse results in the inability to form normal synovial joints. The homozygous mice exhibit multiple skeletal abnormalities including shortened limbs, loss of proximal interphalangeal joints, bone fusion and abnormal knee joints (Storm *et al.*, 1994). The heterozygous mice do not show obvious abnormalities, however they have been shown to develop an osteoarthritis-like phenotype when challenged (Settle Jr *et al.*, 2003; Daans *et al.*, 2011). Human chondrodysplasias caused by mutations in *GDF5* include Hunter-Thompson syndrome, Grebe syndrome and Brachydactyly type C. Hunter-Thompson syndrome is an autosomal recessive condition caused by a tandem duplication of 22 bp, resulting in 43 out-of-frame amino acids in *GDF5*, producing a non-functional protein (Thomas *et al.*, 1996). Grebe syndrome is an autosomal recessive chondrodysplasia caused by a non synonymous mutation, producing an abnormal *GDF5* protein. The mutant protein does not contain 1 of 7 highly conserved cysteine residues, which disrupts correct protein folding, resulting in the inability of the protein to be processed or secreted (Thomas *et al.*, 1997). Brachydactyly type C is an autosomal dominant chondrodysplasia, caused by single base pair insertion or deletion mutations in *GDF5* that create a premature stop codon, giving rise to a non-functional protein (Polinkovsky *et al.*, 1997). These three conditions are associated with the failure to form normal joints (Table 3.1).

Disease	Gene abnormality	Phenotype	Reference
Hunter-Thompson syndrome	22 bp frame shift	Short limbs, absent carpal bones and middle phalanx of fifth finger	Thomas <i>et al.</i> , 1996
Grebe syndrome	Point mutation	Short limbs, fusion of carpal and tarsal bones, loss of metacarpal and tarsal bones and proximal and middle phalanges	Thomas <i>et al.</i> , 1997; Costa <i>et al.</i> , 1998
Brachydactyly type C	Point mutation	Fusion of phalanges, loss of middle phalanges	Polinkovsky <i>et al.</i> , 1997

Table 3.1: Human conditions associated with *GDF5* mutations. (Adapted from Edwards and Francis-West, 2001)

As the role of *GDF5* in skeletogenesis is well established, *GDF5* was utilised in a candidate analysis to identify genes that harbour OA susceptibility loci in Japanese and Han Chinese populations (Miyamoto *et al.*, 2007). The authors identified a single nucleotide polymorphism (SNP) in the 5' untranslated region (UTR) of *GDF5* (rs143383, C/T) which was reported as being associated with OA. This was then replicated in a European study (Chapman *et al.*, 2008). The major T- allele was found to be more common in OA cases (a frequency of 74% in controls versus 84% in cases) in the Asian study (Miyamoto *et al.*, 2007). The same group reported that the T- allele mediated reduced *GDF5* expression compared to the C- allele in an *in-vitro* functional study using a luciferase reporter assay and a chondrogenic cell line. Furthermore, Southam *et al.* (2007) reported that there was up to 27% reduced transcription from the T- allele relative to the C- allele in cartilage of OA patients heterozygous at this SNP. Also, Valdes et al (2011) conducted a combined meta-analysis, which showed that harbouring the T-allele at rs143383 led to a 17% increased risk for knee OA, with an odds ratio of 1.17 and P-value of 6.2×10^{-11} .

Aside from OA, the T-allele mediates increased susceptibility to other musculoskeletal conditions. For example, individuals homozygous for the T-allele were shown to have twice the risk of developing Achilles tendon pathology (Posthumus *et al.*, 2010). Furthermore, the T-allele was also shown to be associated to congenital dysplasia of the hip in Han Chinese populations (Dai *et al.*, 2008) and in Caucasians (Rouault *et al.*,

2010), and to lumbar disc degeneration in Northern European women (Williams *et al.*, 2011). These findings suggest that a slight reduction in *GDF5* expression increases the risk for OA and for some other musculoskeletal diseases.

Several animal studies have reported on the use of GDF5 in therapeutics. Studies in rats have shown that GDF5 can be used to stimulate tendon healing (Forslund *et al.*, 2003; Rickert *et al.*, 2005). GDF5 has also been shown to be effective in repair or slowing down the degeneration of intervertebral discs in mouse, rabbit and bovine models (Walsh *et al.*, 2004; Chujo *et al.*, 2006; Liang *et al.*, 2010). Also, human clinical trials are underway for the use of GDF5 in regenerative periodontal therapy and recombinant GDF5 is being pursued as a therapeutic for intervertebral disc repair (Zhang *et al.*, 2011; Windisch *et al.*, 2012). Also, it has been reported that GDF5 enhanced chondrogenic differentiation and hypertrophy of human MSCs, thus showing potential to be used as a therapeutic in fracture repair (Coleman *et al.*, 2013).

Two publications have shown promising results of the stimulatory effects of GDF5 on matrix synthesis in human articular chondrocytes *in vitro*. Bobacz *et al.* (2002) used hip cartilage from 17 individuals with no OA and 13 OA patients. The authors showed an increase in glycosaminoglycan (GAG) synthesis in normal and OA chondrocytes cultured with GDF5, using [³⁵S] sulphate incorporation assays. They also observed an increase in *ACAN* mRNA levels using northern blot analysis, but no change in *COL2A1* expression. Chubinskaya *et al.*, (2008) carried out alginate bead culture of chondrocytes harvested from ankle joints of 9 donors with no history of joint disease. Culturing in the presence of GDF5 led to an increase in GAG synthesis, measured by radiolabeled sulphate incorporation assays.

The fact that the OA associated T-allele of rs143383 mediates reduced expression of *GDF5* has led to us hypothesising that one means of alleviating this genetic deficit could be via the supply of exogenous GDF5 to chondrocytes. Investigating the logistics of this is the aim of this chapter. Chondrocytes harvested from patients that had undergone total hip or total knee replacement surgery were cultured with or without recombinant GDF5. I then assessed whether this triggers expression changes of genes involved in metabolic processes in chondrocytes.

3.2 Results

3.2.1 GDF5 receptor gene expression in OA and NOF tissue

In order to investigate the effect of adding exogenous GDF5 to chondrocytes, it was important to first assess whether chondrocytes expressed the genes that encode the receptors that GDF5 binds to (*BMPR-II*, *BMPR-IA* and *BMPR-IB*). Complimentary DNAs (cDNAs) were synthesised from RNA extracted from the cartilage of 3 hip OA and 7 knee OA patients and from 10 neck-of-femur fracture (NOF) patients, the latter representing healthy cartilage. Gene expression was assessed using real time PCR assays designed for *BMPR-II*, *BMPR-IA* and *BMPR-IB* (Chapter 2.17, Table 2.2).

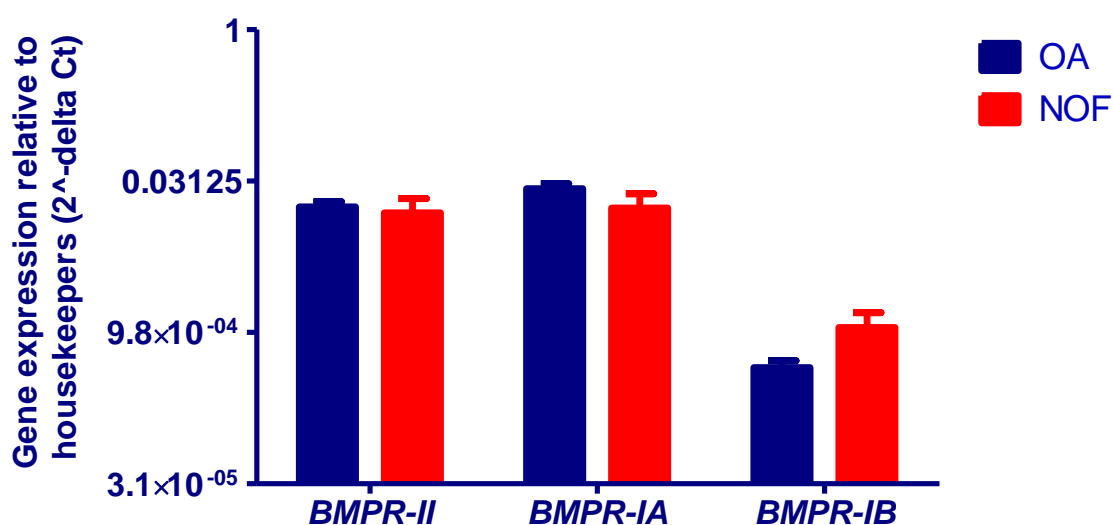


Figure 3.2: GDF5 receptor gene expression profile in 10 OA and 10 NOF cartilage tissue. Gene expression was measured relative to three housekeepers, *18S*, *GAPDH* and *HPRT1*. The error bars represent the standard error of the mean.

OA and NOF chondrocytes expressed all three genes analysed, in particular, *BMPR-II* and *BMPR-IA* (Figure 3.2). The expression of *BMPR-IA*, which encodes the alternative type I receptor that GDF5 binds to, was 60 ($P=7.2 \times 10^{-7}$) and 16 fold ($P=0.02$) higher in OA and NOF cartilage respectively, compared to *BMPR-IB*, which encodes the receptor towards which GDF5 shows preferentially activity. There was no significant difference ($P<0.05$) in the expression of *BMPR-II*, *BMPR-IA* or *BMPR-IB* when OA was compared to NOF.

I next measured the gene expression of *BMPR-II*, *BMPR-IA* and *BMPR-IB* in chondrocytes that had been extracted from OA cartilage and then cultured in monolayer, to assess if the gene expression profile would change under culture

conditions. These cells showed a similar gene expression pattern to that observed in cartilage, with a 22 fold ($P=0.02$) higher *BMPR-IA* expression compared to *BMPR-IB* expression (Figure 3.3).

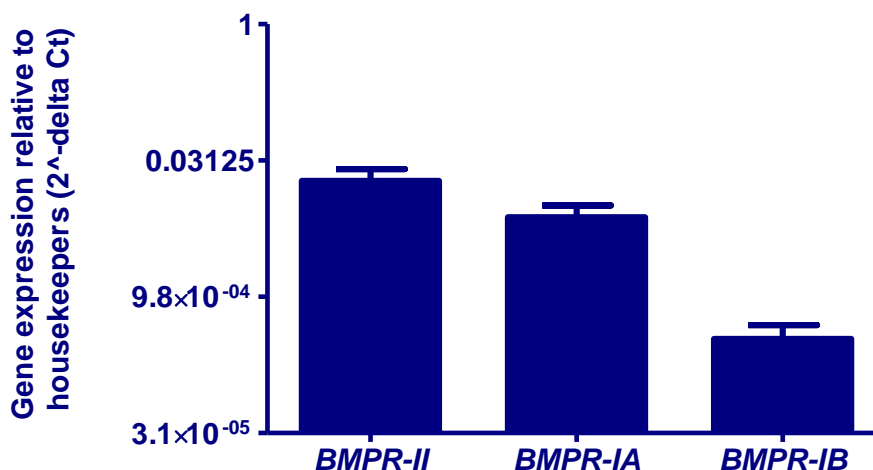


Figure 3.3: GDF5 receptor gene expression profile in OA chondrocytes cultured in monolayer. Gene expression was measured relative to three housekeepers, *18S*, *GAPDH* and *HPRT1*. The error bars represent the standard error of the mean.

3.2.2 The GDF5 proteins used

The above results showed that the expression of *BMPR-IA* was higher in chondrocytes compared to expression of *BMPR-IB*. Therefore, I chose to use a recombinant GDF5 protein that was designed by Biopharm GmbH (Heidelberg, Germany) to show increased specificity for *BMPR-IA* compared to *BMPR-IB*. I also used another variant that was designed by Biopharm, which is insensitive to the GDF5 antagonist noggin. Therefore, I have used four different recombinant GDF5 proteins in total; wildtype mouse (R&D Biosystems), wildtype human (Biopharm) and the two variants (A and B). All recombinant proteins used are the mature form of GDF5. The amino acid sequence difference between the mature forms of recombinant wildtype mouse GDF5 and the wildtype human GDF5 is a single amino acid: asparagine at position 380 in mouse is a threonine at the comparable position (386) in human. Table 3.2 shows the sequence of the four GDF5 proteins encompassing the changes introduced in variants A and B. Human GDF5 variant A was designed by introducing two point mutations in GDF5 to swap two methionine residues to valine residues at positions 453 and 456 (Kasten *et*

al., 2010). Variant B was designed by exchanging the asparagine residue at position 445 in GDF5 to threonine (Seemann *et al.*, 2009).

Wildtype mGDF5	430 PLRSHLEPTNHAVIQTLMNNSMDPESTPPTCCVPTRL 466
Wildtype hGDF5	436 PLRSHLEPTNHAVIQTLMNNSMDPESTPPTCCVPTRL 472
hGDF5 variant A	436 PLRSHLEPTNHAVIQTLVNSVDPESTPPTCCVPTRL 472
hGDF5 variant B	436 PLRSHLEPTTHAVIQTLMNNSMDPESTPPTCCVPTRL 472

Table 3.2: Partial amino acid sequences of the GDF5 proteins used.

The amino acid sequences from 430-466 for mouse GDF5 and from 436-472 for human GDF5 proteins are shown with the change in amino acid sequence in variant A and B highlighted in red. (mGDF5, mouse GDF5; hGDF5, human GDF5)

3.2.3 Analysis of dose-dependent response to exogenous GDF5 in SW1353 cells using a luciferase reporter assay

Previous reports have shown the optimal dose of GDF5 to be used for the stimulation of chondrocytes in monolayer is 100 ng/ml (Erlacher *et al.*, 1998). In order to test this, I carried out a dose response analysis using a Smad 1/5/8 reporter assay, which is a pGL3 basic vector containing Smad 1/5/8 binding elements that drive firefly luciferase transcription (Mitchell *et al.*, 2010). I transfected OA chondrocytes with the vector and stimulated cells with 10 ng/ml, 30 ng/ml, 100 ng/ml and 300 ng/ml exogenous GDF5 24 hours post transfection (Chapter 2.9). Unfortunately, I was unable to transfect OA chondrocytes. I therefore used instead the human SW1353 chondrosarcoma cell line to carry out the dose response analyses.

Initially, I transfected the cells with an empty (no insert) pGL3 basic plasmid vector (as a negative control) in addition to the Smad 1/5/8 reporter vector. The cells were cultured with 100 ng/ml of wildtype human GDF5 24 hours post transfection. The cells were also cultured with 100 ng/ml of human BMP2 (Chubinskaya *et al.*, 2008) and 5 ng/ml of human TGF- β 1 (Baugé *et al.*, 2008) as positive controls. The cells were lysed at 6 hours and 24 hours post stimulation and luciferase activity was measured (Figure 3.4).

At both time points, luciferase activity was significantly increased after stimulation with GDF5, BMP2 and TGF- β 1 in the cells transfected with the Smad 1/5/8 reporter vector. There was no significant increase in luciferase activity between the different

treatments in the cells transfected with the empty pGL3 vector. This showed that the SW1353 cells are responsive to exogenous GDF5, BMP2 and TGF- β 1 at the doses used.

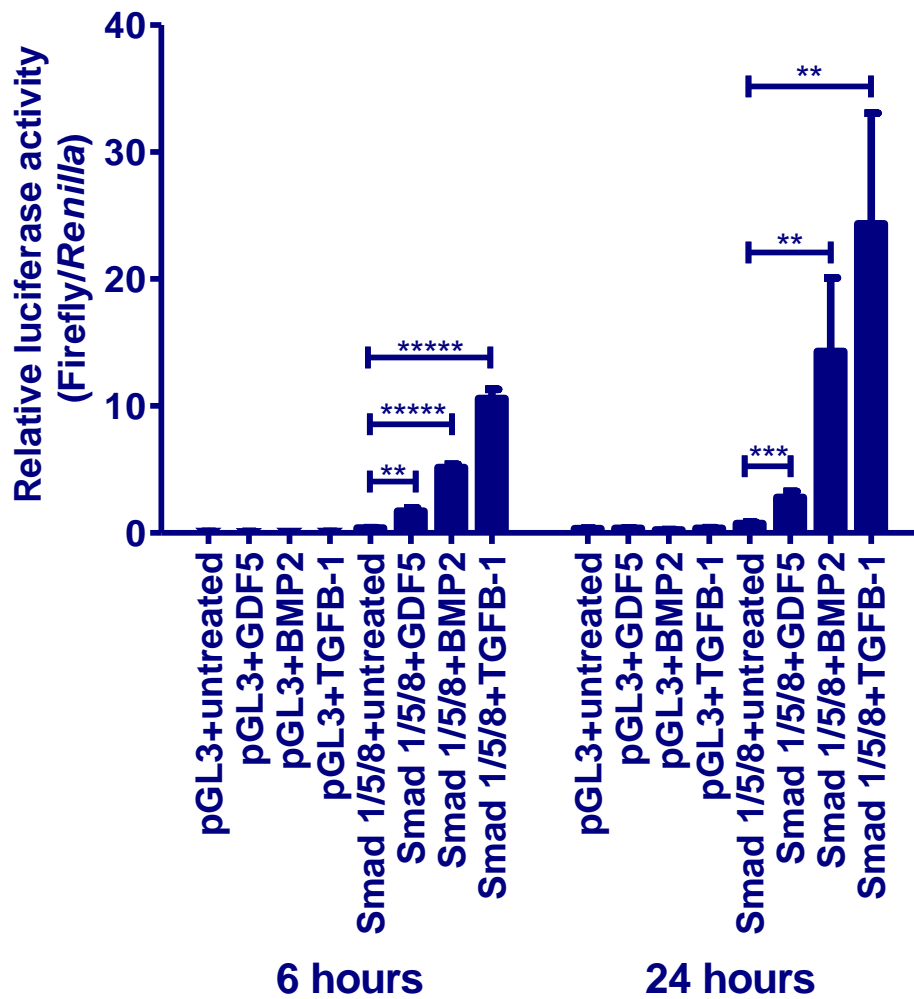


Figure 3.4: Luciferase activity in response to GDF5 treatment, post transfection with empty pGL3 vector as negative control and with pGL3 vector containing Smad 1/5/8 reporter insert. BMP2 and TFG- β 1 stimulations were used as positive controls. The error bars represent the standard error of the mean.

** $P \leq 0.01$, *** $P \leq 0.001$, **** $P \leq 0.0001$, ***** $P \leq 0.00001$

I next stimulated the cells with all four recombinant GDF5 proteins at 10ng/ml, 30 ng/ml, 100 ng/ml and 300 ng/ml post transfection with the Smad 1/5/8 reporter vector. The cells were lysed at four time points, 6, 12, 24 and 48 hours post stimulation (Chapter 2.11.1, Figure 3.5). BMP2 and TGF- β 1 were again used as positive controls at each time point.

The cells stimulated with 10 ng/ml and 30 ng/ml of mouse GDF5 showed a significant increase in luciferase activity at 6 hours after stimulation, compared to untreated cells. However a significant effect was not seen at these doses at the two other time points analysed. The cells treated with 100 ng/ml and 300 ng/ml of mouse GDF5 showed a significant increase in luciferase activity compared to untreated cells at all time points analysed.

Stimulation of cells with 10 ng/ml of wildtype human GDF5 did not increase luciferase activity compared to untreated cells at any of the time points analysed. Stimulation with 30 ng/ml increased luciferase activity only at 6 hours after stimulation. Cells cultured with 100 ng/ml GDF5 showed a significant increase in luciferase readings at all time points. Treatment with 300 ng/ml of wildtype human GDF5 resulted in a significant increase in luciferase activity at 6, 12 and 48 hour time points, but not at 24 hours.

Stimulation of cells with 10 ng/ml of human GDF5 variant A did not result in a significant increase in luciferase activity, and cells stimulated with 30 ng/ml of GDF5 variant A showed a significant increase only at 6 hours post stimulation. Cells cultured with 100 ng/ml of GDF5 variant A showed a significant increase in luciferase readings at all time points. Stimulation with 300 ng/ml of GDF5 variant A resulted in a significant increase in luciferase at 6, 24 and 48 hours post stimulation, but not at 12 hours.

The cells cultured with 10 ng/ml of GDF5 variant B showed an increase in luciferase activity at 6 and 12 hours, but not at 24 or 48 hours after stimulation. The cells cultured with 30 ng/ml, 100 ng/ml and 300 ng/ml of this variant showed significantly higher luciferase activity at all time points.

At all four time points, stimulation with BMP2 and TGF- β 1 resulted in a significant increase in luciferase activity. Furthermore, BMP2 and TGF- β 1 stimulations clearly

elicit a greater response at all time points than do any of the GDF5 proteins. Stimulation with 100 ng/ml of each of the four recombinant GDF5 proteins consistently and significantly increased luciferase activity at all time points. Furthermore, there was no significant difference between the luciferase readings generated in cells stimulated with 100 ng/ml and 300 ng/ml of GDF5 protein. In addition, a previous report has shown that 100 ng/ml is the optimal concentration of recombinant GDF5 to be used in chondrocyte culture (Erlacher *et al.*, 1998). Based on my results and this previous data, I therefore chose to use 100 ng/ml GDF5 for the stimulation of OA and NOF chondrocytes in subsequent experiments.

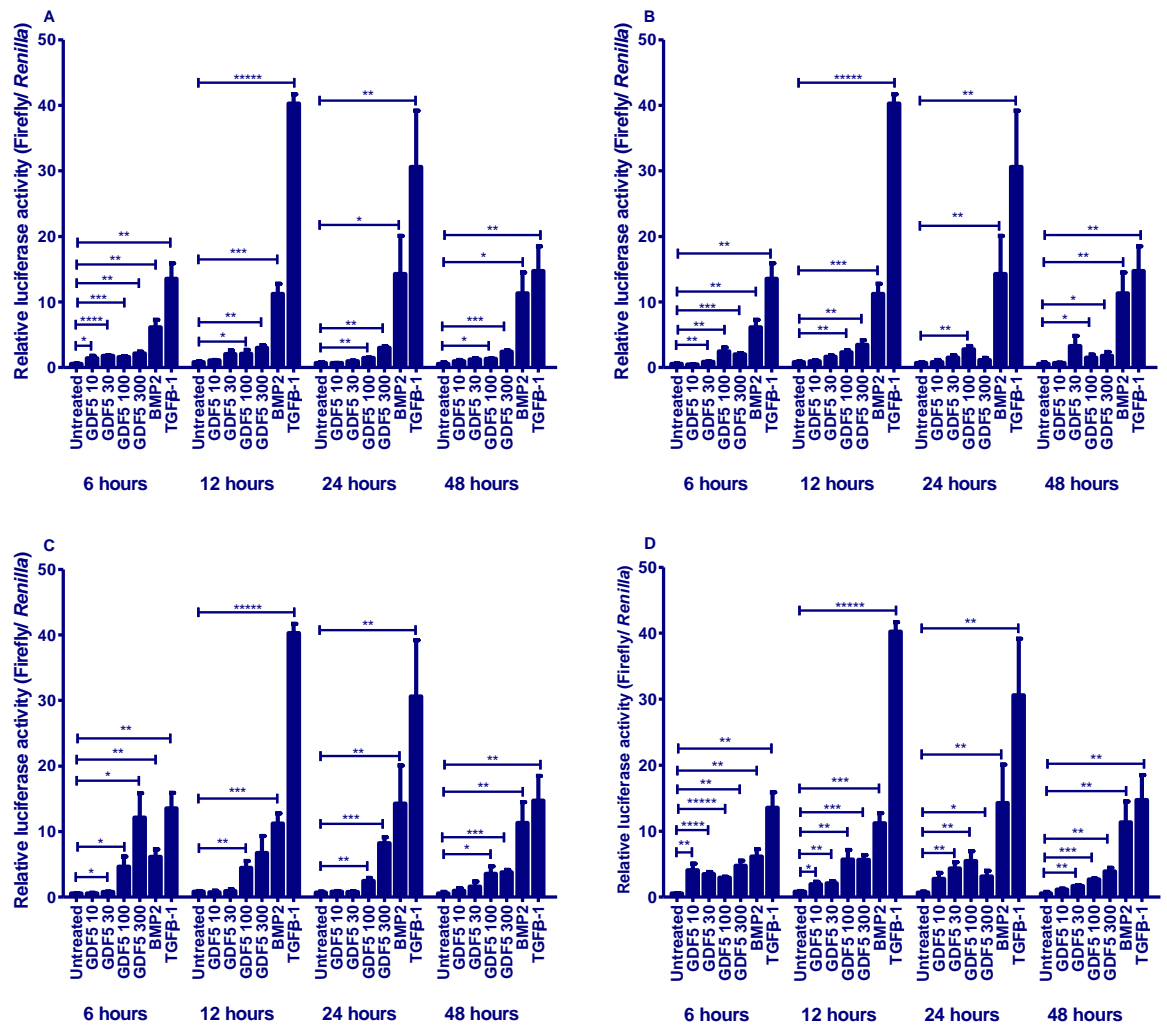


Figure 3.5: Luciferase activity readings generated in SW1353 cells in response to exogenous wildtype mouse GDF5 (A), wildtype human GDF5 (B), human GDF5 variant A (C) and human GDF5 variant B (D) at 6, 12, 24 and 48 hours post stimulation.

BMP2 and TGF-β1 stimulations were used as positive controls. Error bars represent standard error of the mean. GDF5 10, 10 ng/ml; GDF 30, 30 ng/ml; GDF5 100, 100 ng/ml; GDF5 300, 300 ng/ml

* P<0.05, ** P<0.01, *** P<0.001, **** P<0.0001, ***** P<0.00001

3.2.4 Activation of Smad signalling in chondrocytes after stimulation with GDF5

Chondrocytes from two OA patients were cultured in monolayer with or without 100 ng/ml of exogenous GDF5 for 15 minutes, 30 minutes, 1 hour and 2 hours (Chapter 2.11.2). Protein extracted from the cells was subjected to western blot analysis using an antibody against phospho-Smad 1/5/8 (Chapter 2.13, 2.14 and 2.15). The cells were also stimulated with TGF- β 1 for 1 hour as a positive control. Anti- β -actin antibody was used as a loading control for western blot analysis. The data for one of the two individuals is shown in Figure 3.6. The second individual produced the same results. This experiment may need to be repeated in more individuals to determine if this result can be replicated multiple times.

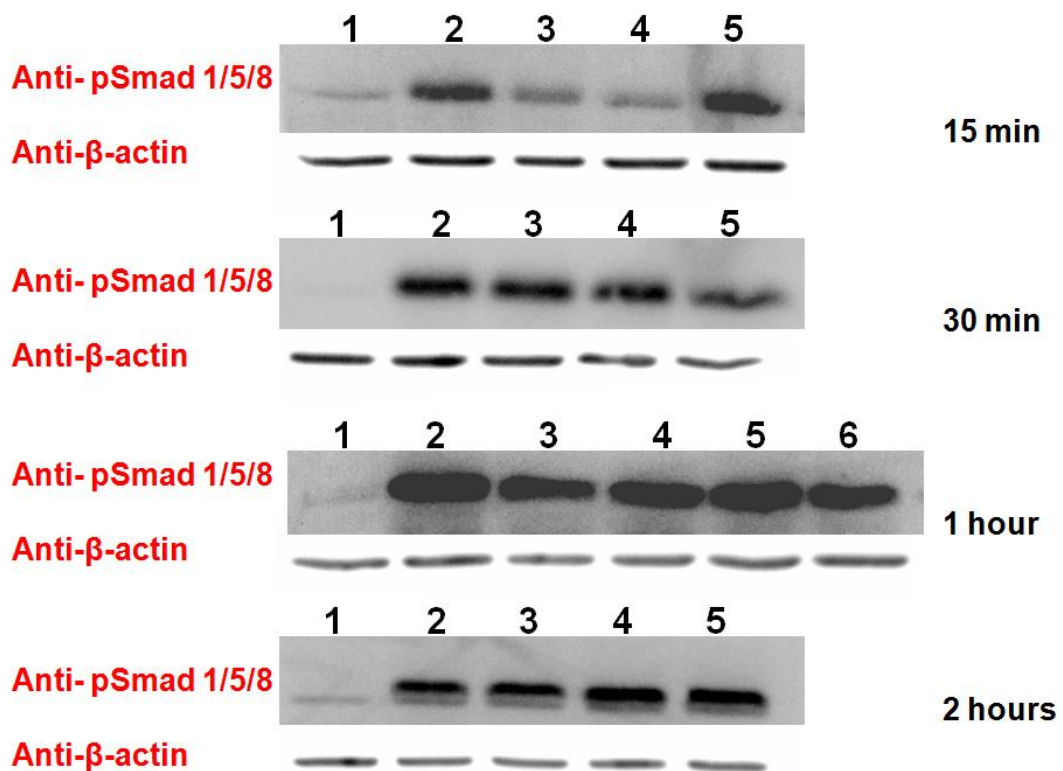


Figure 3.6: Western blot images at 15 minutes, 30 minutes, 1 hour and 2 hours post stimulation with GDF5.

TGF- β 1 stimulation was used as a positive control. Lane 1, Untreated; 2, wildtype mouse GDF5; 3, wildtype human GDF5; 4, human GDF5 variant A; 5, human GDF5 variant B and 6, human TGF- β 1. Anti-pSmad 1/5/8, Anti-phospho-Smad1 (Ser463/465)/ Smad5 (Ser463/465)/ Smad8 (Ser426/428)

The Smad 1/5/8 signalling pathway was activated in response to stimulation with all types of GDF5 proteins used at all time points analysed.

In summary of the above two sections, all four of the exogenous GDF5 proteins were able to activate the Smad 1/5/8 signalling pathway in SW1353 cells, as demonstrated by a luciferase reporter assay, and in chondrocytes, as confirmed by western blot analysis, at a concentration of 100 ng/ml. Having established that the chondrocytes respond to stimulation by the GDF5 proteins, I next assessed the effect that this stimulation has on the expression of a panel of relevant genes.

3.2.5 Changes in gene expression in response to exogenous GDF5 in OA chondrocytes

Chondrocytes harvested from 20 OA patients (Patients A-T, Table 3.3) were cultured with (treated) or without (untreated) 100 ng/ml of each of the GDF5 proteins (Chapter 2.11.3). Nine of the 20 were cultured with wildtype mouse GDF5 (patients A-I), three of whom were also separately cultured with TGF- β 1 (patients G-I). Seven of the 20 were cultured with wildtype human GDF5 (patients J, K and N-R), five of whom were also separately cultured with variant A and separately with variant B (patients N-R). Two of the 20 were cultured with variant A and separately with variant B (patients L and M). Finally, two of the 20 were cultured only with TGF- β 1 (patients S and T). To reiterate, none of the culturing was performed with two or more of the GDF5 proteins in the same culture mix.

The cells were lysed at four time points after stimulation (6, 12, 24 and 48 hours; Chapter 2.16). Changes in the expression of six genes that code for proteins that have anabolic and catabolic roles in chondrocyte biology were then assessed by quantitative real time PCR (Chapter 2.17). The genes studied were *COL2A1*, *ACAN*, *SOX9*, *TIMP1*, *MMP1* and *MMP13*. As a positive control, chondrocytes from patients A-F and J-R were stimulated with TGF- β 1 for 48 hours. The relative gene expression of the test genes was compared between the treated and the untreated cells by performing a student's two tailed *t*-test. Values of $P < 0.05$ were considered significant.

The significant up/down changes in gene expression in response to stimulation with the GDF5 proteins and with TGF- β 1 were then plotted and are shown in Figures 3.7 to 3.11. The actual values of these significant changes are listed in Tables 3.4-3.8. A

Wilcoxon signed rank test was performed to assess whether the chondrocytes showed a significant trend in response to each GDF5 and to TGF- β 1. P-values are listed in Table 3.9.

Patient	Age at surgery	Sex	Joint	Growth factor
A	59	M	Knee	Wildtype mGDF5
B	70	M	Knee	Wildtype mGDF5
C	68	F	Knee	Wildtype mGDF5
D	45	F	Knee	Wildtype mGDF5
E	75	M	Knee	Wildtype mGDF5
F	46	M	Knee	Wildtype mGDF5
G	73	F	Knee	Wildtype mGDF5, TGF- β 1
H	77	M	Knee	Wildtype mGDF5, TGF- β 1
I	68	M	Knee	Wildtype mGDF5, TGF- β 1
J	66	M	Hip	Wildtype hGDF5
K	64	F	Knee	Wildtype hGDF5
L	63	M	Knee	hGDF5 variant A, hGDF5 variant B
M	78	F	Knee	hGDF5 variant A, hGDF5 variant B
N	84	M	Hip	Wildtype hGDF5 and hGDF5 variant A, hGDF5 variant B
O	82	M	Knee	Wildtype hGDF5 and hGDF5 variant A, hGDF5 variant B
P	70	F	Knee	Wildtype hGDF5 and hGDF5 variant A, hGDF5 variant B
Q	70	F	Knee	Wildtype hGDF5 and hGDF5 variant A, hGDF5 variant B
R	68	F	Knee	Wildtype hGDF5 and hGDF5 variant A, hGDF5 variant B
S	67	F	Knee	TGF- β 1
T	58	F	Knee	TGF- β 1

Table 3.3: Details of the OA patients studied in this section and of the growth factors used to stimulate their chondrocytes.

F, female; M, male; mGDF5, mouse GDF5; hGDF5, human GDF5

My results show that OA chondrocytes respond to exogenous GDF5, but not in a consistent manner. Some patients did not show a significant response to GDF5 stimulation at all (for example, patient B), and where a response was observed at one time point, this did not persist through to further time points. For example, patient I showed a 1.64 fold significant upregulation of *MMP13*, 6 hours post stimulation with wildtype mouse GDF5. But, there was no change in *MMP13* expression at 12, 24 or 48 hours post stimulation (Table 3.4). Also, the changes in gene expression observed were not predictable, in that they were not always in the same direction. For example,

MMP13 was both up and down regulated in response to wildtype mouse, wildtype human and human variant A GDF5.

All five patients cultured with TGF- β 1 did however respond in a clearly consistent manner, showing an upregulation of *TIMP1* (P=0.0005) and *COL2A1* (P<0.0001) and a down regulation of *MMP13* (P=0.035), *MMP1* (P=0.0001), *ACAN* (P=0.042) and *SOX9* (P=0.0021; Table 3.9).

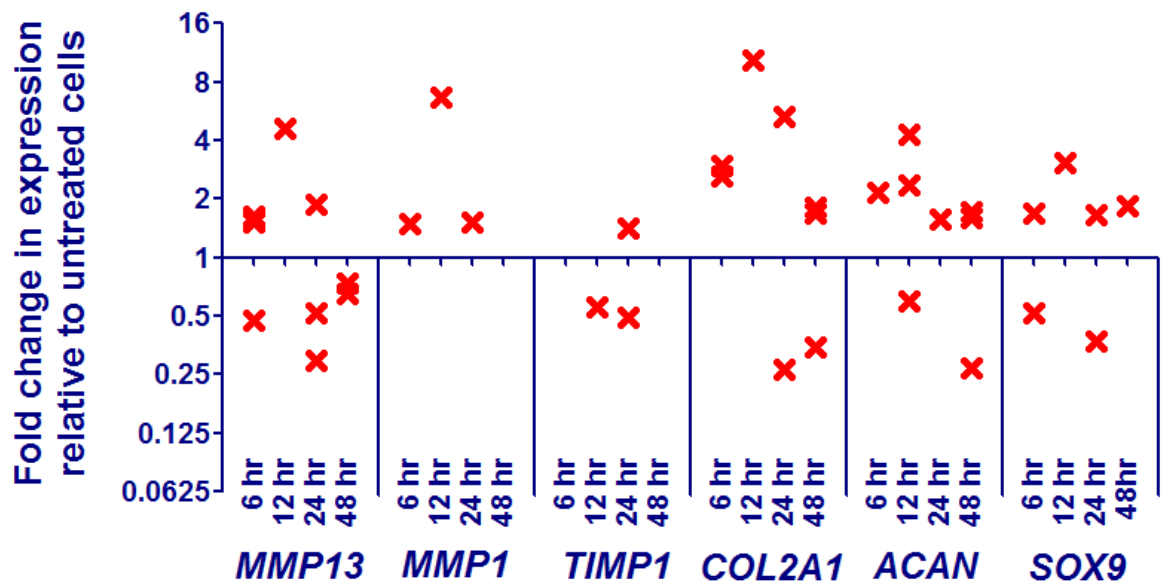


Figure 3.7: Gene expression changes in cells treated with mouse GDF5 compared to untreated cells. Each cross represents a significant ($P < 0.05$) up/down regulation of gene expression relative to untreated cells in one patient. Nine patients were studied in total.

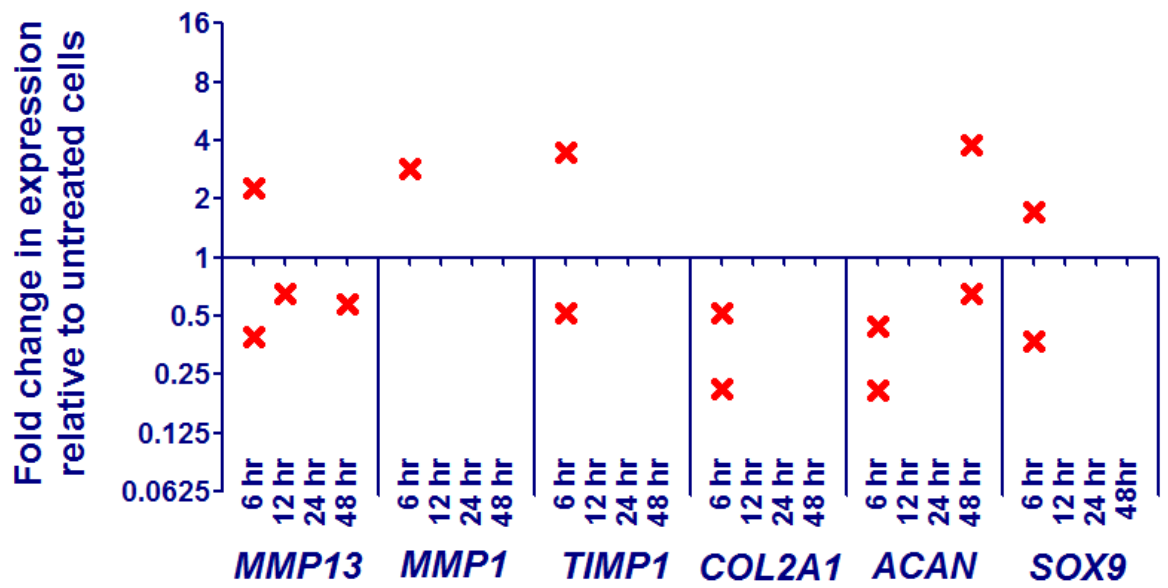


Figure 3.8: Gene expression changes in cells treated with wildtype human GDF5 compared to untreated cells. Each cross represents a significant ($P < 0.05$) up/down regulation of gene expression relative to untreated cells in one patient. Seven patients were studied in total.

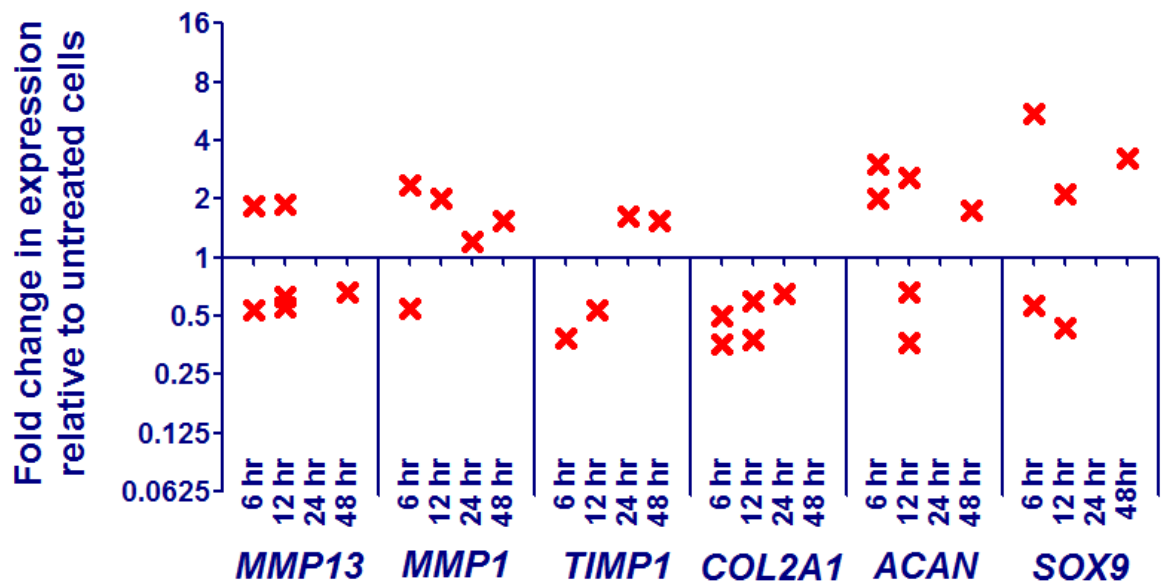


Figure 3.9: Gene expression changes in cells treated with human GDF5 variant A compared to untreated cells. Each cross represents a significant ($P < 0.05$) up/down regulation of gene expression relative to untreated cells in one patient. Seven patients were studied in total.

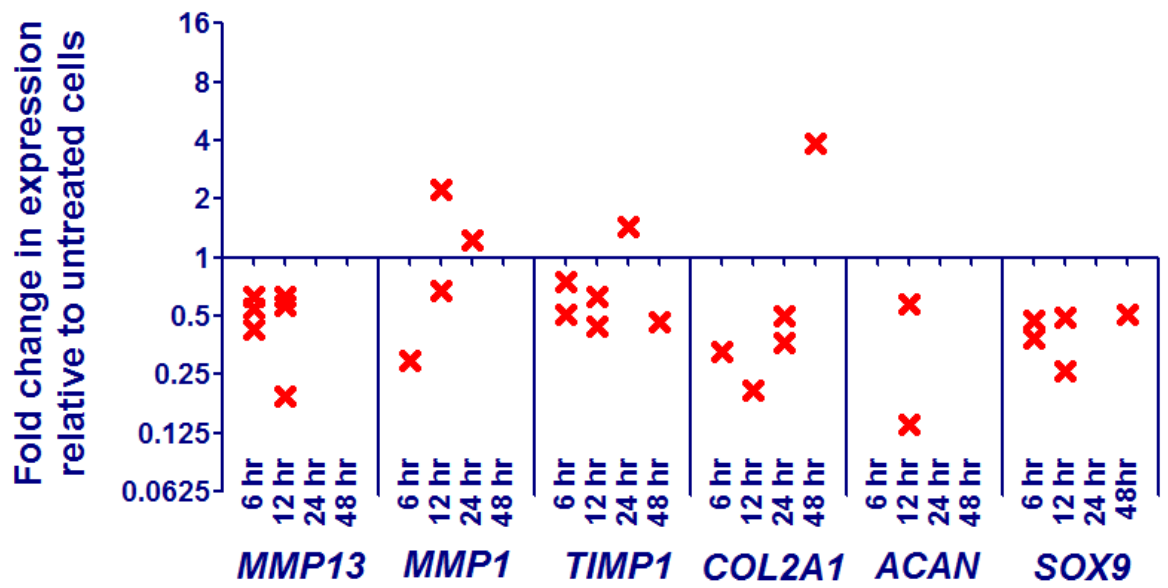


Figure 3.10: Gene expression changes in cells treated with human GDF5 variant B compared to untreated cells. Each cross represents a significant ($P < 0.05$) up/down regulation of gene expression relative to untreated cells in one patient. Seven patients were studied in total.

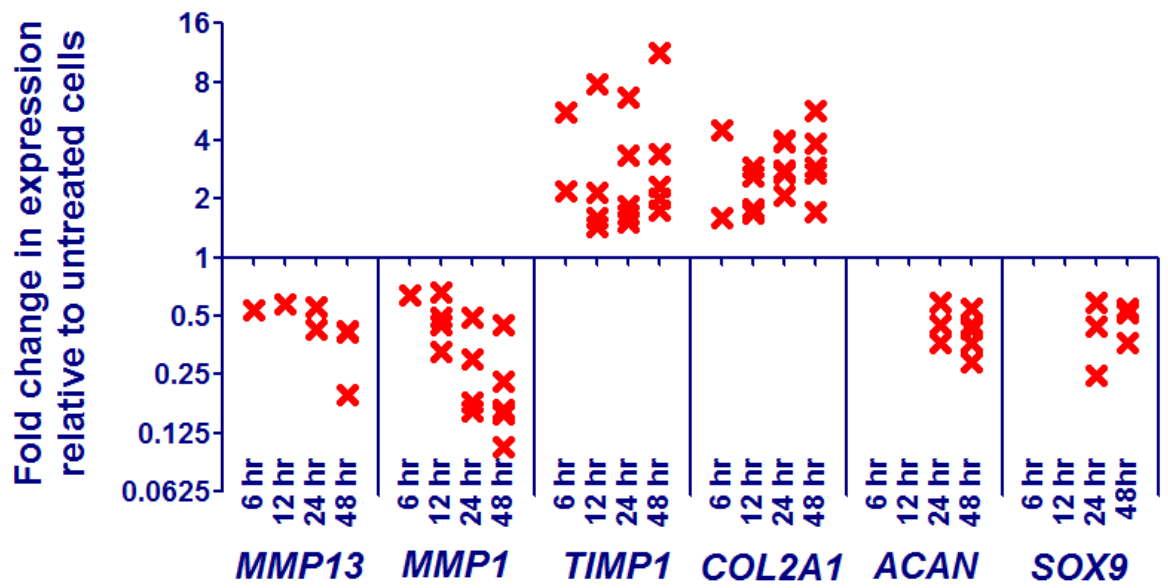


Figure 3.11: Gene expression changes in cells treated with human TGF- β 1 compared to untreated cells. Each cross represents a significant ($P < 0.05$) up/down regulation of gene expression relative to untreated cells in one patient. Five patients were studied in total.

Gene	Time point after stimulation	Patient								
		A	B	C	D	E	F	G	H	I
<i>MMP13</i>	6 hours	0.48	-	-	1.57	1.53	-	-	-	1.64
	12 hours	-	-	-	4.62	-	-	-	-	-
	24 hours	-	-	-	0.30	1.89	-	0.52	-	-
	48 hours	0.65	-	-	-	-	-	0.74	-	-
<i>MMP1</i>	6 hours	-	-	-	1.50	-	-	-	-	-
	12 hours	-	-	-	6.62	-	-	-	-	-
	24 hours	-	-	-	-	-	1.52	-	-	-
	48 hours	-	-	-	-	-	-	-	-	-
<i>TIMP1</i>	6 hours	-	-	-	-	-	-	-	-	-
	12 hours	-	-	-	-	0.56	-	-	-	-
	24 hours	-	-	-	0.49	-	1.41	-	-	-
	48 hours	-	-	-	-	-	-	-	-	-
<i>COL2A1</i>	6 hours	-	-	-	2.97	-	-	-	2.63	-
	12 hours	-	-	-	10.30	-	-	-	-	-
	24 hours	-	-	5.28	0.27	-	-	-	-	-
	48 hours	-	-	0.35	-	-	-	-	1.68	1.80
<i>ACAN</i>	6 hours	-	-	-	2.18	-	-	-	-	-
	12 hours	-	-	4.28	2.37	0.59	-	-	-	-
	24 hours	-	-	-	-	1.57	-	-	-	-
	48 hours	-	-	1.61	0.27	-	-	-	1.72	-
<i>SOX9</i>	6 hours	-	-	-	0.52	1.69	-	-	-	-
	12 hours	-	-	3.08	-	-	-	-	-	-
	24 hours	-	-	-	0.37	-	-	-	1.65	-
	48 hours	-	-	-	-	-	-	-	1.84	-

Table 3.4: Significant ($P < 0.05$) fold changes in gene expression in response to stimulation with wildtype mouse GDF5 at 6, 12, 24 and 48 hours post stimulation in 9 OA patients, relative to untreated cells. A value greater than 1 denotes a significant upregulation of gene expression and a value less than 1 denotes a significant down regulation of gene expression. A dash (-) indicates no significant change in gene expression.

Gene	Time point after stimulation	Patient						
		J	K	N	O	P	Q	R
MMP13	6 hours	-	0.39	-	-	-	2.27	-
	12 hours	-	0.65	-	-	-	-	-
	24 hours	-	-	-	-	-	-	-
	48 hours	-	-	-	-	-	0.58	-
MMP1	6 hours	-	-	-	2.87	-	-	-
	12 hours	-	-	-	-	-	-	-
	24 hours	-	-	-	-	-	-	-
	48 hours	-	-	-	-	-	-	-
TIMP1	6 hours	-	0.52	-	3.46	-	-	-
	12 hours	-	-	-	-	-	-	-
	24 hours	-	-	-	-	-	-	-
	48 hours	-	-	-	-	-	-	-
COL2A1	6 hours	-	0.52	-	-	0.21	-	-
	12 hours	-	-	-	-	-	-	-
	24 hours	-	-	-	-	-	-	-
	48 hours	-	-	-	-	-	-	-
ACAN	6 hours	-	0.44	-	-	0.21	-	-
	12 hours	-	-	-	-	-	-	-
	24 hours	-	-	-	-	-	-	-
	48 hours	-	-	-	-	3.80	0.65	-
SOX9	6 hours	-	-	1.72	-	0.37	-	-
	12 hours	-	-	-	-	-	-	-
	24 hours	-	-	-	-	-	-	-
	48 hours	-	-	-	-	-	-	-

Table 3.5: Significant ($P < 0.05$) fold change in gene expression in response to stimulation with wildtype human GDF5 at 6, 12, 24 and 48 hours post stimulation in 7 OA patients, relative to untreated cells.

A value greater than 1 denotes a significant upregulation of gene expression and a value less than 1 denotes a significant down regulation of gene expression. A dash (-) indicated no significant change in gene expression.

Gene	Time point after stimulation	Patient						
		L	M	N	O	P	Q	R
MMP13	6 hours	0.54	-	-	1.83	-	-	-
	12 hours	0.56	1.88	0.63	-	-	-	-
	24 hours	-	-	-	-	-	-	-
	48 hours	-	-	-	-	-	0.67	-
MMP1	6 hours	0.55	-	-	2.34	-	-	-
	12 hours	-	2.01	-	-	-	-	-
	24 hours	-	1.21	-	-	-	-	-
	48 hours	-	1.55	-	-	-	-	-
TIMP1	6 hours	0.39	-	-	-	-	-	-
	12 hours	-	-	0.54	-	-	-	-
	24 hours	-	1.64	-	-	-	-	-
	48 hours	-	1.54	-	-	-	-	-
COL2A1	6 hours	0.50	-	-	-	0.36	-	-
	12 hours	0.60	-	-	-	0.38	-	-
	24 hours	-	0.65	-	-	-	-	-
	48 hours	-	-	-	-	-	-	-
ACAN	6 hours	-	-	2.00	3.03	-	-	-
	12 hours	0.66	2.58	-	-	0.36	-	-
	24 hours	-	-	-	-	-	-	-
	48 hours	1.75	-	-	-	-	-	-
SOX9	6 hours	-	-	-	5.54	0.56	-	-
	12 hours	-	2.13	-	-	0.43	-	-
	24 hours	-	-	-	-	-	-	-
	48 hours	-	-	3.22	-	-	-	-

Table 3.6: Significant ($P < 0.05$) fold change in gene expression in response to stimulation with human GDF5 variant A at 6, 12, 24 and 48 hours post stimulation in 7 OA patients, relative to untreated cells.

A value greater than 1 denotes a significant upregulation of gene expression and a value less than 1 denotes a significant down regulation of gene expression. A dash (-) indicates no significant change in gene expression.

Gene	Time point after stimulation	Patient						
		L	M	N	O	P	Q	R
MMP13	6 hours	0.63	0.55	-	-	-	-	0.42
	12 hours	0.63	-	0.57	-	-	-	0.19
	24 hours	-	-	-	-	-	-	-
	48 hours	-	-	-	-	-	-	-
MMP1	6 hours	-	-	-	-	0.30	-	-
	12 hours	-	-	0.67	-	2.23	-	-
	24 hours	-	1.22	-	-	-	-	-
	48 hours	-	-	-	-	-	-	-
TIMP1	6 hours	0.51	0.75	-	-	-	-	-
	12 hours	0.44	-	0.63	-	-	-	-
	24 hours	-	1.45	-	-	-	-	-
	48 hours	0.47	-	-	-	-	-	-
COL2A1	6 hours	-	0.33	-	-	-	-	-
	12 hours	-	-	-	-	0.21	-	-
	24 hours	0.50	0.37	-	-	-	-	-
	48 hours	-	-	3.85	-	-	-	-
ACAN	6 hours	-	-	-	-	-	-	-
	12 hours	-	-	0.58	-	0.14	-	-
	24 hours	-	-	-	-	-	-	-
	48 hours	-	-	-	-	-	-	-
SOX9	6 hours	0.47	-	-	-	0.39	-	-
	12 hours	-	-	-	-	0.26	-	0.49
	24 hours	-	-	-	-	-	-	-
	48 hours	0.51	-	-	-	-	-	-

Table 3.7: Significant ($P < 0.05$) fold change in gene expression in response to stimulation with human GDF5 variant B at 6, 12, 24 and 48 hours post stimulation in 7 OA patients, relative to untreated cells.

A value greater than 1 denotes a significant upregulation of gene expression and a value less than 1 denotes a significant down regulation of gene expression. A dash (-) indicates no significant change in gene expression.

Gene	Time point after stimulation	Patient				
		G	H	I	S	T
MMP13	6 hours	-	-	-	0.54	-
	12 hours	-	-	-	0.58	-
	24 hours	0.43	0.56	-	-	-
	48 hours	0.20	0.41	-	0.42	-
MMP1	6 hours	-	-	0.64	-	-
	12 hours	0.50	0.33	0.45	0.67	-
	24 hours	0.18	0.30	0.49	0.16	-
	48 hours	0.11	0.16	0.23	0.17	0.45
TIMP1	6 hours	5.55	2.21	-	-	-
	12 hours	7.85	2.15	1.61	1.45	-
	24 hours	6.73	3.34	1.66	1.85	1.52
	48 hours	11.30	3.40	2.31	1.75	2.00
COL2A1	6 hours	-	4.56	-	1.60	-
	12 hours	1.69	2.91	1.79	1.71	2.61
	24 hours	2.70	3.95	2.80	2.09	4.01
	48 hours	5.67	1.72	3.84	2.91	2.70
ACAN	6 hours	-	-	-	-	-
	12 hours	-	-	-	-	-
	24 hours	0.59	-	0.36	-	0.45
	48 hours	0.43	0.29	0.45	0.54	0.37
SOX9	6 hours	-	-	-	-	-
	12 hours	-	-	-	-	-
	24 hours	0.25	-	0.45	0.59	-
	48 hours	0.36	0.52	-	0.55	-

Table 3.8: Significant ($P < 0.05$) fold change in gene expression in response to stimulation with TGF- β 1 at 6, 12, 24 and 48 hours post stimulation in 5 OA patients, relative to untreated cells.

A value greater than 1 denotes a significant upregulation of gene expression and a value less than 1 denotes a significant down regulation of gene expression. A dash (-) indicates no significant change in gene expression.

Target gene	Growth factor				
	wildtype mGDF5	wildtype hGDF5	hGDF5 A	hGDF5 B	TGF- β 1
<i>MMP13</i>	0.8015	0.1300	0.0314	0.2794	0.035
<i>MMP1</i>	0.5144	0.1299	0.9546	0.4123	0.0001
<i>TIMP1</i>	0.8314	0.2146	0.7413	0.2794	0.0005
<i>COL2A1</i>	0.0974	0.8287	0.2896	0.3331	< 0.0001
<i>ACAN</i>	0.0552	0.3109	0.3109	0.4592	0.042
<i>SOX9</i>	0.9812	0.1035	0.5164	0.2597	0.0021

Table 3.9: P-values calculated using the Wilcoxon signed rank test for each target gene following growth factor stimulation.

mGDF5, mouse GDF5; hGDF5, human GDF5. P<0.05 are highlighted in red.

In summary, chondrocytes from OA patients did not respond consistently to exogenous GDF5, whereas chondrocytes from OA patients showed a very consistent response to stimulation with TGF- β 1.

3.2.6 Changes in gene expression in response to IL-1 α and oncostatin M in OA chondrocytes

In order to determine if the chondrocytes are able to respond to exogenous stimuli other than members of the TGF- β superfamily, chondrocytes harvested from the 20 OA patients used in section 3.2.5 were cultured with IL-1 α (0.05ng/ml) and recombinant oncostatin M (OSM; 10ng/ml) for 24 hours (Chapter 2.11.3). IL-1 α and OSM stimulations have been shown previously to significantly increase *MMP1* and *MMP13* gene expression (Koshy *et al.*, 2002). All patients studied showed a significant upregulation of *MMP1* (P<0.0001) and *MMP13* (P<0.0001) expression in response to IL-1 α and OSM stimulation, therefore, these cells are capable of responding to these cytokines (Figure 3.12, Table 3.10 and 3.11).

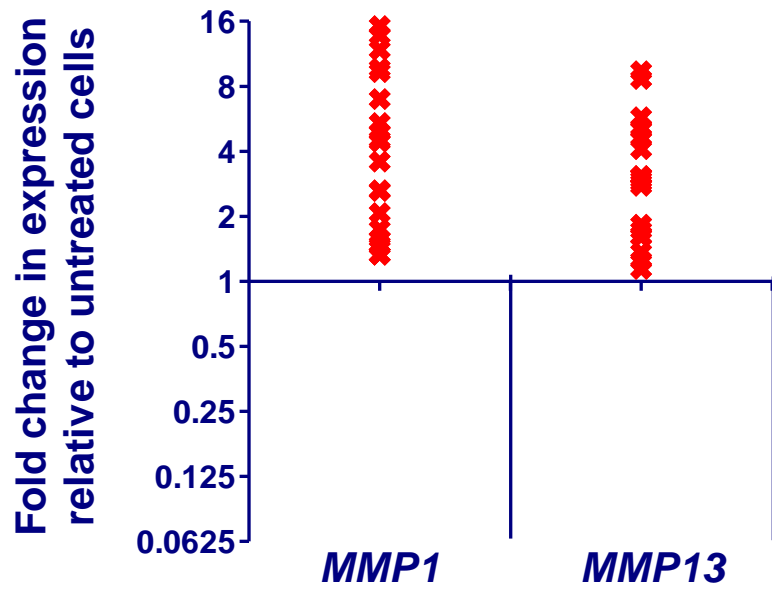


Figure 3.12: Fold change in *MMP1* and *MMP13* gene expression in response to IL-1 α and OSM simulation for 24 hours. Each cross represents a significant ($P < 0.05$) up/down regulation of gene expression relative to untreated cells in one patient. Twenty patients were studied in total.

Patient	Gene	
	<i>MMP1</i>	<i>MMP13</i>
A	2.07	1.62
B	1.33	1.25
C	3.59	1.61
D	1.48	1.72
E	4.53	3.06
F	1.33	1.83
G	9.67	5.03
H	1.45	1.14
I	2.62	1.36
J	4.43	3.05
K	13.80	8.64
L	1.57	2.77
M	5.41	3.08
N	1.74	2.95
O	9.32	9.40
P	2.64	4.09
Q	15.20	4.66
R	4.90	2.86
S	6.98	5.76
T	11.80	5.07

Table 3.10: Significant ($P < 0.05$) fold change in gene expression in response to stimulation with IL-1 α and OSM at 24 hours post stimulation in 20 OA patients, relative to untreated cells.

Target gene	IL-1 α and OSM
<i>MMP1</i>	< 0.0001
<i>MMP13</i>	< 0.0001

Table 3.11: P-values calculated using the Wilcoxon signed rank test for each target gene following IL-1 α and OSM stimulation.

3.3 Discussion

Chondrocytes from OA patients express the genes coding for the GDF5 receptors, in particular, *BMPR-II* and *BMPR-IA*. The gene expression of *BMPR-IB*, which encodes the type I receptor that GDF5 preferentially binds to, was 60 and 16 fold lower in OA and NOF cartilage respectively, than that of the alternative type I receptor *BMPR-IA*.

Drabobinac *et al.*, 2008 have carried out immunohistochemistry on OA and normal articular cartilage to examine the expression pattern of *BMPR-II*, *BMPR-IA* and *BMPR-IB*. They observed strong expression of *BMPR-II* and *BMPR-IA* with no difference in expression levels between OA and normal cartilage. However, the expression of *BMPR-IB* was low in normal cartilage and was not detected in OA cartilage (Drabobinac *et al.*, 2008). My results show a 2.5 fold lower expression of *BMPR-IB* in OA cartilage compared to NOF cartilage, however this was not significant. In addition to wildtype forms of GDF5 from mouse and human, I have also utilised two variants of human GDF5 in this study, which were designed by Biopharm. One was designed to preferentially bind to *BMPR-IA*, and the other variant was insensitive to the GDF5 antagonist noggin. This allowed me to determine if chondrocytes will better respond to these variants, compared to the wildtype form.

Stimulation of SW1353 with all four forms of GDF5 at 100 ng/ml significantly increased luciferase activity of the Smad 1/5/8 vector at 6, 12, 24 and 48 hours after stimulation. This suggests that the GDF5 signal was translocated to the nucleus.

Western blots carried out using phosphorylated Smad 1/5/8 antibody showed that stimulation of chondrocytes with all four types of recombinant GDF5 protein activates this signalling pathway.

I then carried out real time PCR analysis on a panel of genes that encode anabolic and catabolic markers after stimulation of the chondrocytes with the four GDF5 proteins. The proteins triggered gene expression changes of all genes analysed, however, a predictable response was not seen among patients with any of the four different forms of GDF5. Although variant A has been manufactured to show higher affinity to *BMPR-IA*, which chondrocytes abundantly express, and variant B is insensitive to noggin, a consistent response was not observed in cells treated with these variant forms of GDF5.

In contrast, TGF- β 1 treatment in these cells upregulated *TIMP1*, *COL2A1* and down regulated *MMP1*, *MMP13*, *SOX9* and *ACAN* in all patients analysed. Also, IL-1 α and OSM treatment upregulated *MMP1* and *MMP13* in all patients. The chondrocytes were therefore clearly capable of responding to exogenous stimuli, including to growth factors of the TGF- β superfamily.

Together, these data indicate that the cells are not responding to exogenous GDF5 in a consistent manner, whereas a consistent response was observed in these cells when treated with exogenous TGF- β 1.

Age-related reduction in chondrocytes' response to growth factors may account for the observed inconsistency in response to exogenous GDF5. Guerne *et al.* (1995) have shown a reduction in proliferative response with increasing age in chondrocytes in response to exogenous growth factors. In that study chondrocytes were harvested from the articular cartilage of donors aged 11-83 years and who had no history of joint disease. The cells were cultured in the presence of PDGF-AA, FGF-2, IGF-1 and TGF- β 1, and the rate of cell proliferation was measured by ^3H -thymidine incorporation. The proliferative response of chondrocytes to all growth factors tested was reduced with increasing age. Interestingly, the authors observed that TGF- β 1 was the most potent stimulant analysed, and was the only factor that consistently and significantly increased the proliferation rate in chondrocytes from older donors (those aged 44 and above).

Loeser *et al.* (2000) assessed the effect of ageing and OA on the response of chondrocytes to IGF-1 in cynomolgus monkeys that have naturally occurring OA. The authors observed a significant reduction in response to IGF-1 with increasing age and histologic OA score, as measured by radiolabeled sulphate and proline incorporation assays. The authors suggest that possible causes for a reduction in response may include an age-related reduction in the levels of IGF-1 receptors, defective signal transduction or a change in the synthesis of certain molecules necessary to achieve the full response to IGF-1.

My results showed that the Smad 1/5/8 signalling pathway was activated in chondrocytes in response to exogenous GDF5. However, other intracellular events downstream of Smad 1/5/8 may be suboptimal, which may explain the cells' inability

to show a consistent response to exogenous GDF5. It has been reported that the cellular environment within a damaged joint can alter the response to members of the BMP family. For example IL-1 β , which is upregulated in OA can increase the expression of Smad 7 (an inhibitor of BMP intracellular signalling; Goldring and Berenbaum, 2004; Baugé *et al.*, 2008). Also, fibroblast growth factor (FGF) signalling can directly inhibit Smad 1 activity, which in turn inhibits BMP intracellular signalling (Kretzschmar *et al.*, 1997). FGFs have also been shown to down regulate BMPR-IB expression in avian limb cells (Merino *et al.*, 1998).

Therefore, the loss of the chondrocytes' response to growth factors, including GDF5, can be a cause or a consequence of the OA disease process. A loss of response to growth factors during ageing may contribute to the development and progression of OA, resulting in an altered balance between anabolism and catabolism. Furthermore, an increase in cytokine production during the disease process can result in defective downstream signalling that may give rise to the observed inconsistency in response to exogenous GDF5. Hence, it is important to develop a means to enhance the responsive capacity of chondrocytes to exogenous growth factors if treatment with GDF5 is going to be advanced as a potential therapeutic to overcome the genetic deficit mediated by the OA risk allele at rs143383.

Chapter 4: Allelic expression analysis of the osteoarthritis susceptibility locus that maps to *MICAL3*

4.1 Introduction

Stage one of the arcOGEN GWAS with over 67,000 individuals of European descent identified an association to SNP rs2277831 (A/G), with a P-value of 2.3×10^{-5} and an odds ratio for allele G of 1.07 in knee and/or hip OA (Panoutsopoulou *et al.*, 2011).

rs2277831 is located within an intron of the *MICAL3* gene, which codes for the microtubule-associated monooxygenase, calponin and LIM domain containing 3 protein. The *MICAL3* protein is thought to be involved in the vesicle transport system in mammalian cells through the interaction with Rabs, which are small GTPases (Fischer *et al.*, 2005; Grigoriev *et al.*, 2011). Two additional genes map close by and are encompassed by the association signal. These are *BCL2L13*, which codes for the BCL2-like 13 (also known as BCL-Rambo) protein, and *BID*, which codes for the BH3 interacting domain death agonist protein.

The *BCL2L13* protein is a pro-apoptotic member of the BCL2 family of proteins. It has been reported that *BCL2L13* induces apoptosis by reducing the mitochondrial membrane potential, which results in the activation of Caspase-3 (Kataoka *et al.*, 2001; Kim *et al.*, 2012). The *BID* protein is another member of the BCL2 family of proteins and also has pro-apoptotic roles. *BID* is cleaved by Caspase-8, which once cleaved, translocates to the mitochondria where it forms heterodimers with *BAX*, triggering the release of cytochrome *c*. This leads to the activation of apoptotic pathways (Desagher *et al.*, 1999). *BID* can also be phosphorylated in response to DNA damage, which is mediated by ataxia-telangiectasia mutated (*ATM*) kinase. This results in cell cycle arrest at the S phase, which is important for maintaining genomic stability through activating DNA repair pathways or by triggering apoptosis (Zinkel *et al.*, 2005; Gross, 2006).

As chondrocyte apoptosis is a characteristic of OA, it is interesting that the OA associated locus maps closely to two genes whose products belong to the BCL2 family of proteins that play crucial roles in apoptosis. Furthermore, it has been documented that OA cartilage shows increased expression of BCL2 and Caspase-3, which correlates with chondrocyte apoptosis and OA lesions (Kim *et al.*, 2000; Blanco *et al.*, 2004). Also,

OA chondrocytes have been shown to have a reduced mitochondrial membrane potential, which is associated with mitochondrial swelling, disruption of the outer membrane of the mitochondria and the release of cytochrome *c* (Crompton, 1999).

Scrutinizing public databases reveals that *BCL2L13*, *BID* and *MICAL3* are expressed in various tissue types, including adipose tissue, blood, bone, brain, cartilage, heart, liver, kidney and muscle.

BCL2L13 has 14 transcript isoforms, of which 8 are protein coding (Figure 4.1). Ensembl transcript ID ENST00000317582 codes for the longest *BCL2L13* protein isoform, which is 485 amino acids in length. *BID* has 10 transcript isoforms, of which 6 are protein coding (Figure 4.2). The longest *BID* protein isoform, which is 241 amino acids in length, is coded by ENST00000317361 transcript isoform. *MICAL3* has 19 transcript isoforms, of which 15 are protein coding (Figure 4.3). The longest *MICAL3* protein isoform is 2002 amino acids in length and is coded for by transcript isoform ENST00000441493. rs2277831 resides in an intron in 3 of the 19 *MICAL3* transcript isoforms, which are all protein coding. The SNP resides in intron 27 of ENST00000441493 and in intron 2 of ENST00000577821 and ENST00000579997.

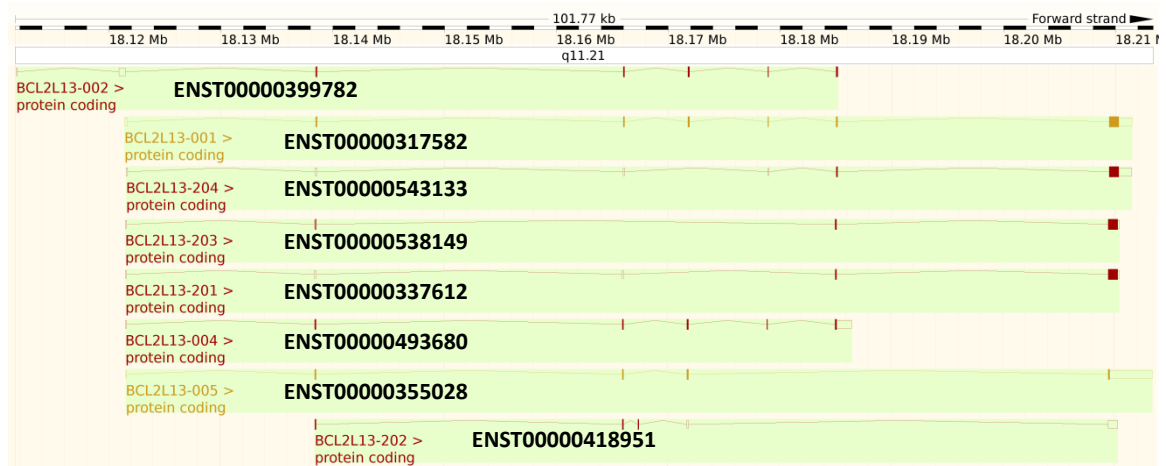


Figure 4.1: The eight protein coding transcript isoforms of *BCL2L13* (from www.ensembl.org). The horizontal bar across the top of the figure shows the forward strand of chromosome 22q11.21 from left to right. The transcript isoforms of *BCL2L13* are shown as horizontal lines and rectangles within the area highlighted in green. The shaded rectangles represent the coding part of exons, whilst the unshaded rectangles represent the UTRs. The horizontal lines show the introns of *BCL2L13*. The ensembl transcript IDs are shown below each transcript.

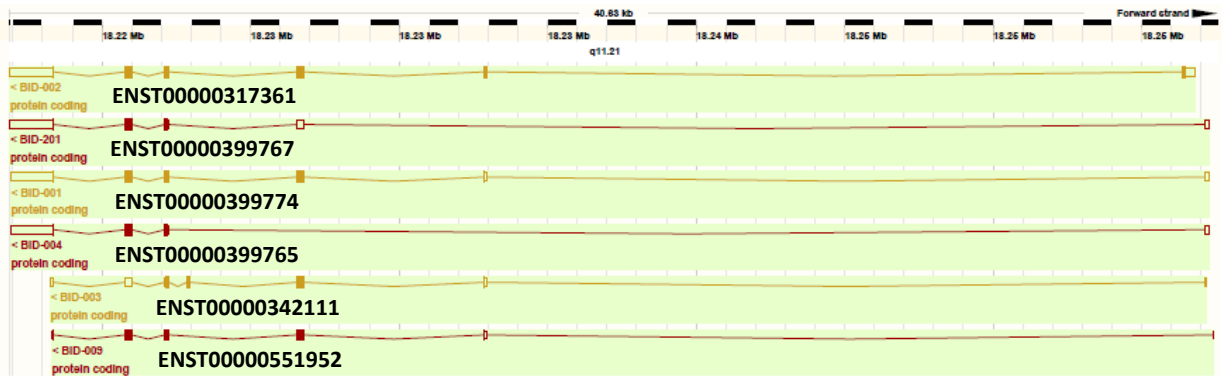


Figure 4.2: The six protein coding transcript isoforms of *BID* (from www.ensembl.org). The horizontal bar across the top of the figure shows the forward strand of chromosome 22q11.21 from left to right. The transcript isoforms of *BID* are shown as horizontal lines and rectangles within the area highlighted in green. The shaded rectangles represent the coding part of exons, whilst the unshaded rectangles represent the UTRs. The horizontal lines show the introns of *BID*. The ensembl transcript IDs are shown below each transcript.

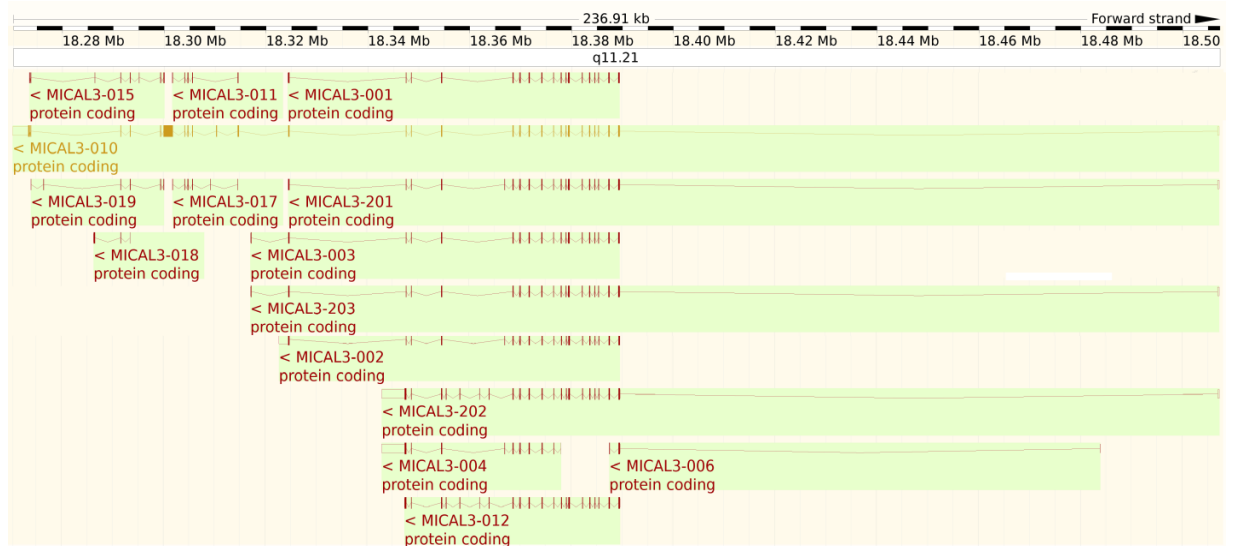


Figure 4.3: The fifteen protein coding transcript isoforms of *MICAL3* (from www.ensembl.org). The horizontal bar across the top of the figure shows the forward strand of chromosome 22q11.21 from left to right. The transcript isoforms of *MICAL3* are shown as horizontal lines and rectangles within the area highlighted in green. The shaded rectangles represent the coding part of exons, whilst the unshaded rectangles represent the UTRs. The horizontal lines show the introns of *MICAL3*. The transcript names are shown below each transcript, and the corresponding ensembl transcript IDs are listed in Table 4.1.

Transcript name	Ensembl transcript ID
MICAL3-001	ENST00000383094
MICAL3-002	ENST00000414725
MICAL3-003	ENST00000400561
MICAL3-004	ENST00000461307
MICAL3-006	ENST00000424046
MICAL3-010	ENST00000441493
MICAL3-011	ENST00000498573
MICAL3-012	ENST00000585038
MICAL3-015	ENST00000577821
MICAL3-017	ENST00000578984
MICAL3-018	ENST00000584751
MICAL3-019	ENST00000579997
MICAL3-201	ENST00000207726
MICAL3-202	ENST00000429452
MICAL3-203	ENST00000444520

Table 4.1: The fifteen protein coding *MICAL3* transcript isoform names and their corresponding ensembl transcript IDs

As the number of susceptibility loci that are identified for common human diseases increases, it is becoming clear that many, if not the majority, of associated alleles contribute to disease risk by acting as expression quantitative trait loci (eQTLs), influencing the expression or stability of a transcript (Cookson *et al.*, 2009; Montgomery and Dermitzakis, 2011). In the majority of cases eQTLs act in an organ or even tissue specific manner. It is important therefore to study RNA extracted from tissues relevant to the disease when assessing the potential effect of eQTLs.

I hypothesised that the OA association to rs2277831 may be marking an eQTL. To assess this I have measured the overall expression of *BCL2L13*, *BID* and *MICAL3* using real time PCR and stratified the expression by the genotype at rs2277831. I also tested for allelic expression imbalance (AEI) of *BCL2L13*, *BID* and *MICAL3* using transcript SNPs and assays that can accurately discriminate and quantify the mRNA synthesised from each allele. I examined RNA extracted from the joint tissues of patients undergoing elective joint replacement surgery.

4.2 Results

4.2.1 Qualitative gene expression analysis of *BCL2L13*, *BID* and *MICAL3* in joint tissue cDNAs

In order to assess if *BCL2L13*, *BID* and *MICAL3* were expressed in joint tissues, RNA extracted from cartilage, fatpad, synovium, cancellous bone and osteophytes from OA patients were reverse transcribed to synthesise complimentary DNAs (cDNAs; Chapter 2.3). These were then PCR amplified using primers listed in Table 2.4 (Chapter 2.4).

The primers that were designed for *BCL2L13* targeted common regions in 4 of 8 protein coding transcript isoforms (ENST00000317582, ENST00000543133, ENST00000538149 and ENST00000337612) of the gene. These transcript isoforms were the only isoforms that carry the SNPs which were later selected for AEI analyses. *BCL2L13* was expressed in all tissues of the joint analysed, with particularly high levels observed in cartilage, fatpad and cancellous bone (Figure 4.4).

The primers designed for *BID* targeted all 6 protein coding transcript isoforms of this gene. *BID* was expressed in all tissues of the joint analysed, with particularly high levels observed in cartilage, fatpad and synovium (Figure 4.5).

Initially, *MICAL3* expression in joint tissues was assessed using primers that targeted common regions in 9 of 15 protein coding transcript isoforms. These transcripts of *MICAL3* were expressed in all tissues of the joint analysed, with particularly high levels observed in synovium, cancellous bone and osteophyte tissue (Figure 4.6).

The expression of transcript isoforms derived from the part of the *MICAL3* gene that harbours the associated SNP rs2277831 were assessed using a different set of primers listed in Table 2.4 (*MICAL3* (2), Chapter 2.4). This amplicon targeted common regions of ENST00000441493, ENST00000577821 and ENST00000579997. The primer pair used in this experiment targeted exons 26 and 28 of ENST00000441493 and exons 1 and 3 of ENST00000579997, producing a PCR product of 177 bp in length. The expression of at least one of these two transcript isoforms were observed in all tissues of the joint analysed, with particularly high levels observed in cancellous bone (Figure 4.7). ENST00000577821 contains an additional 51 bp exon, which is absent in

ENST00000441493 and ENST00000579997, producing a PCR product of 228 bp in length. The expression of ENST00000577821 was observed in cartilage and synovium tissue and was absent in other tissues of the joint analysed (Figure 4.7). Expression of ensembl transcript IDs ENST00000461307, ENST00000498573, ENST00000578984 and ENST00000584751 were not assessed in this experiment.

In summary of section 4.2.1, *BCL2L13*, *BID* and *MICAL3* were expressed in all joint tissues tested.

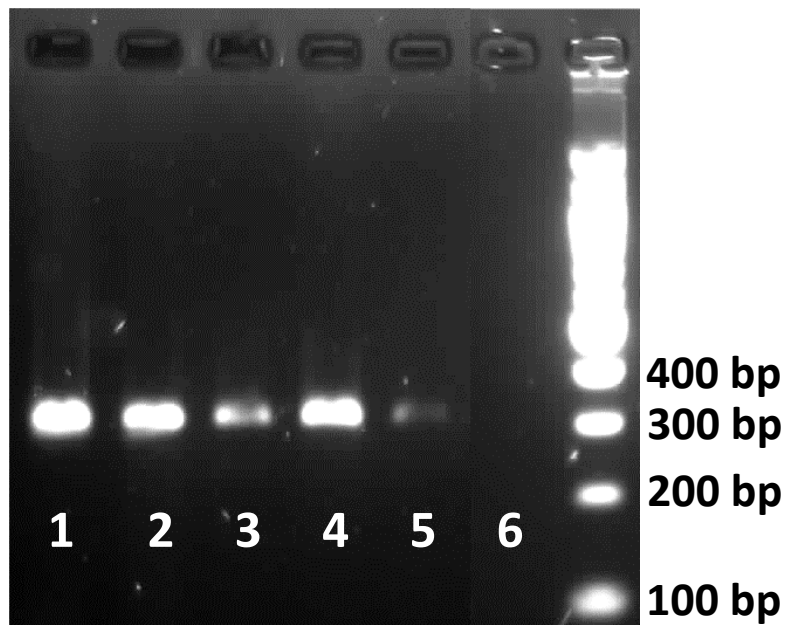


Figure 4.4: *BCL2L13* expression in joint tissue cDNAs.

Lane 1: cartilage, 2: fatpad, 3: synovium, 4: cancellous bone, 5: osteophyte, 6: PCR blank. The PCR products were run on a 2% agarose gel containing ethidium bromide. A 100 bp DNA ladder was used for sizing of PCR products.

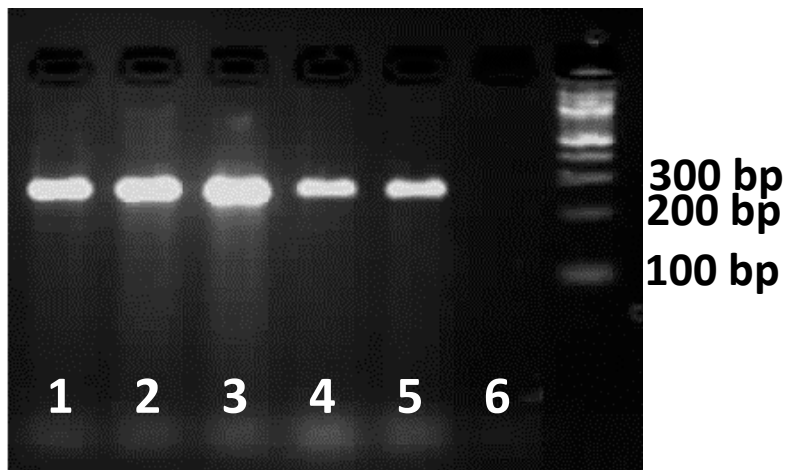


Figure 4.5: *BID* expression in joint tissue cDNAs.

Lane 1: cartilage, 2: fatpad, 3: synovium, 4: cancellous bone, 5: osteophyte, 6: PCR blank.
The PCR products were run on a 2% agarose gel containing ethidium bromide. A 100 bp DNA ladder was used for sizing of PCR products.

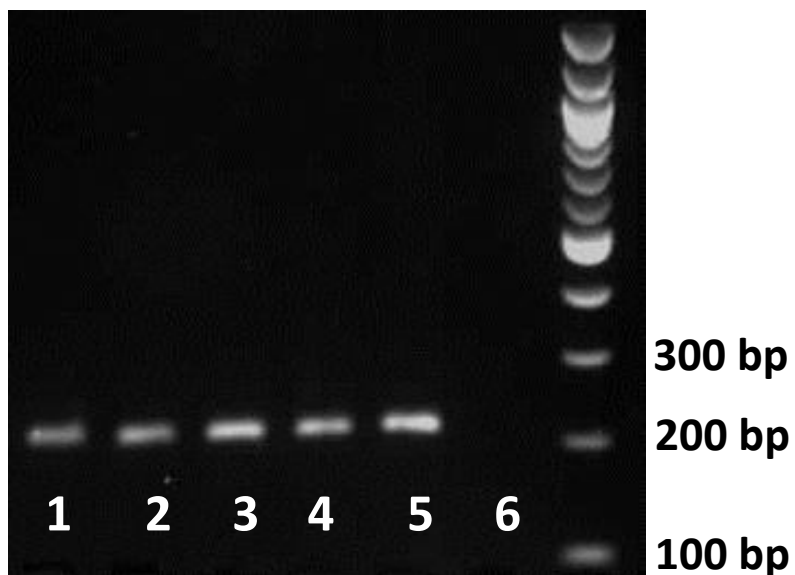


Figure 4.6: *MICAL3* expression in joint tissue cDNAs.

Lane 1: cartilage, 2: fatpad, 3: synovium, 4: cancellous bone, 5: osteophyte, 6: PCR blank.
The PCR products were run on a 2% agarose gel containing ethidium bromide. A 100 bp DNA ladder was used for sizing of PCR products.

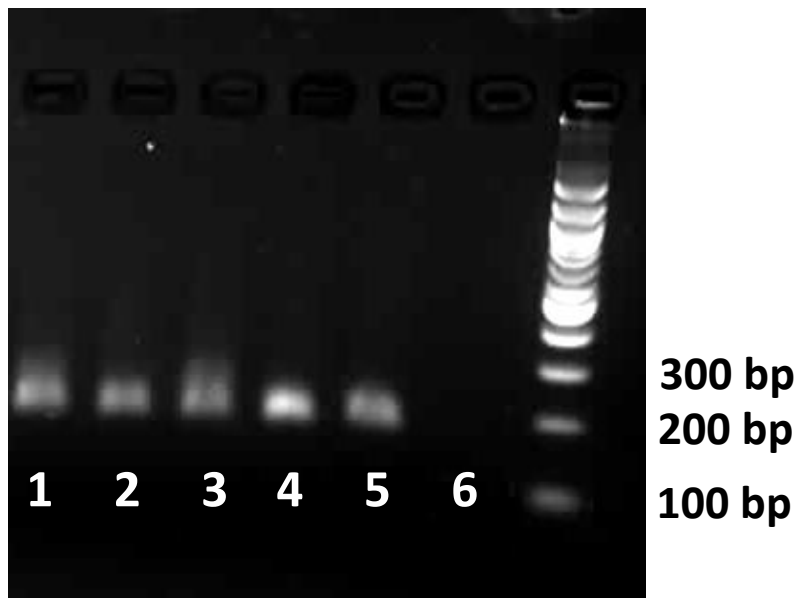


Figure 4.7: *MICAL3* ensembl transcript IDs ENST00000441493, ENST00000577821 and ENST00000579997 expression in joint tissue cDNAs.

Lane 1: cartilage, 2: fatpad, 3: synovium, 4: cancellous bone, 5: osteophyte, 6: PCR blank. The PCR products were run on a 2% agarose gel containing ethidium bromide. A 100 bp DNA ladder was used for sizing of PCR products.

4.2.2 *BCL2L13*, *BID* and *MICAL3* expression in cartilage tissue stratified by genotype at rs2277831

To assess whether the OA association to rs2277831 can influence the expression of *BCL2L13*, *BID* or *MICAL3*, I measured the expression of these genes quantitatively using real time PCR and cDNA synthesised from RNA that had been extracted from cartilage tissue. A total of 55 OA patients were studied, 12 who had hip OA and 43 who had knee OA. Cartilage tissue was analysed as this is the principle tissue type involved in OA. Gene expression was measured using the real time PCR assays listed in Table 2.2 (Chapter 2.17). The real time PCR assay for *BCL2L13* captures 4 of the 8 protein coding transcript isoforms (ENST00000399782, ENST00000317582, ENST00000543133 and ENST00000493680) and that for *BID* captures all 6 protein coding transcript isoforms. The real time PCR assay for *MICAL3* targets 9 of 15 protein coding transcript isoforms: ENST00000383094, ENST00000414725, ENST00000400561, ENST00000461307, ENST00000441493, ENST00000585038, ENST00000207726, ENST00000429452 and ENST00000444520. The expression data were then stratified by the genotype at rs2277831. This SNP was genotyped using DNA extracted from the cartilage samples

(Chapter 2.20). Linear regression was then performed to determine if the gene expression relative to genotype differed significantly from the null (Figure 4.8).

Of the 55 OA patients analysed, three patients were homozygous GG, 21 were heterozygous and 31 were homozygous AA. There was no significant correlation between genotype at rs2277831 and the expression of *BCL2L13*, *BID* or *MICAL3*, with P-values of 0.06, 0.51 and 0.38, respectively (Figure 4.8).

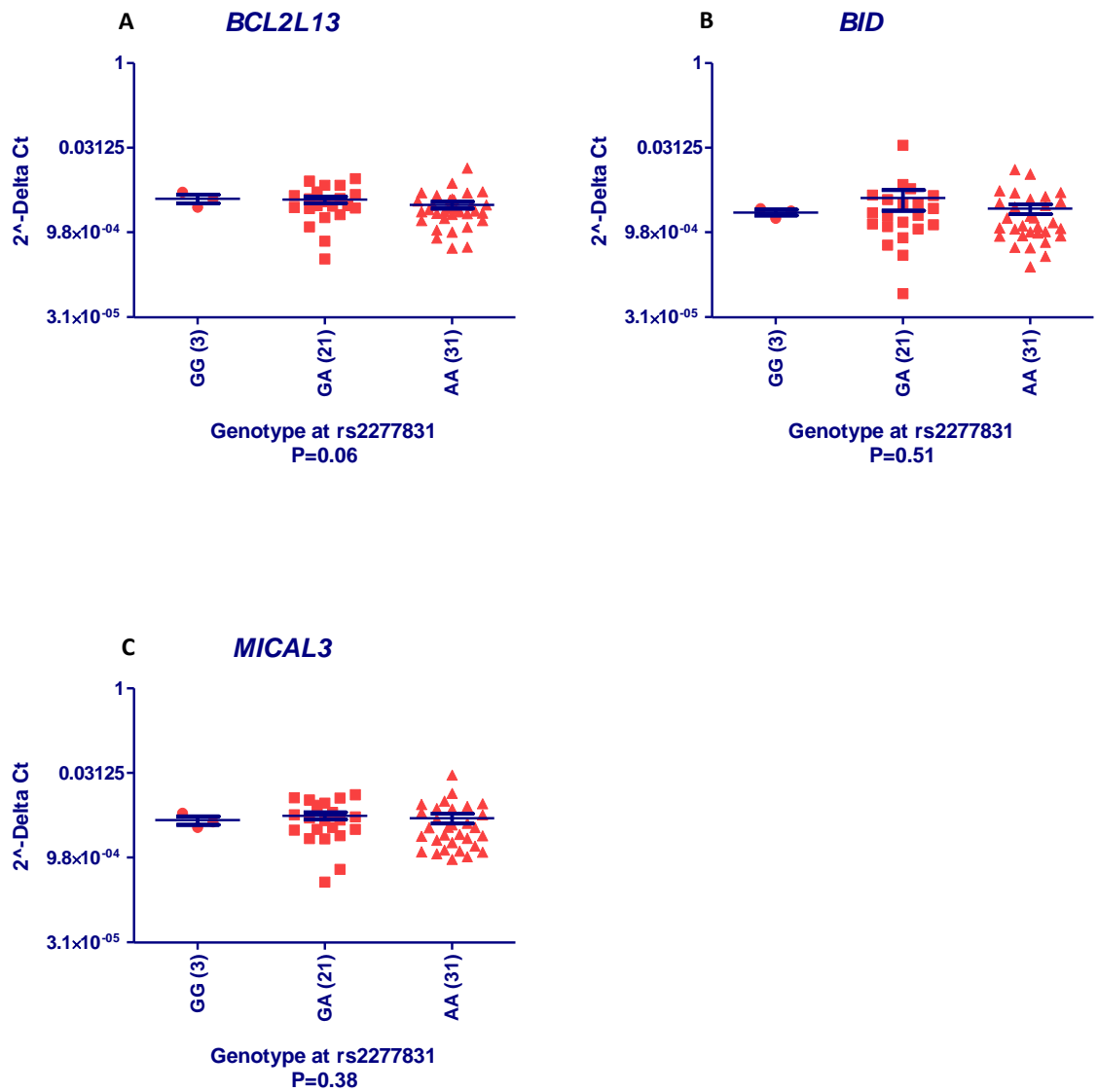


Figure 4.8: Expression of (A) *BCL2L13*, (B) *BID* and (C) *MICAL3* stratified by the genotype at the OA associated SNP rs2277831 in cartilage tissue from 55 OA patients. The data points represent the average of three technical replicates for each sample. The expression of *BCL2L13*, *BID* and *MICAL3* were compared to the average of the housekeeping genes and the $2^{-\Delta\text{Ct}}$ values were plotted against genotype. The horizontal bars represent the mean plus the standard error of the mean. A linear regression was performed to assess the correlation between gene expression and genotype and the P-values are shown below each graph.

Correlating genotype with overall gene expression is vulnerable to the natural fluctuation in gene expression, which can be influenced by patient gender, age and ethnic background. Therefore this technique is liable to generating false-negative results, due to the reduced sensitivity and accuracy of this method (Johnson *et al.*, 2008). Directly testing for allelic expression differences can overcome this, therefore this was the technique that I then used.

4.2.3 Database searching for polymorphisms

HapMap genome browser (<http://hapmap.ncbi.nlm.nih.gov/>) was used to query the genotype frequency and linkage disequilibrium (LD) database to search for polymorphisms on chromosome 22q11.21 that have been genotyped in the CEU population (individuals of European ancestry). Transcribed polymorphisms in *BCL2L13*, *BID* and *MICAL3* with high minor allele frequency (MAF) of more than 15% in the population were selected using the National Centre for Biotechnology Information (NCBI) variation database (dbSNP; <http://www.ncbi.nlm.nih.gov/projects/SNP/>).

Eight transcribed SNPs were selected on chromosome 22q11.21: rs4488761, rs2587100, rs9967, rs11538, rs5992854, rs11917, rs1057721 and rs4819639. These transcribed SNPs were used to carry out AEI analyses (Table 4.2, Figure 4.9).

SNP	Position on chr. 22 on NCBI genome build 37.3	Alleles	MAF*	Gene	Location of SNP in gene	Pairwise linkage disequilibrium relative to the OA associated SNP rs2277831	
						D'	r ²
rs4488761	18209613	A/G	0.46	<i>BCL2L13</i>	3'UTR/exonic [^]	0.11	0.00
rs2587100	18210704	C/G	0.40	<i>BCL2L13</i>	3'UTR	0.02	0.00
rs9967	18211205	C/T	0.38	<i>BCL2L13</i>	3'UTR	0.21	0.01
rs11538	18220831	T/C	0.18	<i>BID</i>	3'UTR/exonic [^]	0.12	0.00
rs5992854	18300240	T/C	0.32	<i>MICAL3</i>	exonic	1.00	0.71
rs11917	18343011	G/T	0.41	<i>MICAL3</i>	3'UTR	0.76	0.11
rs1057721	18343843	G/A	0.41	<i>MICAL3</i>	3'UTR	0.78	0.13
rs4819639	18347127	C/T	0.29	<i>MICAL3</i>	3'UTR	0.74	0.06

Table 4.2: The eight transcript SNPs studied at chr22q11.21

*Minor Allele Frequency in Europeans (dbSNP (<http://www.ncbi.nlm.nih.gov/projects/SNP/>))

[^]Multiple predicted splice isoforms result in different potential locations in the transcript

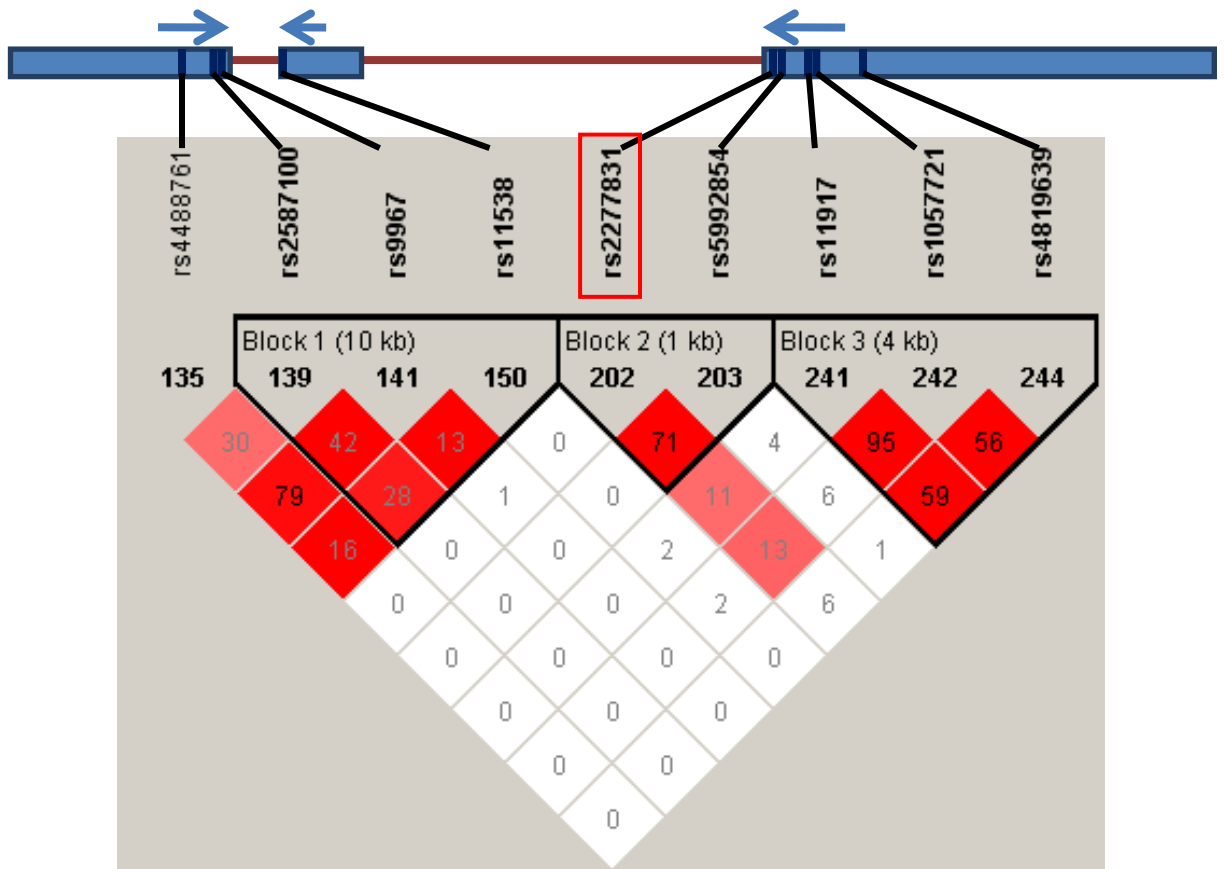


Figure 4.9: Linkage disequilibrium around *BCL2L13*, *BID* and *MICAL3* showing the eight transcript SNPs and the associated SNP rs2277831, outlined in red (<http://hapmap.ncbi.nlm.nih.gov/>). The numbers within boxes represent the r^2 values between each SNP. The blocks illustrate a group of SNPs which are in high linkage disequilibrium with each other. Arrows indicate the direction in which each gene is transcribed.

4.2.4 Allelic expression imbalance at *BCL2L13*, *BID* and *MICAL3* in cartilage tissue

I identified 33 patients who were heterozygous at one or more of the eight transcript SNPs using RFLP assays listed in Table 2.6 (Chapter 2.20). Thirty-two of the 33 were OA patients whereas patient 15 had undergone joint surgery due to a neck-of-femur (NOF) fracture. For two of the OA patients, more than one tissue type was collected: fatpad and synovium for patient 25, cancellous bone and osteophyte for patient 33. For all other patients only one tissue type per patient was collected (Table 4.3). I performed AEI analysis on cDNA synthesised from the RNA extracted from the patient tissues either by using Sequenom iPLEX assays or real time quantitative PCR genotyping assays (Chapter 2.21 and Chapter 2.22). The patients' genomic DNA (gDNA) from the

corresponding tissues were used to normalise the allelic expression ratios, and a two-tailed Mann-Whitney exact test was performed to compare the distribution between allelic ratios of gDNA and cDNA replicates. A patient was considered to show AEI if the P-value was less than 0.05 and the AEI observed was 20% or greater (Chapter 2.32.4).

Twenty-eight of the 33 patients were heterozygous for one or more of the three *BCL2L13* transcript SNPs. Twelve of the 28 demonstrated AEI (data highlighted in yellow in Table 4.3). Of these 12 patients, three were heterozygous for the associated SNP rs2277831 (patients 6, 27 and 28), three were homozygous GG at rs2277831 and six were homozygous AA at rs2277831. AEI at *BCL2L13* did not therefore correlate with the genotype at rs2277831. The largest allelic ratio observed at *BCL2L13* was 2.82 (P=0.004) at transcript SNP rs2587100 for patient 11 (Figure 4.10), who is homozygous AA at rs2277831.

Eleven patients were heterozygous for the *BID* transcript SNP rs11538. Three of the eleven demonstrated AEI, patients 8, 30 and 31 (data highlighted in blue in Table 4.3). There was no correlation between genotype at rs2277831 and AEI at *BID*, with all three patients being homozygous AA at this SNP. The largest allelic ratio observed at *BID* was 2.09 (P=0.001) in patient 30 (Figure 4.10).

Twenty-seven patients were heterozygous for one or more of the four *MICAL3* transcript SNPs, of which 19 demonstrated AEI (data highlighted in green in Table 4.3). Of these 19, five were heterozygous for the associated SNP rs2277831 (patients 4, 6, 18, 28 and 32), one was homozygous GG at rs2277831 and 13 were homozygous AA. AEI at *MICAL3* did not therefore correlate with genotype at rs2277831. The largest allelic ratio observed at *MICAL3*, and at any of the three genes studied, was 5.47 (P=0.001) at transcript SNP rs5992854 for patient 9 (Figure 4.10), who is homozygous AA at rs2277831.

The average allelic expression ratios for the heterozygotes at the eight transcript SNPs were plotted and stratified by genotype at rs2277831 (Figure 4.11). At any of the transcribed SNPs, a Kruskal-Wallis test showed no significant evidence of a difference in the allelic expression ratios between the different genotypes at rs2277831 (P-values of 0.45 at rs4488761, 0.11 at rs2587100, 0.20 at rs9967, 0.15 at rs11538, 0.88 at rs5992854, 0.35 at rs11917, 0.41 at rs1057721 and 0.53 at rs4819639).

Overall, I have studied hip cartilage, knee cartilage, fatpad, synovium, cancellous bone and osteophyte tissue in OA patients and hip cartilage from a NOF patient. Although I observed AEI for one or more of the tissues in each gene, the AEI does not correlate with genotype at the OA associated SNP rs2277831.

Patient number	Sex	Age at surgery (years)	Tissue*	BCL2L13				BID				MICAL3								
				rs4488761		rs2587100		rs9967		rs11538		rs2277831	rs5992854		rs11917		rs1057721		rs4819639	
				Gen [^]	AER† (A/G)	Gen [^]	AER† (C/G)	Gen [^]	AER† (C/T)	Gen [^]	AER† (T/C)	Gen [^]	Gen [^]	AER† (T/C)	Gen [^]	AER† (T/G)	Gen [^]	AER† (G/A)	Gen [^]	AER† (C/T)
1	F	55	Cart (K)	AG	1.04	CG	0.67	CT	0.71	TC	0.90	GG	CC	-	GG	-	AA	-	CC	-
2	M	74	Cart (K)	AG	1.15	CG	1.03	CT	0.91	TT	-	GG	CC	-	GG	-	AA	-	CC	-
3	M	82	Cart (K)	AA	-	CG	0.83	TT	-	TC	1.10	GA	TC	1.13	GG	-	AA	-	CT	0.96
4	M	57	Cart (K)	AG	0.95	CG	0.87	CT	1.09	TC	1.06	GA	TC	0.56	TG	1.30	GA	2.10	CT	1.38
5	F	57	Cart (K)	AA	-	GG	-	TT	-	TT	-	GA	TC	1.14	TG	0.88	GA	0.84	CT	0.90
6	M	58	Cart (K)	AA	-	CG	0.78	TT	-	TT	-	GA	TC	1.30	TG	1.11	GA	0.87	CT	1.02
7	M	71	Cart (K)	GG	-	GG	-	CC	-	TT	-	GA	TC	1.02	GG	-	AA	-	CC	-
8	F	72	Cart (K)	AG	1.09	CG	0.91	CT	1.15	TC	1.54	AA	TT	-	TG	1.51	GA	0.85	CT	0.87
9	M	64	Cart (K)	AG	0.91	CG	1.01	CT	1.09	TT	-	AA	TC	5.47	TT	-	GG	-	CC	-
10	M	76	Cart (K)	GG	-	CG	0.88	CT	1.33	TT	-	AA	TT	-	TG	1.01	GA	1.51	CT	0.82
11	F	66	Cart (K)	AG	1.40	CG	2.82	CT	0.57	TT	-	AA	TC	1.22	TT	-	GG	-	TT	-
12	F	67	Cart (H)	AG	1.67	CG	1.98	CT	1.01	TT	-	AA	TC	0.83	TT	-	GG	-	TT	-
13	F	76	Cart (H)	AG	1.04	CG	0.99	CT	1.22	TC	1.01	AA	TT	-	TG	0.76	GA	1.14	CT	1.49
14	F	50	Cart (H)	GG	-	CG	0.94	CC	-	TT	-	AA	TT	-	TT	-	GG	-	CT	0.83
15	M	83	Cart (H)	AG	0.97	CG	1.00	CT	1.18	TC	0.96	AA	TC	1.03	TG	1.00	GA	1.16	CT	0.93
16	M	62	Fatpad	AG	1.06	CG	1.00	CT	1.01	TC	0.94	GG	CC	-	TG	1.09	GA	1.39	CC	-
17	M	57	Fatpad	AG	1.01	GG	-	CT	0.80	TT	-	GG	TT	-	GG	-	AA	-	CC	-

18	M	76	Fatpad	GG	-	GG	-	CC	-	TT	-	GA	TC	1.92	GG	-	AA	-	CC	-
19	M	79	Fatpad	GG	-	GG	-	CC	-	TT	-	GA	TC	0.96	TG	1.03	GA	1.13	CT	1.02
20	M	58	Fatpad	AG	0.99	CC	-	TT	-	TT	-	GA	TT	-	GG	-	AA	-	CC	-
21	M	58	Fatpad	AG	1.02	CG	1.00	CT	1.36	TT	-	AA	TT	-	TG	0.80	GA	0.63	CT	1.09
22	F	42	Fatpad	AG	1.05	CG	0.94	CT	1.15	TT	-	AA	TT	-	TG	2.13	GA	1.22	CT	0.92
23	M	71	Fatpad	GG	-	CG	1.00	CT	1.13	TT	-	AA	TT	-	TG	1.27	GA	1.23	CC	-
24	F	67	Fatpad	AG	0.95	CG	1.05	CT	0.95	TT	-	AA	TC	0.75	TT	-	GG	-	TT	-
25	F	78	Fatpad	AG	1.15	CG	0.89	CT	0.92	TT	-	AA	TT	-	GG	-	AA	-	CC	-
26	M	74	Syn	AG	0.80	GG	-	CT	1.33	TT	-	GG	CC	-	GG	-	AA	-	CC	-
27	M	62	Syn	AG	0.99	CG	0.85	CT	1.23	TT	-	GA	TC	1.12	GG	-	AA	-	CC	-
28	M	67	Syn	AG	0.97	CG	0.98	CT	1.32	TC	0.83	GA	TC	0.81	TG	0.57	GA	0.75	CT	1.24
29	M	60	Syn	AG	1.11	GG	-	CT	1.14	TT	-	AA	TT	-	TG	1.19	GA	1.32	CC	-
30	M	69	Syn	AG	0.85	CG	1.98	CT	0.72	TC	2.09	AA	TT	-	TT	-	GG	-	CT	0.77
31	F	54	Syn	AG	0.90	CG	1.16	CT	1.19	TC	1.56	AA	TT	-	TG	1.85	GA	1.89	CC	-
25	F	78	Syn	AG	1.00	CG	0.95	CT	1.02	TT	-	AA	TT	-	GG	-	AA	-	CC	-
32	F	72	Can bn	AA	-	CG	1.10	TT	-	TC	1.14	GA	TC	0.96	TG	0.86	GA	1.23	CT	1.07
33	M	86	Can bn	GG	-	GG	-	CC	-	TT	-	AA	TT	-	TG	1.43	GA	1.10	CC	-
33	M	86	OP	GG	-	GG	-	CC	-	TT	-	AA	TT	-	TG	1.27	GA	1.31	CC	-

Table 4.3: Allelic expression imbalance analysis for 33 patients

*Cart (H), hip cartilage; Cart (K), knee cartilage; Syn, synovium; Can bn, cancellous bone; OP, osteophyte. ^Gen, genotype. †AER, allelic expression ratio. Text highlighted in yellow, blue and green denote AEI at the 20% threshold at *BCL2L13*, *BID* and *MICAL3* respectively.

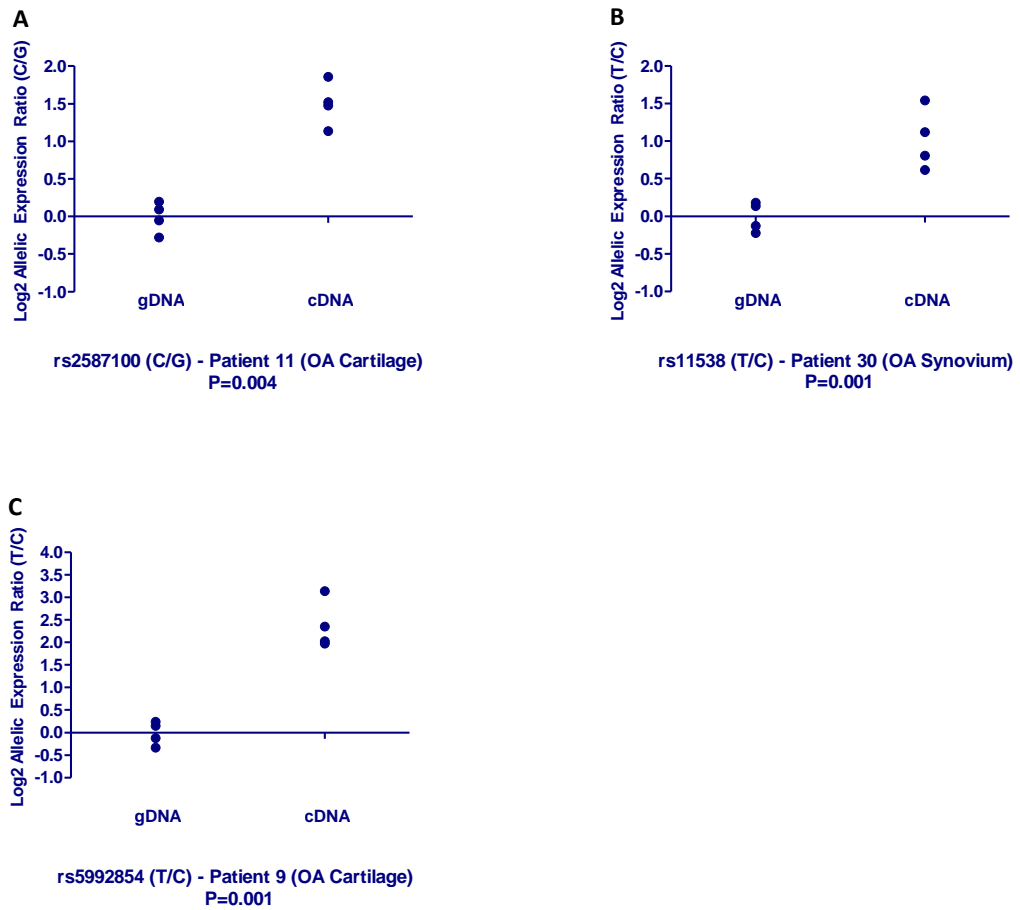


Figure 4.10: Allelic expression imbalance in patients 11, 30 and 9, who showed the largest allelic ratios at *BCL2L13* (rs2587100), *BID* (rs11538) and *MICAL3* (rs5992854) respectively.

Data points represent log₂ of the normalised allelic ratio of genomic DNA (gDNA) or cDNA for each replicate. A value of 0 on the Y-axis denotes an allelic ratio of 1:1. A two-tailed Mann-Whitney exact test was performed to compare the distribution between allelic ratios of gDNA and cDNA replicates. (A) Patient 11 demonstrated a 2.82 fold greater expression of the C allele relative to the G allele (P=0.004) at *BCL2L13* SNP rs2587100. (B) Patient 30 demonstrated a 2.09 fold greater expression of the T allele relative to the C allele (P=0.001) at *BID* SNP rs11538. (C) Patient 9 demonstrated a 5.47 fold greater expression of the T allele relative to the C allele (P = 0.001) at *MICAL3* SNP rs5992854. Four gDNA and four cDNA replicates are shown.

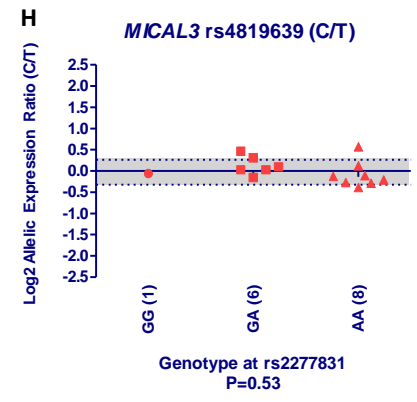
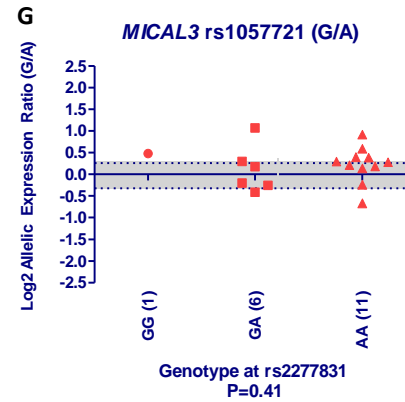
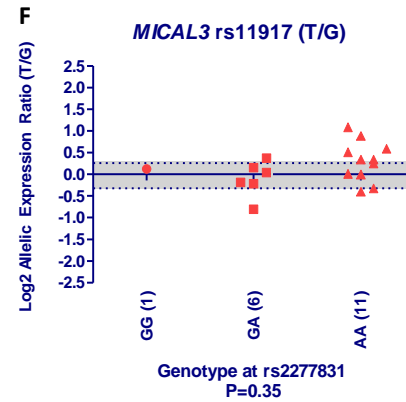
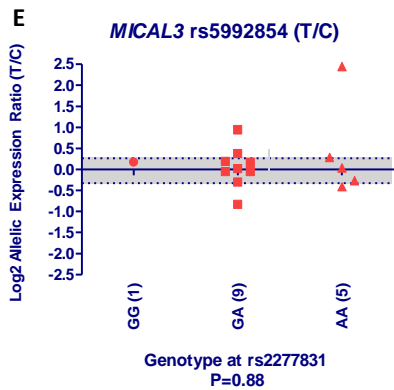
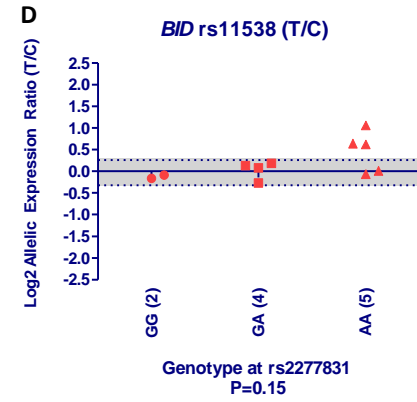
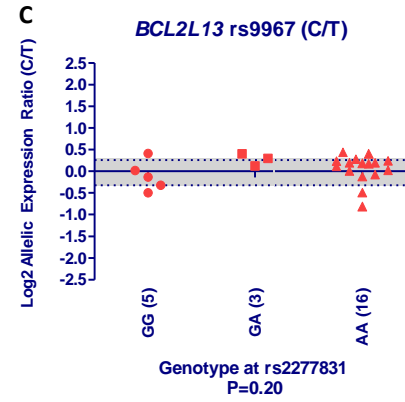
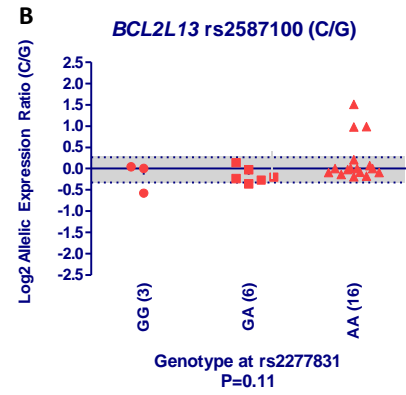
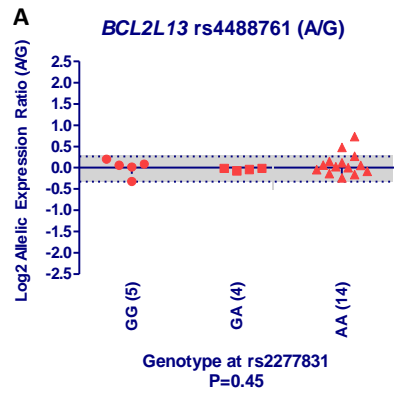


Figure 4.11: Allelic expression imbalance at the transcript SNPs (A) rs4488761, (B) rs25687100, (C) rs9967, (D) rs11538, (E) rs5992854, (F) rs11917, (G) rs1067721 and (H) rs3819639, stratified by genotype at rs2277831.

A total of 33 patients were studied who were heterozygous at one or more of the eight transcript SNPs. The averaged log₂ of the normalised allelic ratios are shown for each patient, categorised according to the genotype at the associated SNP, rs2277831. The shaded area represents a 20% fold difference in expression between the two alleles. A Kruskal-Wallis test was performed to assess the correlation between AEI and the genotype at rs2277831.

4.3 Discussion

It is becoming more apparent that most common traits are influenced by large numbers of alleles that individually have small effects (Allen *et al.*, 2010). It has also been shown that most complex trait alleles influence gene expression by modulating transcription or transcript stability (Montgomery and Dermitzakis, 2011). I therefore hypothesised that the OA association signal that maps to chromosome 22q11.21, detected at SNP rs2277831, may mediate its effect on OA susceptibility by modulating the expression of one or more of the three genes from within the signal. I chose to focus the gene expression studies on joint tissues from patients who had undergone joint replacement surgery rather than a tissue unrelated to OA, such as blood.

I first looked at overall expression of *BCL2L13*, *BID* and *MICAL3* in a variety of joint tissues. The three genes were expressed in all tissue types assessed.

I then quantitatively measured gene expression of *BCL2L13*, *BID* and *MICAL3* in cartilage tissue RNA extracted from OA patients and stratified the expression by genotype at rs2277831, with no significant correlations observed. As the real time PCR assays used to assess *BCL2L13* and *MICAL3* did not capture all transcript isoforms of these two genes, this may have contributed to a false negative result. Therefore, it will be of interest to measure the expression of the other transcript isoforms and stratify the expression by genotype to see if there is a correlation between expression and genotype at rs2277831.

I subsequently tested each gene for the activity of *cis*-regulatory polymorphisms by measuring AEI at eight transcribed SNPs, three residing in *BCL2L13*, one in *BID* and three in *MICAL3*. My results revealed that AEI was common at these loci and was not restricted to a particular tissue type. If the OA associated G allele of rs2277831 is a marker for altered expression of one or more of the three genes tested, then a heterozygote for this SNP would tend to demonstrate AEI. However, I did not observe any correlation between the genotype at rs2277831 and AEI, with an individual heterozygous for rs2277831 being no more likely to demonstrate AEI at one of the three genes than an individual homozygous at this SNP.

Some individuals who were heterozygous for more than one transcript SNP at a particular gene showed an AEI pattern that was not always consistent between the

transcript SNPs. For example, for *BCL2L13* patient 1 shows AEI at rs2587100 (allelic expression ratio; AER; of 0.67) and at rs9967 (AER of 0.71), but not at rs4488761 (AER of 1.04). *BCL2L13* has 14 transcript isoforms and rs4488761 exists in 9 of these whereas, rs2587100 and rs9967 exist in five. Therefore, perhaps isoform specific eQTL effects exist and such variability could account for the AEI differences observed. It will therefore be of interest to utilise AEI assays specific for different transcript isoforms to detect isoform specific AEI.

Although AEI was common in all joint tissues analysed, there was inter and intra-individual variation. For example, AEI at rs9967 was observed in both directions in cartilage tissue in patients 1 and 10. Also, in patient 33, for whom I analysed both cancellous bone and osteophyte tissue, AEI at rs1057721 was apparent only in osteophyte tissue. This suggests that different cellular environments can give rise to differential allelic expression in different tissues in the same individual. This has been shown previously in OA joint tissues in expression studies of the gene *BMP5* (Wilkins *et al.*, 2007).

Overall, *BCL2L13*, *BID* and *MICAL3* are subject to *cis*-acting polymorphisms that influence the expression of the genes in the joint tissues of patients who have undergone surgery. My data do not however support a role for such *cis*-regulation at these genes as accounting for the OA association signal at chromosome 22q11.21 in the tissues that I have looked at. It is possible that there are transcript isoform specific effects or a *cis*-effect related to OA susceptibility at this locus is not active in end stage OA tissue.

Chapter 5: Assessing whether the OA associated locus mapping to chromosome 12q23.3 mediates its effect by influencing the expression of *CHST11*

5.1 Introduction

The arcOGEN GWAS identified an association of hip OA to SNP rs835487 (G/A), with an odds ratio of 1.13 for allele G and a P-value of 1.64×10^{-8} . The SNP is located on chromosome 12q23.3 within intron 2 of *CHST11* (Zeggini *et al.*, 2012). The associated G allele has a frequency of 0.37 in Europeans. As shown in Figure 5.1, the association signal spans approximately 200 kb of the gene and includes exon 2 and regions of intron 1 and 2.

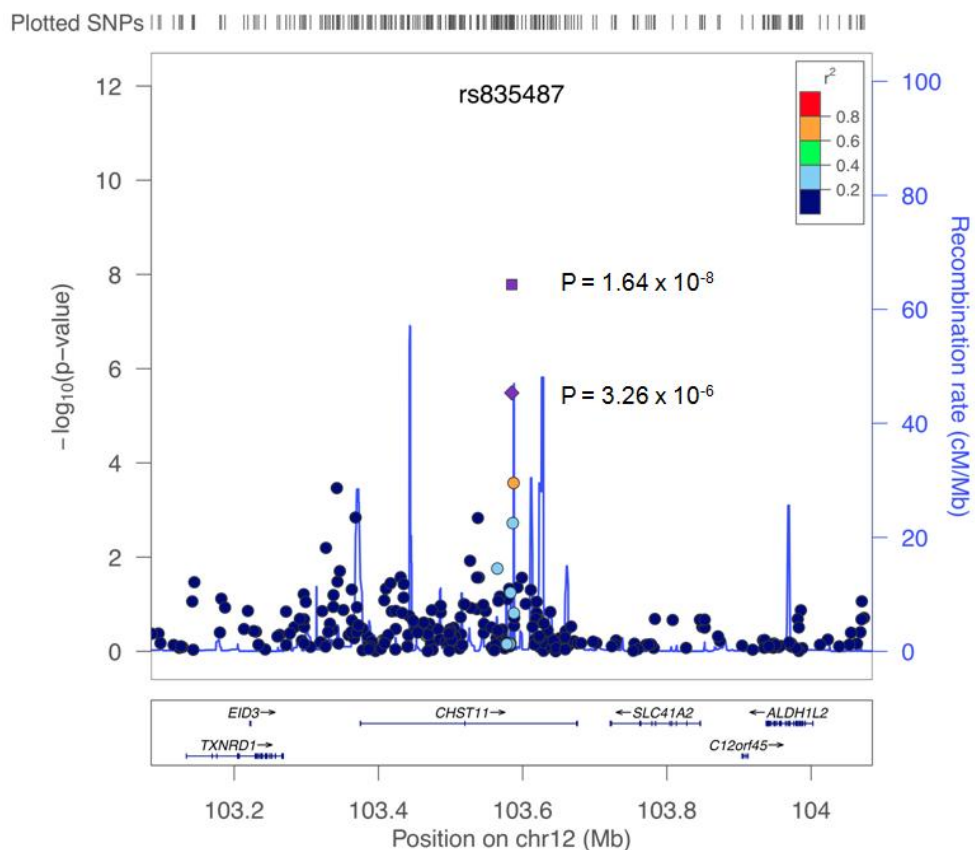


Figure 5.1: Association plot of the chromosome 12q23.3 hip-OA signal from the arcOGEN GWAS. Case-control association results ($-\log_{10}$ p-value) for genotyped SNPs in the discovery set are plotted against genomic position. The rs835487 SNP is denoted by a purple diamond in the discovery set ($p=3.26 \times 10^{-6}$) and by a purple square in the final meta-analysis ($p=1.64 \times 10^{-8}$). The circles indicate association results of genotyped SNPs in the region; the colour reflects the correlation coefficient (r^2) of each genotyped SNP with rs835487 estimated using the CEU HapMap panel. Estimated recombination rates (in centimorgans per megabase) are plotted in light blue. The region shown extends to 500kb upstream and downstream of rs835487. Figure adapted from Zeggini *et al.* (2012).

The gene codes for the Golgi enzyme, carbohydrate sulfotransferase 11 (CHST11), which is also known as chondroitin-4-sulfotransferase-1 (C4ST1). The gene has 6 transcript isoforms, 5 of which are protein coding (Figure 5.2). Of these 5, isoforms ENST00000549260 and ENST00000303694 are the only ones that produce an enzyme molecule containing the catalytic domain. The longest isoform spans 301 kb of genomic sequence and encodes a protein of 352 amino acids, which is the most well characterised. The amino acid identity between human CHST11 and mouse CHST11 is 95% and between human and zebrafish is 78%, suggesting highly conserved functions across species (www.ncbi.nlm.nih.gov). CHST11 is a type II transmembrane protein with an N-terminal cytoplasmic domain, Golgi transmembrane domain and a luminal catalytic domain (Kang et al., 2002). The protein is expressed in a variety of adult tissues, with highest levels observed in lung, placenta, spleen, thymus and peripheral leukocytes (Klüppel, 2010).

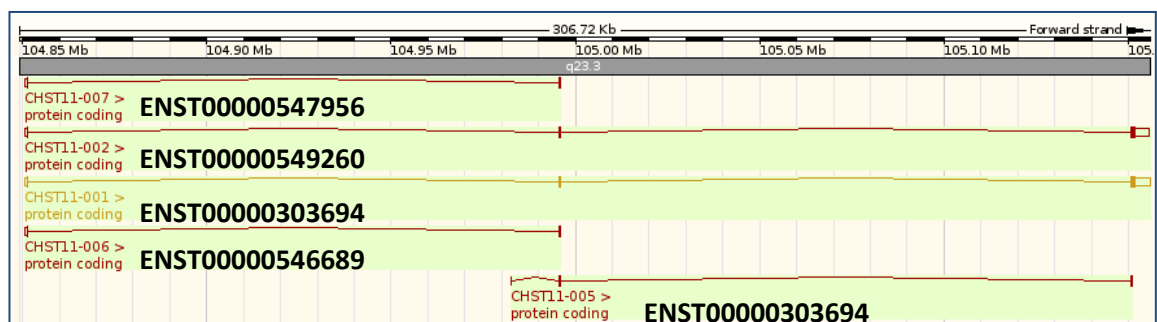


Figure 5.2: The five protein coding transcript isoforms of *CHST11* (from www.ensembl.org). The horizontal bar across the top of the figure shows the forward strand of chromosome 12q23.3 from left to right. The transcript isoforms of *CHST11* are shown as horizontal lines and rectangles within the area highlighted in green. The shaded rectangles represent the coding part of exons whilst the unshaded rectangles represent the UTRs. The horizontal lines show the introns of *CHST11*. The ensembl transcript IDs are shown below each transcript.

CHST11 is a member of the Golgi-associated chondroitin sulfotransferases, which are involved in the modification of chondroitin sulphates in the Golgi apparatus. Chondroitin sulphates are synthesised in the Golgi and undergo sulphation at specific positions on the sugar moieties during chain elongation. CHST11 is one of the enzymes that catalyses the transfer of sulphate groups onto chondroitin at the 4-hydroxyl group of N-acetylgalactosamine (GalNAc) sugars, to form chondroitin-4- sulphate (CS-A; (Klüppel *et al.*, 2010).

Related proteins of CHST11, which also catalyse the transfer of sulphate groups to the 4-hydroxyl position, include CHST12, CHST13 and CHST14. CHST11 and CHST13 preferentially use chondroitin as a substrate, although they also show activity towards dermatan (Mikami *et al.*, 2003). CHST12 and CHST14 show preferential activity towards dermatan disaccharides to form dermatan sulphate (DS or CS-B), but are also able to use chondroitin as a substrate (Mikami *et al.*, 2003). CHST11, CHST12 and CHST14 show a wide spread expression pattern in adult human tissues, but expression of CHST13 is mainly observed in liver, kidney and lymph nodes (Kang *et al.*, 2002). Chondroitin sulphate is a major component of the glycosaminoglycan (GAG) chains, which in cartilage interacts with the core protein to form the proteoglycan aggrecan. This is a major component of the cartilage extracellular matrix and interacts with hyaluronan to form large, complex aggregates. Sulphation of chondroitin provides a strong negative charge to GAG chains, which show a high affinity to water and generate electrostatic forces that help maintain the structural integrity of the cartilage. Chondroitin sulphation is also essential in the interaction of the extracellular matrix with many cationic macro molecules including growth factors (Gama *et al.*, 2006).

It has been shown that CHST11 is involved in cellular signalling events including TGF- β and Wnt signalling. Willis *et al* (2009) identified TGF- β responsive regulatory modules in *CHST11* that can positively and negatively regulate *CHST11* transcription in a cell type specific manner (Willis *et al.*, 2009). They used luciferase reporter assays to show enhanced transcriptional activity of these modules post treatment with TGF- β ligand in human embryonic kidney (HEK293T) and mouse mammary gland (NmuMG) cells. Shortkroff and Yates (2007) have reported that a decrease in chondroitin sulphation or CS levels can lead to a reduction in β -catenin accumulation in articular chondrocytes, which therefore demonstrates a role of CHST11 in the canonical Wnt signalling pathway.

To determine the role of CHST11 in mammalian development, Klüppel *et al.* (2005) generated a loss of function mutation of the gene in mouse embryonic stem cells through gene trapping. This mutation created a fusion transcript of *Chst11* that disrupted the expression of exons 2 and 3, which encode the transmembrane and intra-Golgi catalytic domains of the enzyme. Whilst the heterozygous mice were fertile and viable, the homozygous mice displayed severe dwarfism and died within six hours

of birth due to respiratory distress (Klüppel *et al.*, 2005). The mutant mice showed multiple skeletal abnormalities compared to the wildtype mice, including a smaller rib cage, shortened limbs and a dome-shaped skull. The growth plates of these mutants were disorganised with alterations in the orientation of chondrocyte columns. They also showed a reduction in CS and aggrecan content, which is often observed in osteoarthritis. These results demonstrate an important role for CHST11 in mammalian development.

It has been reported that CHST11 has a role in human diseases, including cancer and OA. There is evidence of an alteration of the pattern of chondroitin sulphation in colon adenocarcinoma, such that the ratio of 4-hydroxyl sulphated and 6-hydroxyl sulphated chondroitin changes from 4:1 in normal colon tissue to 1:3 in malignant cells (Theocharis, 2002). This implies that it is important to tightly regulate the balance and pattern of chondroitin sulphation. A genome-wide gene expression microarray analysis in human subjects identified *CHST11* as one of the genes that showed highly significant upregulation in knee OA cartilage versus normal cartilage, with a 6.8 fold increase observed (Karlsson *et al.*, 2010). Another microarray analysis on cartilage from hip OA and from neck-of-femur (NOF) fracture patients, which is often used as a control cartilage due to the absence of any OA lesions, showed a 1.9 fold upregulation of *CHST11* in OA compared to control cartilage (Xu *et al.*, 2012).

Monoclonal antibodies that specifically recognise native CS/DS sulphation motif epitopes were found to stain positively on newly synthesised aggrecan extracted from human OA cartilage, but not in normal adult human cartilage (Caterson *et al.*, 1990; Slater *et al.*, 1995). Other studies have also shown an increase in expression of native CS/DS sulphation motif epitopes in OA hyaline articular cartilage in early stages of OA (Rizkalla *et al.*, 1992).

Upregulation of *CHST11*, together with an increased expression of native CS/DS motif epitopes, during OA may be a result of the cartilage attempting to repair the damage, and have the potential to be used as biomarkers to monitor the development and progression of OA (Caterson, 2012).

Overall, *CHST11* harbours genetic susceptibility that is relevant to OA disease development at the hip. The gene codes for an enzyme that post-translationally

modifies GAGs, a component of the functionally critical and abundant cartilage protein aggrecan. I hypothesised that the OA susceptibility acted by modulating the expression of *CHST11* and in this chapter I report on the experiments that I performed to test this hypothesis.

5.2 Results

5.2.1 Qualitative gene expression analysis of *CHST11* in joint tissue cDNAs

To assess in which joint tissues *CHST11* was expressed, complimentary DNAs (cDNAs) were synthesised from RNAs extracted from the cartilage, cancellous bone, fatpad, meniscus, synovium and ligament tissues from OA patients (Chapter 2.3). *CHST11* was then PCR amplified using primers listed in Table 2.4 (Chapter 2.4). Initially, the overall expression of *CHST11* was assessed using primers that target a common region in four of the five protein coding transcript isoforms. The primers used were designed to target exon 1 and 2 of ensemble transcript IDs ENST00000303694, ENST00000549260, ENST00000546689 and ENST00000547956. Expression of ensembl transcript ID ENST00000549016 was not assessed in this experiment. *CHST11* was expressed in all tissues of the joint analysed, with particularly high levels observed in cartilage, meniscus and ligament (Figure 5.3).

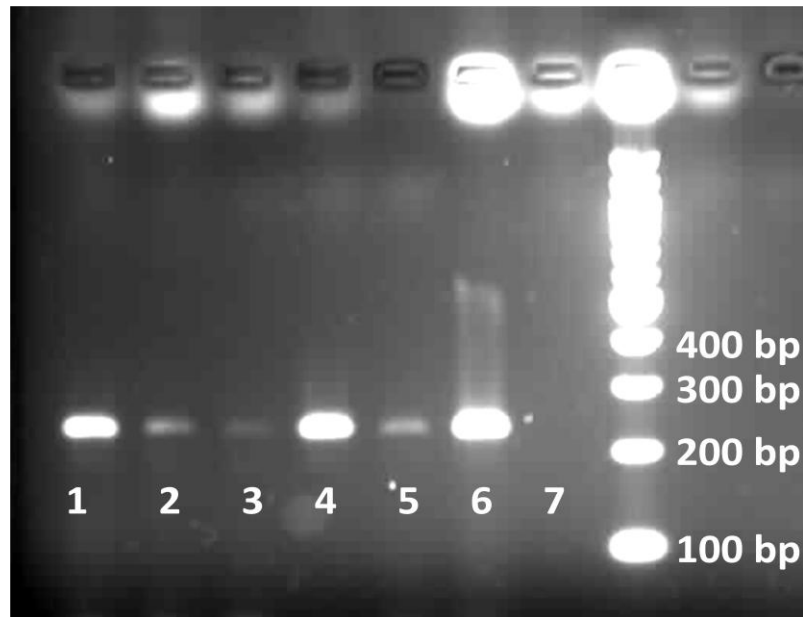


Figure 5.3: *CHST11* expression in joint tissue cDNAs. Lane 1: cartilage, 2: cancellous bone, 3: fatpad, 4: meniscus, 5: synovium, 6: ligament, 7: PCR blank. The PCR products were run on a 2% agarose gel containing ethidium bromide. A 100 bp DNA ladder was used for sizing of PCR products.

The expression of the five protein coding transcript isoforms of *CHST11* were then assessed by PCR using cDNAs synthesised from RNAs extracted from the cartilage, fatpad and synovium of OA patients. Cartilage from a patient who had undergone a NOF fracture was also studied. The primers used are listed in Table 2.5.

The difference between transcript ENST00000303694 and transcript ENST00000549260 (the two longer isoforms; Figure 5.2) is an additional 15 bp at the end of exon 1 of transcript ENST00000549260. Therefore, the forward primer designed for transcript ENST00000549260 contained these 15 bp, whilst that designed for ENST00000303694 spanned the exon-exon boundary, and did not contain the additional 15 bp. Similarly, transcripts ENST00000546689 and ENST00000547956 (the two shorter isoforms) were different in the same additional 15 bp sequence, which is present at the end of exon 1 of ENST00000547956. Hence the same forward primers used to distinguish between the two longer isoforms were utilised, with the reverse primer designed to the unique 3'UTR sequence present in ENST00000546689 and ENST00000547956. Exon 1 of transcript ENST00000549016 is not present in any of the

other transcripts, hence a forward primer was designed to this exon to distinguish this isoform from the others.

Four of the five transcript isoforms were expressed in all the joint tissues analysed, whilst the expression of ENST00000549016 was not detected in any of the tissues analysed (Figure 5.4). Due to the unavailability of a suitable positive control for the PCR of this transcript, I cannot exclude the possibility that my failure to observe its expression is a false negative. However, although this transcript isoform is listed on the ensembl and UCSC genome browsers, it is absent on the NCBI database. I conclude therefore that it is not expressed in the tissues that I have tested.

The intensity of the bands corresponding to the PCR products from cDNAs used in this experiment is not directly comparable with that from the earlier experiment (Figure 5.3). This is probably because the cDNAs used were from different individuals, reflecting inter-individual variation in the level of *CHST11* expression.

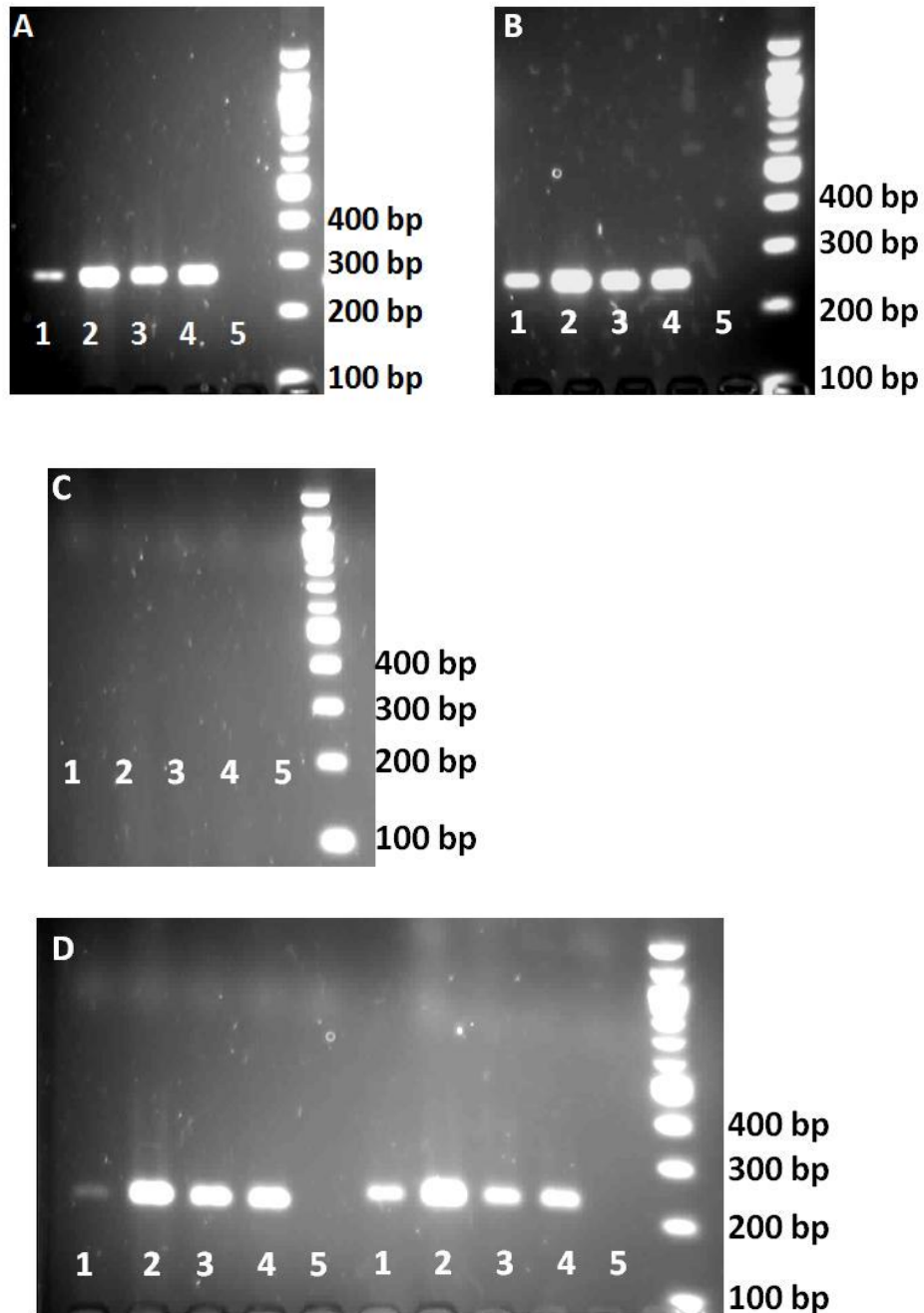


Figure 5.4: *CHST11* transcript isoform expression in joint tissue cDNAs. Different primer pairs were used to amplify ensembl transcript ID ENST00000303694 (A), ENST00000549260 (B), ENST00000549016 (C), ENST00000546689 and ENST00000547956 (D). Lane 1: OA cartilage, 2: NOF cartilage, 3: fatpad, 4: synovium 5: PCR blank. The PCR products were run on a 2% agarose gel containing ethidium bromide. A 100 bp DNA ladder was used for sizing of PCR products.

In summary, *CHST11* expression was observed across all joint tissues analysed. The expression of four of the five protein coding transcript isoforms was also detected across the joint tissues.

5.2.2 Gene expression of *CHST11* in hip OA versus NOF cartilage

It has previously been shown that *CHST11* expression is 6.8 fold higher in OA knee cartilage compared to normal knee cartilage in a study which used whole genome microarray analysis on 5 OA and 8 normal donors (Karlsson *et al.*, 2010), whilst a microarray analysis on 9 OA hip and 10 NOF patients revealed a 1.9 fold increase in *CHST11* expression in hip OA (Xu *et al.*, 2012).

The *CHST11* genetic association is to hip OA and I therefore set out to confirm the observation of an increased expression of the gene in a larger sample. I used real time quantitative PCR gene expression analysis and a cohort of 28 hip OA patients and 19 NOF patients (Chapter 2.17). *CHST11* expression was measured using the assay listed in Table 2.2. The gene showed a 2.6 fold greater expression in hip OA compared to NOF cartilage with a P-value of 0.007 (Figure 5.5). This result is clearly comparable to that from the microarray study.

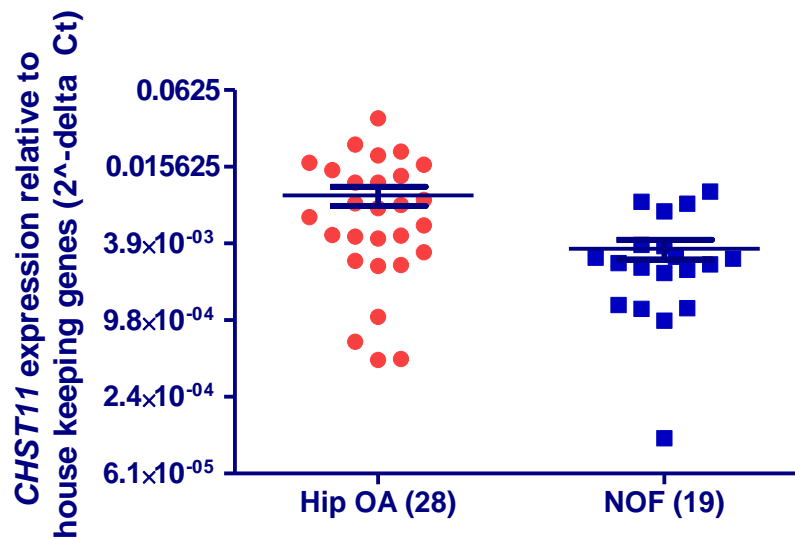


Figure 5.5: *CHST11* expression relative to housekeeping genes in cartilage from hip OA and NOF patients. The error bars represent the mean plus the standard error.

5.2.3 Database searching for common non-synonymous mutations in CHST11

In order to determine if the OA association to *CHST11* is caused by an amino acid substitution, I searched the ensembl online database (www.ensembl.org) for common variants within the *CHST11* coding region, in particular, within exon 2, which lies within the association interval.

There are no common (minor allele frequency greater than 15%) non-synonymous SNPs in the gene that can account for the association signal.

5.2.4 CHST11 expression in cartilage, fatpad and synovium tissue stratified by genotype at rs835487

If the OA association at *CHST11* influences expression of the gene, then one way to assess this is to measure *CHST11* expression in a large number of individuals and to then stratify expression level by genotype at rs835487; a correlation would support an effect of the association signal on *CHST11* expression. I was able to perform this analysis on cartilage from OA patients. My group also has a biobank of cartilage from NOF patients and of fatpad and synovium tissue from knee OA patients. These were also studied.

CHST11 expression was measured using the real time PCR assay listed in Table 2.2 (Chapter 2.17). Linear regression was performed to determine if the gene expression relative to genotype differed significantly from the null.

Of a total of 113 patient cartilage cDNAs analysed, 94 were synthesised from OA knee and OA hip cartilage RNAs whilst 19 were from NOF cartilage RNAs. Of the 94 OA patients, 14 were homozygous GG, 42 were heterozygous and 38 were homozygous AA at rs835487. There was no significant correlation between genotype at rs835487 and *CHST11* expression, with a P-value of 0.67 (Figure 5.6). As the association of this SNP is seen in hip OA, the hip cartilage samples were analysed separately from the knee cartilage samples. Of the 94 cartilages, 28 were from the hip joints of OA patients. There was no correlation between genotype at rs835487 and *CHST11* expression in these hip OA cartilage samples, with a P-value of 0.76 (Figure 5.6). *CHST11* expression in NOF cartilage was also stratified by genotype at rs835487. Of the 19 NOF samples, 6 were heterozygous and 13 were homozygous AA. There were no

homozygous GG patients in this cohort. Again, there was no correlation between *CHST11* expression and genotype, with a P-value of 0.83 (Figure 5.6).

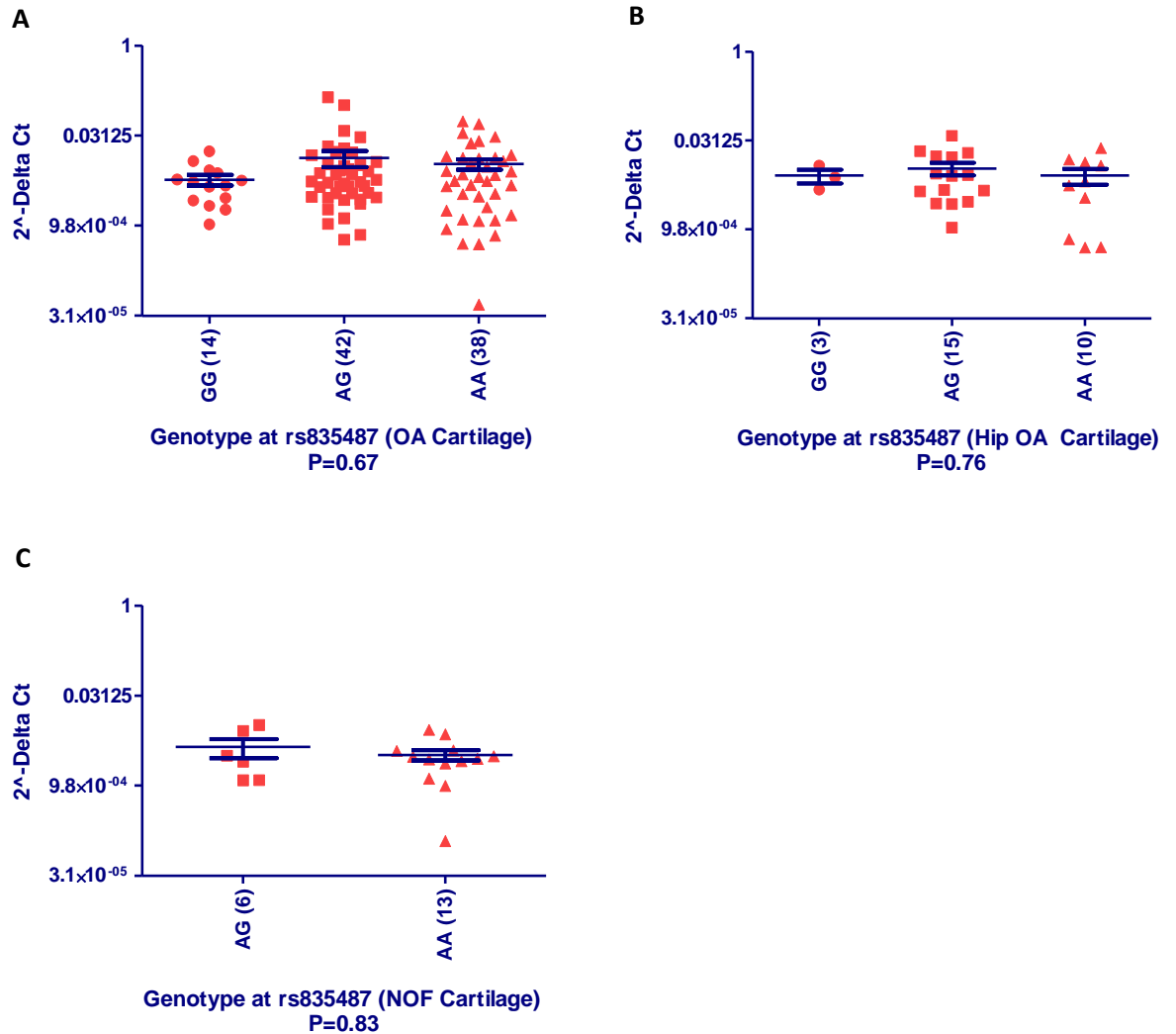


Figure 5.6: Expression of *CHST11* stratified by the genotype at the OA associated SNP rs835487 in (A) hip or knee cartilage of 94 OA patients (B) hip cartilage of 28 OA patients and (C) hip cartilage of 19 NOF patients. The data points represent the average of the three replicates for each sample. The expression of *CHST11* was compared to the average of the housekeeping genes and the 2⁻delta Ct values were plotted against genotype. The horizontal bars represent the mean plus the standard error of the mean. A linear regression (A and B) and a two-tailed Mann-Whitney exact test (C) were performed to assess the correlation between gene expression and genotype. The P-values are shown below each graph.

Of the 30 fatpad samples from knee OA patients, 5 were homozygous GG, 12 were heterozygous and 13 were homozygous AA for rs835487. Of the 25 synovium samples from knee OA patients, 3 were homozygous GG, 12 were heterozygous and 10 were homozygous AA for the SNP. No significant correlation between *CHST11* expression and the genotype at rs835487 was observed in the fatpad or synovium samples, with P-values of 0.37 and 0.27 respectively (Figure 5.7).

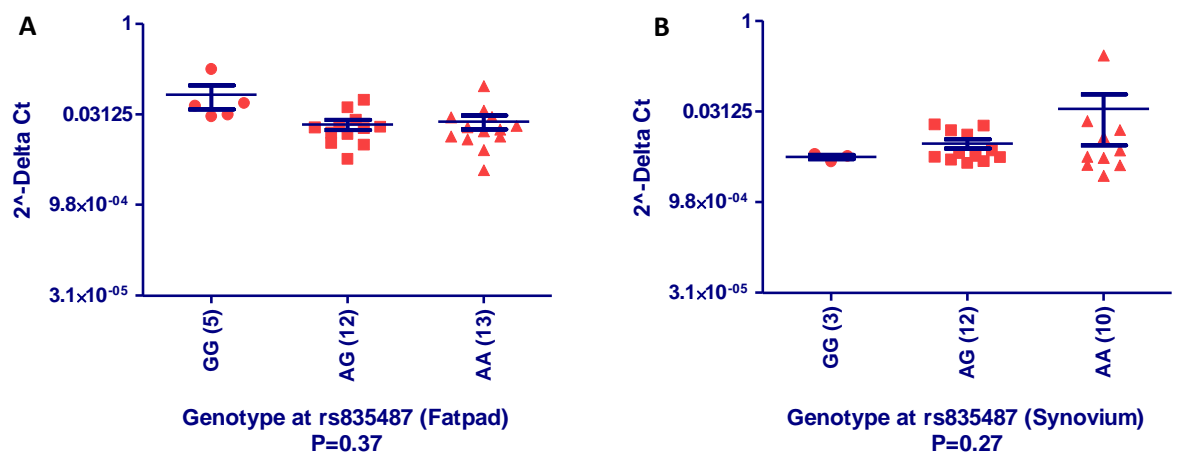


Figure 5.7: Expression of *CHST11* stratified by the genotype at the OA associated SNP rs835487 in (A) fatpad of 30 OA patients and (B) synovium of 25 OA patients. The data points represent the average of the three replicates for each sample. The expression of *CHST11* was compared to the average of the house keeping genes and the 2^{-delta Ct} values were plotted against genotype. The horizontal bars represent the mean plus the standard error of the mean. A linear regression was performed to assess the correlation between gene expression and genotype. The P-values are shown below each graph.

In summary, this analysis did not find evidence for a correlation between *CHST11* expression in cartilage, fatpad and synovium tissue and genotype at the associated SNP rs835487.

5.2.5 Allelic expression imbalance of *CHST11* in cartilage, fatpad and synovium tissue

The above technique of measuring the expression of a gene and then stratifying this by genotype is vulnerable to the natural fluctuation in gene expression, which can decrease the technique's sensitivity and accuracy and potentially lead to false negative results (Johnson *et al.*, 2008). Therefore I directly measured allelic expression which can circumvent this possibility.

Since *CHST11* does not harbour any common variants (minor allele frequency greater than 15%) in its coding region, the SNP rs2463018, located in the 3'UTR of the gene was used to test for allelic expression imbalance (AEI; Table 2.9). Of the five protein coding transcript isoforms of *CHST11*, ENST00000303694 and ENST00000549260 harbour this polymorphism. These are the only two isoforms that produce the functional enzyme. The SNP was selected as it has a high minor allele frequency in the European population (29%; Table 5.1) and because there is a validated real time PCR genotyping assay available for it from Applied Biosystems (Chapter 2.22).

The allelic expression ratios (AERs) were calculated using the formula $(2^{-\text{FAM Ct}})/(2^{-\text{VIC Ct}})$ and normalised to the allelic expression ratios of genomic DNA (Chapter 2.22).

I initially performed AEI analysis on cDNA synthesised from the RNA extracted from the cartilage tissue of knee and hip OA patients. I then separated the hip cartilage samples. The average AERs were plotted against the genotype at rs835487 to assess whether there was a correlation between AEI and genotype at the SNP, using a Kruskal-Wallis test. I also carried out AEI analysis on NOF cartilage, on fatpad and on synovium tissue.

SNP	Position on chr. 12 on NCBI genome build 37.3	Alleles	MAF*	Location of SNP in <i>CHST11</i>	Pairwise linkage disequilibrium relative to the OA associated SNP rs835487	
					D'	r ²
rs2463018	18343843	C/T	0.29	3'UTR	0.05	0.002

Table 5.1: The SNPs studied for AEI analysis of *CHST11*.

* Minor allele frequency in Europeans (dbSNP (<http://www.ncbi.nlm.nih.gov/projects/SNP/>)).

Of 96 cartilages analysed, 39 patients were heterozygous at rs2463018. The normalised AERs for those heterozygotes are summarised in Table 5.2. Of the 39, 10 patients demonstrated AEI at a value of 20% or greater and with a P-value of less than 0.05. Two were homozygous GG, 6 were heterozygous and 2 were homozygous AA at the OA associated SNP rs835487. The largest AER observed was 2.08 for patient 12, who is heterozygous at rs835487 (P=0.008, Figure 5.8). Of the 39 heterozygotes, 11 were hip OA patients, of which 3 demonstrated AEI. Two of these 3 were heterozygous and one was homozygous AA at the associated SNP rs835487.

Five of 19 NOF patients used in this study were heterozygous at rs2463018 (Table 5.3). Two of five showed AEI at the 20% threshold and a P-value of less than 0.05, and both were homozygous AA at rs835487. The largest AER observed in NOF cartilage was 0.70 in patient 44 (P=0.001, Figure 5.8).

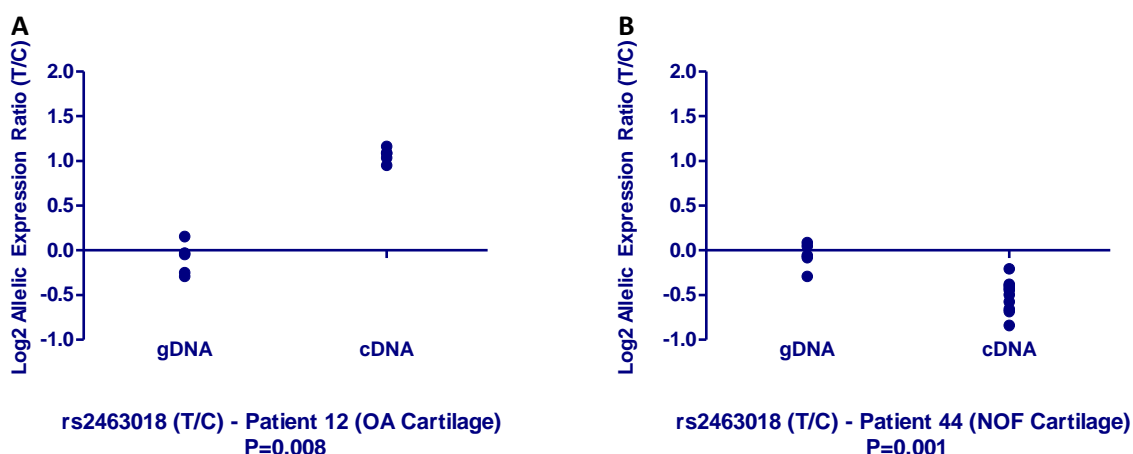


Figure 5.8: Allelic expression imbalance in patients 12 and 44, who showed the largest allelic ratios in OA cartilage and NOF cartilage, respectively. Data points represent log₂ of the normalised allelic ratio of genomic DNA (gDNA) or cDNA for each replicate. A value of 0 on the Y-axis denotes an allelic ratio of 1:1. A two-tailed Mann-Whitney exact test was performed to compare the distribution between allelic ratios of gDNA and cDNA replicates. (A) Patient 12 demonstrated a 2.08 fold greater expression of the T allele relative to the C allele (P=0.008). Five genomic DNA and five cDNA replicates are shown. (B) Patient 44 demonstrated a 0.70 fold lower expression of the T allele relative to the C allele (P=0.001). Five gDNA and 10 cDNA replicates are shown.

The average AERs at rs2463018 were then plotted against the genotype at rs835487. There were no significant correlations between AERs and genotype at rs835487 in OA cartilage, in OA hip cartilage or in NOF cartilage, with P-values of 0.32, 0.92 and 0.80 respectively (Figure 5.9).

Of 30 fatpad samples analysed, 17 were heterozygous at rs2463018. Of the 17, 6 showed AEI at 20% or greater with a P-value less than 0.05 at rs2463018 (Table 5.4). One was homozygous GG, 2 were heterozygous and 3 were homozygous AA at rs835487. The largest AER observed was 1.61 in patient 51, who was heterozygous at the associated SNP (P=0.02, Figure 5.10).

Twelve of 25 synovium samples analysed were heterozygous at rs2463018. At rs2463018, 4 patients showed AEI at the 20% threshold with a P-value less than 0.05 (Table 5.5). One patient was heterozygous at the associated SNP (patient 16) and showed the largest AER, with a ratio of 1.68 (P=0.008, Figure 5.10). The remaining three patients were homozygous AA at rs835487.

The average AERs for the fatpad and synovium tissues were then stratified by the genotype at the associated SNP and a Kruskal-Wallis test was performed to assess the association between AERs and rs835487 genotype (Figure 5.11). No significant correlations were observed.

Of the OA patients who were subject to AEI analyses, for 8 of them multiple joint tissues were collected. The 8 patients were: Patient 1 and 27, for whom cartilage, fatpad and synovium were collected; patient 5, 12 and 31, for whom cartilage and fatpad were collected, patient 16 and 28, for whom cartilage and synovium were collected and patient 54, for whom fatpad and synovium were collected. Patient 27 did not demonstrate AEI at either one of the tissues analysed. However, AEI observed in one tissue type was not necessarily replicated in other tissue types. For example, patient 16 did not demonstrate AEI in cartilage tissue, but showed a 1.68 fold AEI in synovium. Similarly, patient 54 showed a 1.21 fold AEI in fatpad, but did not demonstrate AEI in synovium tissue.

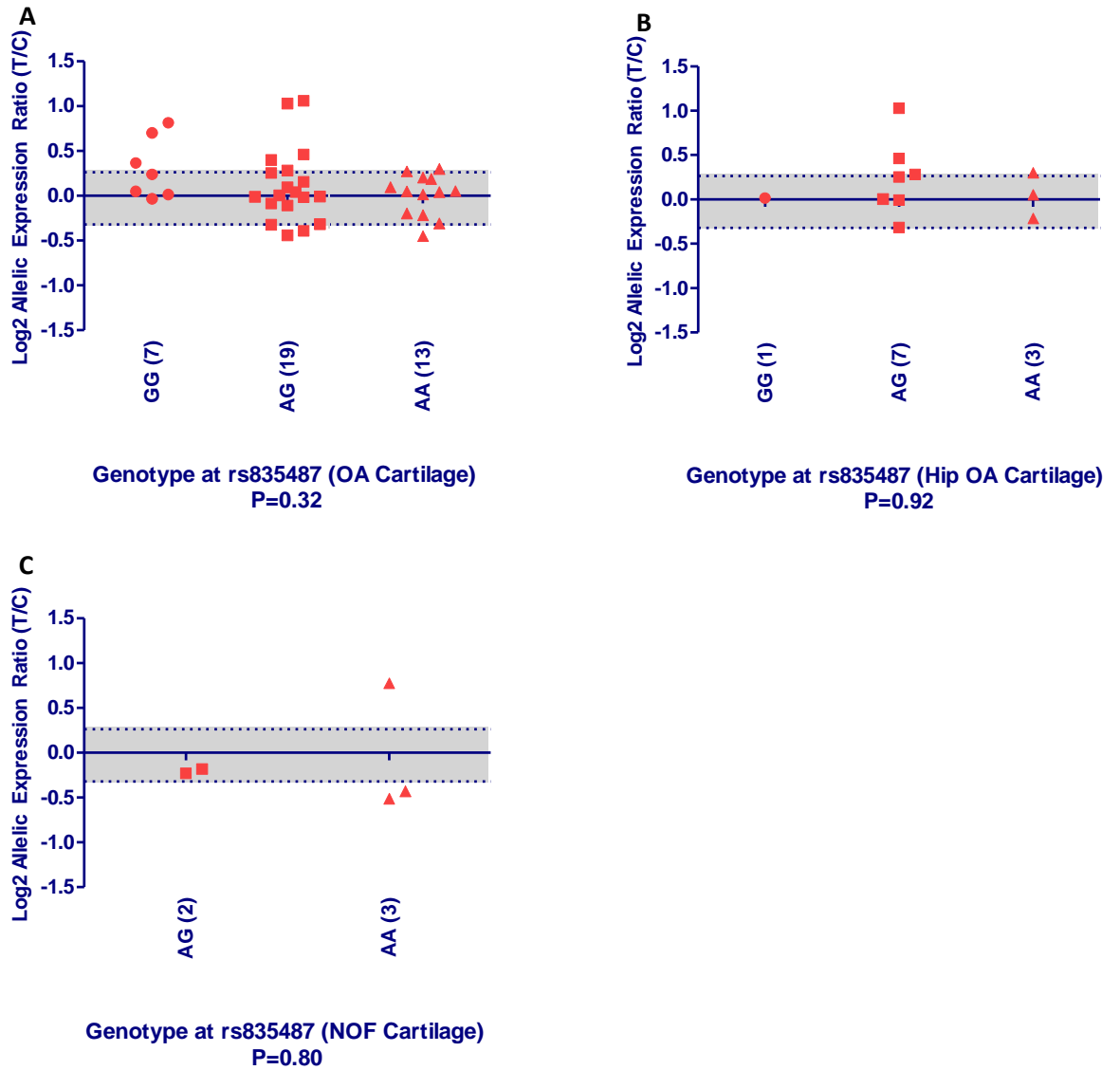


Figure 5.9: Allelic expression imbalance stratified by genotype at rs835487 in (A) the 39 hip or knee OA patients, (B) the 11 hip OA patients and (C) the 5 NOF patients all heterozygous at rs2463018. The averaged log₂ of the normalised allelic ratios are shown for each patient, categorised according to the genotype at the associated SNP, rs835487. The shaded area represents a 20% fold difference in expression between the two alleles of rs2463018. A Kruskal-Wallis test was performed in OA cartilage (A and B) and a two-tailed Mann-Whitney exact test was performed in NOF cartilage (C) to assess the correlation between AEI and the genotype at rs835487.

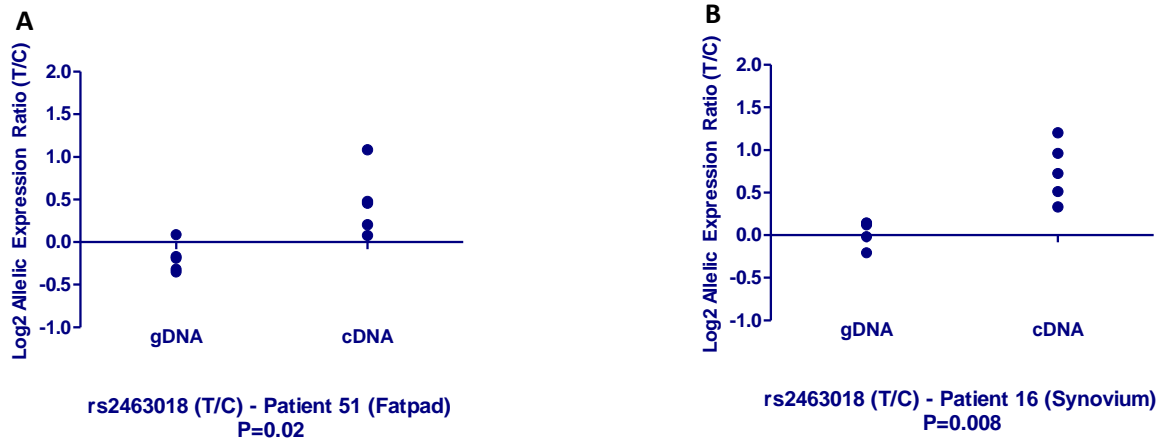


Figure 5.10: Allelic expression imbalance in patients 51 and 16, who showed the largest allelic ratios in fatpad and synovium, respectively. Data points represent log₂ of the normalised allelic ratio of genomic or cDNA for each replicate. A value of 0 on the Y-axis denotes an allelic ratio of 1:1. A two-tailed Mann-Whitney exact test was performed to compare the distribution between allelic ratios of gDNA and cDNA replicates. Five genomic DNA and five cDNA replicates are shown. (A) Patient 51 demonstrated a 1.61 fold greater expression (P=0.02) and (B) patient 16 demonstrated a 1.68 fold greater expression (P=0.008), both of the T allele relative to the C allele.

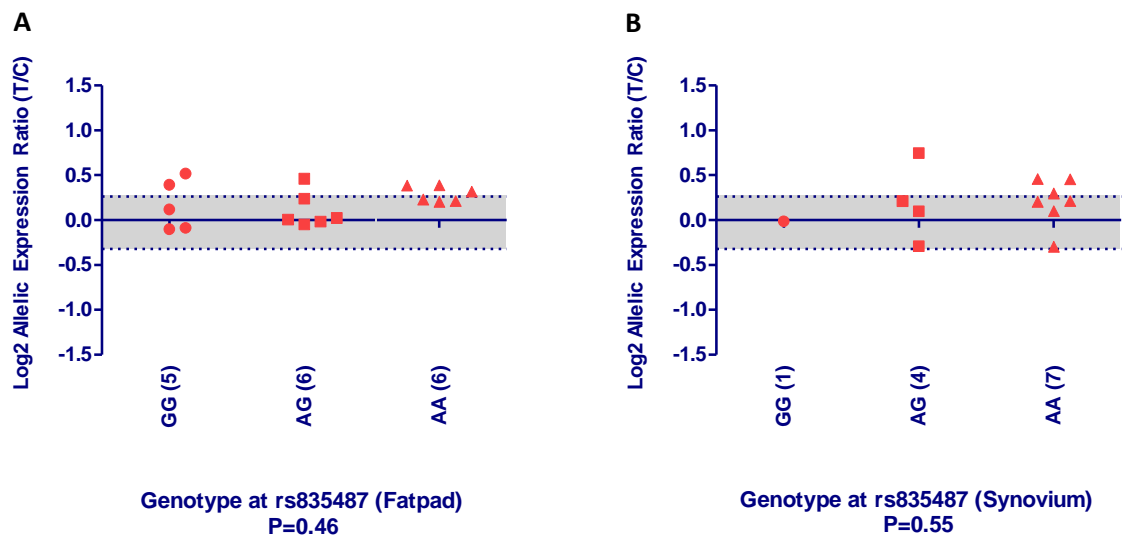


Figure 5.11: Allelic expression imbalance stratified by genotype at rs835487 in (A) the fatpad from 17 OA patients and (B) the synovium from 12 OA patients, all heterozygous at rs2463018. The averaged log₂ of the normalised allelic ratios are shown for each patient, categorised according to the genotype at the associated SNP, rs835487. The shaded area represents a 20% fold difference in expression between the two alleles of rs2463018. A Kruskal-Wallis test was performed to assess the correlation between AEI and the genotype at rs835487.

In summary, although AEI at *CHST11* was observed in all tissues analysed, this did not correlate with the genotype at the associated SNP, rs835487.

Patient number	Sex	Age at surgery	Tissue*	Gen^ at rs835487	AER† at rs2463018	log2 standard error
1	M	74	Cart (K)	GG	1.04	0.07
2	M	76	Cart (K)	GG	1.29	0.12
3	M	63	Cart (K)	GG	1.62	0.26
4	M	70	Cart (K)	GG	1.18	0.11
5	M	71	Cart (K)	GG	1.76	0.39
6	M	74	Cart (K)	GG	0.98	0.17
7	M	71	Cart (H)	GG	1.01	0.16
8	M	50	Cart (K)	AG	0.76	0.07
9	F	81	Cart (K)	AG	1.11	0.22
10	M	74	Cart (K)	AG	1.03	0.17
11	M	82	Cart (K)	AG	0.93	0.32
12	F	69	Cart (K)	AG	2.08	0.04
13	F	67	Cart (K)	AG	0.80	0.10
14	F	73	Cart (K)	AG	1.32	0.46
15	F	80	Cart (K)	AG	1.07	0.11
16	M	67	Cart (K)	AG	0.99	0.12
17	M	64	Cart (K)	AG	0.99	0.11
18	F	64	Cart (K)	AG	0.74	0.38
19	F	80	Cart (K)	AG	0.94	0.14
20	F	58	Cart (H)	AG	2.04	0.13
21	F	78	Cart (H)	AG	0.80	0.07
22	F	69	Cart (H)	AG	1.22	0.15
23	F	77	Cart (H)	AG	1.38	0.67
24	F	71	Cart (H)	AG	0.99	0.26
25	F	65	Cart (H)	AG	1.00	0.13
26	F	50	Cart (H)	AG	1.19	0.47
27	F	78	Cart (K)	AA	1.15	0.09
28	M	56	Cart (K)	AA	1.04	0.19
29	F	66	Cart (K)	AA	0.87	0.13
30	M	68	Cart (K)	AA	1.14	0.16
31	F	67	Cart (K)	AA	0.81	0.12
32	F	64	Cart (K)	AA	1.03	0.09
33	F	67	Cart (K)	AA	1.01	0.20
34	M	86	Cart (K)	AA	1.07	0.15
35	M	46	Cart (K)	AA	1.21	0.21
36	F	62	Cart (K)	AA	0.73	0.38
37	F	67	Cart (H)	AA	0.86	0.10
38	M	66	Cart (H)	AA	1.04	0.12

39	F	67	Cart (H)	AA	1.23	0.17
----	---	----	----------	----	-------------	------

Table 5.2: Allelic expression analysis of *CHST11* in cartilage from 39 OA patients, heterozygous at rs2463018.

***Cart (H), hip cartilage; Cart (K), knee cartilage; ^Gen, genotype; †AER, allelic expression ratio. Bold text denotes allelic expression imbalance (AEI) at the 20% threshold and with a P-value less than 0.05.**

Patient number	Sex	Age at surgery	Gen [^] at rs835487	AER [†] at rs2463018	log2 standard error
40	F	84	AG	0.85	0.40
41	F	89	AG	0.88	0.14
42	F	79	AA	0.74	0.51
43	F	94	AA	1.71	0.32
44	F	91	AA	0.70	0.06

Table 5.3: Allelic expression analysis of *CHST11* in cartilage from 5 NOF patients, heterozygous at rs2463018.

[^]Gen, genotype; [†]AER, allelic expression ratio. Bold text denotes allelic expression imbalance (AEI) at the 20% threshold and with a P-value less than 0.05.

Patient number	Sex	Age at surgery	Gen [^] at rs835487	AER [†] at rs2463018	log2 standard error
1	M	74	GG	1.19	0.02
5	M	71	GG	0.94	0.03
45	F	65	GG	1.00	0.01
46	F	60	GG	1.13	0.03
47	F	68	GG	1.45	0.06
12	F	69	AG	0.96	0.02
48	F	81	AG	1.10	0.03
49	F	88	AG	1.05	0.06
50	F	81	AG	1.34	0.03
51	M	63	AG	1.61	0.05
52	M	85	AG	1.05	0.02
27	F	78	AA	1.14	0.03
31	F	67	AA	1.19	0.01
53	M	71	AA	1.17	0.04
54	F	64	AA	1.21	0.02
55	F	62	AA	1.21	0.02
56	F	82	AA	1.32	0.04

Table 5.4: Allelic expression analysis of *CHST11* in fatpad from 17 OA patients, heterozygous at rs2463018.

[^]Gen, genotype; [†]AER, allelic expression ratio. Bold text denotes allelic expression imbalance (AEI) at the 20% threshold and with a P-value less than 0.05.

Patient number	Sex	Age at surgery	Gen [^] at rs835487	AER [†] at rs2463018	log ₂ standard error
1	M	74	GG	0.99	0.31
16	M	67	AG	1.68	0.16
57	F	73	AG	1.07	0.22
58	M	75	AG	0.82	0.11
59	F	64	AG	1.16	0.19
27	F	78	AA	1.07	0.06
28	M	56	AA	1.16	0.08
60	F	72	AA	1.37	0.12
61	F	69	AA	1.23	0.11
62	M	69	AA	1.37	0.44
54	F	64	AA	1.15	0.08
63	M	72	AA	0.81	0.08

Table 5.5: Allelic expression analysis of *CHST11* in synovium from 12 OA patients, heterozygous at rs2463018.

[^]Gen, genotype; [†]AER, allelic expression ratio. Bold text denotes allelic expression imbalance (AEI) at the 20% threshold and with a P-value less than 0.05.

5.3 Discussion

I have initially looked for overall gene expression, then the expression of five protein coding transcript isoforms of *CHST11* in a variety of joint tissues. *CHST11* was expressed in all tissue types assessed, and the expression of four of five transcript isoforms was detected in the joint tissues that I have looked at.

It has been reported that the expression of *CHST11* is elevated in OA knee and hip cartilage compared to healthy cartilage by 6.2 and 1.9 fold respectively (Karlsson *et al.*, 2010; Xu *et al.*, 2012). These studies used micro array analysis to measure gene expression changes. I have used real time PCR to quantify *CHST11* expression in hip OA cartilage and in NOF cartilage using a larger sample size. I observed a 2.6 fold difference in *CHST11* expression in OA versus NOF cartilage. This increase in gene expression can perhaps be a cause or a consequence of cartilage damage. An increase in *CHST11* expression may result in an altered sulphation balance of chondroitin, leading to a reduction in cartilage extra cellular matrix synthesis, or an increase in

CHST11 can be a result of the damaged cartilage attempting to repair itself by upregulating genes, whose products are involved in cartilage anabolism.

In order to look for possible causes for the OA association to *CHST11*, I have searched online databases for common coding SNPs in exon 2 of *CHST11*, which is the only *CHST11* exon that maps within the association signal. *CHST11* does not harbour any common coding SNPs. Therefore, the association to rs835487 is not mediated by an amino acid change.

Hence my hypothesis was that the association to rs835487 on *CHST11* was marking an expression quantitative trait locus (eQTL), which may influence the expression of *CHST11*. Therefore I have followed the same approach I used to characterise the locus on *MICAL3* (Chapter 4). I initially measured overall gene expression of *CHST11* in cartilage, fatpad and synovium and stratified this by the genotype at rs835487. There was no correlation between gene expression and the genotype in the tissues that I have analysed. Then I have tested for AEI of *CHST11* using a transcript SNP in the 3'UTR of *CHST11* to quantify the amount of mRNA synthesised from each allele. I stratified the allelic expression ratios from the two alleles by the genotype at rs835487 in cartilage, fatpad and synovium tissue. There was no correlation between allelic expression and the genotype at the OA associated SNP in the tissues I have looked at. A heterozygote at this SNP was no more likely to show AEI than would a homozygote at this SNP, therefore, rs835487 was unlikely to have an influence on *CHST11* expression in these tissues.

Although AEI was common in all joint tissues analysed, there was inter and intra-individual variation. In individuals for whom more than one tissue type was available, in some instances, AEI was apparent in one tissue type, but not in others. Also, in some individuals AEI was observed in every tissue analysed, but to different extents, and also in opposite directions. This suggests that different cellular environments can give rise to differential allelic expression in different tissues in the same individual. This has been shown previously for a locus on *BMP5* across osteoarthritic and joint tissues from the same patient (Wilkins *et al.*, 2007).

My results show no evidence for a role for *cis* regulation at *CHST11* that can account for the association signal at chromosome 12q23.3 in the tissues that I have analysed. It

can be presumed that the *cis*-effect at this locus may not be active in adult tissue obtained from end-stage OA patients. A role for CHST11 during mammalian development has previously been characterised (Klüppel *et al.*, 2005), hence it may mean that *cis* regulation of *CHST11* is more important during early developmental stages in mammals, hence is absent in adult tissue. Therefore, cartilage from OA patients may not be a suitable tissue type to be used for the search for functional effects at this locus.

Chapter 6: Sequence analysis of *CHST11* coding exons

6.1 Introduction

As mentioned in Chapter 5.2.3, there are no common (MAF $\geq 15\%$) coding variants in *CHST11* as suggested by online DNA variant databases. My aim was to search for rare penetrant variants in *CHST11* that can account for OA susceptibility. The online databases contain population controls, therefore, I directly looked at hip OA patients, as *CHST11* association was to hip OA.

6.2 Results

Primers listed in Table 2.10 were used to PCR amplify the coding region of *CHST11* in 192 hip OA patients (Chapter 2.24, Figure 2.1). The sequences were analysed for novel mutations using the Sequencing Analysis software (Applied Biosystems). One mutation was observed in a male patient, involving a G to C transition that would result in the non conservative amino acid change of lysine to asparagine (Figure 6.1).

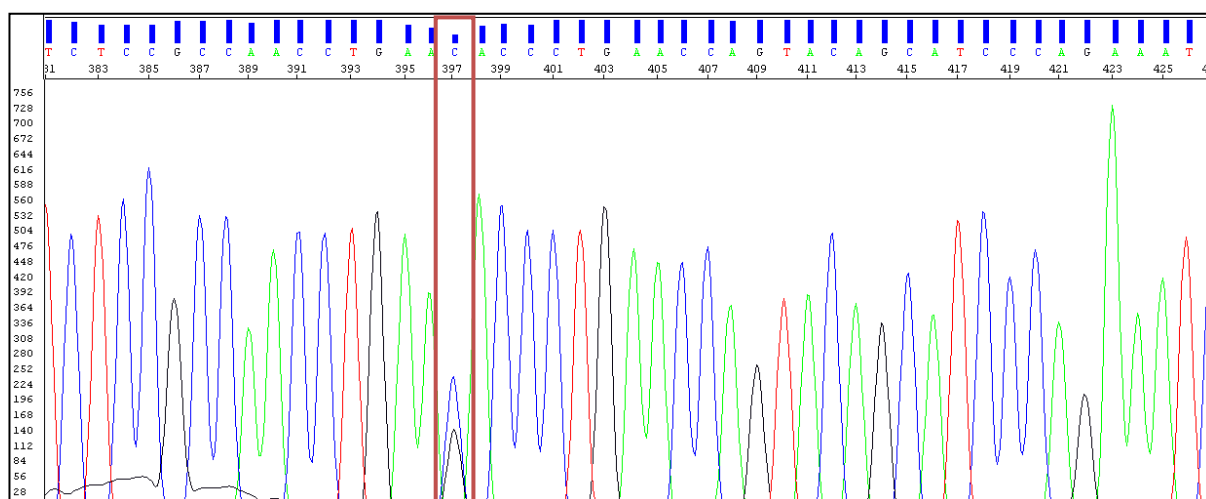


Figure 6.1: Electropherogram showing the partial sequence of *CHST11* exon 3, that harbours the novel mutation (G/C).

The Y-axis denotes the relative fluorescent units. The different colours of the peaks represent different dyes used to detect the alleles: red, T; blue, C; black, G and green, A. The novel mutation is boxed in red.

An additional 599 OA hip patients were genotyped for this novel mutation to assess its frequency. The genotyping was performed using the RFLP assay listed in Table 2.6. The

mutation was absent in these additional samples. A representative assay is shown in Figure 6.2. The allele frequency of this mutation is estimated to be at most 0.063%.

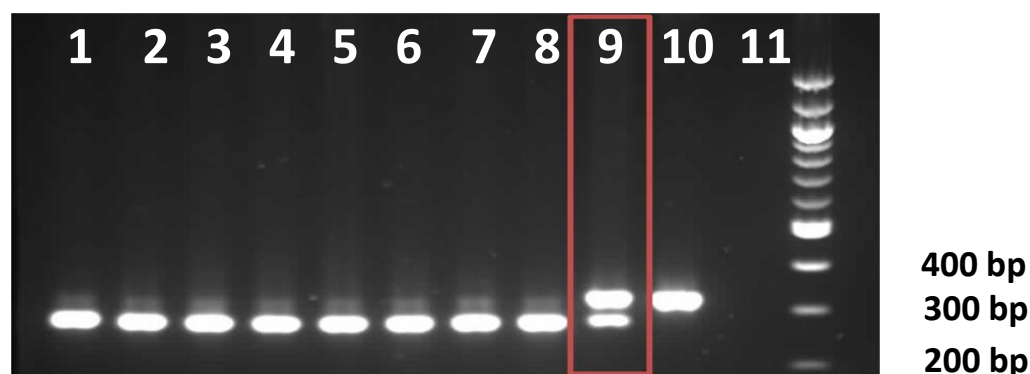


Figure 6.2: RFLP carried out on hip OA patients.

Lane 1 to 9: Digestion products of PCR amplified DNA from Hip OA patients, Lane 10: Undigested PCR product, Lane 11: PCR blank. The heterozygote carrying the rare variant is boxed. The digestion products were run on a 2% agarose gel containing ethidium bromide. A 100 bp DNA ladder was used for sizing of PCR products.

6.3 Discussion

Of 192 hip OA patients that were sequenced for the *CHST11* coding region, one carried a novel mutation in exon 3 of *CHST11*. This is a G to C transition resulting in a non conservative amino acid change from lysine to asparagine. The mutation was absent in an additional 599 hip OA patients that were subsequently genotyped for this variant. The allele frequency of this mutation is estimated therefore to be 0.063%.

Therefore, I did not find any variants in the *CHST11* coding region that can contribute to OA susceptibility at a population level.

Chapter 7: The role of CHST11 in chondrocyte differentiation

7.1 Introduction

Studies carried out in mouse and zebrafish have shown the importance of CHST11 during development. Klüppel *et al.* (2005) generated a *Chst11* knockout mouse which showed severe chondrodysplasia, alterations in cartilage growth plate morphogenesis, and disturbed TGF β signalling in the cartilage growth plate (Chapter 5.1). A study in zebrafish where *Chst11* was knocked-down with the use of specific antisense morpholino oligonucleotides showed reduced 4-O sulphation and reduced chondroitin sulphate (CS) levels in the mutant embryos (Mizumoto *et al.*, 2009). The mutants also showed multiple embryonic morphological defects including a ventrally bent trunk and a curled tail. A recent study that used a forward genetic screen of zebrafish to screen for cartilage and bone phenotypes that resemble OA, identified *chst11* as the mutant gene (CL Hammond, personal communication, 18th July 2012). The mutants showed an alteration in the assembly of the cartilage matrix, premature chondrocyte hypertrophy and osteoblast formation. Hence there is clear evidence for a role of CHST11/*Chst11* during embryonic development in mouse and zebrafish.

As discussed in Chapter 5, the OA association to rs835487 in *CHST11* was not mediated by a change in *CHST11* expression in adult OA joint tissues. Hence I have now hypothesised that the *cis* effect is active during development but not active in the adult OA tissues that I had analysed in that chapter. Therefore, I concluded that adult OA tissue was not a suitable tissue type to be used for functional studies of *CHST11*. Hence I have now utilised mesenchymal stem cells (MSCs) extracted from human hip joints to assess and explore the role of CHST11 in MSCs during chondrogenesis. That is the principle aim of this chapter.

Under appropriate culture conditions, MSCs are capable of undergoing differentiation into chondrocytes, osteoblasts and adipocytes (Dominici *et al.*, 2006). Many cell culture methods have been developed to drive MSCs towards chondrogenesis, including monolayer culture, pellet culture, micromass culture and polymer or biomaterial based scaffold culture (Djouad *et al.*, 2006). It has been shown by Murdoch *et al.* (2007) that Transwell culture is a more efficient method for MSC differentiation since it results in greater cartilage-like matrix synthesis and deposition compared to

other established methods. This is primarily because the cells that are cultured in Transwell inserts have access to the nutrient supply from above and below the permeable insert, which creates a strong pro-chondrogenic environment. In this chapter, I have used the Transwell culture method to differentiate MSCs into chondrocytes after *CHST11* knockdown, to assess the role of *CHST11* during chondrogenesis. To complement the MSCs study I have also investigated the role of *CHST11* in adult chondrocytes, also by *CHST11* knockdown.

7.2 Results

7.2.1 Validation of the Transwell culture of mesenchymal stem cells as a tool to investigate chondrogenesis

The gene expression changes that take place during the differentiation of MSCs from a donor (black, male, aged 22) from day 0 to 14 in Transwell culture were previously analysed by Dr. Matt Barter (Newcastle University; Figure 1A; Appendix 2; Chapter 2.25 and 2.27). The gene expression of cartilage specific genes *COL2A1* and *ACAN* were elevated approximately 1000 and 100 fold by day 1 of chondrogenesis respectively, and the gene expression levels were maintained up to 14 days. The expression of *SOX9*, which encodes a chondrogenic transcription factor, showed an approximately 10 fold increase by day 1, and varied during the 14 day time course. Expression of *COL1A1* and *RUNX2*, which encode osteogenic markers, and *MMP13*, which encodes a hypertrophic marker, were down regulated during chondrogenesis. The upregulation of chondrocyte marker genes and the down regulation of osteogenic and hypertrophic marker genes demonstrated that the MSCs progressed towards chondrogenesis. However, the expression of *COL10A1*, which encodes a marker of hypertrophy, followed a similar pattern to *COL2A1*, where the gene expression was elevated by approximately 1000 fold by day 1, and remained at similar levels up to day 14. The large increase in *COL2A1* and *COL10A1* expression at the same time during chondrogenesis has been reported previously in MSC Transwell disc culture (Murdoch *et al.*, 2007). However, the authors suggest that the down regulation of *RUNX2*, upregulation of its repressor *BAPX1*, down regulation of *MATN1* (gene expressed in growth plate cartilage) and increased expression of *MATN3* (gene expressed in articular cartilage) together show that there is no clear evidence for the progression towards hypertrophy in these cells.

7.2.2 *CHST11* expression in mesenchymal stem cells during differentiation into chondrocytes

To assess how the expression of *CHST11* varies during chondrogenesis, I drove MSCs from towards chondrogenesis and measured *CHST11* expression at days 0, 3, 7 and 14 using the real time PCR assay listed in Table 2.2 (Chapter 2.17 and Chapter 2.27). This experiment was performed on the MSCs from two donors (Chapter 2.25).

CHST11 expression was highest at day 7 and decreased 2.2 and 3.6 fold by day 14 in donor A and B respectively (Figure 7.1).

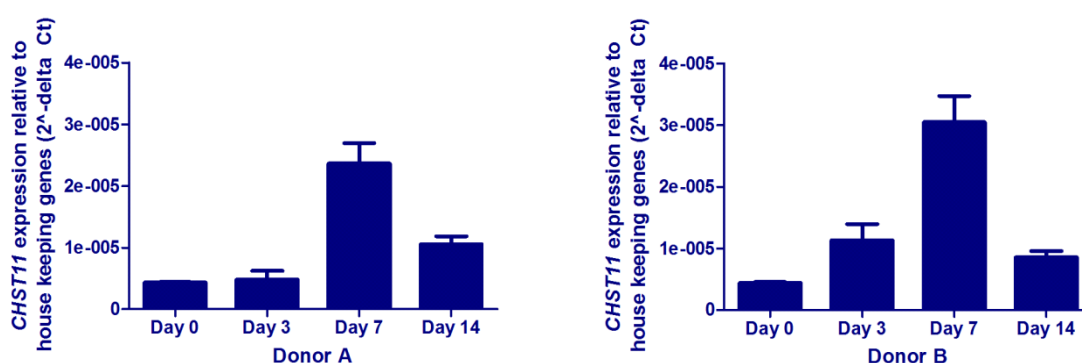


Figure 7.1: *CHST11* expression relative to housekeeping genes in MSCs from donors A and B during differentiation into chondrocytes. The gene expression was measured at 4 time points; days 0, 3, 7 and 14. The error bars represent standard error of the mean of three technical replicates.

7.2.3 Effect of *CHST11* knockdown in human mesenchymal stem cells during differentiation into chondrocytes

Effect on wet mass of cartilage discs

To assess the role of *CHST11* during chondrogenesis, I knocked-down *CHST11* in the MSCs from the two donors (Chapter 2.26). I used MSCs transfected with a non-targeting siRNA as a negative control. *CHST11* knockdown was confirmed using real time PCR at each time point (Figure 7.2) and *CHST11* protein knockdown in day 7 discs was confirmed with western blot analysis (Chapter 2.15). Western blots showed two bands, one at the predicted size for *CHST11* protein (42 kDa), and one slightly larger (Figure 7.3). Both bands disappeared when *CHST11* was knocked-down. It has been

reported that CHST11 undergoes post-translational *N*-glycosylation, which can increase its molecular weight, producing the larger band (Yusa et al., 2005).

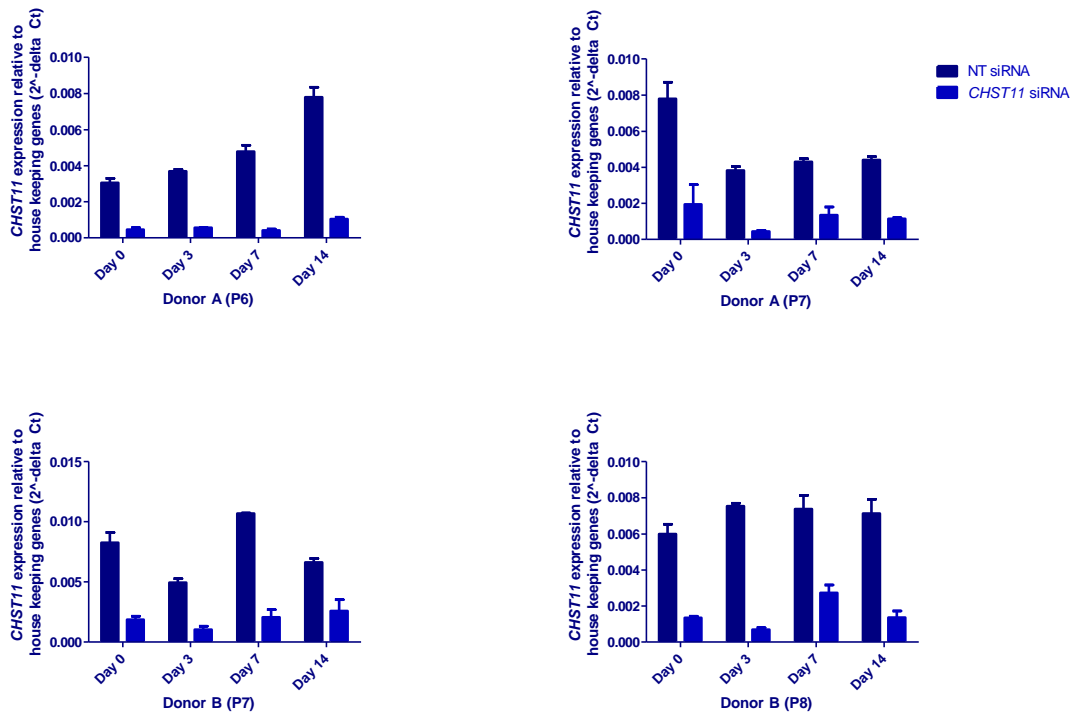


Figure 7.2: *CHST11* expression in MSCs transfected with a non-targeting (NT) siRNA and with an anti-*CHST11* siRNA. The error bars represent standard error of the mean (n=3).

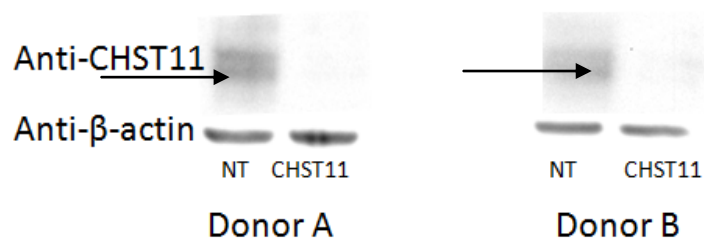


Figure 7.3: Western blot analysis on protein extracted from day 7 cartilage discs formed during MSC chondrogenesis.

Arrows show the 42 kDa band corresponding to CHST11. Anti-β-actin antibody was used as a loading control. NT, protein extracted from cells transfected with the non-targeting siRNA; CHST11, protein extracted from cells transfected with the anti-*CHST11* siRNA.

As the cells progress towards chondrogenesis, in addition to cell proliferation, a highly hydrated extracellular matrix is deposited in the discs (Tew et al., 2008). I therefore measured the wet mass of the discs at days 3, 7 and 14.

The wet mass of the discs formed by the cells transfected with the non-targeting siRNA control (control cells) and those formed by the *CHST11* knocked-down cells increased during differentiation in both donors (Figure 7.4). Donor A and donor B showed a 3.5 and a 4.6 fold increase in the wet mass of control discs by day 14 compared to day 3, respectively. Similarly, the wet mass of the discs formed in the *CHST11* knocked-down cells increased by 2.7 and 4.8 fold by day 14 compared to day 3 in donor A and B, respectively.

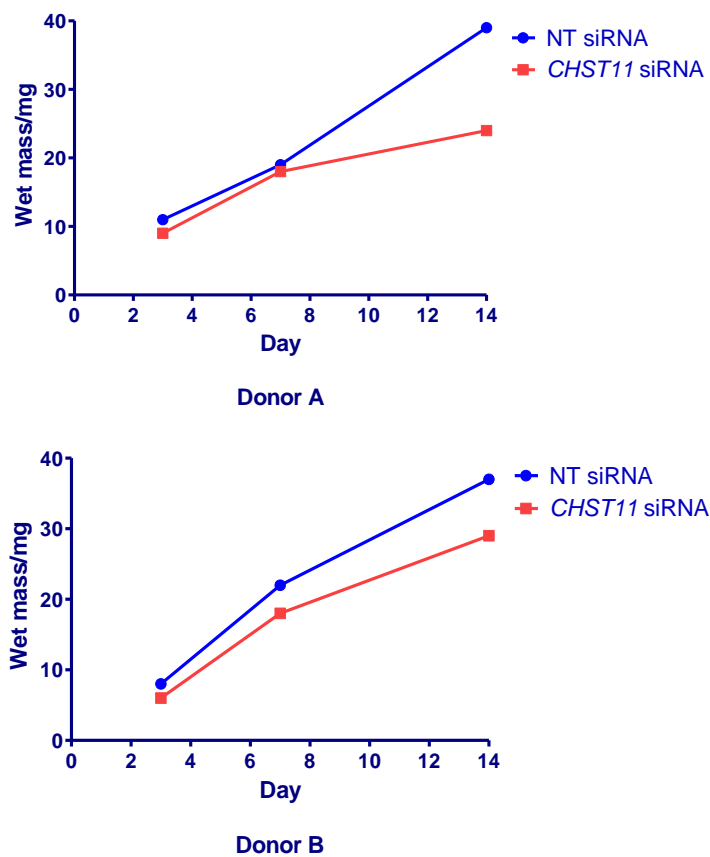


Figure 7.4: The change in wet mass in cartilage discs formed by MSCs from donors A and B during chondrogenesis. The weights were measured at 3 time points; day 3, 7 and 14. NT siRNA, non-targeting siRNA.

However, the wet mass of the cartilage discs formed by the *CHST11* knocked-down cells was lower than that formed by the control cells at all time points and in both donors (Figure 7.4). In donor A, the fold decrease in wet mass was 1.2, 1.1 and 1.6 fold at day 3, 7 and 14, respectively. Donor B showed a 1.3, 1.2 and 1.3 fold decrease in wet mass at day 3, 7 and 14, respectively. This may reflect a reduction in extracellular matrix synthesis in the *CHST11* knocked-down cells compared to the control cells.

Effect on gene expression

I next measured the gene expression changes of a panel of 13 genes in the *CHST11* knocked-down cells compared to the cells transfected with the non-targeting siRNA. The genes tested are listed in Table 7.1. They represent a range of genes whose proteins function in cartilage metabolism. This panel included genes whose products are catabolic, anabolic, osteogenic and hypertrophic markers. For each gene, expression was measured twice in each donor to assess the reproducibility of the experiment. *CHST11* knockdown was successful in both donors at days 0, 3, 7 and 14. Gene expression was tested at these time points (Figure 7.2), whilst western blotting was carried out on protein extracted from day 7 cartilage discs. This showed successful knockdown of *CHST11* (Figure 7.3). A two-tailed student's *t*-test was performed to compare between the gene expression between control cells and the *CHST11* knocked-down cells at all time points. Significant ($P < 0.05$) up/down regulation in gene expression was plotted for the two donors for each time point (Figure 7.5). The actual values of these significant changes are listed in Table 7.2. A Wilcoxon signed rank test was performed to assess whether gene expression in the cells showed a significant trend, following *CHST11* knockdown. The P-values are listed in Table 7.3.

Gene	Gene product	Role in cartilage
<i>COL2A1</i>	α -1 chain of type 2 collagen	Anabolism
<i>ACAN</i>	Aggrecan	
<i>SOX9</i>	SRY-box 9 transcription factor	
<i>TIMP1</i>	Tissue inhibitor of matrix metalloproteinase 1	Anti-catabolism
<i>MMP1</i>	Matrix metalloproteinase 1, a collagenase	Catabolism
<i>MMP13</i>	Matrix metalloproteinase 13, a collagenase	
<i>ADAMTS4</i>	A disintegrin and metalloproteinase with thrombospondin motifs 4, an aggrecanase	
<i>ADAMTS5</i>	A disintegrin and metalloproteinase with thrombospondin motifs 5, an aggrecanase	
<i>COL1A1</i>	α -1 chain of type 1 collagen	Osteogenesis
<i>BGLAP</i>	Bone γ -carboxyglutamate (gla) protein	
<i>RUNX2</i>	Runt-related transcription factor 2	
<i>IHH</i>	Indian hedgehog	Hypertrophy
<i>COL10A1</i>	α -1 chain of type 10 collagen	

Table 7.1: List of the genes that were studied in this chapter, their protein products and their role in cartilage.

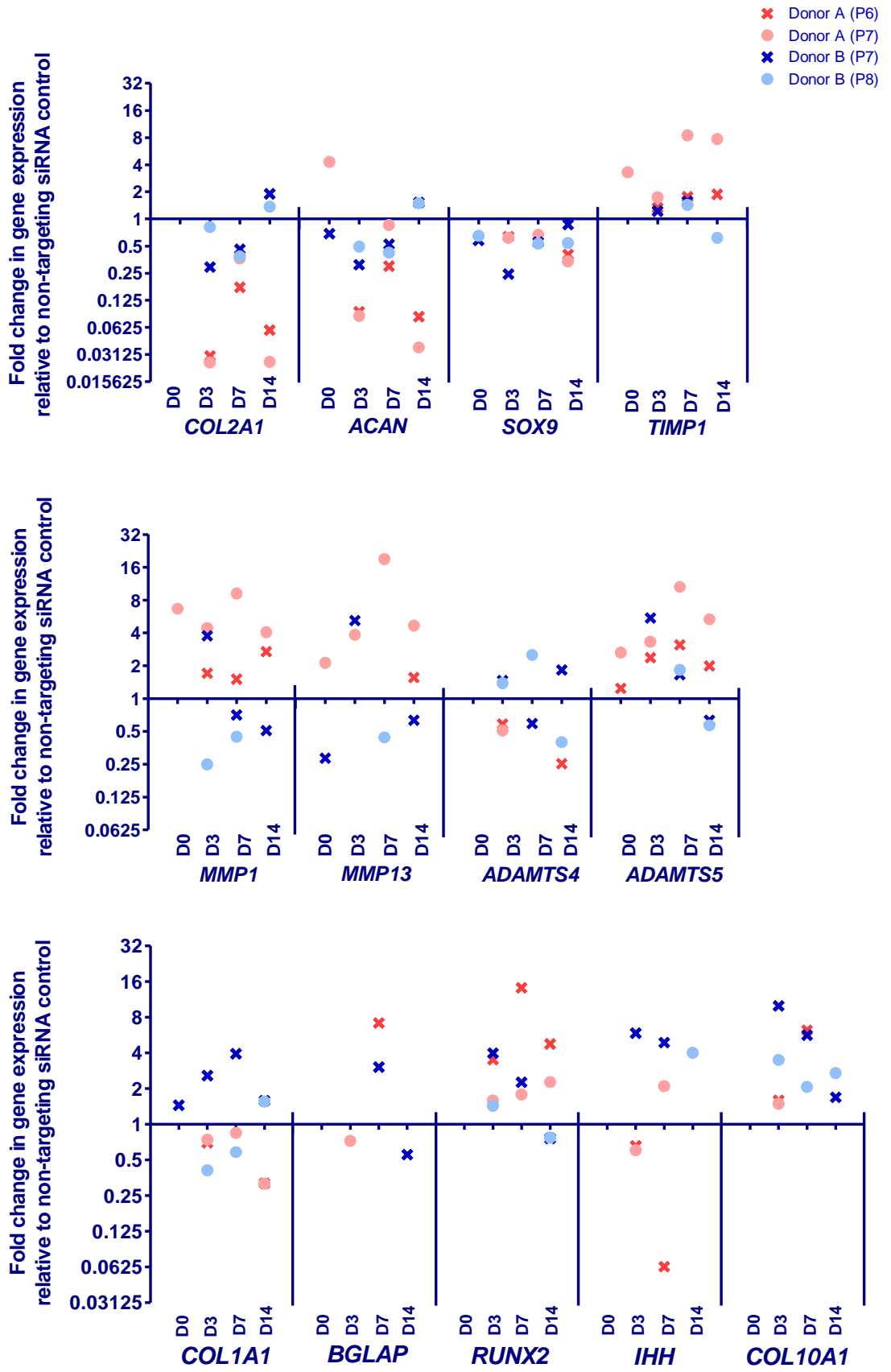


Figure 7.5: Fold change in gene expression in *CHST11* knocked-down cells compared to control cells in MSCs from donors A and B during chondrogenesis.

The passage number of the cells used in each experiment is given within brackets (P6, P7, P8). Gene expression was measured at four time points; days 0, 3, 7 and 14 (D0, D3, D7 and D14). Each data point represents a significant ($P < 0.05$) up/down regulation of gene expression relative to housekeeping genes in response to *CHST11* knockdown at different time points. Data points show results from two independent experiments carried out for each donor.

Gene	Time point	Donor A		Donor B	
		P6	P7	P 7	P8
COL2A1	Day 0				
	Day 3	0.03	0.03	0.29	0.81
	Day 7	0.17	0.36	0.46	0.39
	Day 14	0.06	0.03	1.90	1.37
ACAN	Day 0	-	4.29	0.69	-
	Day 3	0.09	0.08	0.31	0.49
	Day 7	0.30	0.86	0.52	0.42
	Day 14	0.08	0.04	1.52	1.49
SOX9	Day 0	-	-	0.58	0.65
	Day 3	0.64	0.62	0.24	-
	Day 7	-	0.67	0.55	0.53
	Day 14	0.40	0.34	0.87	0.54
TIMP1	Day 0	-	3.29	-	-
	Day 3	1.33	1.74	1.22	-
	Day 7	1.76	8.47	1.57	1.43
	Day 14	1.87	7.69	-	0.62
MMP1	Day 0	-	6.68	-	-
	Day 3	1.71	4.42	3.76	0.25
	Day 7	1.51	9.20	0.71	0.45
	Day 14	2.69	4.06	0.51	-
MMP13	Day 0	-	2.13	0.28	-
	Day 3	-	3.83	5.20	-
	Day 7	-	19.04	-	0.44
	Day 14	1.56	4.66	0.63	-
ADAMTS4	Day 0	-	-	-	-
	Day 3	0.58	0.51	1.46	1.38
	Day 7	-	-	0.59	2.51
	Day 14	0.25	-	1.82	0.40
ADAMTS5	Day 0	1.25	2.64	-	-
	Day 3	2.37	3.31	5.47	-
	Day 7	3.12	10.57	1.66	1.83
	Day 14	1.99	5.33	0.63	0.57
COL1A1	Day 0	-	-	-	1.44
	Day 3	0.74	0.70	0.41	2.57
	Day 7	0.84	-	0.58	3.94
	Day 14	0.31	0.32	1.56	1.58
BGLAP	Day 0	-	-	-	-
	Day 3	0.72	-	-	-
	Day 7	-	7.14	-	3.03
	Day 14	-	-	-	0.55
RUNX2	Day 0	-	-	-	-
	Day 3	1.59	3.50	1.43	3.98
	Day 7	1.78	14.18	-	2.26
	Day 14	2.27	4.75	0.77	0.76
IHH	Day 0	-	-	-	-
	Day 3	0.60	0.66	-	5.88
	Day 7	2.09	0.06	-	4.89
	Day 14	-	-	4.00	-
COL10A1	Day 0				
	Day 3	1.48	1.59	3.49	9.96
	Day 7	-	6.20	2.06	5.64
	Day 14	-	-	2.70	1.69

Table 7.2: Significant ($P < 0.05$) fold change in gene expression following *CHST11* knockdown in days 0, 3, 7 and 14 MSC discs, relative to control discs. A value greater than 1 denotes a significant upregulation of gene expression and a value less than 1 denotes a significant down regulation of gene expression. A dash (-) indicates no significant change in gene expression. *COL2A1* and *COL10A1* expression were not detected at day 0. Gene expression was measured using cDNA synthesised from RNA extracted from discs transfected with non-targeting siRNA and compared to that extracted from *CHST11* knocked-down discs. Three technical replicates were performed for each disc. The experiment was performed twice for each donor.

Gene	P-value
<i>COL2A1</i>	0.0210
<i>ACAN</i>	0.0105
<i>SOX9</i>	0.0005
<i>TIMP1</i>	0.0049
<i>MMP1</i>	0.0525
<i>MMP13</i>	0.0977
<i>ADAMTS4</i>	1.0000
<i>ADAMTS5</i>	0.0024
<i>COL1A1</i>	0.9097
<i>BGLAP</i>	0.6250
<i>RUNX2</i>	0.0049
<i>IHH</i>	0.2188
<i>COL10A1</i>	0.0039

Table 7.3: P-values calculated using the Wilcoxon signed rank test for each target gene following *CHST11* knockdown.

P<0.05 are highlighted in red.

COL2A1

COL2A1 expression was not detected in the MSCs at day 0, before the addition of chondrogenic factors to the growth media. The *CHST11* knocked-down cells from both donors showed a reduced expression of *COL2A1* at day 3 and 7. At day 14, donor A showed a down regulation whilst donor B showed an upregulation of *COL2A1* expression.

ACAN

During differentiation up to day 7, *ACAN* expression was decreased in *CHST11* knocked-down cells from both donors. At day 14, donor A showed a down regulation and donor B showed an upregulation of *ACAN* expression after *CHST11* knockdown.

SOX9

SOX9 expression was down regulated in donor A at all time points and in donor B at day 3, 7 and 14.

TIMP1

TIMP1 expression was increased in donor A at all time points and in donor B at day 3 and 7. At day 14, there was reduced *TIMP1* expression in *CHST11* knocked-down cells in donor B.

MMP1

Donor A showed increased expression of *MMP1* in *CHST11* knocked-down cells at all time points. Donor B showed a down regulation of *MMP1* expression after *CHST11* knockdown at day 7 and 14. This may explain the upregulation of *COL2A1* seen in donor B at day 14 after knockdown of *CHST11*.

MMP13

MMP13 was upregulated in *CHST11* knocked-down cells from donor A, however this effect was not replicated in both experiments. The increased expression of *TIMP1* seen during chondrogenesis in this donor is perhaps a consequence of the cells attempting to regulate the increased levels of *MMP1* and *MMP13* expression. Donor B showed an

initial upregulation of *MMP13* in response to *CHST11* knockdown, and then showed a down regulation after day 3.

ADAMTS4

The expression of *ADAMTS4* was variable between the two donors, as well as between the experimental replicates.

ADAMTS5

ADAMTS5 was upregulated at all time points in *CHST11* knocked-down cells from donor A. Donor B also showed an upregulation of this gene at day 3 and 7. However, *ADAMTS5* was down regulated in this donor at day 14. This may explain the upregulation of *ACAN* at day 14 in the *CHST11* knocked-down cells from this donor.

COL1A1, BGLAP, IHH

A consistent effect was not seen between experiments or donors for *COL1A1*, *BGLAP* or *IHH*.

RUNX2

RUNX2 expression was upregulated in donor A at all time points during chondrogenesis after *CHST11* knockdown. This gene was initially upregulated in donor B, but was down regulated by day 14.

COL10A1

Expression of *COL10A1* was not detected at day 0 in either donor. Donor A showed an increase in *COL10A1* in response to *CHST11* knockdown at day 3. In donor B the gene was upregulated following *CHST11* knockdown at all time points during chondrogenesis.

In summary, *CHST11* knockdown in MSCs led to a significant change in gene expression of anabolic marker genes *COL2A1* ($p=0.02$), *ACAN* (0.01), *SOX9* (0.0005) and *TIMP1* (0.005), catabolic marker gene *ADAMTS5* (0.002) and hypertrophic marker genes *RUNX2* (0.005) and *COL10A1* (0.004).

7.2.4 Proteoglycan quantification in *CHST11* knocked-down mesenchymal stem cells

Since the results from the above section showed a loss of wet mass in cartilage discs formed by the *CHST11* knocked-down cells and a down regulation of *ACAN* during chondrogenesis in response to *CHST11* knockdown, I hypothesised that these cells may produce less extracellular matrix compared to control cells. I therefore used Alcian blue staining to quantify the amount of sulphated GAGs in MSCs (Chapter 2.31). The cells were cultured as high density micromasses after transfection with the non-targeting siRNA and the anti-*CHST11* siRNA (Chapter 2.30). Real time PCR analysis showed a 7 fold and 15 fold decrease in *CHST11* expression in cells transfected with anti-*CHST11* siRNA versus control cells from donor A and B, respectively (Figure 7.6). The subsequent reduction in the level of *CHST11* protein was confirmed using western blot analysis (Figure 7.7). The Alcian blue bound to sulphated glycosaminoglycans (GAGs) was quantified and normalised to the protein content of the *CHST11* knocked-down cells and control cells (Chapter 2.31). Three biological replicates were performed. The *CHST11* knocked-down cells showed significantly reduced Alcian blue staining compared to control cells from both donors, suggesting that there is less sulphated GAGs produced in these cells after *CHST11* knockdown (Figures 7.8 and 7.9).

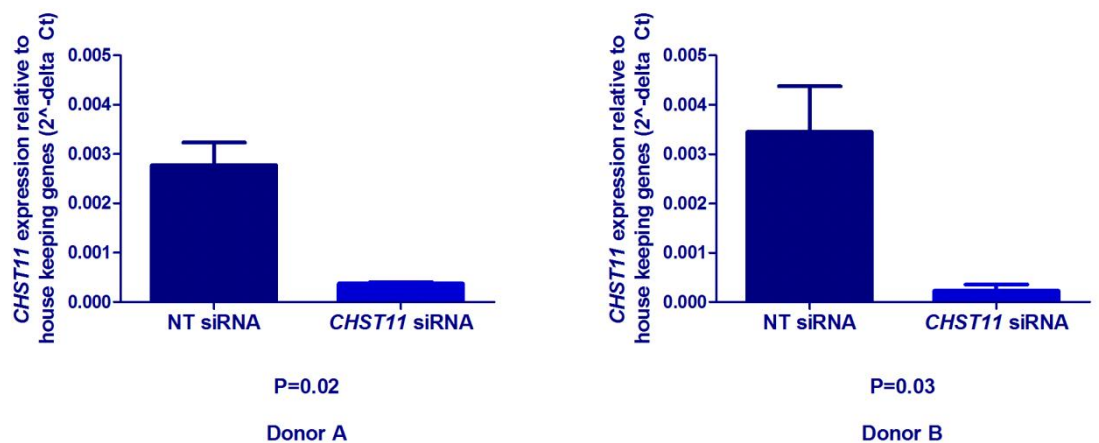


Figure 7.6: *CHST11* expression in MSCs transfected with a non-targeting (NT) siRNA and with an anti-*CHST11* siRNA. The error bars represent standard error of the mean (n=3). A student's *t*-test was performed to calculate the P-value.



Figure 7.7: Western blot analysis on protein extracted from micromass cultures of MSCs from donors A and B. Arrows show the 42 kDa band corresponding to CHST11. Anti-β-actin antibody was used as a loading control.

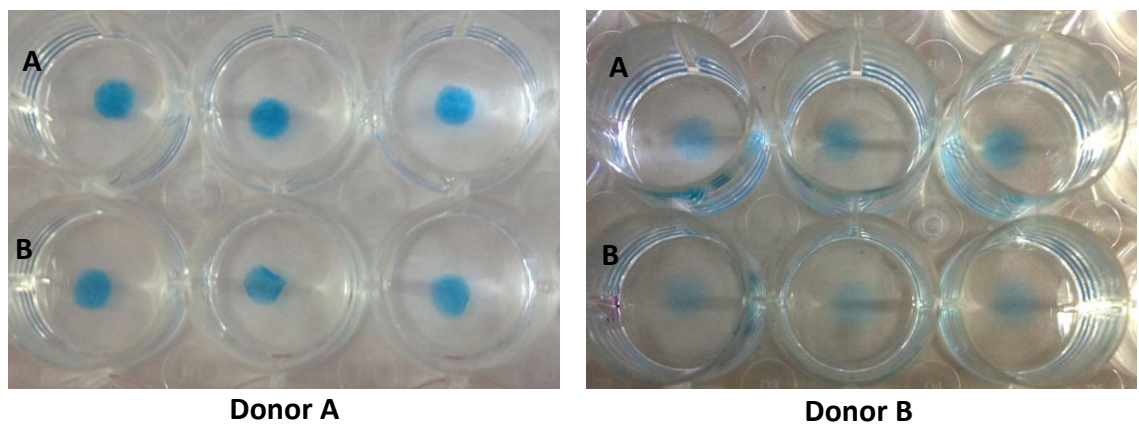


Figure 7.8: Alcian blue staining in micromasses cultured from cells transfected with (A) a non-targeting siRNA and (B) with an anti-*CHST11* siRNA.

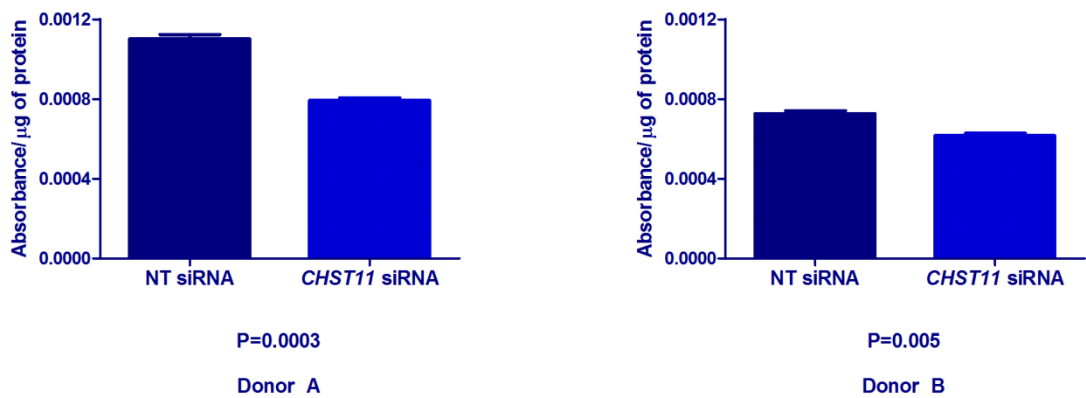


Figure 7.9: Absorbance at 600 nm per microgram of protein in micromasses cultured from MSCs transfected with a non-targeting (NT) siRNA and with an anti-*CHST11* siRNA. The error bars represent the standard error of the mean (n=3). A student's *t*-test was performed to calculate the P-value.

Summary of the *CHST11* MSC data

CHST11 expression peaked at day 7 in MSCs during chondrogenesis, which was then reduced by day 14 (Figure 7.1). The wet mass of the cartilage discs increased during MSC chondrogenesis, however, *CHST11* knockdown resulted in a reduction in the wet mass of the discs formed compared to the controls (Figure 7.4). *CHST11* knockdown also reduced expression of some anabolic marker genes (*COL2A1*, *ACAN* and *SOX9*) and increased expression of *ADAMTS5*, a catabolic marker gene, and *RUNX2* and *COL10A1*, hypertrophic marker genes (Figure 7.5, Tables 7.2 and 7.3). My results also showed that the amount of sulphated GAGs synthesised by the *CHST11* knocked-down cells was significantly lower than that produced by the control cells (Figures 7.8 and 7.9).

Overall, my results clearly demonstrate a role for *CHST11* during chondrogenesis in the MSC model that I have used.

7.2.5 Gene expression changes after *CHST11* knockdown in OA and NOF chondrocytes

My MSC data raise the question whether *CHST11* is only important during the formation of the cartilage or if it also plays a role in mature cartilage. Therefore, I knocked-down *CHST11* in chondrocytes extracted from four hip and four knee joints of

OA patients and from a NOF patient and assessed what effect this had on gene expression (Chapter 2.26). Details regarding the 9 patients are listed in Table 7.4. For gene expression I focused on 6 of the 13 genes listed in Table 7.1: *COL2A1*, *ACAN*, *TIMP1*, *SOX9*, *MMP1* and *MMP13*. Knockdown of *CHST11* was successful in all 9 patients (data not shown). However, due to insufficient amounts of protein extracted from the chondrocytes, I was not able to test for the concomitant reduction in *CHST11* protein.

Complimentary DNA was synthesised from the cell lysates 48 hours post transfection with anti-*CHST11* siRNA (Chapter 2.16). Gene expression was measured in cDNAs synthesised from RNAs from the control cells (cells transfected with a non-targeting siRNA) and the *CHST11* knocked-down cells using real time PCR (Chapter 2.17). A two-tailed student's *t*-test was performed to compare the gene expression in control cells and the *CHST11* knocked-down cells. Significant ($P < 0.05$) up/down regulation in gene expression was plotted for the knee and hip OA patients and for the NOF patient (Figure 7.10). The actual values of these significant data are listed in Table 7.5. A Wilcoxon signed rank test was not performed for these experiments due to the low sample size.

Of the nine patients, only two OA patients (patients C and F) showed a significant down regulation of *COL2A1*. OA patients D, E and F showed elevated levels of *ACAN*. An upregulation of *TIMP1* was seen in the hip OA patients E, F and H, and a down regulation of *TIMP1* was seen in the NOF patient. None of the 9 patients showed an up/down regulation of *SOX9* expression. The knee OA patients A, D and I, and the NOF patient, showed a decreased expression of *MMP1*. *MMP13* expression was elevated only in patient B and was down regulated only in the NOF patient.

In summary, I observed significant effects on gene expression following *CHST11* knockdown in chondrocytes. However, this was not observed in all patients studied.

Patient letter	Age at surgery	Sex	Joint type
A	79	F	OA knee
B	54	M	OA knee
C	63	M	OA knee
D	49	F	OA knee
E	52	F	OA hip
F	67	F	OA hip
G	54	F	OA hip
H	77	M	OA hip
I	80	F	NOF hip

Table 7.4: Details of the nine patients studied.

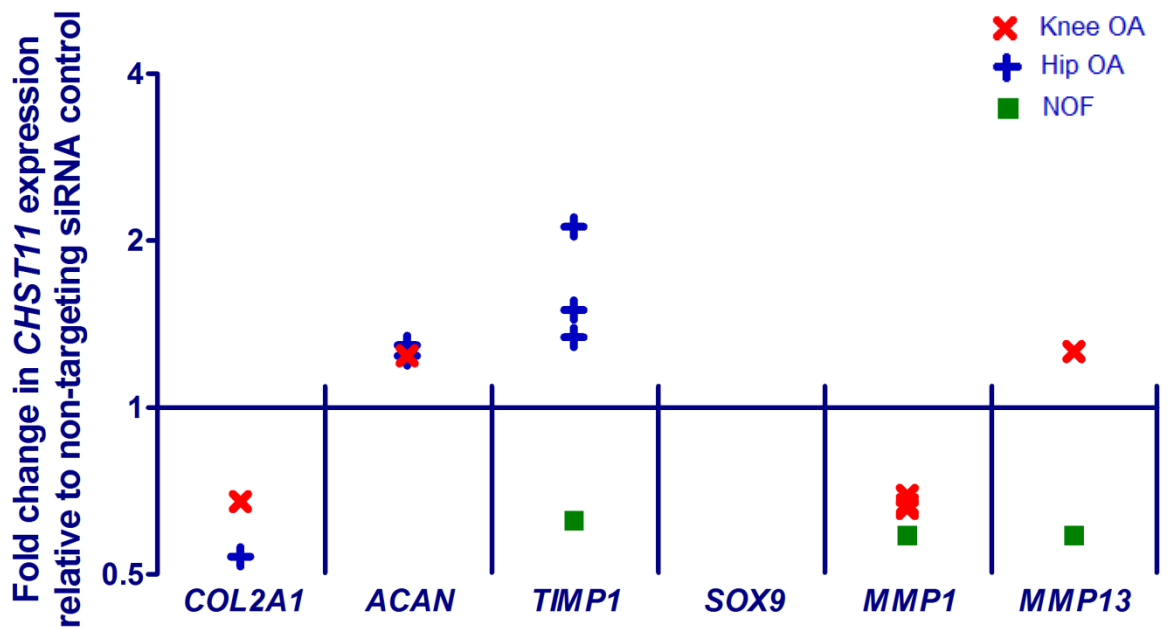


Figure 7.10: Effect of *CHST11* knockdown in knee OA, hip OA and NOF chondrocytes. Each data point represents a significant ($p < 0.05$) up/down regulation of gene expression relative to housekeeping genes in response to *CHST11* knockdown.

Gene	Knee OA				Hip OA				NOF
	A	B	C	D	E	F	G	H	I
<i>COL2A1</i>	-	0.68	-	-	-	-	-	0.54	-
<i>ACAN</i>	-	-	-	1.24	-	-	1.24	1.30	-
<i>TIMP1</i>	-	-	-	-	1.50	-	2.12	1.34	0.63
<i>SOX9</i>	-	-	-	-	-	-	-	-	-
<i>MMP1</i>	-	0.67	0.66	0.69	-	-	-	-	0.59
<i>MMP13</i>	1.26	-	-	-	-	-	-	-	0.59

Table 7.5: Significant ($P < 0.05$) fold change in gene expression following *CHST11* knockdown in days 0, 3, 7 and 14 MSC discs, relative to control discs.

A value greater than 1 denotes a significant upregulation of gene expression and a value less than 1 denotes a significant down regulation of gene expression. A dash (-) indicates no significant change in gene expression.

7.2.6 Proteoglycan quantification in *CHST11* knocked-down OA chondrocytes

To determine if *CHST11* knockdown in adult chondrocytes leads to a reduction in extracellular proteoglycan synthesis, I next cultured chondrocytes extracted from one knee OA patient (an 83 year old female) in high density micromasses for analysis using Alcian blue staining (Chapter 2.30 and 2.31). *CHST11* expression was successfully knocked-down by 8 fold in these cells, which was assessed by real time PCR (Figure 7.11). As above, there was insufficient protein to test for the depletion in *CHST11* protein.

Quantification of Alcian blue staining showed that there was no significant difference in the amount of sulphated GAGs synthesised in the control cells compared to the cells transfected with the anti-*CHST11* siRNA (Figures 7.12 and 7.13).

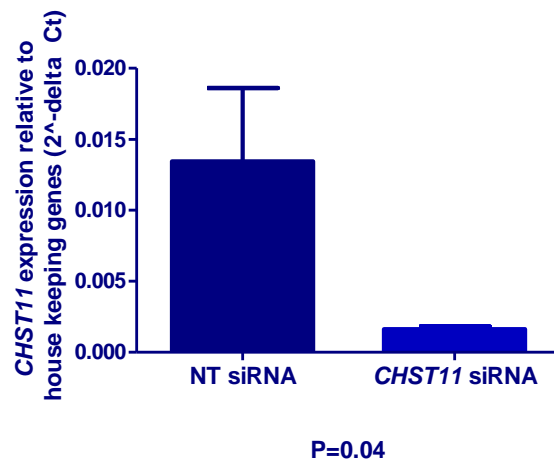


Figure 7.11: *CHST11* expression in cells transfected with a non-targeting (NT) siRNA and with an anti-*CHST11* siRNA. The error bars represent standard error of the mean (n=3). A student's *t*-test was performed to calculate the P-value.

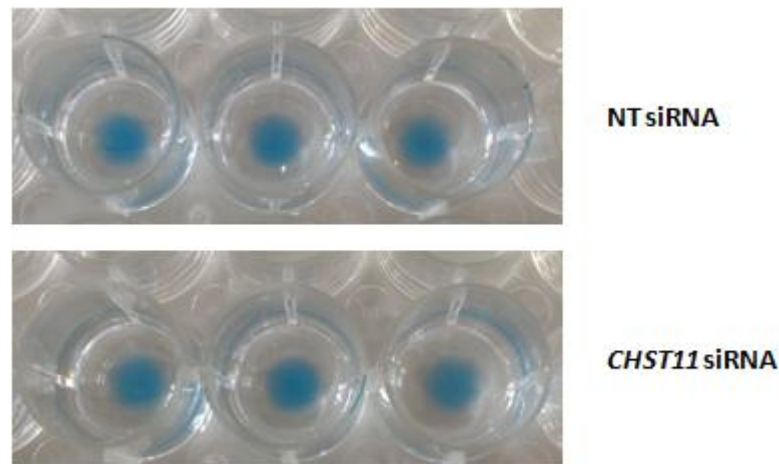


Figure 7.12: Alcian blue staining in micromasses cultured from cells transfected with a non-targeting (NT) siRNA and with an anti-*CHST11* siRNA.

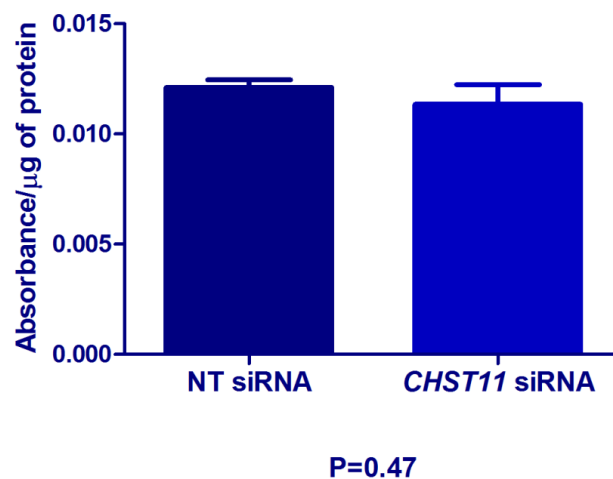


Figure 7.13: Absorbance at 600 nm per microgram of protein in micromasses cultured from cells transfected with a non-targeting (NT) siRNA and with an anti-*CHST11* siRNA. The error bars represent the standard error of the mean (n=3). A student's *t*-test was performed to calculate the P-value.

In summary, *CHST11* knockdown in adult chondrocytes from OA and NOF patients led to a change in gene expression of various genes, although the effect was not consistent among individuals. *CHST11* knockdown did not lead to a change in overall proteoglycan synthesis in OA chondrocytes. However, since I was not able to test for

the concomitant depletion of CHST11 protein, I cannot exclude the possibility that the CHST11 protein levels did not decrease following *CHST11* knockdown.

7.3 Discussion

During MSC differentiation into chondrocytes, *CHST11* expression was highest at day 7 and then decreased by day 14. This suggests that *CHST11* expression is regulated to maintain the correct sulphation balance during chondrogenesis.

The Transwell discs increased in wet mass as the cells progressed towards chondrogenesis, which has been observed previously by Murdoch *et al.* (2007). GAG assays carried out in the discs by those authors showed a linear increase in proteoglycan content, which corresponded to the increase in wet mass that they observed. The discs also stained strongly with Safranin O, which shows further evidence of the formation of a cartilage matrix during chondrogenesis (Murdoch *et al.*, 2007). My results showed that the wet mass of the *CHST11* knocked-down discs increased during differentiation, however the wet mass was lower than that of the discs formed by the control cells at all time points. This suggests that the loss of CHST11 has resulted in these discs being less hydrated, as a correct sulphation balance of GAGs is important for water retention in order to maintain the structural integrity of the cartilage (Gama *et al.*, 2006).

Gene expression analysis on *CHST11* knocked-down MSC discs showed a down regulation of anabolic marker genes *COL2A1*, *ACAN* and *SOX9*. It is of interest that *ACAN* expression was down regulated in response to *CHST11* knockdown, which may correspond to the loss of wet mass seen in these discs compared to the controls, as aggrecan plays a role in water retention in cartilage. Catabolic marker genes *MMP13* and *MMP1* were upregulated in one donor and *ADAMTS5* was upregulated in both donors after *CHST11* knockdown. These results support a role of CHST11 in chondrogenesis. *CHST11* knockdown resulted in an increase in *RUNX2* expression in both donors, which may suggest that CHST11 is not involved in driving cells towards osteogenesis. *COL10A1* expression follows a similar pattern to that of *COL2A1* expression during MSC chondrogenesis (Figure 1A; Appendix 2). However in *CHST11* knocked-down cells, *COL10A1* expression was elevated, whereas *COL2A1* expression

was decreased, suggesting that CHST11 plays a role in chondrogenesis and does not promote chondrocyte hypertrophy.

As *CHST11* expression was initially upregulated until day 7 of chondrogenesis and then down regulated by day 14, it could be that *CHST11* expression is regulated to achieve the correct sulphation balance during chondrogenesis. The correct sulphation pattern and balance of GAGs is crucial for the interaction of the extracellular matrix with growth factors (Klüppel *et al.*, 2005). Different signalling pathways may interact in these cells at different time points during chondrogenesis, and the absence of CHST11 can disrupt the response of these cells to external growth factors, which can alter the expression of several genes involved in chondrogenesis. This may lead to the decrease in anabolism and increase in catabolism, osteogenesis and hypertrophy as observed. In some instances, an inconsistent response was seen, for example, *COL2A1* expression was down regulated initially in donor B, but was upregulated at day 14. This may be a result of other signalling pathways being activated to counteract the loss of CHST11 during chondrogenesis.

CHST11 knockdown also led to a significant reduction in the amount of sulphated GAGs in MSCs from both donors, which corresponds to the reduction in wet mass observed in the Transwell discs after *CHST11* knockdown.

Having seen a role of CHST11 during MSC chondrogenesis, my next aim was to determine if CHST11 was important in adult chondrocytes. Hence I assessed the gene expression changes in response to *CHST11* knockdown in adult OA and NOF chondrocytes. The results showed significant changes in gene expression, however, there was no consistent effect among patients. Also, there was no change in the amount of sulphated GAGs produced in these cells in response to *CHST11* knockdown.

My results show that CHST11 is important during chondrogenesis, the loss of which leads to changes in gene expression during MSC differentiation, a reduction in the wet mass of cartilage discs and a decrease in the amount of sulphated GAGs produced during differentiation. However this effect was not replicated in adult OA and NOF cartilage. Therefore, these results may explain the lack of evidence for *cis* regulation at *CHST11* in OA tissue that can account for the OA association signal at chromosome

12q23.3. Therefore, MSCs can perhaps be used as a more suitable tissue type for functional studies of *CHST11*.

Chapter 8: General discussion

Many epidemiological studies have shown a genetic link to OA, therefore OA is recognised as a polygenic and multifactorial disease (Loughlin, 2011). A number of OA associated polymorphisms have been identified through candidate gene studies, genome-wide linkage studies and genome-wide association scans.

Functional studies on some OA associated polymorphisms have shown that these affect the structure of the protein encoded or affect the expression of the gene through *cis* regulation. An example of a polymorphism that affects protein structure is a polymorphism in the aspartic acid (D) repeat sequence in *ASPN* that showed association to OA. Harboursing the D14 allele of the repeat sequence resulted in greater inhibition of the TGF- β signalling pathway (Kizawa *et al.*, 2005). A good example of a polymorphism that affects gene expression through *cis* regulation is a 5'UTR SNP in *GDF5*, rs143383. This is a T to C transition and showed compelling association to OA in European and Asian cohorts (reviewed in Loughlin, 2011). Functional studies have suggested that rs143383 is perhaps the polymorphism influencing OA susceptibility at this locus, with the OA associated T allele mediating reduced *GDF5* transcription relative to the C allele in all joint tissues so far tested (Egli *et al.*, 2009).

OA chondrocytes respond discordantly to GDF5

In Chapter 3 I hypothesised that this deficit in *GDF5* could be attenuated by the application of exogenous *GDF5* protein and I assessed what effect such application will have on primary OA chondrocyte gene expression.

Key findings of Chapter 3:

1. OA cartilage expressed genes that code for the three *GDF5* receptors, in particular *BMPR-II* and *BMPR-IA*. The expression of *BMPR-IA*, which encodes the alternative type I receptor that *GDF5* binds to, was significantly higher in OA and NOF cartilage compared to *BMPR-IB*, which encodes the receptor towards which *GDF5* shows preferential activity. The same receptor expression pattern was observed in OA chondrocytes cultured in monolayer.
2. I chose to use two *GDF5* proteins, one that was designed to show increased specificity for *BMPR-IA* compared to *BMPR-IB*, and another that was insensitive to

GDF5 antagonist noggin. I used four different recombinant GDF5 proteins in total; wildtype mouse, wildtype human and the two variants (A and B). All four of the exogenous GDF5 proteins were able to activate the Smad 1/5/8 signalling pathway in SW1353 cells, as demonstrated by a luciferase reporter assay, and in chondrocytes, as confirmed by western blot analysis, at a concentration of 100 ng/ml.

3. Gene expression analyses of a panel of chondrocyte marker genes revealed that OA chondrocytes respond to exogenous GDF5 in an inconsistent manner, whereas a consistent response was observed in cells stimulated with exogenous TGF- β 1 and stimulation with IL-1 α and OSM in combination.

My results show that the inconsistency in response to GDF5 will need to be surmounted if treatment with exogenous GDF5 is going to be advanced as a potential means of alleviating the genetic deficit mediated by OA susceptibility at the gene *GDF5*.

Carrying out gene expression analyses in chondrocytes cultured in monolayer has several limitations. Inter-patient variability due to genetic and epigenetic factors and co-morbidity can be problematic in assessing a trend in response to GDF5. To overcome this, a larger sample size is needed, although this is challenging due to the limited availability of samples. Monolayer culture of chondrocytes can also add to this variability as the chondrocyte phenotype is difficult to maintain in culture. Chondrocytes expanded in monolayer have been shown to have a low proliferative capacity and undergo dedifferentiation (Harrison *et al.*, 2000; Dell'Accio *et al.*, 2001). Therefore, it may be more suitable to carry out these studies using *in vitro* culture techniques that provide a three-dimensional cellular environment and use agarose, fibrin or alginate as scaffolds for chondrocytes to adhere to (Buschmann *et al.*, 1992; Schultz *et al.*, 1997; Andreas *et al.*, 2008). High density micromass culture is also being used as a simple and effective culture model and has been used for anti-rheumatic drug screening (Ibold *et al.*, 2007; Andreas *et al.*, 2009) and in regenerative medicine to investigate cartilage formation and the influence of environmental and culture conditions (Anderer and Libera, 2002; Tallheden *et al.*, 2004; Grogan *et al.*, 2007; Dehne *et al.*, 2009). Chondrocyte pellet culture is also another culture technique that is

widely used and has been suggested as transplants in cartilage repair (Anderer and Libera, 2002).

Allelic expression analysis of the OA susceptibility locus that maps to MICAL3

As candidate gene studies focused on genes whose protein products play roles in joint biology, these required prior knowledge of the disease process. Genome-wide association scans have instead yielded more novel loci that show association in OA. Recent findings suggest that OA susceptibility appears to be mediated by polymorphisms in genes whose protein products are involved in pathways that regulate joint maintenance and development, instead of genes encoding structural proteins of the ECM (Reynard and Loughlin, 2013). For example, the arcOGEN GWAS produced OA association signals to *RUNX2* and *PTHLH* genes, which encode proteins involved in endochondral ossification and to *CHST11*, whose protein product is involved in proteoglycan synthesis (Zeggini *et al.*, 2012).

Having identified OA susceptibility loci, it is important to further investigate these to explore whether the susceptibility is mediated through altered gene expression or protein function. Apart from the functional studies that were carried out on the *GDF5* SNP rs143383, as described above and in Chapter 3.1, recent studies have generated functional data for the chromosome 7q22 signal from the Rotterdam GWAS and for the chromosome 14q31.1 locus that maps to *DIO2*, that was produced through a candidate gene study (reviewed in Reynard and Loughlin, 2013). The chromosome 7q22 signal contained, amongst other genes, *HBP1* and *DUS4L*, and reduced expression of *HBP1* was seen in cartilage and synovium tissue, and reduced expression of *DUS4L* was seen in fatpad tissue, in carriers of the OA associated allele (Raine *et al.*, 2012). The authors also carried out allelic expression imbalance (AEI) analyses at *HBP1* and observed that the pattern of AEI demonstrated by carriers of the OA associated allele was significantly different from that seen in non-carriers. Functional studies on *DIO2* showed that AEI was present at the OA associated SNP rs225014 in this gene, with a significant increase in expression from the C allele relative to the T allele in cartilage tissue (Bos *et al.*, 2012).

Aside from OA, AEI analyses have commonly been used to identify *cis* regulatory polymorphisms that account for changes in gene expression in a variety of human tissue types including blood (Pant *et al.*, 2006), brain (Pinsonneault *et al.*, 2006; Zhang *et al.*, 2007), lung (Heighway *et al.*, 2003), liver (Hirota *et al.*, 2004) and adipose tissue (Pastinen *et al.*, 2004).

In chapter 4 I have carried out functional studies on rs2277831, an OA associated SNP identified through stage 1 of the arcOGEN GWAS, with a P-value of 2.3×10^{-5} . The SNP on chromosome 22q11.21, maps to an intron in *MICAL3*. The association signal encompasses two other genes, *BCL2L13* and *BID*, whose proteins have roles in apoptosis. This was of interest as chondrocyte apoptosis is a hallmark of OA (Kim *et al.*, 2000; Blanco *et al.*, 2004).

I carried out gene and allelic expression analyses on *BCL2L13*, *BID* and *MICAL3* in cartilage, fatpad, synovium, cancellous bone and osteophyte tissue as it is important to conduct such analyses in pathologically relevant tissues. For example, Emilsson *et al.* (2008) showed that there is a significant difference in the gene expression profile in blood and adipose tissue in obesity. This suggests that eQTLs can act in a tissue specific manner. My hypothesis was that the OA associated locus highlighted by rs2277831 can be marking an eQTL, affecting the gene expression of either *MICAL3* or its two neighbouring genes.

Key findings of Chapter 4:

1. *BCL2L13*, *BID* and *MICAL3* were expressed in all joint tissues that were tested.
2. There was no correlation between *BCL2L13*, *BID* and *MICAL3* gene expression and genotype at rs2277831.
3. AEI was observed at *BCL2L13*, *BID* and *MICAL3* in all tissue types analysed, however this did not correlate with genotype at rs2277831.

Therefore, my results did not support a role for *cis*-regulation at *BCL2L13*, *BID* or *MICAL3* as accounting for the OA association signal at chromosome 22q11.21. There is a possibility that the original discovery of the OA association to rs2277831 was a false positive, and may account for the lack of correlation seen between gene expression and genotype at this locus.

Assessing whether the OA associated locus that maps to chromosome 12q23.3 mediates its effect by influencing the gene expression of CHST11

I subsequently focused on a second locus that was identified through the arcOGEN GWAS. The OA associated SNP is rs835487 and is located at chromosome 12q23.3. The association surpassed the genome-wide significance threshold, with a P-value of 1.64×10^{-8} . The SNP is located in intron 2 of *CHST11*, which encodes an enzyme that catalyses the sulphation of glycosaminoglycans, hence making it a highly interesting locus to study in the context of OA. Again I hypothesised that the association to rs835487 may influence the gene expression of *CHST11*. I carried out gene expression and AEI analyses on tissue types relevant to OA; cartilage, fatpad and synovium, as well as in NOF cartilage.

Key findings of Chapter 5:

1. The expression of *CHST11* was observed in all joint tissues analysed.
2. The expression of *CHST11* was significantly higher in OA cartilage compared to NOF cartilage.
3. *CHST11* expression in OA cartilage, fatpad and synovium tissue and in NOF cartilage did not correlate with the genotype at the associated SNP rs835487.
4. Although AEI at *CHST11* was observed in OA cartilage, fatpad and synovium tissue and in NOF cartilage, this did not correlate with the genotype at the associated SNP, rs835487. Therefore, perhaps there are eQTLs operating in adult tissues, but an eQTL, if present, that correlates with rs835487 may not be operating in end stage OA tissue.

I speculated that since a role for *CHST11* during development has been well established in mouse (Klüppel *et al.*, 2005) and zebrafish (Mizumoto *et al.*, 2009), perhaps tissue from OA patients may not be a suitable tissue type to carry out functional studies on *CHST11*. Therefore, to understand how the OA susceptibility marked by rs835487 affects *CHST11* expression, it may be necessary to analyse AEI in MSCs that are undergoing chondrogenic differentiation, and to follow the pattern of AEI during chondrogenesis in these cells. Also, *in vitro* assays such as luciferase

reporter assays and electrophoretic mobility shift assays (EMSAs) could be used to study the functionality of a particular allele. However results from these *in vitro* assays need to be interpreted with caution as the variants are assayed outside of their natural context. For example, the DNA sequences used in these approaches lack the naturally occurring chromatin configuration and also, the function of a SNP may be dependent on the naturally occurring haplotypes around the SNP of interest (Knight, 2005).

Sequence analysis of CHST11 coding exons

In Chapter 6 I set out to look for rare variants in the *CHST11* coding sequence in OA patients. The DNA variant databases suggested that there were no common coding SNPs in *CHST11*. These databases are based on population samples, and therefore I looked directly at an OA cohort for potentially rare but penetrant risk alleles.

Key findings of Chapter 6:

1. One of 192 hip OA patients that were sequenced carried a novel mutation, in exon 3 of *CHST11*. This is a G to C transition resulting in a non conservative amino acid change from lysine to asparagine.
2. The mutation was absent in an additional 599 hip OA patients that were subsequently genotyped for this variant. The allele frequency of this mutation is estimated therefore to be 0.063%.

There are therefore no variants in the coding exons of *CHST11* that can contribute to OA disease susceptibility at a population level.

Role of CHST11 in chondrocyte differentiation

In Chapter 7, I aimed to look for the role of *CHST11* during chondrogenesis. For this, I differentiated iliac crest derived MSCs from two young donors into chondrocytes after *CHST11* knockdown, and then analysed changes in gene expression of anabolic, catabolic and hypertrophic marker genes.

Key findings of Chapter 7:

1. During chondrogenesis, the expression of *CHST11* was highest at day 7, and was down regulated by day 14.

2. The wet mass of the *CHST11* knocked-down discs increased through chondrogenesis, but was lower than the control discs at each time point. This suggests a reduction in water retention due to altered sulphation of GAGs in the *CHST11* knocked-down discs.
3. Gene expression analysis on *CHST11* knocked-down discs showed a down regulation of anabolic marker genes *COL2A1*, *ACAN* and *SOX9* and an upregulation of catabolic marker gene *ADAMTS5* and the hypertrophic marker genes *RUNX2* and *COL10A1*.
4. *CHST11* knockdown also resulted in a significant reduction in the amount of sulphated GAGs as measured by Alcian blue staining.
5. Having seen a role of *CHST11* during chondrogenesis, I assessed the gene expression changes in response to *CHST11* knockdown in adult OA and NOF chondrocytes. The results showed significant changes in gene expression, however, there was no consistent effect among patients.
6. There was no change in the amount of sulphated GAGs produced by OA chondrocytes as measured by Alcian blue staining.

My results showed the importance of *CHST11* during chondrogenesis, the loss of which results in gene expression changes during MSC differentiation, reduction in wet mass of cartilage discs and a reduction in sulphated GAGs produced during differentiation.

As *CHST11* expression is increased in knee OA (Karlsson *et al.*, 2010) and in hip OA (Xu *et al.*, 2012; Chapter 5.2.2), it will be interesting to assess what effect the overexpression of *CHST11* will have on gene expression of chondrocyte marker genes and the sulphation of GAGs during differentiation of MSCs into chondrocytes.

CHST11 catalyses the transfer of sulphate groups in chondroitin to the 4-hydroxyl group of N-acetylgalactosamine (GalNAc) sugars, to form chondroitin-4- sulphate (CS-A). *CHST11* also shows activity towards dermatan (Mikami *et al.*, 2003), to form dermatan sulphate (DS, also known as CS-B). Other enzymes that catalyse the transfer of sulphate groups to the 4-hydroxyl position include *CHST12*, *CHST13* and *CHST14*. In addition, *CHST3* and *CHST7* catalyse the addition of sulphate groups to the 6-hydroxyl group of chondroitin disaccharides, to form chondroitin-6-sulphate (CS-C; Caterson, 2012). As Alcian blue is a global measure of sulphated GAGs, it is not a specific stain to

detect CS-A alone. It is possible to use antibodies that recognise different sulphation motifs of CS and DS GAG chains (Caterson, 2012). Hence, it will be of interest to assess the effect of *CHST11* knockdown on the sulphation of specific CSs, and also to determine if *CHST12*, *CHST13* or *CHST14*, which also catalyse the synthesis of CS-A, can compensate for the lack of *CHST11*.

It is reported that in colon adenocarcinoma, the ratio of 4-hydroxyl sulphated and 6-hydroxyl sulphated chondroitin changes from 4:1 in normal colon tissue to 1:3 in malignant cells (Theocharis, 2002). As the expression of *CHST11* is increased in OA (Karlsson *et al.*, 2010; Xu *et al.*, 2012), it will also be of interest to assess if there is an alteration in the pattern of chondroitin sulphation in OA cartilage compared to normal cartilage, which can perhaps be used as a biomarker for the development and progression of OA.

In summary, the aim of my thesis was to explore the functional effects of OA susceptibility loci. I have showed that OA chondrocytes respond discordantly to GDF5, a protein encoded by an OA susceptibility gene. I have explored the functional effects of two OA associated variants residing on *MICAL3* and *CHST11*, but did not see a correlation between the genotype of the associated SNP and gene expression. I sequenced *CHST11* coding exons in hip OA patients to look for rare variants, and did not find evidence for any that could account for disease susceptibility. I have then assessed the role of *CHST11* during MSC differentiation into chondrocytes, and I observed that *CHST11* knockdown leads to gene expression changes in anabolic, catabolic and hypertrophic marker genes, and a reduction in the synthesis of sulphated GAGs.

As OA is a polygenic disorder, risk alleles will only have a very small effect on overall disease susceptibility, hence their use as a diagnostic tool is currently limited (Rodriguez-Fontenla *et al.*, 2012). However, identifying the key pathways that the genes harbouring these OA risk alleles are involved in, may prove to be beneficial in the development of new therapies for OA (Reynard and Loughlin, 2013).

Appendix

Appendix 1:

Ethics statement

The Newcastle and North Tyneside research ethics committees granted ethical approval for the collection of cartilage from patients undergoing hip or knee joint replacement for primary OA (REC reference number 09/H0906/72). Each donor provided informed consent. The project was discussed with the donor verbally by a trained research nurse and if the donor agreed to participate written consent was then taken. This consent procedure was approved by the ethics committee and the written consent was then filed by the consenting nurse. OA status was confirmed using pre-operative records. All patients had full-thickness cartilage lesions.

Appendix 2:

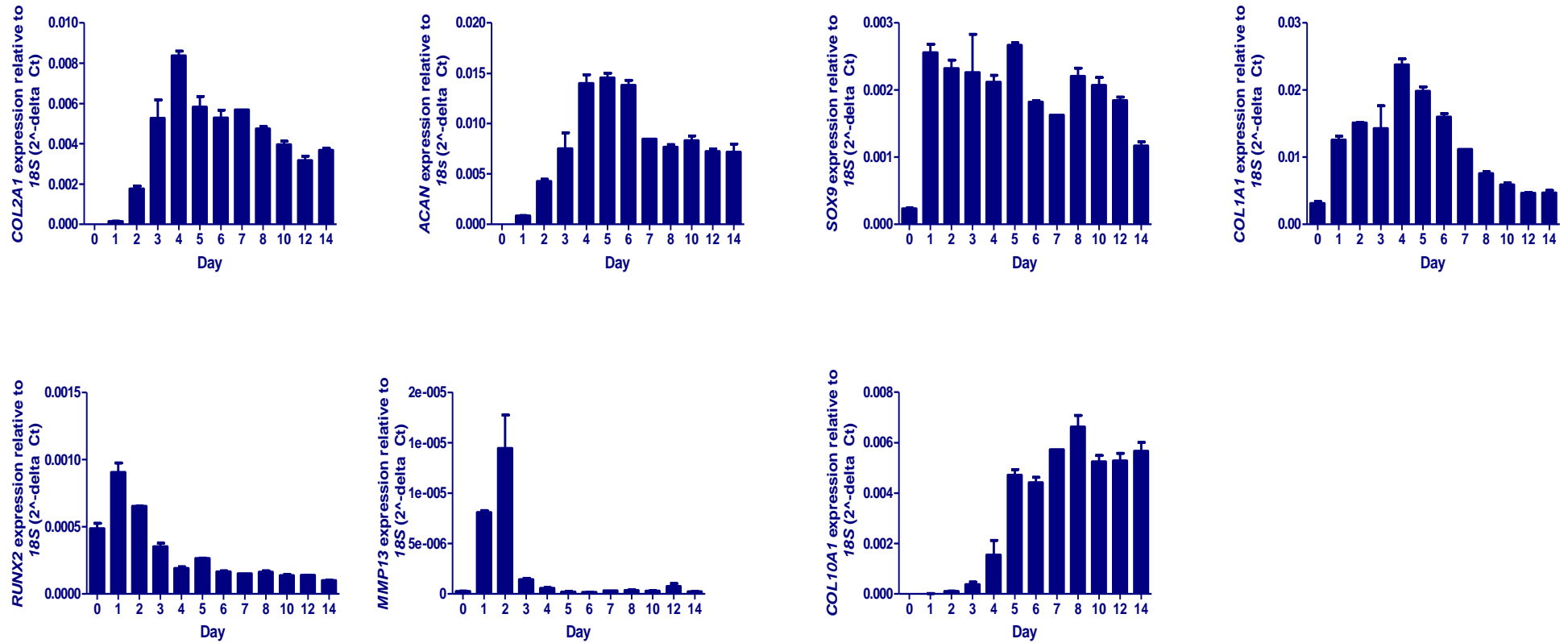


Figure 1A: Gene expression changes that undergo during day 0 to day 14 of MSC chondrogenesis.

These experiments were performed by Dr Matt Barter (Newcastle University). Error bars represent standard error of the mean.

Conference attendances

OA Research Society International 2010 (Brussels)

British Society of Matrix Biology (BSMB) 2011 (Newcastle)

OA Research Society International 2012 (Barcelona) – Poster Presentation

Publications

Ratnayake M., Reynard L.N., Raine E.V., Santibanez-Koref M., Loughlin J. (2012). Allelic expression analysis of the osteoarthritis susceptibility locus that maps to *MICAL3*. *BMC Medical Genetics*.13 (1):12.

Zeggini, E., Panoutsopoulou, K., Southam, L., Rayner, N. W., Day-Williams, A. G., Lopes, M. C., Boraska, V., Esko, T., Evangelou, E., Hoffman, A., Houwing-Duistermaat, J. J., Ingvarsson, T., Jonsdottir, I., Jonsson, H., Kerkhof, H. J., Kloppenburg, M., Bos, S. D., Mangino, M., Metrustry, S., Slagboom, P. E., Thorleifsson, G., Raine, E. V., Ratnayake, M., Ricketts, M., Beazley, C., Blackburn, H., Bumpstead, S., Elliott, K. S., Hunt, S. E., Potter, S. C., Shin, S. Y., Yadav, V. K., Zhai, G., Sherburn, K., Dixon, K., Arden, E., Aslam, N., Battley, P. K., Carluke, I., Doherty, S., Gordon, A., Joseph, J., Keen, R., Koller, N. C., Mitchell, S., O'Neill, F., Paling, E., Reed, M. R., Rivadeneira, F., Swift, D., Walker, K., Watkins, B., Wheeler, M., Birrell, F., Ioannidis, J. P., Meulenbelt, I., Metspalu, A., Rai, A., Salter, D., Stefansson, K., Stykarsdottir, U., Uitterlinden, A. G., Van Meurs, J. B., Chapman, K., Deloukas, P., Ollier, W. E., Wallis, G. A., Arden, N., Carr, A., Doherty, M., Mccaskie, A., Willkinson, J. M., Ralston, S. H., Valdes, A. M., Spector, T. D. and Loughlin, J. (2012). Identification of new susceptibility loci for osteoarthritis (arcOGEN): a genome-wide association study. *Lancet*. 380: 815-23.

Ratnayake M., Plöger F., Santibanez-Koref M., Loughlin J. (2013) Human chondrocytes respond discordantly to the protein encoded by the osteoarthritis susceptibility gene *GDF5*. Manuscript submitted to PLOS ONE.

References

- Abramson, S. B. (2008). Osteoarthritis and nitric oxide. *Osteoarthritis and Cartilage*. 16: S15-S20.
- Aerssens, J., Dequeker, J., Peeters, J., Breemans, S. and Boonen, S. (1998). Lack of association between osteoarthritis of the hip and gene polymorphisms of VDR, COL1a1, and COL2a1 in postmenopausal women. *Arthritis and Rheumatism*. 41: 1946-1950.
- Ahmad, R., Sylvester, J., Ahmad, M. and Zafarullah, M. (2009). Adaptor proteins and ras synergistically regulate IL-1-induced ADAMTS-4 expression in human chondrocytes. *Journal of Immunology*. 182: 5081-5087.
- Aigner, T. and Mckenna, L. (2002). Molecular pathology and pathobiology of osteoarthritic cartilage. *Cellular and Molecular Life Sciences*. 59: 5-18.
- Aigner, T., Sachse, A., Gebhard, P. M. and Roach, H. I. (2006a). Osteoarthritis: Pathobiology-targets and ways for therapeutic intervention. *Advanced Drug Delivery Reviews*. 58: 128-149.
- Aigner, T., Söder, S., Gebhard, P. M., Mcalinden, A. and Haag, J. (2007). Mechanisms of Disease: Role of chondrocytes in the pathogenesis of osteoarthritis - Structure, chaos and senescence. *Nature Clinical Practice Rheumatology*. 3: 391-399.
- Aigner, T., Soeder, S. and Haag, J. (2006b). IL-1 β and BMPS - Interactive players of cartilage matrix degradation and regeneration. *European Cells and Materials*. 12: 49-56.
- Allan, D. A. (1998). Structure and physiology of joints and their relationship to repetitive strain injuries. *Clinical Orthopaedics and Related Research*. 32-38.
- Allen, H. L., Estrada, K., Lettre, G., Berndt, S. I., Weedon, M. N., Rivadeneira, F., Willer, C. J., Jackson, A. U., Vedantam, S., Raychaudhuri, S., Ferreira, T., Wood, A. R., Weyant, R. J., Segrè, A. V., Speliotes, E. K., Wheeler, E., Soranzo, N., Park, J. H., Yang, J., Gudbjartsson, D., Heard-Costa, N. L., Randall, J. C., Qi, L., Smith, A. V., Mägi, R., Pastinen, T., Liang, L., Heid, I. M., Luan, J., Thorleifsson, G., Winkler, T. W., Goddard, M. E., Lo, K. S., Palmer, C., Workalemahu, T., Aulchenko, Y. S., Johansson, Å., Zillikens, M. C., Feitosa, M. F., Esko, T., Johnson, T., Ketkar, S., Kraft, P., Mangino, M., Prokopenko, I., Absher, D., Albrecht, E., Ernst, F., Glazer, N. L., Hayward, C., Hottenga, J. J., Jacobs, K. B., Knowles, J. W., Kutalik, Z., Monda, K. L.,

Polasek, O., Preuss, M., Rayner, N. W., Robertson, N. R., Steinthorsdottir, V., Tyrer, J. P., Voight, B. F., Wiklund, F., Xu, J., Zhao, J. H., Nyholt, D. R., Pellikka, N., Perola, M., Perry, J. B., Surakka, I., Tammesoo, M. L., Altmaier, E. L., Amin, N., Aspelund, T., Bhangale, T., Boucher, G., Chasman, D. I., Chen, C., Coin, L., Cooper, M. N., Dixon, A. L., Gibson, Q., Grundberg, E., Hao, K., Juntila, M. J., Kaplan, L. M., Kettunen, J., König, I. R., Kwan, T., Lawrence, R. W., Levinson, D. F., Lorentzon, M., Mcknight, B., Morris, A. P., Müller, M., Ngwa, J. S., Purcell, S., Rafelt, S., Salem, R. M., Salvi, E., Sanna, S., Shi, J., Sovio, U., Thompson, J. R., Turchin, M. C., Vandenput, L., Verlaan, D. J., Vitart, V., White, C. C., Ziegler, A., Almgren, P., Balmforth, A. J., Campbell, H., Citterio, L., De Grandi, A., Dominiczak, A., Duan, J., Elliott, P., Elosua, R., Eriksson, J. G., Freimer, N. B., Geus, E. J. C., Glorioso, N., Haiqing, S., Hartikainen, A. L., Havulinna, A. S., Hicks, A. A., Hui, J., Igl, W., Illig, T., Jula, A., Kajantie, E., Kilpeläinen, T. O., Koiranen, M., Kolcic, I., Koskinen, S., Kovacs, P., Laitinen, J., Liu, J., Lokki, M. L., Marusic, A., Maschio, A., Meitinger, T., Mulas, A., Paré, G., Parker, A. N., Peden, J. F., Petersmann, A., Pichler, I., Pietiläinen, K. H., Pouta, A., Ridderstråle, M., Rotter, J. I., Sambrook, J. G., Sanders, A. R., Schmidt, C. O., Sinisalo, J., Smit, J. H., Stringham, H. M., Walters, G. B., Widen, E., Wild, S. H., Willemsen, G., Zagato, L., Zgaga, L., Zitting, P., Alavere, H., Farrall, M., Mcardle, W. L., Nelis, M., Peters, M. J., Ripatti, S., Van Meurs, J. B. J., Aben, K. K., Ardlie, K. G., Beckmann, J. S., Beilby, J. P., Bergman, R. N., Bergmann, S., Collins, F. S., Cusi, D., Den Heijer, M., Eiriksdottir, G., Gejman, P. V., Hall, A. S., Hamsten, A., Huikuri, H. V., Iribarren, C., Kähönen, M., Kaprio, J., Kathiresan, S., Kiemeny, L., Kocher, T., Launer, L. J., Lehtimäki, T., Melander, O., Mosley Jr, T. H., Musk, A. W., Nieminen, M. S., O'donnell, C. J., Ohlsson, C., Oostra, B., Palmer, L. J., Raitakari, O., Ridker, P. M., Rioux, J. D., Rissanen, A., Rivolta, C., Schunkert, H., Shuldiner, A. R., Siscovick, D. S., Stumvoll, M., Tönjes, A., Tuomilehto, J., Van Ommen, G. J., Viikari, J., Heath, A. C., Martin, N. G., Montgomery, G. W., Province, M. A., Kayser, M., Arnold, A. M., D.Atwood, L., Boerwinkle, E., Chanock, S. J., Deloukas, P., Gieger, C., Grönberg, H., Hall, P., Hattersley, A. T., Hengstenberg, C., Hoffman, W., Lathrop, G. M., Salomaa, V., Schreiber, S., Uda, M., Waterworth, D., Wright, A. F., Assimes, T. L., Barroso, I., Hofman, A., Mohlke, K. L., Boomsma, D. I., Caulfield, M. J., Cupples, L. A., Erdmann, J., Fox, C. S., Gudnason, V., Gyllensten, U., Harris, T. B., Hayes, R. B., Jarvelin, M. R.,

- Mooser, V., Munroe, P. B., Ouwehand, W. H., Penninx, B. W., Pramstaller, P. P., Quertermous, T., Rudan, I., Samani, N. J., Spector, T. D., Völzke, H., Watkins, H., Wilson, J. F., Groop, L. C., Haritunians, T., Hu, F. B., Kaplan, R. C., Metspalu, A., North, K. E., Schlessinger, D., Wareham, N. J., Hunter, D. J., O'Connell, J. R., Strachan, D. P., Wichmann, H. E., Borecki, I. B., Van Duijn, C. M., Schadt, E. E., Thorsteinsdottir, U., Peltonen, L., Uitterlinden, A. G., Visscher, P. M., Chatterjee, N., Loos, R. J. F., Boehnke, M., McCarthy, M. I., Ingelsson, E., Lindgren, C. M., Abecasis, G. R., Stefansson, K., Frayling, T. M. and Hirschhorn, J. N. (2010). Hundreds of variants clustered in genomic loci and biological pathways affect human height. *Nature*. 467: 832-838.
- Allen, R. T., Robertson, C. M., Harwood, F. L., Sasho, T., Williams, S. K., Pomerleau, B. A. and Amiel, D. (2004). Characterization of mature vs aged rabbit articular cartilage: Analysis of cell density, apoptosis-related gene expression and mechanisms controlling chondrocyte apoptosis. *Osteoarthritis and Cartilage*. 12: 917-923.
- Anderer, U. and Libera, J. (2002). In vitro engineering of human autogenous cartilage. *Journal of Bone and Mineral Research*. 17: 1420-1429.
- Anderson, J. J. and Felson, D. T. (1988). Factors associated with osteoarthritis of the knee in the first National Health and Nutrition Examination Survey (HANES I). Evidence for an association with overweight, race, and physical demands of work. *American Journal of Epidemiology*. 128: 179-189.
- Andreas, K., Häupl, T., Lübke, C., Ringe, J., Morawietz, L., Wachtel, A., Sittinger, M. and Kaps, C. (2009). Antirheumatic drug response signatures in human chondrocytes: Potential molecular targets to stimulate cartilage regeneration. *Arthritis Research and Therapy*. 11.
- Andreas, K., Lübke, C., Häupl, T., Dehne, T., Morawietz, L., Ringe, J., Kaps, C. and Sittinger, M. (2008). Key regulatory molecules of cartilage destruction in rheumatoid arthritis: An in vitro study. *Arthritis Research and Therapy*. 10.
- Archer, C. W., Dowthwaite, G. P. and Francis-West, P. (2003). Development of synovial joints. *Birth Defects Research Part C - Embryo Today: Reviews*. 69: 144-155.
- Arroll, B. and Goodyear-Smith, F. (2004). Corticosteroid injections for osteoarthritis of the knee: Meta-analysis. *British Medical Journal*. 328: 869-870.

- Arthritis and Musculoskeletal Alliance (2004). *Standards of care for people with osteoarthritis*. London.
- Arthritis Research Campaign (2002). *Arthritis: The big picture*. London.
- Bandrés, E., Pombo, I., González-Huarriz, M., Rebollo, A., López, G. and García-Foncillas, J. (2005). Association between bone mineral density and polymorphisms of the VDR, ER α , COL1A1 and CTR genes in Spanish postmenopausal women. *Journal of Endocrinological Investigation*. 28: 312-321.
- Bannuru, R. R., Natov, N. S., Obadan, I. E., Price, L. L., Schmid, C. H. and McAlindon, T. E. (2009). Therapeutic trajectory of hyaluronic acid versus corticosteroids in the treatment of knee osteoarthritis: A systematic review and meta-analysis. *Arthritis Care and Research*. 61: 1704-1711.
- Barrett, J. C. and Cardon, L. R. (2006). Evaluating coverage of genome-wide association studies. *Nature Genetics*. 38: 659-662.
- Baugé, C., Attia, J., Leclercq, S., Pujol, J. P., Galéra, P. and Boumédiene, K. (2008). Interleukin-1 β up-regulation of Smad7 via NF- κ B activation in human chondrocytes. *Arthritis and Rheumatism*. 58: 221-226.
- Bergink, A. P., Van Meurs, J. B., Loughlin, J., Arp, P. P., Fang, Y., Hofman, A., Van Leeuwen, J. P. T. M., Van Duijn, C. M., Uitterlinden, A. G. and Pols, H. a. P. (2003). Estrogen receptor α gene haplotype is associated with radiographic osteoarthritis of the knee in elderly men and women. *Arthritis and Rheumatism*. 48: 1913-1922.
- Blagojevic, M., Jinks, C., Jeffery, A. and Jordan, K. P. (2010). Risk factors for onset of osteoarthritis of the knee in older adults: a systematic review and meta-analysis. *Osteoarthritis and Cartilage*. 18: 24-33.
- Blanco, F. J., Guitian, R., Vázquez-Martul, E., De Toro, F. J. and Galdo, F. (1998). Osteoarthritis chondrocytes die by apoptosis: A possible pathway for osteoarthritis pathology. *Arthritis and Rheumatism*. 41: 284-289.
- Blanco, F. J., López-Armada, M. J. and Maneiro, E. (2004). Mitochondrial dysfunction in osteoarthritis. *Mitochondrion*. 4: 715-728.
- Blaney Davidson, E. N., Scharstuhl, A., Vitters, E. L., Van Der Kraan, P. M. and Van Den Berg, W. B. (2005). Reduced transforming growth factor-beta signaling in cartilage of old mice: role in impaired repair capacity. *Arthritis research & therapy*. 7: R1338-1347.

- Bobacz, K., Gruber, R., Soleiman, A., Graninger, W. B., Luyten, F. P. and Erlacher, L. (2002). Cartilage-derived morphogenetic protein-1 and -2 are endogenously expressed in healthy and osteoarthritic human articular chondrocytes and stimulate matrix synthesis. *Osteoarthritis and Cartilage*. 10: 394-401.
- Bondeson, J., Wainwright, S. D., Lauder, S., Amos, N. and Hughes, C. E. (2006). The role of synovial macrophages and macrophage-produced cytokines in driving aggrecanases, matrix metalloproteinases, and other destructive and inflammatory responses in osteoarthritis. *Arthritis Research and Therapy*. 8.
- Bos, S. D., Bove e, J. V. M. G., Duijnisveld, B. J., Raine, E. V. A., Dalen, W. J., Ramos, Y. F. M., Van Der Breggen, R., Nelissen, R. G. H. H., Slagboom, P. E., Loughlin, J. and Meulenbelt, I. (2012). Increased type II deiodinase protein in OA-affected cartilage and allelic imbalance of OA risk polymorphism rs225014 at DIO2 in human OA joint tissues. *Annals of the Rheumatic Diseases*. 71: 1254-1258.
- Brenner, D. A., O'hara, M., Angel, P., Chojkier, M. and Karin, M. (1989). Prolonged activation of jun and collagenase genes by tumour necrosis factor- α . *Nature*. 337: 661-663.
- Brittberg, M., Lindahl, A., Nilsson, A., Ohlsson, C., Isaksson, O. and Peterson, L. (1994). Treatment of deep cartilage defects in the knee with autologous chondrocyte transplantation. *New England Journal of Medicine*. 331: 889-895.
- Brunet, L. J., McMahon, J. A., McMahon, A. P. and Harland, R. M. (1998). Noggin, cartilage morphogenesis, and joint formation in the mammalian skeleton. *Science*. 280: 1455-1457.
- Buckland-Wright, C. (2004). Subchondral bone changes in hand and knee osteoarthritis detected by radiography. *Osteoarthritis and Cartilage*. 12: S10-S19.
- Buckland-Wright, J. C., Macfarlane, D. G., Fogelman, I., Emery, P. and Lynch, J. A. (1991). Technetium 99m methylene diphosphonate bone scanning in osteoarthritic hands. *European Journal of Nuclear Medicine*. 18: 12-16.
- Burr, D. B. (2004). Anatomy and physiology of the mineralized tissues: Role in the pathogenesis of osteoarthrosis. *Osteoarthritis and Cartilage*. 12: S20-S30.
- Buschmann, M. D., Gluzband, Y. A., Grodzinsky, A. J., Kimura, J. H. and Hunziker, E. B. (1992). Chondrocytes in agarose culture synthesize a mechanically functional extracellular matrix. *Journal of Orthopaedic Research*. 10: 745-758.

- Callaghan, J. J., Brand, R. A. and Pedersen, D. R. (1985). Hip arthrodesis. A long-term follow-up. *Journal of Bone and Joint Surgery - Series A*. 67: 1328-1335.
- Caterson, B. (2012). Fell-Muir lecture: Chondroitin sulphate glycosaminoglycans: Fun for some and confusion for others. *International Journal of Experimental Pathology*. 93: 1-10.
- Caterson, B., Griffin, J., Mahmoodian, F. and Sorrell, J. M. (1990). Monoclonal antibodies against chondroitin sulphate isomers: their use as probes for investigating proteoglycan metabolism. *Biochem Soc Trans*. 18: 820-3.
- Chang, S. C., Hoang, B., Thomas, J. T., Vukicevic, S., Luyten, F. P., Ryba, N. J. P., Kozak, C. A., Reddi, A. H. and Moos Jr, M. (1994). Cartilage-derived morphogenetic proteins: New members of the transforming growth factor- β superfamily predominantly expressed in long bones during human embryonic development. *Journal of Biological Chemistry*. 269: 28227-28234.
- Chanock, S. J., Manolio, T., Boehnke, M., Boerwinkle, E., Hunter, D. J., Thomas, G., Hirschhorn, J. N., Abecasis, G., Altshuler, D., Bailey-Wilson, J. E., Brooks, L. D., Cardon, L. R., Daly, M., Donnelly, P., Fraumeni Jr, J. F., Freimer, N. B., Gerhard, D. S., Gunter, C., Guttmacher, A. E., Guyer, M. S., Harris, E. L., Hoh, J., Hoover, R., Kong, C. A., Merikangas, K. R., Morton, C. C., Palmer, L. J., Phimister, E. G., Rice, J. P., Roberts, J., Rotimi, C., Tucker, M. A., Vogan, K. J., Wacholder, S., Wijsman, E. M., Winn, D. M. and Collins, F. S. (2007). Replicating genotype-phenotype associations. *Nature*. 447: 655-660.
- Chapman, K., Takahashi, A., Meulenbelt, I., Watson, C., Rodriguez-Lopez, J., Egli, R., Tsezou, A., Malizos, K. N., Kloppenburg, M., Shi, D., Southam, L., Van Der Breggen, R., Donn, R., Qin, J., Doherty, M., Slagboom, P. E., Wallis, G., Kamatani, N., Jiang, Q., Gonzalez, A., Loughlin, J. and Ikegawa, S. (2008). A meta-analysis of European and Asian cohorts reveals a global role of a functional SNP in the 5' UTR of GDF5 with osteoarthritis susceptibility. *Human Molecular Genetics*. 17: 1497-1504.
- Chen, W. H., Lo, W. C., Lee, J. J., Su, C. H., Lin, C. T., Liu, H. Y., Lin, T. W., Lin, W. C., Huang, T. Y. and Deng, W. P. (2006). Tissue-engineered intervertebral disc and chondrogenesis using human nucleus pulposus regulated through TGF- β 1 in platelet-rich plasma. *Journal of Cellular Physiology*. 209: 744-754.

- Chevalier, X. and Tyler, J. A. (1996). Production of binding proteins and role of the insulin-like growth factor I binding protein 3 in human articular cartilage explants. *British Journal of Rheumatology*. 35: 515-522.
- Cho, K. W. Y. and Blitz, I. L. (1998). BMPs, Smads and metalloproteases: Extracellular and intracellular modes of negative regulation. *Current Opinion in Genetics and Development*. 8: 443-449.
- Chubinskaya, S., Segalite, D., Pikovsky, D., Hakimiyan, A. A. and Rueger, D. C. (2008). Effects induced by BMPS in cultures of human articular chondrocytes: Comparative studies. *Growth Factors*. 26: 275-283.
- Chujo, T., An, H. S., Akeda, K., Miyamoto, K., Muehleman, C., Attawia, M., Andersson, G. and Masuda, K. (2006). Effects of growth differentiation factor-5 on the intervertebral disc - In vitro bovine study and in vivo rabbit disc degeneration model study. *Spine*. 31: 2909-2917.
- Coleman, C. M., Vaughan E.E., Browe D.C., Mooney E., Howard L., Barry F. (2013) Growth differentiation factor-5 enhances in vitro mesenchymal stromal cell chondrogenesis and hypertrophy. *Stem Cells and Development*. 22(13):1968-76.
- Colizza, W. A., Insall, J. N. and Scuderi, G. R. (1995). The posterior stabilized total knee prosthesis: Assessment of polyethylene damage and osteolysis after a ten-year-minimum follow-up. *Journal of Bone and Joint Surgery - Series A*. 77: 1713-1720.
- Conca, W., Kaplan, P. B. and Krane, S. M. (1989). Increases in levels of procollagenase mRNA in human fibroblasts induced by interleukin-1, tumor necrosis factor-alpha, or serum follow c-jun expression and are dependent on new protein synthesis. *Transactions of the Association of American Physicians*. 102: 195-203.
- Conway, J. D., Mont, M. A. and Bezwada, H. P. (2004). Arthrodesis of the Knee. *Journal of Bone and Joint Surgery - Series A*. 86: 835-848.
- Cookson, W., Liang, L., Abecasis, G., Moffatt, M. and Lathrop, M. (2009). Mapping complex disease traits with global gene expression. *Nature Reviews Genetics*. 10: 184-194.
- Costa, T., Ramsby, G., Cassia, F., Peters, K. R., Soares, J., Correa, J., Quelce-Salgado, A. and Tsipouras, P. (1998). Grebe syndrome: Clinical and radiographic findings in affected individuals and heterozygous carriers. *American Journal of Medical Genetics*. 75: 523-529.

- Coventry, M. B. (1979). Upper tibial osteotomy for gonarthrosis. The evolution of the operation in the last 18 years and long term results. *Orthopedic Clinics of North America*. 10: 191-210.
- Crompton, M. (1999). The mitochondrial permeability transition pore and its role in cell death. *Biochemical Journal*. 341: 233-249.
- Daans, M., Luyten, F. P. and Lories, R. J. U. (2011). GDF5 deficiency in mice is associated with instability-driven joint damage, gait and subchondral bone changes. *Annals of the Rheumatic Diseases*. 70: 208-213.
- Dai, J., Shi, D., Zhu, P., Qin, J., Ni, H., Xu, Y., Yao, C., Zhu, L., Zhu, H., Zhao, B., Wei, J., Liu, B., Ikegawa, S., Jiang, Q. and Ding, Y. (2008). Association of a single nucleotide polymorphism in growth differentiate factor 5 with congenital dysplasia of the hip: A case-control study. *Arthritis Research and Therapy*. 10.
- Dehne, T., Karlsson, C., Ringe, J., Sittinger, M. and Lindahl, A. (2009). Chondrogenic differentiation potential of osteoarthritic chondrocytes and their possible use in matrix-associated autologous chondrocyte transplantation. *Arthritis Research and Therapy*. 11.
- Delaunay, C., Petit, I., Learmonth, I. D., Oger, P. and Vendittoli, P. A. (2010). Metal-on-metal bearings total hip arthroplasty: The cobalt and chromium ions release concern. *Orthopaedics and Traumatology: Surgery and Research*. 96: 894-904.
- Dell'accio, F., De Bari, C. and Luyten, F. P. (2001). Molecular markers predictive of the capacity of expanded human articular chondrocytes to form stable cartilage in vivo. *Arthritis and Rheumatism*. 44: 1608-1619.
- Desagher, S., Osen-Sand, A., Nichols, A., Eskes, R., Montessuit, S., Lauper, S., Maundrell, K., Antonsson, B. and Martinou, J. C. (1999). Bid-induced conformational change of Bax is responsible for mitochondrial cytochrome c release during apoptosis. *Journal of Cell Biology*. 144: 891-901.
- Dieppe, P. A. and Lohmander, L. S. (2005). Pathogenesis and management of pain in osteoarthritis. *Lancet*. 365: 965-973.
- Djouad, F., Mrugala, D., Noel, D. and Jorgensen, C. (2006). Engineered mesenchymal stem cells for cartilage repair. *Regen Med*. 1: 529-37.
- Dominici, M., Le Blanc, K., Mueller, I., Slaper-Cortenbach, I., Marini, F. C., Krause, D. S., Deans, R. J., Keating, A., Prockop, D. J. and Horwitz, E. M. (2006). Minimal criteria

- for defining multipotent mesenchymal stromal cells. The International Society for Cellular Therapy position statement. *Cytotherapy*. 8: 315-317.
- Dowthwaite, G. P., Edwards, J. C. W. and Pitsillides, A. A. (1998). An essential role for the interaction between hyaluronan and hyaluronan binding proteins during joint development. *Journal of Histochemistry and Cytochemistry*. 46: 641-651.
- Drabobinac, G., Španjol, J., Marinović, M., Cvek, S. Z., Marić, I., Cicvarić, T., Fučkar, D., Markić, D. and Vojniković, B. (2008). Expression of bone morphogenetic proteins, cartilage-derived morphogenetic proteins and related receptors in normal and osteoarthritic human articular cartilage. *Collegium Antropologicum*. 32: 83-87.
- Edwards, C. J. and Francis-West, P. H. (2001). Bone morphogenetic proteins in the development and healing of synovial joints. *Seminars in Arthritis and Rheumatism*. 31: 33-42.
- Edwards, D. R., Murphy, G., Reynolds, J. J., Whitham, S. E., Docherty, A. J., Angel, P. and Heath, J. K. (1987). Transforming growth factor beta modulates the expression of collagenase and metalloproteinase inhibitor. *EMBO Journal*. 6: 1899-1904.
- Egli, R. J., Southam, L., Wilkins, J. M., Lorenzen, I., Pombo-Suarez, M., Gonzalez, A., Carr, A., Chapman, K. and Loughlin, J. (2009). Functional analysis of the osteoarthritis susceptibility-associated GDF5 regulatory polymorphism. *Arthritis and Rheumatism*. 60: 2055-2064.
- Ellsworth, J. L., Berry, J., Bukowski, T., Claus, J., Feldhaus, A., Holderman, S., Holdren, M. S., Lum, K. D., Moore, E. E., Raymond, F., Ren, H., Shea, P., Sprecher, C., Storey, H., Thompson, D. L., Waggle, K., Yao, L., Fernandes, R. J., Eyre, D. R. and Hughes, S. D. (2002). Fibroblast growth factor-18 is a trophic factor for mature chondrocytes and their progenitors. *Osteoarthritis and Cartilage*. 10: 308-320.
- Emilsson, V., Thorleifsson, G., Zhang, B., Leonardson, A. S., Zink, F., Zhu, J., Carlson, S., Helgason, A., Walters, G. B., Gunnarsdottir, S., Mouy, M., Steinthorsdottir, V., Eiriksdottir, G. H., Bjornsdottir, G., Reynisdottir, I., Gudbjartsson, D., Helgadottir, A., Jonasdottir, A., Jonasdottir, A., Styrkarsdottir, U., Gretarsdottir, S., Magnusson, K. P., Stefansson, H., Fossdal, R., Kristjansson, K., Gislason, H. G., Stefansson, T., Leifsson, B. G., Thorsteinsdottir, U., Lamb, J. R., Gulcher, J. R., Reitman, M. L., Kong, A., Schadt, E. E. and Stefansson, K. (2008). Genetics of gene expression and its effect on disease. *Nature*. 452: 423-428.

- Englund, M., Guermazi, A. and Lohmander, L. S. (2009). The Meniscus in Knee Osteoarthritis. *Rheumatic Disease Clinics of North America*. 35: 579-590.
- Erlacher, L., McCartney, J., Piek, E., Ten Dijke, P., Yanagishita, M., Oppermann, H. and Luyten, F. P. (1998). Cartilage-derived morphogenetic proteins and osteogenic protein-1 differentially regulate osteogenesis. *Journal of Bone and Mineral Research*. 13: 383-392.
- Ethgen, O., Bruyère, O., Richy, F., Dardennes, C. and Reginster, J. Y. (2004). Health-Related Quality of Life in Total Hip and Total Knee Arthroplasty: A Qualitative and Systematic Review of the Literature. *Journal of Bone and Joint Surgery - Series A*. 86: 963-974.
- Eviatar, T., Kauffman, H. and Maroudas, A. (2003). Synthesis of insulin-like growth factor binding protein 3 in vitro in human articular cartilage cultures. *Arthritis and Rheumatism*. 48: 410-417.
- Fischer, J., Weide, T. and Barnekow, A. (2005). The MICAL proteins and rab1: A possible link to the cytoskeleton? *Biochemical and Biophysical Research Communications*. 328: 415-423.
- Forslund, C., Rueger, D. and Aspenberg, P. (2003). A comparative dose-response study of cartilage-derived morphogenetic protein (CDMP)-1, -2 and -3 for tendon healing in rats. *Journal of Orthopaedic Research*. 21: 617-621.
- Francis-West, P. H., Abdelfattah, A., Chen, P., Allen, C., Parish, J., Ladher, R., Allen, S., Macpherson, S., Luyten, F. P. and Archer, C. W. (1999a). Mechanisms of GDF-5 action during skeletal development. *Development*. 126: 1305-1315.
- Francis-West, P. H., Parish, J., Lee, K. and Archer, C. W. (1999b). BMP/GDF-signalling interactions during synovial joint development. *Cell and Tissue Research*. 296: 111-119.
- Freund E. (1940). The pathological significance of intra-articular pressure. *Edinburgh Med J*. 192-203.
- Fukui, N., Zhu, Y., Maloney, W. J., Clohisy, J. and Sandell, L. J. (2003). Stimulation of BMP-2 expression by pro-inflammatory cytokines IL-1 and TNF- α in normal and osteoarthritic chondrocytes. *Journal of Bone and Joint Surgery - Series A*. 85: 59-66.

- Fytily, P., Giannatou, E., Papanikolaou, V., Stripeli, F., Karachalios, T., Malizos, K. and Tsezou, A. (2005). Association of repeat polymorphisms in the estrogen receptors α , β , and androgen receptor genes with knee osteoarthritis. *Clinical Genetics*. 68: 268-277.
- Gabriel, S., Ziaugra, L. and Tabbaa, D. (2009). SNP genotyping using the sequenom massARRAY iPLEX Platform. *Current Protocols in Human Genetics*. 2.12.1-2.12.18.
- Gama, C. I., Tully, S. E., Sotogaku, N., Clark, P. M., Rawat, M., Vaidehi, N., Goddard, W. A., 3rd, Nishi, A. and Hsieh-Wilson, L. C. (2006). Sulfation patterns of glycosaminoglycans encode molecular recognition and activity. *Nat Chem Biol*. 2: 467-73.
- Garstang, S. V. and Stitik, T. P. (2006). Osteoarthritis: Epidemiology, risk factors, and pathophysiology. *American Journal of Physical Medicine and Rehabilitation*. 85: S2-S12.
- Giannoni, P., Pagano, A., Maggi, E., Arbicò, R., Randazzo, N., Grandizio, M., Cancedda, R. and Dozin, B. (2005). Autologous chondrocyte implantation (ACI) for aged patients: Development of the proper cell expansion conditions for possible therapeutic applications. *Osteoarthritis and Cartilage*. 13: 589-600.
- Goldring, M. B. (2006). Update on the biology of the chondrocyte and new approaches to treating cartilage diseases. *Best Practice and Research: Clinical Rheumatology*. 20: 1003-1025.
- Goldring, M. B. and Berenbaum, F. (2004). The regulation of chondrocyte function by proinflammatory mediators: Prostaglandins and nitric oxide. *Clinical Orthopaedics and Related Research*. S37-S46.
- Goldring, M. B. and Goldring, S. R. (2010). Articular cartilage and subchondral bone in the pathogenesis of osteoarthritis.
- Goldring, M. B., Suen, L. F., Yamin, R. and Lai, W. F. T. (1996). Regulation of collagen gene expression by prostaglandins and interleukin-1 β in cultured chondrocytes and fibroblasts. *American Journal of Therapeutics*. 3: 9-16.
- Grigoriev, I., Yu, K. L., Martinez-Sanchez, E., Serra-Marques, A., Smal, I., Meijering, E., Demmers, J., Peränen, J., Pasterkamp, R. J., Van Der Sluijs, P., Hoogenraad, C. C. and Akhmanova, A. (2011). Rab6, Rab8, and MICAL3 cooperate in controlling docking and fusion of exocytotic carriers. *Current Biology*. 21: 967-974.

- Grogan, S. P., Barbero, A., Diaz-Romero, J., Cleton-Jansen, A. M., Soeder, S., Whiteside, R., Hogendoorn, P. C. W., Farhadi, J., Aigner, T., Martin, I. and Mainil-Varlet, P. (2007). Identification of markers to characterize and sort human articular chondrocytes with enhanced in vitro chondrogenic capacity. *Arthritis and Rheumatism*. 56: 586-595.
- Gross, A. (2006). BID as a double agent in cell life and death. *Cell Cycle*. 5: 582-584.
- Guccione, A. A., Felson, D. T., Anderson, J. J., Anthony, J. M., Zhang, Y., Wilson, P. W. F., Kelly-Hayes, M., Wolf, P. A., Kreger, B. E. and Kannel, W. B. (1994). The effects of specific medical conditions on the functional limitations of elders in the Framingham study. *American Journal of Public Health*. 84: 351-358.
- Guerne, P. A., Blanco, F., Kaelin, A., Desgeorges, A. and Lotz, M. (1995). Growth factor responsiveness of human articular chondrocytes in aging and development. *Arthritis and Rheumatism*. 38: 960-968.
- Haara, M. M., Heliövaara, M., Kröger, H., Arokoski, J. P. A., Manninen, P., Kärkkäinen, A., Knekt, P., Impivaara, O. and Aromaa, A. (2004). Osteoarthritis in the carpometacarpal joint of the thumb: Prevalence and associations with disability and mortality. *Journal of Bone and Joint Surgery - Series A*. 86: 1452-1457.
- Hammond C.L. (University of Bristol). 18th July 2012.
- Hanna, F. S., Wluka, A. E., Bell, R. J., Davis, S. R. and Cicuttini, F. M. (2004). Osteoarthritis and the postmenopausal woman: Epidemiological, magnetic resonance imaging, and radiological findings. *Seminars in Arthritis and Rheumatism*. 34: 631-636.
- Hardingham, T. E., Oldershaw, R. A. and Tew, S. R. (2006). Cartilage, SOX9 and Notch signals in chondrogenesis. *Journal of Anatomy*. 209: 469-480.
- Harrison, P. E., Ashton, I. K., Johnson, W. E. B., Turner, S. L., Richardson, J. B. and Ashton, B. A. (2000). The in vitro growth of human chondrocytes. *Cell and Tissue Banking*. 1: 255-260.
- Hartman, C. and Tabin, C. J. (2000). Dual roles of Wnt signaling during chondrogenesis in the chicken limb. *Development*. 127: 3141-3159.
- Hashimoto, M., Nakasa, T., Hikata, T. and Asahara, H. (2008). Molecular network of cartilage homeostasis and osteoarthritis. *Medicinal Research Reviews*. 28: 464-481.

- Hata, A., Lagna, G., Massagué, J. and Hemmati-Brivanlou, A. (1998). Smad6 inhibits BMP/Smad1 signaling by specifically competing with the Smad4 tumor suppressor. *Genes and Development*. 12: 186-197.
- Häuselmann, H. J., Stefanovic-Racic, M., Michel, B. A. and Evans, C. H. (1998). Differences in nitric oxide production by superficial and deep human articular chondrocytes: Implications for proteoglycan turnover in inflammatory joint diseases. *Journal of Immunology*. 160: 1444-1448.
- Hawker, G. A., Badley, E. M., Croxford, R., Coyte, P. C., Glazier, R. H., Guan, J., Harvey, B. J., Williams, J. I. and Wright, J. G. (2009). A population-based nested case-control study of the costs of hip and knee replacement surgery. *Medical Care*. 47: 732-741.
- Heighway, J., Margison, G. P. and Santibáñez-Koref, M. F. (2003). The alleles of the DNA repair gene O6-alkylguanine-DNA alkyltransferase are expressed at different levels in normal human lung tissue. *Carcinogenesis*. 24: 1691-1694.
- Heldin, C. H., Miyazono, K. and Ten Dijke, P. (1997). TGF- β signalling from cell membrane to nucleus through SMAD proteins. *Nature*. 390: 465-471.
- Heuts, P. H. T. G., Vlaeyen, J. W. S., Roelofs, J., De Bie, R. A., Aretz, K., Van Weel, C. and Van Schayck, O. C. P. (2004). Pain-related fear and daily functioning in patients with osteoarthritis. *Pain*. 110: 228-235.
- Hiraide, A., Yokoo, N., Xin, K. Q., Okuda, K., Mizukami, H., Ozawa, K. and Saito, T. (2005). Repair of articular cartilage defect by intraarticular administration of basic fibroblast growth factor gene, using adeno-associated virus vector. *Human Gene Therapy*. 16: 1413-1421.
- Hiraoka, N., Nakagawa, H., Ong, E., Akama, T. O., Fukuda, M. N. and Fukuda, M. (2000). Molecular cloning and expression of two distinct human chondroitin 4-O-sulfotransferases that belong to the HNK-1 sulfotransferase gene family. *J Biol Chem*. 275: 20188-96.
- Hirota, T., Ieire, I., Takane, H., Maegawa, S., Hosokawa, M., Kobayashi, K., Chiba, K., Nanba, E., Oshimura, M., Sato, T., Higuchi, S. and Kenji, O. (2004). Allelic expression imbalance of the human CYP3A4 gene and individual phenotypic status. *Human Molecular Genetics*. 13: 2959-2969.

- Hogan, B. L. M. (1996). Bone morphogenetic proteins: Multifunctional regulators of vertebrate development. *Genes and Development*. 10: 1580-1594.
- Huang, J., Ushiyama, T., Inoue, K., Kawasaki, T. and Hukuda, S. (2000). Vitamin D receptor gene polymorphisms and osteoarthritis of the hand, hip, and knee: A case-control study in Japan. *Rheumatology*. 39: 79-84.
- Huber, M., Reinisch, G., Zenz, P., Zweymüller, K. and Lintner, F. (2010). Postmortem study of femoral osteolysis associated with metal-on-metal articulation in total hip replacement: An analysis of nine cases. *Journal of Bone and Joint Surgery - Series A*. 92: 1720-1731.
- Hutton, C. W., Higgs, E. R. and Jackson, P. C. (1986). 99mTc HMDP bone scanning in generalised nodal osteoarthritis. II. The four hour bone scan image predicts radiographic change. *Annals of the Rheumatic Diseases*. 45: 622-626.
- Ibold, Y., Frauenschuh, S., Kaps, C., Sittinger, M., Ringe, J. and Goetz, P. M. (2007). Development of a high-throughput screening assay based on the 3-dimensional pannus model for rheumatoid arthritis. *Journal of Biomolecular Screening*. 12: 956-965.
- Im, H. J., Li, X., Muddasani, P., Kim, G. H., Davis, F., Rangan, J., Forsyth, C. B., Ellman, M. and Thonar, E. J. M. A. (2008). Basic fibroblast growth factor accelerates matrix degradation via a neuro-endocrine pathway in human adult articular chondrocytes. *Journal of Cellular Physiology*. 215: 452-463.
- Imamura, T., Takase, M., Nishihara, A., Oeda, E., Hanai, J. I., Kawabata, M. and Miyazono, K. (1997). Smad6 inhibits signalling by the TGF- β superfamily. *Nature*. 389: 622-626.
- Insall, J. N. (1967). Intra-articular surgery for degenerative arthritis of the knee. A report of the work of the late K. H. Pridie. *Journal of Bone and Joint Surgery - Series B*. 49: 211-228.
- International Hapmap Project. (2013). *International HapMap Project* [Online]. Available: <http://hapmap.ncbi.nlm.nih.gov/> [Accessed 8th September 2013].
- Iwamoto, M., Higuchi, Y., Koyama, E., Enomoto-Iwamoto, M., Kurisu, K., Yeh, H., Abrams, W. R., Rosenbloom, J. and Pacifici, M. (2000). Transcription factor ERG variants and functional diversification of chondrocytes during limb long bone development. *Journal of Cell Biology*. 150: 27-39.

- Izumi, T., Scully, S. P., Heydemann, A. and Bolander, M. E. (1992). Transforming growth factor β 1 stimulates type II collagen expression in cultured periosteum-derived cells. *Journal of Bone and Mineral Research*. 7: 115-121.
- Jakkula, E., Melkonieni, M., Kiviranta, I., Lohiniva, J., Räninä, S. S., Perälä, M., Warman, M. L., Ahonen, K., Kröger, H., Göring, H. H. H. and Ala-Kokko, L. (2005). The role of sequence variations within the genes encoding collagen II, IX and XI in non-syndromic, early-onset osteoarthritis. *Osteoarthritis and Cartilage*. 13: 497-507.
- Jin, S. Y., Hong, S. J., Yang, H. I., Park, S. D., Yoo, M. C., Lee, H. J., Hong, M. S., Park, H. J., Yoon, S. H., Kim, B. S., Yim, S. V., Park, H. K. and Chung, J. H. (2004). Estrogen receptor-alpha gene haplotype is associated with primary knee osteoarthritis in Korean population. *Arthritis research & therapy*. 6: R415-421.
- Johnson, A. D., Zhang, Y., Papp, A. C., Pinsonneault, J. K., Lim, J. E., Saffen, D., Dai, Z., Wang, D. and Sadée, W. (2008). Polymorphisms affecting gene transcription and mRNA processing in pharmacogenetic candidate genes: Detection through allelic expression imbalance in human target tissues. *Pharmacogenetics and Genomics*. 18: 781-791.
- Jones, G., White, C., Sambrook, P. and Eisman, J. (1998). Allelic variation in the vitamin D receptor, lifestyle factors and lumbar spinal degenerative disease. *Annals of the Rheumatic Diseases*. 57: 94-99.
- Jordan, K. M., Arden, N. K., Doherty, M., Bannwarth, B., Bijlsma, J. W. J., Dieppe, P., Gunther, K., Hauselmann, H., Herrero-Beaumont, G., Kaklamanis, P., Lohmander, S., Leeb, B., Lequesne, M., Mazieres, B., Martin-Mola, E., Pavelka, K., Pendleton, A., Punzi, L., Serni, U., Swoboda, B., Verbruggen, G., Zimmerman-Gorska, I. and Dougados, M. (2003). EULAR Recommendations 2003: An evidence based approach to the management of knee osteoarthritis: Report of a Task Force of the Standing Committee for International Clinical Studies Including Therapeutic Trials (ESCISIT). *Annals of the Rheumatic Diseases*. 62: 1145-1155.
- Kang, H. G., Evers, M. R., Xia, G., Baenziger, J. U. and Schachner, M. (2002). Molecular cloning and characterization of chondroitin-4-O-sulfotransferase-3. A novel member of the HNK-1 family of sulfotransferases. *J Biol Chem*. 277: 34766-72.
- Karlson, E. W., Mandl, L. A., Awch, G. N., Sangha, O., Liang, M. H. and Grodstein, F. (2003). Total hip replacement due to osteoarthritis: The importance of age,

- obesity, and other modifiable risk factors. *American Journal of Medicine*. 114: 93-98.
- Karlsson, C., Dehne, T., Lindahl, A., Brittberg, M., Pruss, A., Sittinger, M. and Ringe, J. (2010). Genome-wide expression profiling reveals new candidate genes associated with osteoarthritis. *Osteoarthritis and Cartilage*. 18: 581-592.
- Kasten, P., Beyen, I., Bormann, D., Luginbühl, R., Plöger, F. and Richter, W. (2010). The effect of two point mutations in GDF-5 on ectopic bone formation in a β -tricalciumphosphate scaffold. *Biomaterials*. 31: 3878-3884.
- Kataoka, T., Holler, N., Micheau, O., Martinon, F., Tinel, A., Hofmann, K. and Tschopp, J. (2001). Bcl-rambo, a Novel Bcl-2 Homologue That Induces Apoptosis via Its Unique C-terminal Extension. *Journal of Biological Chemistry*. 276: 19548-19554.
- Keen, R. W., Hart, D. J., Lanchbury, J. S. and Spector, T. D. (1997). Association of early, osteoarthritis of the knee with a Taq I polymorphism of the vitamin D receptor gene. *Arthritis and Rheumatism*. 40: 1444-1449.
- Kellgren, J. H. and Lawrence, J. S. (1963). *Atlas of standard radiographs.*, Oxford (UK): Oxford University Press.
- Kellgren, J. H., Lawrence, J. S. and Bier, F. (1963). GENETIC FACTORS IN GENERALIZED OSTEO-ARTHRITIS. *Annals of the rheumatic diseases*. 22: 237-255.
- Kerkhof, H. J. M., Lories, R. J., Meulenbelt, I., Jonsdottir, I., Valdes, A. M., Arp, P., Ingvarsson, T., Jhamai, M., Jonsson, H., Stolk, L., Thorleifsson, G., Zhai, G., Zhang, F., Zhu, Y., Van Der Breggen, R., Carr, A., Doherty, M., Doherty, S., Felson, D. T., Gonzalez, A., Halldorsson, B. V., Hart, D. J., Hauksson, V. B., Hofman, A., Ioannidis, J. P. A., Kloppenburg, M., Lane, N. E., Loughlin, J., Luyten, F. P., Nevitt, M. C., Parimi, N., Pols, H. a. P., Rivadeneira, F., Slagboom, E. P., Styrkársdóttir, U., Tsezou, A., Van De Putte, T., Zmuda, J., Spector, T. D., Stefansson, K., Uitterlinden, A. G. and Van Meurs, J. B. J. (2010). A genome-wide association study identifies an osteoarthritis susceptibility locus on chromosome 7q22. *Arthritis and Rheumatism*. 62: 499-510.
- Khan, W. S., Johnson, D. S. and Hardingham, T. E. (2010). The potential of stem cells in the treatment of knee cartilage defects. *Knee*. 17: 369-374.

- Khan, W. S., Malik, A. A. and Hardingham, T. E. (2009). Stem cell applications and tissue engineering approaches in surgical practice. *Journal of perioperative practice*. 19: 130-135.
- Kiaer, T., Pedersen, N. W., Kristensen, K. D. and Starklint, H. (1990). Intra-osseous pressure and oxygen tension in avascular necrosis and osteoarthritis of the hip. *Journal of Bone and Joint Surgery - Series B*. 72: 1023-1030.
- Kim, H. A., Lee, Y. J., Seong, S. C., Choe, K. W. and Song, Y. W. (2000). Apoptotic chondrocyte death in human osteoarthritis. *Journal of Rheumatology*. 27: 455-462.
- Kim, J. Y., So, K. J., Lee, S. and Park, J. H. (2012). Bcl-rambo induces apoptosis via interaction with the adenine nucleotide translocator. *FEBS Letters*. 586: 3142-3149.
- Kizawa, H., Kou, I., Iida, A., Sudo, A., Miyamoto, Y., Fukuda, A., Mabuchi, A., Kotani, A., Kawakami, A., Yamamoto, S., Uchida, A., Nakamura, K., Notoya, K., Nakamura, Y. and Ikegawa, S. (2005). An aspartic acid repeat polymorphism in asporin inhibits chondrogenesis and increases susceptibility to osteoarthritis. *Nature Genetics*. 37: 138-144.
- Klüppel, M. (2010). The roles of chondroitin-4-sulfotransferase-1 in development and disease. *Prog Mol Biol Transl Sci*. 93: 113-32.
- Klüppel, M., Wight, T. N., Chan, C., Hinek, A. and Wrana, J. L. (2005). Maintenance of chondroitin sulfation balance by chondroitin-4-sulfotransferase 1 is required for chondrocyte development and growth factor signaling during cartilage morphogenesis. *Development*. 132: 3989-4003.
- Knight, J. C. (2005). Regulatory polymorphisms underlying complex disease traits. *Journal of Molecular Medicine*. 83: 97-109.
- Knudson, C. B. and Knudson, W. (2001). Cartilage proteoglycans. *Seminars in Cell and Developmental Biology*. 12: 69-78.
- Koch, O., Kwiatkowski, D. P. and Udalova, I. A. (2006). Context-specific functional effects of IFNGR1 promoter polymorphism. *Human Molecular Genetics*. 15: 1475-1481.
- Komori, T. (2010). Regulation of bone development and extracellular matrix protein genes by RUNX2. *Cell and Tissue Research*. 339: 189-195.

- Koshy, P. J. T., Lundy, C. J., Rowan, A. D., Porter, S., Edwards, D. R., Hogan, A., Clark, I. M. and Cawston, T. E. (2002). The modulation of matrix metalloproteinase and ADAM gene expression in human chondrocytes by interleukin-1 and oncostatin M: A time-course study using real-time quantitative reverse transcription-polymerase chain reaction. *Arthritis and Rheumatism*. 46: 961-967.
- Kretzschmar, M., Doody, J. and Massagué, J. (1997). Opposing BMP and EGF signalling pathways converge on the TGF- β family mediator Smad1. *Nature*. 389: 618-622.
- Kriegstein, K., Suter-Crazzolaro, C., Hotten, G., Pohl, J. and Unsicker, K. (1995). Trophic and protective effects of growth/differentiation factor 5, a member of the transforming growth factor- β superfamily, on midbrain dopaminergic neurons. *Journal of Neuroscience Research*. 42: 724-732.
- Kronenberg, H. M. (2003). Developmental regulation of the growth plate. *Nature*. 423: 332-336.
- Kronenberg, H. M. (2006). PTHrP and skeletal development.
- Kühn, K., D'lima, D. D., Hashimoto, S. and Lotz, M. (2004). Cell death in cartilage. *Osteoarthritis and Cartilage*. 12: 1-16.
- Lajeunesse, D. and Reboul, P. (2003). Subchondral bone in osteoarthritis: A biologic link with articular cartilage leading to abnormal remodeling. *Current Opinion in Rheumatology*. 15: 628-633.
- Landells, J. W. (1953). The bone cysts of osteoarthritis. *The Journal of bone and joint surgery. British volume*. 35 B: 643-649.
- Lane, L. B. and Bullough, P. G. (1980). Age-related changes in the thickness of the calcified zone and the number of tidemarks in adult human articular cartilage. *Journal of Bone and Joint Surgery - Series B*. 62: 372-375.
- Leach, R. E., Baumgard, S. and Broom, J. (1973). Obesity: its relationship to osteoarthritis of the knee. *CLIN.ORTHOP*. 93: 271-273.
- Lefebvre, V., Peeters-Joris, C. and Vaes, G. (1990). Modulation by interleukin 1 and tumor necrosis factor α of production of collagenase, tissue inhibitor of metalloproteinases and collagen types in differentiated and dedifferentiated articular chondrocytes. *BBA - Molecular Cell Research*. 1052: 366-378.

- Li, X., An, H. S., Ellman, M., Phillips, F., Thonar, E. J., Park, D. K., Udayakumar, R. K. and Im, H. J. (2008). Action of fibroblast growth factor-2 on the intervertebral disc. *Arthritis Research and Therapy*. 10.
- Liang, H., Ma, S. Y., Feng, G., Shen, F. H. and Joshua Li, X. (2010). Therapeutic effects of adenovirus-mediated growth and differentiation factor-5 in a mice disc degeneration model induced by annulus needle puncture. *Spine Journal*. 10: 32-41.
- Loeser, R. F., Chubinskaya, S., Pacione, C. and Im, H. J. (2005). Basic fibroblast growth factor inhibits the anabolic activity of insulin-like growth factor 1 and osteogenic protein 1 in adult human articular chondrocytes. *Arthritis and Rheumatism*. 52: 3910-3917.
- Loeser, R. F., Shanker, G., Carlson, C. S., Gardin, J. F., Shelton, B. J. and Sonntag, W. E. (2000). Reduction in the chondrocyte response to insulin-like growth factor 1 in aging and osteoarthritis: Studies in a non-human primate model of naturally occurring disease. *Arthritis and Rheumatism*. 43: 2110-2120.
- Lohmander, L. S. (2000). What can we do about osteoarthritis? *Arthritis Research*. 2: 95-100.
- Lorenz, H. and Richter, W. (2006). Osteoarthritis: Cellular and molecular changes in degenerating cartilage. *Progress in Histochemistry and Cytochemistry*. 40: 135-163.
- Loughlin, J. (2001). Genetic epidemiology of primary osteoarthritis. *Current Opinion in Rheumatology*. 13: 111-116.
- Loughlin, J. (2002). Genome studies and linkage in primary osteoarthritis. *Rheumatic Disease Clinics of North America*. 28: 95-109.
- Loughlin, J. (2003). Genetics of osteoarthritis and potential for drug development. *Current Opinion in Pharmacology*. 3: 295-299.
- Loughlin, J. (2005a). The genetic epidemiology of human primary osteoarthritis: Current status. *Expert Reviews in Molecular Medicine*. 7.
- Loughlin, J. (2005b). Polymorphism in signal transduction is a major route through which osteoarthritis susceptibility is acting. *Current Opinion in Rheumatology*. 17: 629-633.

- Loughlin, J. (2011). Genetics of osteoarthritis. *Current Opinion in Rheumatology*. 23: 479-483.
- Loughlin, J., Dowling, B., Chapman, K., Marcelline, L., Mustafa, Z., Southam, L., Ferreira, A., Ciesielski, C., Carson, D. A. and Corr, M. (2004). Functional variants within the secreted frizzled-related protein 3 gene are associated with hip osteoarthritis in females. *Proceedings of the National Academy of Sciences of the United States of America*. 101: 9757-9762.
- Loughlin, J., Sinsheimer, J. S., Mustafa, Z., Carr, A. J., Clipsham, K., Bloomfield, V. A., Chitnavis, J., Bailey, A., Sykes, B. and Chapman, K. (2000). Association analysis of the vitamin D receptor gene, the type I collagen gene COL1A1, and the estrogen receptor gene in idiopathic osteoarthritis. *Journal of Rheumatology*. 27: 779-784.
- Luyten, F. P. (1997). Cartilage-derived morphogenetic protein-1. *International Journal of Biochemistry and Cell Biology*. 29: 1241-1244.
- Luyten, F. P., Hascall, V. C., Nissley, S. P., Morales, T. I. and Reddi, A. H. (1988). Insulin-like growth factors maintain steady-state metabolism of proteoglycans in bovine articular cartilage explants. *Archives of Biochemistry and Biophysics*. 267: 416-425.
- Macgregor, A. J., Antoniadou, L., Matson, M., Andrew, T. and Spector, T. D. (2000). The genetic contribution to radiographic hip osteoarthritis in women: Results of a classic twin study. *Arthritis and Rheumatism*. 43: 2410-2416.
- Makris, E. A., Hadidi, P. and Athanasiou, K. A. (2011). The knee meniscus: Structure-function, pathophysiology, current repair techniques, and prospects for regeneration. *Biomaterials*. 32: 7411-7431.
- Maleki-Fischbach, M. and Jordan, J. M. (2010). New developments in osteoarthritis. Sex differences in magnetic resonance imaging-based biomarkers and in those of joint metabolism. *Arthritis Research and Therapy*. 12.
- Manek, N. J., Hart, D., Spector, T. D. and Macgregor, A. J. (2003). The association of body mass index and osteoarthritis of the knee joint: An examination of genetic and environmental influences. *Arthritis and Rheumatism*. 48: 1024-1029.
- Marks, R. and Allegrante, J. P. (2002). Body mass indices in patients with disabling hip osteoarthritis. *Arthritis Research*. 4: 112-116.
- Martin, J. A. and Buckwalter, J. A. (2002). Aging, articular cartilage chondrocyte senescence and osteoarthritis. *Biogerontology*. 3: 257-264.

- Massagué, J. (1998). TGF- β signal transduction. *Annual Review of Biochemistry*. 67:753-791.
- Merino, R., Gañan, Y., Macias, D., Economides, A. N., Sampath, K. T. and Hurle, J. M. (1998). Morphogenesis of digits in the avian limb is controlled by FGFs, TGF β s, and noggin through BMP signaling. *Developmental Biology*. 200: 35-45.
- Merino, R., Macias, D., Gañan, Y., Economides, A. N., Wang, X., Wu, Q., Stahl, N., Sampath, K. T., Varona, P. and Hurle, J. M. (1999a). Expression and function of gdf-5 during digit skeletogenesis in the embryonic chick leg bud. *Developmental Biology*. 206: 33-45.
- Merino, R., Rodriguez-Leon, J., Macias, D., Gañan, Y., Economides, A. N. and Hurle, J. M. (1999b). The BMP antagonist Gremlin regulates outgrowth, chondrogenesis and programmed cell death in the developing limb. *Development*. 126: 5515-5522.
- Meulenbelt, I., Seymour, A. B., Nieuwland, M., Huizinga, T. W. J., Van Duijn, C. M. and Slagboom, P. E. (2004). Association of the Interleukin-1 Gene Cluster With Radiographic Signs of Osteoarthritis of the Hip. *Arthritis and Rheumatism*. 50: 1179-1186.
- Middleton, J., Manthey, A. and Tyler, J. (1996). Insulin-like growth factor (IGF) receptor, IGF-I, interleukin-1 β (IL-1 β), and IL-6 mRNA expression in osteoarthritic and normal human cartilage. *Journal of Histochemistry and Cytochemistry*. 44: 133-141.
- Mikami, T., Mizumoto, S., Kago, N., Kitagawa, H. and Sugahara, K. (2003). Specificities of three distinct human chondroitin/dermatan N-acetylgalactosamine 4-O-sulfotransferases demonstrated using partially desulfated dermatan sulfate as an acceptor: Implication of differential roles in dermatan sulfate biosynthesis. *Journal of Biological Chemistry*. 278: 36115-36127.
- Mikic, B. (2004). Multiple effects of GDF-5 deficiency on skeletal tissues: Implications for therapeutic bioengineering. *Annals of Biomedical Engineering*. 32: 466-476.
- Minas, T. and Bryant, T. (2005). The role of autologous chondrocyte implantation in the patellofemoral joint. *Clinical Orthopaedics and Related Research*. 30-39.
- Mitchell, E. A., Chaffey, B. T., Mccaskie, A. W., Lakey, J. H. and Birch, M. A. (2010). Controlled spatial and conformational display of immobilised bone morphogenetic

- protein-2 and osteopontin signalling motifs regulates osteoblast adhesion and differentiation in vitro. *BMC Biology*. 8.
- Miyamoto, Y., Mabuchi, A., Shi, D., Kubo, T., Takatori, Y., Saito, S., Fujioka, M., Sudo, A., Uchida, A., Yamamoto, S., Ozaki, K., Takigawa, M., Tanaka, T., Nakamura, Y., Jiang, Q. and Ikegawa, S. (2007). A functional polymorphism in the 5' UTR of GDF5 is associated with susceptibility to osteoarthritis. *Nature Genetics*. 39: 529-533.
- Mizumoto, S., Mikami, T., Yasunaga, D., Kobayashi, N., Yamauchi, H., Miyake, A., Itoh, N., Kitagawa, H. and Sugahara, K. (2009). Chondroitin 4-O-sulfotransferase-1 is required for somitic muscle development and motor axon guidance in zebrafish. *Biochemical Journal*. 419: 387-399.
- Montgomery, S. B. and Dermitzakis, E. T. (2011). From expression QTLs to personalized transcriptomics. *Nature Reviews Genetics*. 12: 277-282.
- Moore, E. E., Bendele, A. M., Thompson, D. L., Littau, A., Waggie, K. S., Reardon, B. and Ellsworth, J. L. (2005). Fibroblast growth factor-18 stimulates chondrogenesis and cartilage repair in a rat model of injury-induced osteoarthritis. *Osteoarthritis and Cartilage*. 13: 623-631.
- Moskowitz R.W., Altman R.D., Hochberg M.C., Buckwalter J.A. and Goldberg V.M. (2007). *Osteoarthritis*. USA, Lippincott Williams and Wilkins.
- Muddasani, P., Norman, J. C., Ellman, M., Van Wijnen, A. J. and Im, H. J. (2007). Basic fibroblast growth factor activates the MAPK and NFκB pathways that converge on Elk-1 to control production of matrix metalloproteinase-13 by human adult articular chondrocytes. *Journal of Biological Chemistry*. 282: 31409-31421.
- Murakami, S., Lefebvre, V. and De Crombrughe, B. (2000). Potent inhibition of the master chondrogenic factor Sox9 gene by interleukin-1 and tumor necrosis factor-α. *Journal of Biological Chemistry*. 275: 3687-3692.
- Murdoch, A. D., Grady, L. M., Ablett, M. P., Katopodi, T., Meadows, R. S. and Hardingham, T. E. (2007). Chondrogenic differentiation of human bone marrow stem cells in transwell cultures: Generation of scaffold-free cartilage. *Stem Cells*. 25: 2786-2796.
- Murphy, L., Schwartz, T. A., Helmick, C. G., Renner, J. B., Tudor, G., Koch, G., Dragomir, A., Kalsbeek, W. D., Luta, G. and Jordan, J. M. (2008). Lifetime risk of symptomatic knee osteoarthritis. *Arthritis and rheumatism*. 59: 1207-1213.

- Nakajima, M., Takahashi, A., Kou, I., Rodriguez-Fontenla, C., Gomez-Reino, J. J., Furuichi, T., Dai, J., Sudo, A., Uchida, A., Fukui, N., Kubo, M., Kamatani, N., Tsunoda, T., Malizos, K. N., Tsezou, A., Gonzalez, A., Nakamura, Y. and Ikegawa, S. (2010). New sequence variants in HLA Class II/III region associated with susceptibility to knee Osteoarthritis identified by genome-wide association study. *PLoS ONE*. 5.
- Nevitt, M. C., Felson, D. T., Williams, E. N. and Grady, D. (2001). The effect of estrogen plus progestin on knee symptoms and related disability in postmenopausal women: The heart and estrogen/progestin replacement study, a randomized, double-blind, placebo-controlled trial. *Arthritis and Rheumatism*. 44: 811-818.
- Newman, B. and Wallis, G. A. (2002). Is osteoarthritis a genetic disease? *Clinical and Investigative Medicine*. 25: 139-149.
- Nishitoh, H., Ichijo, H., Kimura, M., Matsumoto, T., Makishima, F., Yamaguchi, A., Yamashita, H., Enomoto, S. and Miyazono, K. (1996). Identification of type I and type II serine/threonine kinase receptors for growth/differentiation factor-5. *Journal of Biological Chemistry*. 271: 21345-21352.
- Niu, J., Zhang, Y. Q., Torner, J., Nevitt, M., Lewis, C. E., Aliabadi, P., Sack, B., Clancy, M., Sharma, L. and Felson, D. T. (2009). Is obesity a risk factor for progressive radiographic knee osteoarthritis? *Arthritis Care and Research*. 61: 329-335.
- Noble, J. and Hamblen, D. L. (1975). The pathology of the degenerate meniscus lesion. *Journal of Bone and Joint Surgery - Series B*. 57: 180-186.
- Okuda, T., Mita, S., Yamauchi, S., Matsubara, T., Yagi, F., Yamamori, D., Fukuta, M., Kuroiwa, A., Matsuda, Y. and Habuchi, O. (2000). Molecular cloning, expression, and chromosomal mapping of human chondroitin 4-sulfotransferase, whose expression pattern in human tissues is different from that of chondroitin 6-sulfotransferase. *Journal of Biochemistry*. 128: 763-770.
- Oldershaw, R. A. (2012). Cell sources for the regeneration of articular cartilage: The past, the horizon and the future. *International Journal of Experimental Pathology*. 93: 389-400.
- Oliveria, S. A., Felson, D. T., Reed, J. I., Cirillo, P. A. and Walker, A. M. (1995). Incidence of symptomatic hand, hip, and knee osteoarthritis among patients in a health maintenance organization. *Arthritis and Rheumatism*. 38: 1134-1141.

- Olsen, B. R. (1995). Mutations in collagen genes resulting in metaphyseal and epiphyseal dysplasias. *Bone*. 17: 45S-49S.
- Orito, K., Koshino, T. and Saito, T. (2003). Fibroblast growth factor 2 in synovial fluid from an osteoarthritic knee with cartilage regeneration. *Journal of Orthopaedic Science*. 8: 294-300.
- Pacifici, M., Koyama, E. and Iwamoto, M. (2005). Mechanisms of synovial joint and articular cartilage formation: Recent advances, but many lingering mysteries. *Birth Defects Research Part C - Embryo Today: Reviews*. 75: 237-248.
- Panoutsopoulou, K., Southam, L., Elliott, K. S., Wrayner, N., Zhai, G., Beazley, C., Thorleifsson, G., Arden, N. K., Carr, A., Chapman, K., Deloukas, P., Doherty, M., Mccaskie, A., Ollier, W. E. R., Ralston, S. H., Spector, T. D., Valdes, A. M., Wallis, G. A., Wilkinson, J. M., Arden, E., Battley, K., Blackburn, H., Blanco, F. J., Bumpstead, S., Cupples, L. A., Day-Williams, A. G., Dixon, K., Doherty, S. A., Esko, T., Evangelou, E., Felson, D., Gomez-Reino, J. J., Gonzalez, A., Gordon, A., Gwilliam, R., Halldorsson, B. V., Hauksson, V. B., Hofman, A., Hunt, S. E., Ioannidis, J. P. A., Ingvarsson, T., Jonsdottir, I., Jonsson, H., Keen, R., Kerkhof, H. J. M., Kloppenburg, M. G., Koller, N., Lakenberg, N., Lane, N. E., Lee, A. T., Metspalu, A., Meulenbelt, I., Nevitt, M. C., O'Neill, F., Parimi, N., Potter, S. C., Rego-Perez, I., Riancho, J. A., Sherburn, K., Slagboom, P. E., Stefansson, K., Styrkarsdottir, U., Sumillera, M., Swift, D., Thorsteinsdottir, U., Tsezou, A., Uitterlinden, A. G., Van Meurs, J. B. J., Watkins, B., Wheeler, M., Mitchell, S., Zhu, Y., Zmuda, J. M., Zeggini, E. and Loughlin, J. (2011). Insights into the genetic architecture of osteoarthritis from stage 1 of the arcOGEN study. *Annals of the Rheumatic Diseases*. 70: 864-867.
- Pant, P. V. K., Tao, H., Beilharz, E. J., Ballinger, D. G., Cox, D. R. and Frazer, K. A. (2006). Analysis of allelic differential expression in human white blood cells. *Genome Research*. 16: 331-339.
- Pastinen, T., Sladek, R., Gurd, S., Sammak, A., Ge, B., Lepage, P., Lavergne, K., Villeneuve, A., Gaudin, T., Brändström, H., Beck, A., Verner, A., Kingsley, J., Harmsen, E., Labuda, D., Morgan, K., Vohl, M. C., Naumova, A. K., Sinnett, D. and Hudson, T. J. (2004). A survey of genetic and epigenetic variation affecting human gene expression. *Physiological Genomics*. 16: 184-193.

- Pe'er, I., De Bakker, P. I. W., Maller, J., Yelensky, R., Altshuler, D. and Daly, M. J. (2006). Evaluating and improving power in whole-genome association studies using fixed marker sets. *Nature Genetics*. 38: 663-667.
- Peach, C. A., Carr, A. J. and Loughlin, J. (2005). Recent advances in the genetic investigation of osteoarthritis. *Trends in Molecular Medicine*. 11: 186-191.
- Piccolo, S., Sasai, Y., Lu, B. and De Robertis, E. M. (1996). Dorsoventral patterning in *Xenopus*: Inhibition of ventral signals by direct binding of chordin to BMP-4. *Cell*. 86: 589-598.
- Pinsonneault, J. K., Papp, A. C. and Sadée, W. (2006). Allelic mRNA expression of X-linked monoamine oxidase a (MAOA) in human brain: Dissection of epigenetic and genetic factors. *Human Molecular Genetics*. 15: 2636-2649.
- Polinkovsky, A., Robin, N. H., Thomas, J. T., Irons, M., Lynn, A., Goodman, F. R., Reardon, W., Kant, S. G., Brunner, H. G., Van Der Burgt, I., Chitayat, D., Mcgaughran, J., Donnai, D., Luyten, F. P. and Warman, M. L. (1997). Mutations in CDMP1 cause autosomal dominant brachydactyly type C. *Nature genetics*. 17: 18-19.
- Poole, A.R. (2005). Cartilage in health and disease. In: KOOPMAN WJ & MORELAND LW (eds.) *Arthritis and Allied Conditions. A Textbook of Rheumatology*. 15th ed. Philadelphia: Lippincott Williams & Wilkins.
- Posthumus, M., Collins, M., Cook, J., Handley, C. J., Ribbans, W. J., Smith, R. K. W., Schwellnus, M. P. and Raleigh, S. M. (2010). Components of the transforming growth factor- β family and the pathogenesis of human achilles tendon pathology- a genetic association study. *Rheumatology*. 49: 2090-2097.
- Raine, E. V. A., Wreglesworth, N., Dodd, A. W., Reynard, L. N. and Loughlin, J. (2012). Gene expression analysis reveals HBP1 as a key target for the osteoarthritis susceptibility locus that maps to chromosome 7q22. *Annals of the Rheumatic Diseases*. 71: 2020-2027.
- Reginato, A. M. and Olsen, B. R. (2002). The role of structural genes in the pathogenesis of osteoarthritic disorders. *Arthritis Research*. 4: 337-345.
- Reinhold, M. I., Abe, M., Kapadia, R. M., Liao, Z. and Naski, M. C. (2004). FGF18 represses noggin expression and is induced by calcineurin. *Journal of Biological Chemistry*. 279: 38209-38219.

- Resnick D (1995). *Diagnosis of Bone and Joint Disorders*. London: WB Saunders Co.
- Revell, P. A., Pirie, C., Amir, G., Rashad, S. and Walker, F. (1990). Metabolic activity in the calcified zone of cartilage: Observations on tetracycline labelled articular cartilage in human osteoarthritic hips. *Rheumatology International*. 10: 143-147.
- Reynard, L. N. and Loughlin, J. (2013). The genetics and functional analysis of primary osteoarthritis susceptibility. *Expert Reviews in Molecular Medicine*. 15.
- Richmond, R. S., Carlson, C. S., Register, T. C., Shanker, G. and Loeser, R. F. (2000). Functional estrogen receptors in adult articular cartilage: Estrogen replacement therapy increases chondrocyte synthesis of proteoglycans and insulin-like growth factor binding protein 2. *Arthritis and Rheumatism*. 43: 2081-2090.
- Rickert, M., Wang, H., Wieloch, P., Lorenz, H., Steck, E., Sabo, D. and Richter, W. (2005). Adenovirus-mediated gene transfer of growth and differentiation factor-5 into tenocytes and the healing rat achilles tendon. *Connective Tissue Research*. 46: 175-183.
- Rizkalla, G., Reiner, A., Bogoch, E. and Poole, A. R. (1992). Studies of the articular cartilage proteoglycan aggrecan in health and osteoarthritis. Evidence for molecular heterogeneity and extensive molecular changes in disease. *J Clin Invest*. 90: 2268-77.
- Roberts, S., Genever, P., Mccaskie, A. and Bari, C. D. (2011). Prospects of stem cell therapy in osteoarthritis. *Regenerative Medicine*. 6: 351-366.
- Rockman, M. V. and Wray, G. A. (2002). Abundant raw material for cis-regulatory evolution in humans. *Molecular Biology and Evolution*. 19: 1991-2004.
- Rodriguez-Fontenla, C., López-Golán, Y., Calaza, M., Pombo-Suarez, M., Gómez-Reino, J. J. and González, A. (2012). Genetic risk load and age at symptom onset of knee osteoarthritis. *Journal of Orthopaedic Research*. 30: 905-909.
- Rouault, K., Scotet, V., Autret, S., Gaucher, F., Dubrana, F., Tanguy, D., Yaacoub El Rassi, C., Fenoll, B. and Férec, C. (2010). Evidence of association between GDF5 polymorphisms and congenital dislocation of the hip in a Caucasian population. *Osteoarthritis and Cartilage*. 18: 1144-1149.
- Saklatvala, J. (1986). Tumour necrosis factor α stimulates resorption and inhibits synthesis of proteoglycan in cartilage. *Nature*. 322: 547-549.
- Salter, D. M. (1998). (II) Cartilage. *Current Orthopaedics*. 12: 251-257.

- Sasaki, K., Hattori, T., Fujisawa, T., Takahashi, K., Inoue, H. and Takigawa, M. (1998). Nitric oxide mediates interleukin-1-induced gene expression of matrix metalloproteinases and basic fibroblast growth factor in cultured rabbit articular chondrocytes. *Journal of Biochemistry*. 123: 431-439.
- Sayer, A. A., Poole, J., Cox, V., Kuh, D., Hardy, R., Wadsworth, M. and Cooper, C. (2003). Weight from birth to 53 years: A longitudinal study of the influence on clinical hand osteoarthritis. *Arthritis and Rheumatism*. 48: 1030-1033.
- Schlaak, J. F., Pfers, I., Meyer Zum Büschenfelde, K. H. and Märker-Hermann, E. (1996). Different cytokine profiles in the synovial fluid of patients with osteoarthritis, rheumatoid arthritis and seronegative spondylarthropathies. *Clinical and Experimental Rheumatology*. 14: 155-162.
- Schultz, O., Keyszer, G., Zacher, J., Sittinger, M. and Burmester, G. R. (1997). Development of in vitro model systems for destructive joint diseases: Novel strategies for establishing inflammatory pannus. *Arthritis and Rheumatism*. 40: 1420-1428.
- Seemann, P., Brehm, A., König, J., Reissner, C., Stricker, S., Kuss, P., Haupt, J., Renninger, S., Nickel, J., Sebald, W., Groppe, J. C., Plöger, F., Pohl, J., Kegler, M. S. V., Walther, M., Gassner, I., Rusu, C., Janecke, A. R., Dathe, K. and Mundlos, S. (2009). Mutations in GDF5 reveal a key residue mediating BMP inhibition by NOGGIN. *PLoS Genetics*. 5.
- Sekiya, I., Tsuji, K., Koopman, P., Watanabe, H., Yamada, Y., Shinomiya, K., Nifuji, A. and Noda, M. (2000). SOX9 enhances aggrecan gene promoter/enhancer activity and is up-regulated by retinoic acid in a cartilage-derived cell line, TC6. *Journal of Biological Chemistry*. 275: 10738-10744.
- Settle Jr, S. H., Rountree, R. B., Sinha, A., Thacker, A., Higgins, K. and Kingsley, D. M. (2003). Multiple joint and skeletal patterning defects caused by single and double mutations in the mouse Gdf6 and Gdf5 genes. *Developmental Biology*. 254: 116-130.
- Sharma, L., Kapoor, D. and Issa, S. (2006). Epidemiology of osteoarthritis: An update. *Current Opinion in Rheumatology*. 18: 147-156.

- Shortkroff, S. and Yates, K. E. (2007). Alteration of matrix glycosaminoglycans diminishes articular chondrocytes' response to a canonical Wnt signal. *Osteoarthritis Cartilage*. 15: 147-54.
- Sitcheran, R., Cogswell, P. C. and Baldwin Jr, A. S. (2003). NF- κ B mediates inhibition of mesenchymal cell differentiation through a posttranscriptional gene silencing mechanism. *Genes and Development*. 17: 2368-2373.
- Slater, R. R., Jr., Bayliss, M. T., Lachiewicz, P. F., Visco, D. M. and Caterson, B. (1995). Monoclonal antibodies that detect biochemical markers of arthritis in humans. *Arthritis Rheum*. 38: 655-9.
- Solovieva, S., Hirvonen, A., Siivola, P., Vehmas, T., Luoma, K., Riihimäki, H. and Leino-Arjas, P. (2006). Vitamin D receptor gene polymorphisms and susceptibility of hand osteoarthritis in Finnish women. *Arthritis research & therapy*. 8.
- Song, R. H., Tortorella, M. D., Malfait, A. M., Alston, J. T., Yang, Z., Arner, E. C. and Griggs, D. W. (2007). Aggrecan degradation in human articular cartilage explants is mediated by both ADAMTS-4 and ADAMTS-5. *Arthritis and Rheumatism*. 56: 575-585.
- Southam, L., Dowling, B., Ferreira, A., Marcelline, L., Mustafa, Z., Chapman, K., Bentham, G., Carr, A. and Loughlin, J. (2004). Microsatellite association mapping of a primary osteoarthritis susceptibility locus on chromosome 6p12.3-q13. *Arthritis and Rheumatism*. 50: 3910-3914.
- Southam, L., Rodriguez-Lopez, J., Wilkins, J. M., Pombo-Suarez, M., Snelling, S., Gomez-Reino, J. J., Chapman, K., Gonzalez, A. and Loughlin, J. (2007). An SNP in the 5'-UTR of GDF5 is associated with osteoarthritis susceptibility in Europeans and with in vivo differences in allelic expression in articular cartilage. *Human Molecular Genetics*. 16: 2226-2232.
- Spector, T. D., Cicuttini, F., Baker, J., Loughlin, J. and Hart, D. (1996). Genetic influences on osteoarthritis in women: A twin study. *British Medical Journal*. 312: 940-944.
- Spector, T. D. and Macgregor, A. J. (2004). Risk factors for osteoarthritis: genetics. *Osteoarthritis and Cartilage*. 12 Suppl A: S39-44.
- Srikanth, V. K., Fryer, J. L., Zhai, G., Winzenberg, T. M., Hosmer, D. and Jones, G. (2005). A meta-analysis of sex differences prevalence, incidence and severity of osteoarthritis. *Osteoarthritis and Cartilage*. 13: 769-781.

- Stecher, R. M. (1941). HEBERDEN'S NODES: Heredity in Hypertrophic Arthritis of the Finger Joints. *The American Journal of the Medical Sciences*. 201: 801-809.
- Stefánsson, S. E., Jónsson, H., Ingvarsson, T., Manolescu, I., Jónsson, H. H., Ólafsdóttir, G., Pálsdóttir, E., Stefánsdóttir, G., Sveinbjörnsdóttir, G., Frigge, M. L., Kong, A., Gulcher, J. R. and Stefánsson, K. (2003). Genomewide scan for hand osteoarthritis: A novel mutation in matrilin-3. *American Journal of Human Genetics*. 72: 1448-1459.
- Stokes, D. G., Liu, G., Dharmavaram, R., Hawkins, D., Piera-Velazquez, S. and Jimenez, S. A. (2001). Regulation of type-II collagen gene expression during human chondrocyte de-differentiation and recovery of chondrocyte-specific phenotype in culture involves Sry-type high-mobility-group box (SOX) transcription factors. *Biochemical Journal*. 360: 461-470.
- Storm, E. E., Huynh, T. V., Copeland, N. G., Jenkins, N. A., Kingsley, D. M. and Lee, S. J. (1994). Limb alterations in brachypodism mice due to mutations in a new member of the TGF β -superfamily. *Nature*. 368: 639-643.
- Storm, E. E. and Kingsley, D. M. (1996). Joint patterning defects caused by single and double mutations in members of the bone morphogenetic protein (BMP) family. *Development*. 122: 3969-3979.
- Storm, E. E. and Kingsley, D. M. (1999). GDF5 coordinates bone and joint formation during digit development. *Developmental Biology*. 209: 11-27.
- Sun, Y., Mauerhan, D. R., Honeycutt, P. R., Kneisl, J. S., Norton, H. J., Zinchenko, N., Hanley Jr, E. N. and Gruber, H. E. (2010). Calcium deposition in osteoarthritic meniscus and meniscal cell culture. *Arthritis Research and Therapy*. 12.
- Tallheden, T., Karlsson, C., Brunner, A., Van Der Lee, J., Hagg, R., Tommasini, R. and Lindahl, A. (2004). Gene expression during redifferentiation of human articular chondrocytes. *Osteoarthritis and Cartilage*. 12: 525-535.
- Taskiran, D., Stefanic-Racic, M., Georgescu, H. and Evans, C. (1994). Nitric oxide mediates suppression of cartilage proteoglycan synthesis by interleukin-1. *Biochemical and Biophysical Research Communications*. 200: 142-148.
- Tew, S. R., Murdoch, A. D., Rauchenberg, R. P. and Hardingham, T. E. (2008). Cellular methods in cartilage research: primary human chondrocytes in culture and chondrogenesis in human bone marrow stem cells. *Methods*. 45: 2-9.

- Theocharis, A. D. (2002). Human colon adenocarcinoma is associated with specific post-translational modifications of versican and decorin. *Biochimica et Biophysica Acta - Molecular Basis of Disease*. 1588: 165-172.
- Thomas, J. T., Kilpatrick, M. W., Lin, K., Erlacher, L., Lembessis, P., Costa, T., Tsiouras, P. and Luyten, F. P. (1997). Disruption of human limb morphogenesis by a dominant negative mutation in CDMP1. *Nature Genetics*. 17: 58-64.
- Thomas, J. T., Lin, K., Nandedkar, M., Camargo, M., Cervenka, J. and Luyten, F. P. (1996). A human chondrodysplasia due to a mutation in a TGF- β superfamily member. *Nature Genetics*. 12: 315-317.
- Thorén, S. and Jakobsson, P. J. (2000). Coordinate up- and down-regulation of glutathione-dependent prostaglandin E synthase and cyclooxygenase-2 in A549 cells: Inhibition by NS-398 and leukotriene C4. *European Journal of Biochemistry*. 267: 6428-6434.
- Trippel, S. B., Corvol, M. T., Dumontier, M. F., Rappaport, R., Hung, H. H. and Mankin, H. J. (1989). Effect of somatomedin-C/Insulin-like growth factor I and growth hormone on cultured growth plate and articular chondrocytes. *Pediatric Research*. 25: 76-82.
- Uitterlinden, A. G., Burger, H., Huang, Q., Odding, E., Van Duijn, C. M., Hofman, A., Birkenhäger, J. C., Van Leeuwen, J. P. T. M. and Pols, H. a. P. (1997). Vitamin D receptor genotype is associated with radiographic osteoarthritis at the knee. *Journal of Clinical Investigation*. 100: 259-263.
- Uitterlinden, A. G., Burger, H., Van Duijn, C. M., Huang, Q., Hofman, A., Birkenhäger, J. C., Van Leeuwen, J. P. T. M. and Pols, H. a. P. (2000). Adjacent genes, for COL2A1 and the vitamin D receptor, are associated with separate features of radiographic osteoarthritis of the knee. *Arthritis and Rheumatism*. 43: 1456-1464.
- Vahlensieck, M., Linneborn, G., Schild, H. H. and Schmidt, H. M. (2002). Hoffa's recess: Incidence, morphology and differential diagnosis of the globular-shaped cleft in the infrapatellar fat pad of the knee on MRI and cadaver dissections. *European Radiology*. 12: 90-93.
- Vallièrès, M. and Du Souich, P. (2010). Modulation of inflammation by chondroitin sulfate. *Osteoarthritis and Cartilage*. 18: S1-S6.

- Van Der Kraan, P. M. and Van Den Berg, W. B. (2007). Osteophytes: relevance and biology. *Osteoarthritis and Cartilage*. 15: 237-244.
- Varga, A. C. and Wrana, J. L. (2005). The disparate role of BMP in stem cell biology. *Oncogene*. 24: 5713-5721.
- Videman, T., Leppävuori, J., Kaprio, J., Battié, M. C., Gibbons, L. E., Peltonen, L. and Koskenvuo, M. (1998). Intragenic polymorphisms of the vitamin D receptor gene associated with intervertebral disc degeneration. *Spine*. 23: 2477-2485.
- Vincenti, M. P. and Brinckerhoff, C. E. (2002). Transcriptional regulation of collagenase (MMP-1, MMP-13) genes in arthritis: Integration of complex signaling pathways for the recruitment of gene-specific transcription factors. *Arthritis Research*. 4: 157-164.
- Vlad, S. C., Lavalley, M. P., Mcalindon, T. E. and Felson, D. T. (2007). Glucosamine for pain in osteoarthritis: why do trial results differ? *Arthritis & Rheumatism*. 56: 2267-77.
- Walsh, A. J. L., Bradford, D. S. and Lotz, J. C. (2004). In Vivo Growth Factor Treatment of Degenerated Intervertebral Discs. *Spine*. 29: 156-163.
- Wandel, S., Jüni, P., Tendal, B., Nüesch, E., Villiger, P. M., Welton, N. J., Reichenbach, S. and Trelle, S. (2010). Effects of glucosamine, chondroitin, or placebo in patients with osteoarthritis of hip or knee: network meta-analysis. *BMJ (Clinical research ed.)*. 341.
- Wang, D. and Sadée, W. (2006). Searching for polymorphisms that affect gene expression and mRNA processing: Example ABCB1 (MDR1). *AAPS Journal*. 8: E515-E520.
- Wehrli, F. W. (2007). Structural and functional assessment of trabecular and cortical bone by micro magnetic resonance imaging. *Journal of Magnetic Resonance Imaging*. 25: 390-409.
- WHO Scientific Group on the Burden of Musculoskeletal Conditions at the Start of the New Millennium (2003). The burden of musculoskeletal conditions at the start of the new millennium. *World Health Organization Technical Report Series*. 919: i-x, 1-218, back cover.

- Wieland, H. A., Michaelis, M., Kirschbaum, B. J. and Rudolphi, K. A. (2005). Osteoarthritis - an untreatable disease? *Nature Reviews. Drug Discovery*. 4: 331-344.
- Wilkins, J. M., Southam, L., Price, A. J., Mustafa, Z., Carr, A. and Loughlin, J. (2007). Extreme context specificity in differential allelic expression. *Human Molecular Genetics*. 16: 537-546.
- Williams, F. M. K., Popham, M., Hart, D. J., De Schepper, E., Bierma-Zeinstra, S., Hofman, A., Uitterlinden, A. G., Arden, N. K., Cooper, C., Spector, T. D., Valdes, A. M. and Van Meurs, J. (2011). GDF5 single-nucleotide polymorphism rs143383 is associated with lumbar disc degeneration in Northern European women. *Arthritis and Rheumatism*. 63: 708-712.
- Willis, C. M., Wrana, J. L. and Kluppel, M. (2009). Identification and characterization of TGFbeta-dependent and -independent cis-regulatory modules in the C4ST-1/CHST11 locus. *Genet Mol Res*. 8: 1331-43.
- Windisch, P., Stavropoulos, A., Molnár, B., Szendrői-Kiss, D., Szilágyi, E., Rosta, P., Horváth, A., Capsius, B., Wikesjö, U. M. E. and Sculean, A. (2012). A phase IIa randomized controlled pilot study evaluating the safety and clinical outcomes following the use of rhGDF-5/ β -TCP in regenerative periodontal therapy. *Clinical Oral Investigations*. 16: 1181-1189.
- Wluka, A. E., Cicuttini, F. M. and Spector, T. D. (2000). Menopause, oestrogens and arthritis. *Maturitas*. 35: 183-199.
- Woo SI-Y, Kwan Mk, Coutts Rd and Akeson Wh (1992). Biomechanical considerations. In: MOSKOWITZ RW, HOWELL DS, GOLDBERG VM & MANKIN HJ (eds.) *Osteoarthritis, Diagnosis and Medical/Surgical Management*. 2nd ed. Philadelphia: WB Saunders Co.
- Wrana, J. L., Attisano, L., Wieser, R., Ventura, F. and Massagué, J. (1994). Mechanism of activation of the TGF- β receptor. *Nature*. 370: 341-347.
- Wu, W., Billingham, R. C., Pidoux, I., Antoniou, J., Zukor, D., Tanzer, M. and Poole, A. R. (2002). Sites of collagenase cleavage and denaturation of type II collagen in aging and osteoarthritic articular cartilage and their relationship to the distribution of matrix metalloproteinase 1 and matrix metalloproteinase 13. *Arthritis and Rheumatism*. 46: 2087-2094.

- Wysolmerski, J. J. (2012). Parathyroid hormone-related protein: An update. *Journal of Clinical Endocrinology and Metabolism*. 97: 2947-2956.
- Xu, Y., Barter, M. J., Swan, D. C., Rankin, K. S., Rowan, A. D., Santibanez-Koref, M., Loughlin, J. and Young, D. A. (2012). Identification of the pathogenic pathways in osteoarthritic hip cartilage: Commonality and discord between hip and knee OA. *Osteoarthritis and Cartilage*. 20: 1029-1038.
- Yan, C. and Boyd, D. D. (2007). Regulation of matrix metalloproteinase expression. *Journal of Cellular Physiology*. 211: 19-26.
- Yan, C., Wang, H. and Boyd, D. D. (2001). KiSS-1 represses 92-kDa type IV collagenase expression by down-regulating NF- κ B binding to the promoter as a consequence of I κ B α -induced block of p65/p50 nuclear translocation. *Journal of Biological Chemistry*. 276: 1164-1172.
- Yan, H., Yuan, W., Velculescu, V. E., Vogelstein, B. and Kinzler, K. W. (2002). Allelic variation in human gene expression. *Science*. 297: 1143.
- Yusa, A., Kitajima, K. and Habuchi, O. (2005). N-linked oligosaccharides are required to produce and stabilize the active form of chondroitin 4-sulphotransferase-1. *Biochem J*. 388: 115-21.
- Zeggini, E., Panoutsopoulou, K., Southam, L., Rayner, N. W., Day-Williams, A. G., Lopes, M. C., Boraska, V., Esko, T., Evangelou, E., Hoffman, A., Houwing-Duistermaat, J. J., Ingvarsson, T., Jonsdottir, I., Jonnson, H., Kerkhof, H. J., Kloppenburg, M., Bos, S. D., Mangino, M., Metrustry, S., Slagboom, P. E., Thorleifsson, G., Raine, E. V., Ratnayake, M., Ricketts, M., Beazley, C., Blackburn, H., Bumpstead, S., Elliott, K. S., Hunt, S. E., Potter, S. C., Shin, S. Y., Yadav, V. K., Zhai, G., Sherburn, K., Dixon, K., Arden, E., Aslam, N., Battley, P. K., Carluke, I., Doherty, S., Gordon, A., Joseph, J., Keen, R., Koller, N. C., Mitchell, S., O'Neill, F., Paling, E., Reed, M. R., Rivadeneira, F., Swift, D., Walker, K., Watkins, B., Wheeler, M., Birrell, F., Ioannidis, J. P., Meulenbelt, I., Metspalu, A., Rai, A., Salter, D., Stefansson, K., Stykarsdottir, U., Uitterlinden, A. G., Van Meurs, J. B., Chapman, K., Deloukas, P., Ollier, W. E., Wallis, G. A., Arden, N., Carr, A., Doherty, M., Mccaskie, A., Wilkinson, J. M., Ralston, S. H., Valdes, A. M., Spector, T. D. and Loughlin, J. (2012). Identification of new susceptibility loci for osteoarthritis (arcOGEN): a genome-wide association study. *Lancet*. 380: 815-23.

- Zhang, W., Nuki, G., Moskowitz, R. W., Abramson, S., Altman, R. D., Arden, N. K., Bierma-Zeinstra, S., Brandt, K. D., Croft, P., Doherty, M., Dougados, M., Hochberg, M., Hunter, D. J., Kwoh, K., Lohmander, L. S. and Tugwell, P. (2010). OARSI recommendations for the management of hip and knee osteoarthritis. Part III: Changes in evidence following systematic cumulative update of research published through January 2009. *Osteoarthritis and Cartilage*. 18: 476-499.
- Zhang, Y., Bertolino, A., Fazio, L., Blasi, G., Rampino, A., Romano, R., Lee, M. L. T., Xiao, T., Papp, A., Wang, D. and Sadée, W. (2007). Polymorphisms in human dopamine D2 receptor gene affect gene expression, splicing, and neuronal activity during working memory. *Proceedings of the National Academy of Sciences of the United States of America*. 104: 20552-20557.
- Zhang, Y., Chee, A., Thonar, E. J. and An, H. S. (2011). Intervertebral disk repair by protein, gene, or cell injection: a framework for rehabilitation-focused biologics in the spine. *PM & R : the journal of injury, function, and rehabilitation*. 3: S88-94.
- Zimmerman, L. B., De Jesús-Escobar, J. M. and Harland, R. M. (1996). The Spemann organizer signal noggin binds and inactivates bone morphogenetic protein 4. *Cell*. 86: 599-606.
- Zinkel, S. S., Hurov, K. E., Ong, C., Abtahi, F. M., Gross, A. and Korsmeyer, S. J. (2005). A role for proapoptotic BID in the DNA-damage response. *Cell*. 122: 579-591.